

University of Belgrade  
School of Electrical Engineering

Natalija M. Katić

**Decoding neural mechanisms using in silico and  
animal models for restoring somatosensory  
feedback with neuroprostheses**

Doctoral Dissertation

Belgrade, 2023

Универзитет у Београду  
Електротехнички факултет

Наталија М. Катић

**Декодирање неуралних механизма помоћу „in silico“ модела и експеримената на животињама са циљем обнављања соматосензорног осећаја променом неуропротеза**

Докторска дисертација

Београд, 2023

# Information About the Mentors and Commission Members

## **Mentors:**

- ❖ Dr Željko Đurović, full professor, School of Electical Engineering, University of Belgrade
- ❖ Dr Milica Janković, associate professor, School of Electical Engineering, University of Belgrade

## **Commission members:**

- ❖ Dr Lazar Saranovac, full professor, School of Electical Engineering, University of Belgrade
- ❖ Dr Goran Kvaščev, assosiate professor, School of Electical Engineering, University of Belgrade
- ❖ Dr Staniša Raspopović, assistant professor, Eidgenössische Technische Hochschule Zürich

## **Date of defense:**

## Подаци о менторима и члановима комисије

### Ментори:

- ❖ Др Жељко Ђуровић, редовни професор, Електротехнички факултет, Универзитет у Београду
- ❖ Др Милица Јанковић, ванредни професор, Електротехнички факултет, Универзитет у Београду

### Чланови комисије:

- ❖ Др Лазар Сарановац, редовни професор, Електротехнички факултет, Универзитет у Београду
- ❖ Др. Горан Квашчев, ванредни професор, Електротехнички факултет, Универзитет у Београду
- ❖ Др Станиша Распоповић, доцент, Eidgenössische Technische Hochschule Zürich

### Датум одбране:



## Acknowledgements

*Good friends help you to find important things when you have lost them:  
your smile, your hope, and your courage.*

I would like to express my deepest gratitude to my research supervisor, prof. Staniša Raspopović, firstly for giving me the opportunity to live in Belgrade and work as an external part of the Neuroengineering lab at ETH Zurich, pursuing the objectives I have always dreamt about. Thank you for trusting me on a challenging project, for the consistent guidance, suggestions, advices and incredible patience. I am particularly grateful for the numerous scientific collaborations you enabled me to be a part of, as well as the enriching travel experiences they entailed. Thank you for allowing me to try and learn things that are rarely part of the PhD path. Witnessing the establishment and growth of your laboratory has been an absolute honor. I am thrilled with all your effort to make such an incredible, funny, close and trustable atmosphere. I aspire to create a similar environment in my future. Just as my parents have shown me what it means to be respected in family and life, you have taught me how empowering it feels when one's opinion is valued and respected in the workplace. Our shared values have been a source of inspiration, and I sincerely hope that we will continue to embark on scientific and other exciting adventures together.

My sincere thanks go to my university mentors, prof. Željko Đurović and prof. Milica Janković. Your suggestions helped the thesis to get its final form. Moreover, your lectures throughout the studies set the bases of knowledge necessary for dealing with challenges nowadays. I would like to thank Prof. Marco Capogrosso, my co-mentor in science. Your sharp mind and inspiring guidance have not only deepened my understanding of neuroscience but also fostered a genuine love for the field. I also express my thanks to all my students and collaborators that contributed to the accomplishment of this thesis.

My warm thanks go to my Neuroengineering lab with whom I've shared everything for nine months, and learned what the team is - team at work and even stronger in life, and created the unbreakable ties. You made me understand that passion is, if not more, equally important as the knowledge. Your presence has been a constant source of inspiration, and I firmly believe that we have countless "crazy ideas" to explore in the years to come. I must admit, I never believed in the concept of creating a home away from home, but you have proven me to be so wrong.

I would like to believe that my dedication played a significant role in shaping my life according to my aspirations. However, I recognize that I was extraordinarily fortunate twice: when I transitioned to a new elementary school and when I arrived in Zurich. Both times, I embarked on new chapters of my life alone, and was immediately accepted as the integral part of the team, surrounded by people who cheered and still cheer up for my every achievement. I felt how strong push the friends can give you, and really find your lost courage, hope and of course bring you such a wide smile. Overwhelmed with this incredible feeling I'm finishing the long pathway of education, hoping I would never lose this essence. I therefore thank all my friends for unreserved support, love and understanding and I can't wait for creating our new adventures, memories, and life chapters.

When people are amazed with the person who managed to finish marathon race, I love to say that running is “easy” when family made it possible to spend so many hours on training. I have to be fair now and say learning and doing a research is easy when my family gave everything to make me be able to focus, enjoy it fully, and never worry about the daily things. Mum and dad, besides the unconditional love, you dedicated the infinite amount of time to make the studying my only responsibility, always. This thesis is mostly your achievement.

Lule, even though it’s now official, it feels like I have forgotten the times when we were not a family. My learning and travel buddy, stress reliever, time manager, my best friend and ultimately my true love, I love seeing us grow. I feel your sincere belief in the things I am doing. Thank you for being the anchor of my life. I would love to make you proud.

Finally, my big thanks go to Stani, a true friend, for being a “psychologist” during challenging times, and a volleyball and basketball coach under the sunny weather. I am happy for fighting all the battles with you in the previous years, I believe they tough us so much. I long for more time to delve into our never-ending discussions, that played a pivotal role in structuring the core of this theses.

# **Decoding neural mechanisms using in silico and animal models for restoring somatosensory feedback with neuroprostheses**

## **Abstract**

Limb amputation is a tragic event that significantly alters patient's quality of life. Although somatosensory feedback is a crucial for motor control and coordination, currently available prostheses are lacking information about the ground interaction or limb position. Because of that, amputees are prone to falls and asymmetrical walking, causing higher fatigue and big cardiovascular problems. Efforts are made to develop a neuroprosthetic device that is able to restore missing sensations. Previous studies demonstrated the ability to restore touch sensation with electrical stimulation, but the naturalness of resulting sensation was limited and often described as unpleasant paresthesia. Restoring the proprioception, sense about the position of the limb, still remains as a big challenge.

This thesis aims to define the proper language to communicate with our nervous system, in order to restore close-to-natural sensory feedback. A computational model of foot sole afferents neural responses was developed and biomimetic paradigms mimicking the natural features of touch designed on its output. Animal models were used for studying the effects of nerve stimulation with different patterns on resulting neural responses along the somatosensory axes, and understanding transmission of artificially induced information from peripheral to the central nervous system. Translational framework for creating new biomimetic strategies is a final outcome of the study. Results imply that the new patterns design should be model-driven, developed approach tested in animals as a proof of concept, and finally validated in the clinical human experiments. Our evidences highlight the remarkable impact of biomimicry, while also holding immense promise in revolutionizing neuroprosthetics.

**Key words:** neuroprosthetics, bionic prostheses, somatosensory feedback, neuromodulation, biomimetic paradigms, computational modeling, proprioception, translational framework, spinal cord, somatosensory cortex

**Scientific field:** technical sciences, electrical engineering

**Scientific subfield:** biomedical engineering

**UDK number:** 621.3

# Декодирање неуралних механизма помоћу „in silico“ модела и експеримената на животињама са циљем обнављања соматосензорног осећаја променом неуропротеза

## Сажетак

Ампутација екстремитета сматра се трагичним догађајем који значајно утиче на здравље и квалитет живота особе. Иако је соматосензорни осећај изузетно важан за координацију покрета, комерцијално доступне протезе не преносе пацијенту информацију о интеракцији са подлогом, или позицији уда у простору. Услед недостатка осећаја из стопала, брзина хода се смањује, јавља се несиметричан ход, замор се последично повећава, и то често доводи до великих кардиоваскуларних проблема. Због наведеног, пуно се улаже у развој неуропротетичких система који би омогућили пацијентима да осећају одговарајуће сензације са периферије. Раније студије показале су да је електричном стимулацијом могуће обновити осећај додира, али је природност осећаја била мала и слична непријатној парестезији. Као додатан изазов јавља се немогућност робусног обнављања осећаја проприоцепције.

Ова теза има за циљ да дефинише одговарајући језик за комуникацију са нашим нервним системом како би се повратио осећај што ближи природном. Развијен је „in silico“ модел који oponаша рад механорецептора на стопалу који механички стимулус пресликава се у специфичан одговор нервних влакана и служи као полазна тачка за дефинисање биомиметичких типова стимулације. Ефекти нервне стимулације различитим парадигмама у кичменој мождини и кортексу, као и њихов начин преноса од периферног до централног нервног система, проучавани су током експеримената на животињама. Крајњи исход студије је концепт за креирање биомиметичких типова стимулације: нове парадигме треба базирати на предикцији модела, примарно тестирати приступ на животињама и коначно потврдити перформансе у клиничким студијама на људима. Представљени резултати истичу важност биомимикрије и омогућавају превазилажење недостатака и напредак у развоју неуропротетичких система.

**Кључне речи:** неуропротетика, бионичка протеза, соматосензорни осећај, неуромодулација, биомиметичке парадигме, рачунарско моделирање, проприоцепција, кичмена мождина, соматосензорни кортекс

**Научна област:** техничке науке, електротехника

**Ужа научна област:** биомедицинско инжењерство

**УДК број:** 621.3

# Contents

|   |           |
|---|-----------|
| <b>General introduction</b>   | <b>1</b>  |
| <b>1.1 Context</b>  | <b>2</b>  |
| <b>1.2 Limitations of neuroprosthetic devices that do not provide sensory feedback</b>                | <b>2</b>  |
| <b>1.3 Somatosensory feedback</b>   | <b>2</b>  |
| 1.3.1 Natural sensors detecting and transmitting somatosensory feedback                               | 3         |
| 1.3.1.1 Touch sensation   | 3         |
| 1.3.1.2 Proprioception  | 5         |
| 1.3.1.3 Neural pathways: from detecting stimulus on the periphery to perceiving sensation             | 5         |
| <b>1.4 Neurostimulation technologies for restoring somatosensory feedback</b>                         | <b>7</b>  |
| 1.4.1 Neuromodulation devices   | 7         |
| 1.4.2 Encoding strategies: Lack of natural, physiologically plausible touch                           | 8         |
| 1.4.3 Touch, but not the proprioception.  | 11        |
| 1.4.3.1 Understanding information processing along the somatosensory axes using populational analysis | 13        |
| <b>1.5 Translational framework for novel sensory encoding strategies</b>                              | <b>13</b> |
| <b>1.6 Thesis objectives</b>  | <b>14</b> |
| <b>1.7 Structure of the thesis</b>  | <b>15</b> |
| <b><i>In silico modeling of foot afferents</i></b>  | <b>16</b> |
| <b>2.1 Introduction</b>   | <b>17</b> |
| <b>2.2 Methods</b>  | <b>18</b> |
| 2.2.1 FootSim model overview  | 18        |
| 2.2.2 Fitting model parameters  | 21        |
| 2.2.3 Fitting accuracy testing and model validation   | 23        |
| 2.2.3.1 Firing rate responses   | 24        |
| 2.2.3.2 Afferent firing thresholds  | 24        |
| 2.2.3.3 Receptive Fields  | 24        |
| 2.2.3.4 Ramp-and-hold responses   | 24        |
| 2.2.4 Simulation of neural responses during walking   | 24        |
| 2.2.5 Quantification and statistical analysis   | 25        |
| <b>2.3 Results</b>  | <b>25</b> |
| 2.3.1 FootSim model replicates experimental afferent neural responses                                 | 25        |
| 2.3.1.1 Firing rates  | 25        |
| 2.3.1.2 Response thresholds   | 26        |
| 2.3.2 Model validation  | 27        |
| 2.3.2.1 Receptive fields  | 27        |
| 2.3.2.2 Afferent responses on ramp-and-hold stimuli   | 29        |
| 2.3.3 Robustness of model parameters  | 29        |
| 2.3.3 Neural afferent responses during walking cycle  | 31        |
| <b>2.4 Discussion</b>   | <b>33</b> |
| 2.4.1 FootSim emulates and reveals the role of specific tactile afferents for balance and gait        | 34        |
| 2.4.2 Importance of specific FootSim features   | 35        |
| 2.4.3 FootSim model application in neuroprosthetics   | 36        |
| 2.4.4 Limitations of the study  | 37        |
| <b><i>Animal models can reveal novel insights about artificial somatosensory feedback</i></b>         | <b>39</b> |
| <b>3.1 Introduction</b>   | <b>40</b> |
| <b>3.2 Methods</b>  | <b>42</b> |
| 3.2.1 Animals   | 42        |
| 3.2.2 Surgical procedures   | 42        |

|   |           |
|---|-----------|
| 3.2.3 Electrophysiology in sedated monkeys  | 43        |
| 3.2.4 Data analysis   | 43        |
| 3.2.4.1 Pre-processing  | 43        |
| 3.2.4.2 Identification of sensory volleys resulting from muscle nerve stimulation   | 43        |
| 3.2.4.3 Characterization and quantification of neural spiking activity  | 44        |
| 3.2.4.4 Neural manifold and trajectory length   | 44        |
| 3.2.5 Statistical Analysis  | 45        |
| <b>3.3 Results</b>  | <b>45</b> |
| 3.3.1 Simultaneous brain and spinal neural recordings during electrical nerve stimulation of multiple sensory modalities  | 45        |
| 3.3.2 Proprioceptive inputs elicit robust trajectories in the spinal neural manifold  | 47        |
| 3.3.3 Continuous electrical stimulation of the cutaneous nerve disrupts intra-spinal proprioceptive neural trajectories   | 48        |
| 3.3.4 Cutaneous electrical stimulation reduced proprioceptive afferent volleys, spinal cord grey matter field potentials and multiunit responses                  | 51        |
| 3.3.5 Reduction of proprioceptive processing impacts somatosensory cortex   | 55        |
| <b>3.4 Discussion</b>   | <b>57</b> |
| 3.4.1 Population analysis as a tool to explain network-level effects of electrical stimulation  | 57        |
| 3.4.2 Potential underlying neural mechanisms  | 58        |
| 3.4.3 Effects within the brain  | 59        |
| 3.4.4 Conclusions and relevance for other brain circuits  | 59        |
| <b><i>From in silico modeling towards sophisticated application in humans</i></b>   | <b>61</b> |
| <b>4.1 Introduction</b>   | <b>62</b> |
| <b>4.2 Methods</b>  | <b>64</b> |
| 4.2.1 Modeling of all tactile afferents innervating the glabrous skin of the foot (FootSim)   | 65        |
| 4.2.2 Design biomimetic neural stimulations using FootSim   | 65        |
| 4.2.3 Electrophysiology in decerebrated cats  | 65        |
| 4.2.4 Analysis of the animal neural data  | 65        |
| 4.2.4.1 Pre-processing  | 66        |
| 4.2.4.2 Identification of local field potential   | 66        |
| 4.2.4.3 Characterization and quantification of neural spiking activity  | 66        |
| 4.2.5 Patient recruitment and surgical procedure in humans  | 66        |
| 4.2.6 Intraneural stimulation for evoking artificial sensations   | 67        |
| 4.2.6 Assessment of sensation naturalness   | 68        |
| 4.2.7 Real-time biomimetic neurostimulation in a neuro-robotic leg  | 69        |
| 4.2.8 Stairs Task   | 69        |
| 4.2.9 Cognitive double task   | 70        |
| 4.2.10 Self-reported confidence   | 70        |
| 4.2.11 Statistics   | 70        |
| <b>4.3 Results</b>  | <b>70</b> |
| 4.3.1 Biomimetic neurostimulation paradigms are designed by exploiting a realistic in-silico model of foot sole afferents (FootSim).                              | 71        |
| 4.3.2 The neurostimulation dynamics is transferred through somatosensory neuroaxis  | 73        |
| 4.3.3 Neural response evoked by biomimetic stimulation is more similar to the mechanically-induced activity than the one produced by tonic electrical stimulation | 74        |
| 4.3.4 Biomimetic neurostimulation evokes more natural sensations than non-biomimetic neurostimulation paradigms.  | 77        |
| 4.3.5 Biomimetic neurostimulation on a neuro-robotic device allows for a higher mobility and a reduced metal workload   | 80        |
| <b>4.4 Discussion</b>   | <b>83</b> |
| 4.4.1 Multi-level approach for designing new stimulation strategies that would minimize paresthesia sensations  | 83        |
| 4.4.2 Comparing neural responses induced with natural touch and electrical nerve stimulation  | 83        |

|  |    |
|--|----|
| 4.4.3 Biomimetic stimulation in neuromodulation devices is beneficial both for the perceived sensation and its functionality | 84 |
| 4.4.3 Future biomimetic neurostimulation devices   | 85 |

**Conclusion** \_\_\_\_\_ **87**

**5.1 In silico modeling of touch – scientific and engineering tool** \_\_\_\_\_ **88**

**5.2 Understanding neural responses along the somatosensory axes** \_\_\_\_\_ **90**

5.2.1 Unveiling hindered processing limitations with population analysis \_\_\_\_\_ 90

5.2.2 Neural responses to artificial and natural stimuli \_\_\_\_\_ 92

**5.3 Multifaceted framework for creating novel stimulating patterns** \_\_\_\_\_ **92**

**5.4 General outlook: Towards the development of novel neuroprosthetic approaches** \_\_\_\_\_ **93**

**5.5 Limitations of the thesis** \_\_\_\_\_ **94**

**5.6 Opportunities** \_\_\_\_\_ **95**

## List of figures:

|  |    |
|--|----|
| <b>Figure 1.1</b> , Cutaneous afferents.....   | 3  |
| <b>Figure 1.2</b> , Distribution of specific afferent types.....   | 4  |
| <b>Figure 1.3</b> , Major proprioceptors.....  | 5  |
| <b>Figure 1.4</b> , Afferent fibers projecting from the periphery to the spinal cord.....  | 6  |
| <b>Figure 1.5</b> , Touch and proprioception pathways.....   | 6  |
| <b>Figure 1.6</b> Somatosensory Neuroprostheses.....   | 8  |
| <b>Figure 1.7</b> Different sensory encoding strategies.....   | 9  |
| <b>Figure 1.8</b> Contact with an object produces temporal patterns of pressure on a sensor at the fingertip of the prosthesis.....  | 10 |
| <b>Figure 2.1</b> . Overview of the FootSim model mimicking the mechanotransduction process  | 19 |
| <b>Figure 2.2</b> Mechanical model of FootSim simulates skin changes caused by the applied stimuli and its propagation through the sole of the foot.....                                   | 21 |
| <b>Figure 2.3</b> , Response of afferents innervating the great toe with different incorporated skin hardness values.....  | 22 |
| <b>Figure 2.4</b> . Microneurography recordings in human tibial nerve.....   | 23 |
| <b>Figure 2.5</b> , Parameter values for individual models of afferents.....   | 24 |
| <b>Figure 2.6</b> . FootSim accurately simulates afferent firing rates.....  | 27 |
| <b>Figure 2.7</b> . FootSim demonstrates realistic absolute firing threshold values.....   | 28 |
| <b>Figure 2.8</b> . FootStim can produce realistic receptive field sizes and afferent responses to ramp and hold stimuli, replicating the natural behavior of specific afferent types..... | 29 |
| <b>Figure 2.9</b> , Exploring the individual models parameter space.....   | 31 |
| <b>Figure 2.10</b> , Footstim is robust to modifications of parameters values but also to changes of relationships between parameters.....   | 32 |
| <b>Figure 2.11</b> , FootSim can reveal dynamics of activation during the walking cycle.....   | 33 |
| <b>Figure 2.12</b> , The spatial indentation profile and the population responses during different type of steps, analyzed by the location on the foot sole.....                           | 34 |
| <b>Figure 2.13</b> . FootSim possible contribution to biomimetic stimulation patterns for tactile feedback restoration in future neuroprosthetics.....                                     | 38 |
| <b>Figure 3.1</b> , Electrical stimulation disrupts computations of ongoing network processes....  | 42 |
| <b>Figure 3.2</b> , Experimental setup: Schematic illustration of experiments.....   | 47 |
| <b>Figure 3.3</b> , Experimental procedure and electrophysiology details.....  | 47 |
| <b>Figure 3.4</b> , Intra-spinal neural population analysis.....   | 48 |
| <b>Figure 3.5</b> , Neural trajectory lengths.....   | 50 |
| <b>Figure 3.6</b> , Intraspinal neural trajectories.....   | 51 |
| <b>Figure 3.7</b> , Spinal spiking activity induced by concurrent cutaneous nerve stimulation....  | 52 |
| <b>Figure 3.8</b> , Proprioceptive afferent volley peak-to-peak amplitude suppression.....   | 53 |



|   |    |
|---|----|
| <b>Figure 3.9</b> , Peak-to-peak amplitude suppression of spinal cord grey matter response fields.....  | 54 |
| <b>Figure 3.10</b> , Multiunit activity.....  | 55 |
| <b>Figure 3.11</b> , Somatosensory cortex evoked potentials and cortical spiking activity.....  | 57 |
| <b>Figure 4.1</b> . Neuroscience-driven development of a biomimetic neuroprosthetic device.....   | 65 |
| <b>Figure 4.2</b> . Biomimetic neurostimulation patterns designed using a realistic in-silico model of foot sole afferents (FootSim).....             | 73 |
| <b>Figure 4.3</b> . Purposely designed experiments to study neural dynamics through neurostimulation.....   | 74 |
| <b>Figure 4.4</b> Neural response on biomimetic stimulation is more similar to the response to natural touch than to tonic stimulation.....           | 76 |
| <b>Figure 4.5</b> . Synchronization of the neural activity evoked in the spinal cord.....   | 78 |
| <b>Figure 4.6</b> Biomimetic neurostimulations evoke more natural perceptions in implanted humans than non-biomimetic approaches.....                 | 79 |
| <b>Figure 4.7</b> Biomimetic neurostimulation elicits more natural sensations than non-biomimetic approaches in Subject 3.....                        | 80 |
| <b>Figure 4.8</b> Electrically-evoked sensation naturalness related to different projected fields location.....                                       | 81 |
| <b>Figure 4.9</b> Real-time biomimetic neural feedback allows for higher speed and lower cognitive workload while walking.....                        | 82 |
| <b>Figure 4.10</b> Walking speed baseline in the Cognitive Dual Task (CDT).....   | 83 |
| <b>Figure 5.1</b> . FootSim possible contribution to biomimetic stimulation patterns for tactile feedback restoration in future neuroprosthetics..... | 90 |

## **List of tables:**

|   |    |
|---|----|
| <b>Table 1.1</b> , Results with different sensory encoding approaches.....                                | 11 |
| <b>Table 1.2</b> , Review of the reported sensations in examined studies with electrical stimulation..... | 12 |
| <b>Table 4.1</b> . Participants' demographics.....  | 68 |

# Chapter 1

## General introduction

*"Science is magic that works."  
Kurt Vonnegut*

## **1.1 Context**

Limb amputation is a deeply impactful event that significantly alters patients' well-being and diminishes their overall quality of life. Approximately 87 thousand patients per year in European Union (The Global Lower Extremity Amputation Study Group and Unwin 2002; Moxey et al. 2011), and 150 thousand in the United States (Dillingham, Pezzin, and Shore 2005) undergo a lower extremity amputation.

## **1.2 Limitations of neuroprosthetic devices that do not provide sensory feedback**

Somatosensory feedback from the periphery to the brain is a crucial aspect of motor control and coordination. Currently available prostheses in the market are passive devices that lack sensory feedback, depriving users of the ability to explore their environment and perceive sensations from the periphery. This limitation leads to reduced confidence in prostheses, hindering walking pace, and contributing to the development of standing and walking asymmetry (Nolan et al. 2003). These issues are also associated with increased metabolic cost during daily activities (Robert L. Waters and Mulroy 1999), leading to elevated physical and mental fatigue. Furthermore, these conditions are connected to a higher risk of heart failure (R. L. Waters et al. 1976). Due to the inability to detect obstacles with their prostheses, amputees are more prone to falls (W. C. Miller, Speechley, and Deathe 2001). The absence of sensory feedback results in altered integration of prostheses in body perception (Horgan and MacLachlan 2004), leading to a diminished sense of embodiment, mental exhaustion (Heller, Datta, and Howitt 2000), and ultimately, low acceptance of the prostheses (Makin, De Vignemont, and Faisal 2017). Additionally, the lack of physiological feedback from the limb can contribute to phantom limb pain, experienced by approximately 60% of lower limb amputees (Limakatso et al. 2020; Flor, Nikolajsen, and Staehelin Jensen 2006).

Considering the mentioned factors, the implementation of artificial somatosensory feedback in a prosthetic leg holds the potential to enhance prosthesis functionality and alleviate phantom limb pain and emerges as a crucial and unresolved clinical requirement.

## **1.3 Somatosensory feedback**

Somatosensory feedback is a remarkable aspect of our sensory system, allowing us to experience the world through touch and proprioception. It enhances our physical interactions, contributes to our emotional well-being, and forms a crucial part of our overall perception of self and the environment. It encompasses the complex network of receptors, nerves, and brain pathways that allow us to perceive and interpret tactile information, enabling us to interact with the world in a meaningful way. It plays a vital role in our daily lives. It allows us to perceive and manipulate objects with precision, providing essential feedback about their properties such as texture, temperature, and shape. It also contributes to our awareness of our body's position and movement, facilitating coordination and balance.





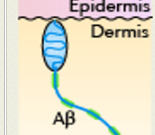
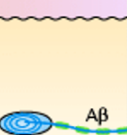
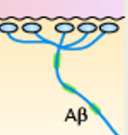
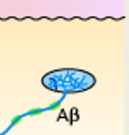
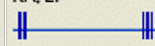



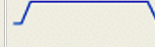
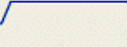
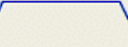
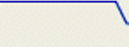

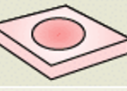


Optimally, neuroprosthetic device would possess the capability to evoke authentic tactile or proprioceptive sensations by transmitting intricate signals to the nervous system, mimicking the signals generated by receptors in the skin, muscles, and joints.

## 1.3.1 Natural sensors detecting and transmitting somatosensory feedback

### 1.3.1.1 Touch sensation

Touch sensation, also known as tactile perception, is the ability to perceive and interpret physical contact and pressure on the skin.

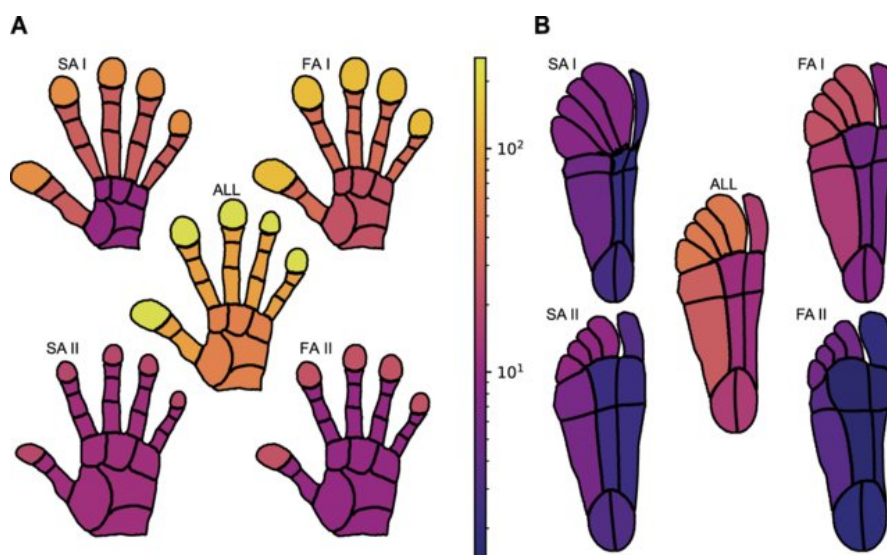
Stimulus detection starts with the specific natural sensors called mechanoreceptors. They are sensitive to mechanical stimuli, such as pressure, vibration, stretching, and deformation. There are four types of mechanoreceptors located in the glabrous skin of the hand palm (Knibestöl and Vallbo 1970) and foot sole (Kennedy and Inglis 2002), each one specialized for detecting specific aspects of tactile stimuli (**Figure 1.1**) (K. Johnson 2001; Iggo 1977). One type of mechanoreceptor is the Merkel cell, also known as a Merkel disc. Merkel cells respond to light touch and are responsible for detecting fine details and textures. Another type is the Meissner's corpuscle, particularly sensitive to gentle touch and low-frequency vibrations. They are detecting the initial contact with an object and provide us with information about its shape, movement, and texture. Pacinian corpuscles are mechanoreceptors located in the deep layers of the skin. They respond to rapid changes in pressure and vibrations. Pacinian corpuscles are responsible for detecting strong or sudden pressure. Ruffini endings are another type of sensors that detects stretching and sustained pressure. They are located in the deeper layers of the skin and respond to prolonged contact or continuous pressure. Ruffini endings play a role in perceiving the skin's deformation and contribute to our sense of skin tension and shape (K. Johnson 2001).

| Receptor subtype     | Meissner corpuscle   | Pacinian corpuscle   | Merkel cell-neurite complex  | Ruffini corpuscle  |
|----------------------|--|--|--|--|
| Skin stimulus        | Dynamic deformation<br> | Vibration<br> | Indentation depth<br> | Stretch<br> |
|                      |                         |               |                       |             |
| Afferent response    | RA, LT<br>              | RA, LT<br>    | SA, LT<br>            | SA, LT<br>  |
| Stimulus             |                         |               |                       |             |
| Receptive field      |                         |               |                       |             |
| Perceptual functions | Skin motion; detecting slipping objects  | Vibratory cues transmitted by body contact when grasping an object                               | Fine tactile discrimination; form and texture perception   | Skin stretch; direction of object motion, hand shape and finger position                         |

**Figure 1.1, Cutaneous afferents.** From top to bottom: Receptor types, typical functions of specific afferent types and their position in glabrous skin tissue, specific afferent responses to the stimuli, stimulus used for classification of sensory afferents (ramp-and-hold stimuli), size of receptive fields and number and position of their hotspots, perceptual functions listed. Adapted from (Delmas, Hao, and Rodat-Despoix 2011) with permission.

Sensory unit refers to the combination of sensory nerve and mechanoreceptor ending. Cutaneous afferents are classified (**Figure 1.1**) based on their ability to respond to sustained tactile stimuli (fast adapting or slowly adapting) as well as their receptive field characteristics (type I or type II) (Knibestöl and Vallbo 1970; Macefield 2005). Fast/rapidly adapting (FA/RA) afferents are sensitive to the change of response and when stimulated with ramp-and-hold stimuli, will respond during on and off phases (Knibestöl 1973; Iggo 1977). Therefore, they are detecting and transmitting vibrations and other dynamic deformations from the periphery (Fig 1.1). On contrary, slow adapting fibers (SA) will fire during the hold part of the stimuli (sustained stimulus) and react to skin stretching (**Figure 1.1**) (Iggo 1977).

Furthermore, cutaneous afferents are classified as type 1 or type 2 based on the characteristic of their receptive fields (Vallbo and Johansson 1984; R S Johansson 1978). Receptive field refers to the area of the body surface or the specific muscle or joint that, when stimulated, activates the corresponding sensory neuron. Based on the size of the receptive field and the number and position of their most sensitive areas, named hotspots, afferents are clustered in two types. Type 1 afferents have smaller receptive fields, with multiple hotspots (Maissner corpuscle - FA1 and Merkel cell - SA1) (Roland S. Johansson and Vallbo 1983; Kennedy and Inglis 2002). In contrary, type 2 afferent innervate one bigger area (Pacinian corpuscle - FA2 and Ruffici corpuscle - SA2) (Kennedy and Inglis 2002).



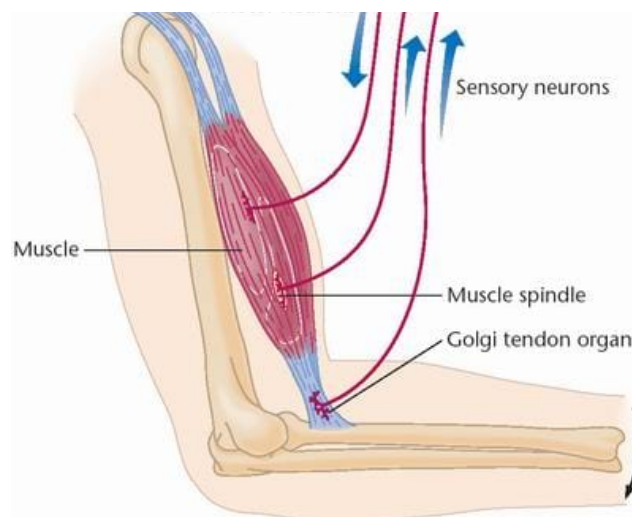
**Figure 1.2, Distribution of specific afferent types (FAI, FAII, SAI, SAI).** A) hand palm B) foot sole. Taken from (Corniani and Saal 2020) with permission.

The cutaneous afferents convey both temporal and spatial characteristics of tactile stimuli (K. O. Johnson and Hsiao 1992). Distribution of mechanoreceptors on the skin surface influences ability to detect small changes in stimulus strength and distinguish spatially distributed points on the skin. Regions of the skin with a higher concentration of afferent fibers, are more likely to detect multiple stimuli through different receptive field areas and activate the units with very low perceptual threshold. Microneurography has been used as a technique to record afferent responses and understand their distribution across the hand palm or sole of the foot. The microelectrodes were inserted into median (for the hand innervation) (R. S. Johansson and Vallbo 1980) or the tibial nerve (for the foot innervation) (Kennedy and Inglis 2002) and the responses on mechanical stimuli of single units were recorded. While in the hand whole afferents are distributed following the same way - number of mechanoreceptors increase from the hand palm to the finger tips (**Figure 1.2a**), the distribution of afferent in the foot sole is slightly different and innervation densities also

are much lower on the foot than on the hand (Corniani and Saal 2020). The foot displays medial-lateral increase in the density of afferents (**Figure 1.2 b**), with the FA1 units being the most prevalent (Strzalkowski et al. 2018). More details about the distribution and the role of afferents in the foot sole are given in the Chapter 2.

### 1.3.1.2 Proprioception

Proprioception is the sense that allows us to perceive the position, movement, and orientation of our body parts in space (Tuthill and Azim 2018). It is essential for coordinating and controlling our movements, maintaining balance, and interacting with our environment. Proprioceptors are natural sensory receptors that provide information necessary for creating sense of proprioception. They are located in our muscles, tendons, joints, and inner ear. Proprioception is the sense that allows us to perceive the relative positions of our body parts and the effort required to move them. It plays a crucial role in coordinating and controlling movements (Ziaul Hasan 1992; Z. Hasan and Stuart 1988). Major proprioceptors important for the motor control are muscle spindles and Golgi tendon organs (**Figure 1.3**), connected to three main types of proprioceptive fibers. Muscle spindles are specialized sensory receptors located within the muscle fibers. They are sensitive to changes in muscle length (type Ia fibres and type II fibres) and the rate of change (type Ia fibres), which helps in detecting muscle stretch and initiating reflexes to maintain muscle tone and control movement. Golgi tendon organs (Type Ib fibres) are found at the junction of muscles and tendons. They are sensitive to changes in muscle tension or force. When the tension in a muscle exceeds a certain threshold, Golgi tendon organs send signals to the central nervous system to inhibit muscle contraction, preventing excessive force and potential injury.



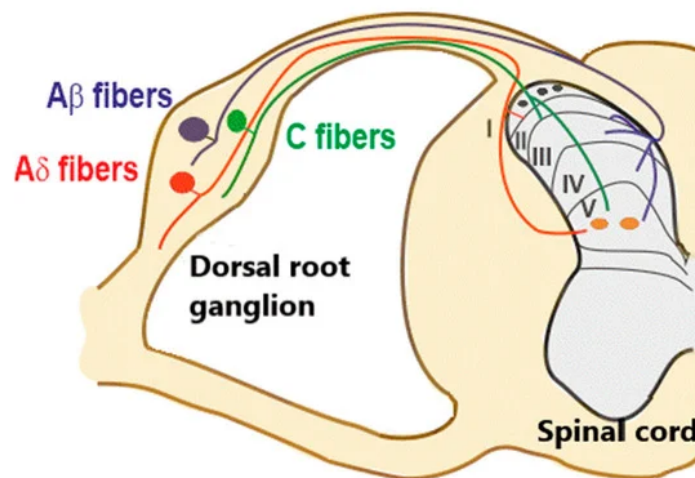
**Figure 1.3, Major proprioceptors.** Muscle spindles and Golgi tendon organs are most important proprioceptors for motor control transmitted by three types of sensory afferents. Adapted from ("Postural Control Part 1 - Proprioception," n.d.) with permission.

### 1.3.1.3 Neural pathways: from detecting stimulus on the periphery to perceiving sensation

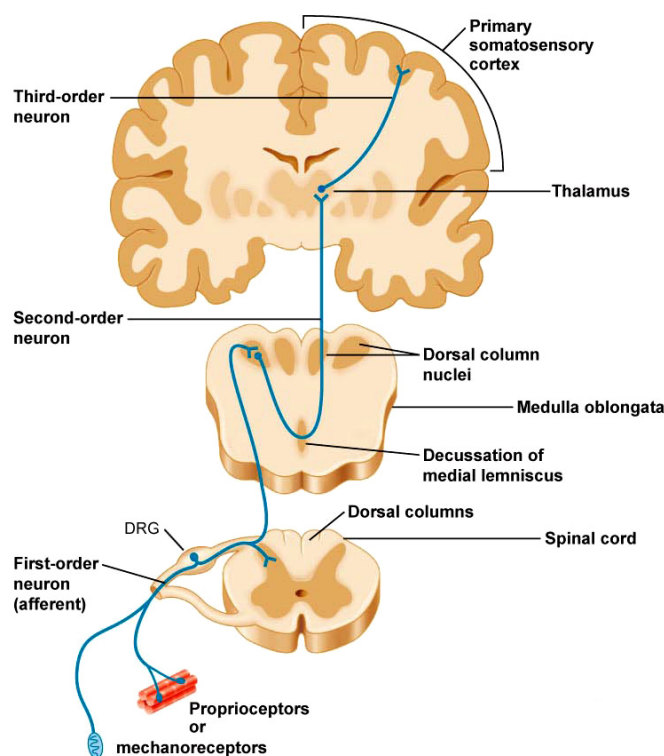
The process of transmitting stimuli from the periphery to the somatosensory cortex involves several stages (Abraira and Ginty 2013). Specialized sensory receptors located in the skin, muscles, tendons, and joints, described in previous sections, detect various sensory information. When these receptors are stimulated, they generate electrical signals called action potentials. These signals are transmitted by the afferent fibers. These signals travel



along afferent nerve fibers, which enter the spinal cord. These fibers are pseudo-unipolar, their somas are located in dorsal root ganglion (DRG), one end is connected to the receptors on the periphery and the other end enters the dorsal horn of spinal cord where they interact with interneurons (**Figure 1.4**).



**Figure 1.4, Afferent fibers projecting from the periphery to the spinal cord.** Somas of pseudo unipolar afferent fibers are located in dorsal root ganglion. One end of the fibers is connected to the receptors on the periphery, while the other end projects to the laminae in dorsal horn of spinal cord gray matter. Taken from (Comitato and Bardoni 2021) with permission.



**Figure 1.5, Touch and proprioception pathways.** First-order neurons transmit the information from the periphery to the spinal cord and through the ascending pathways to the dorsal column nuclei. Second-order neuron carries the information to the thalamus where the information is transmitted to the third-order neuron that brings the sensory signal to the somatosensory cortex. Taken from ("The Sense of Touch," n.d.) with permission.

From the spinal cord, an ascending pathway carries the information to the dorsal column nuclei, which refers to cuneate nucleus and gracile nucleus where the information from the upper and lower extremities arrives, respectively (**Figure 1.5**). From there, the second-order

neuron sends the information to the thalamus, which acts as a relay station. The thalamus then sends the processed sensory information to the primary somatosensory cortex in the parietal lobe through the third-order neuron (**Figure 1.5**). In the primary somatosensory cortex, the sensory information is further processed, integrated with other sensory inputs, and interpreted, allowing for the perception of touch, pressure, temperature, and proprioception. The somatosensory cortex also plays a crucial role in generating appropriate motor responses and integrating sensory information with higher-order cognitive processes.

## 1.4 Neurostimulation technologies for restoring somatosensory feedback

*Segments of this chapter are taken and adapted from: Katic, Natalija, Giacomo Valle, and Stanisa Raspopovic. 2022. "Modeling of the Peripheral Nerve to Investigate Advanced Neural Stimulation (Sensory Neural Prosthesis)." In Handbook of Neuroengineering, edited by Nitish V. Thakor, 1–30. Singapore: Springer Singapore. [https://doi.org/10.1007/978-981-15-2848-4\\_100-1](https://doi.org/10.1007/978-981-15-2848-4_100-1)*

Neuroprosthetics are implantable devices designed to replace or improve the function of a disabled part of the nervous system (Borton et al. 2013). This technology is relatively recent, as the first neuroprosthetic device successfully implanted was a cochlear implant in 1957 (Eisen 2003). Since then, such approach has been expanded to many different applications, among which sensorimotor prosthetics (S. Raspopovic et al. 2014; S. N. Flesher et al. 2016; Francesco Maria Petrini, Valle, et al. 2019), motor prosthetics (Brand et al. 2012; Collinger et al. 2013) and cognitive prosthetics (Andersen, Hwang, and Mulliken 2010).

Restoring sensory feedback to the prosthesis of amputees, is of a paramount importance for future improvements. An ideal device should be able to elicit natural sensations of touch and proprioception that are naturally perceived by the intact limb, by delivering to the nervous system the complex signals closely resembling the information produced by natural sensors, that would be properly interpreted in somatosensory cortex.

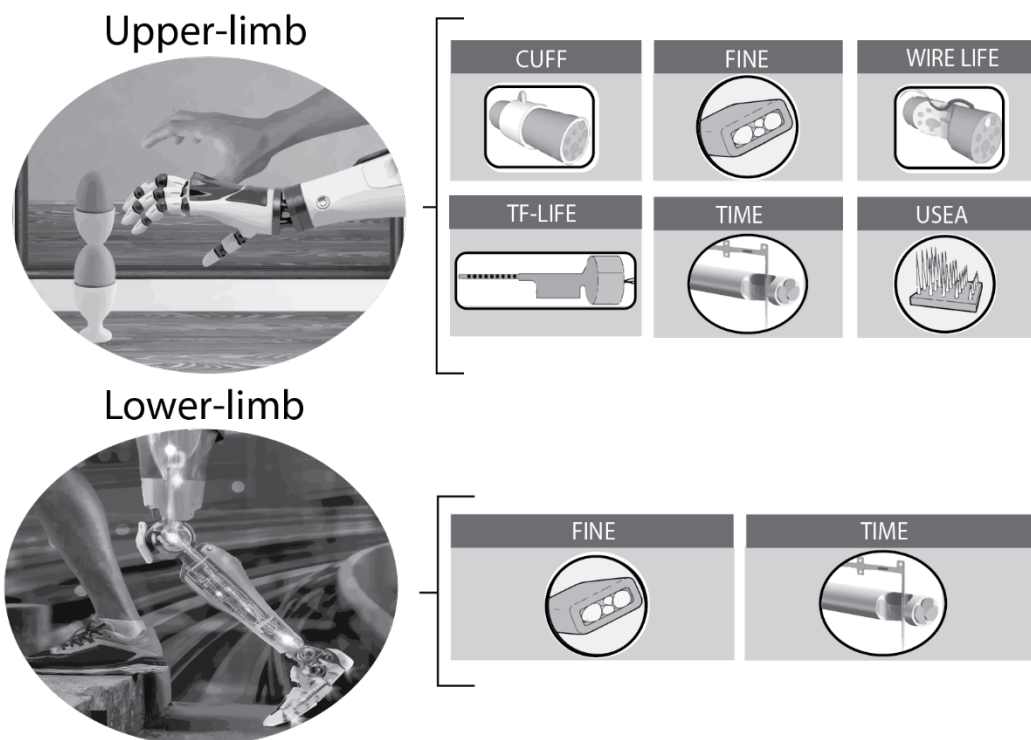
### 1.4.1 Neuromodulation devices

Different approaches have been developed to restore sensory feedback both in upper and lower limb amputees (**Figure 1.6**). Novel surgery techniques (Kuiken et al. 2007; Marasco et al. 2011; Hebert et al. 2014; Clites et al. 2018) and non-invasive methods (Rusaw et al. 2012; Crea et al. 2017; D'Anna et al. 2017; 2019; Dietrich et al. 2018; Osborn et al. 2018; Marasco et al. 2018) were extensively tested. In the last decades, neuroprosthetics for the peripheral nerve have also been developed to a very mature stage, close to the clinical translation. Indeed, several research groups have shown the potential of direct nerve stimulation to restore somatotopic sensations referred to the phantom hand after upper limb amputation by means of implantable electrodes (Navarro et al. 2005) being directly connected to afferent fibers of peripheral nerves (Rossini et al. 2010; Horch et al. 2011; S. Raspopovic et al. 2014; M. Ortiz-Catalan, Hakansson, and Branemark 2014; Daniel W. Tan et al. 2014; Oddo et al. 2016; Davis et al. 2016; E. L. Graczyk et al. 2016; G. Valle et al. 2018; Francesco M. Petrini et al. 2019; Giacomo Valle et al. 2018b). Restoring sensory feedback using somatosensory neuroprostheses (**Figure 1.6**) improved prosthesis control (Daniel W. Tan et al. 2014; Francesco M. Petrini et al. 2019; Francesco Clemente et al. 2019; Giacomo Valle et al. 2018b),



prosthesis embodiment (Rognini et al. 2018; Page et al. 2018; Giacomo Valle et al. 2018b), prosthesis time use (Emily L. Graczyk et al. 2018), visuo-haptic integration (Risso et al. 2019), reduction of phantom limb abnormal representations (Rognini et al. 2018; Emily L. Graczyk et al. 2018; Giacomo Valle et al. 2018b) and phantom limb pain (Page et al. 2018; Granata et al. 2018; Francesco M. Petrini et al. 2019) even in long-term applications (Daniel W. Tan et al. 2014; Francesco M. Petrini et al. 2019). Similar approach held the promise to help also in the case of the lower limb amputation. In humans different types TIME (Francesco Maria Petrini, Bumbasirevic, et al. 2019; Francesco Maria Petrini, Valle, et al. 2019) and FINE (Charkhkar et al. 2018) electrodes were successfully tested for restoring sensations from phantom leg and foot.

The use of neural sensory feedback in lower-limb amputees resulted in spatially selective and distinct sensations of touch, pressure, and vibration. It enabled users the recognition of prostheses movement and avoidance of the obstacles. Moreover, patients were able to walk and climb the stairs faster and experience the reduced cognitive effort needed for daily tasks (Francesco Maria Petrini, Bumbasirevic, et al. 2019). That lead to overall strong health benefits, higher confidence in prostheses and therefore increased acceptance of the device.

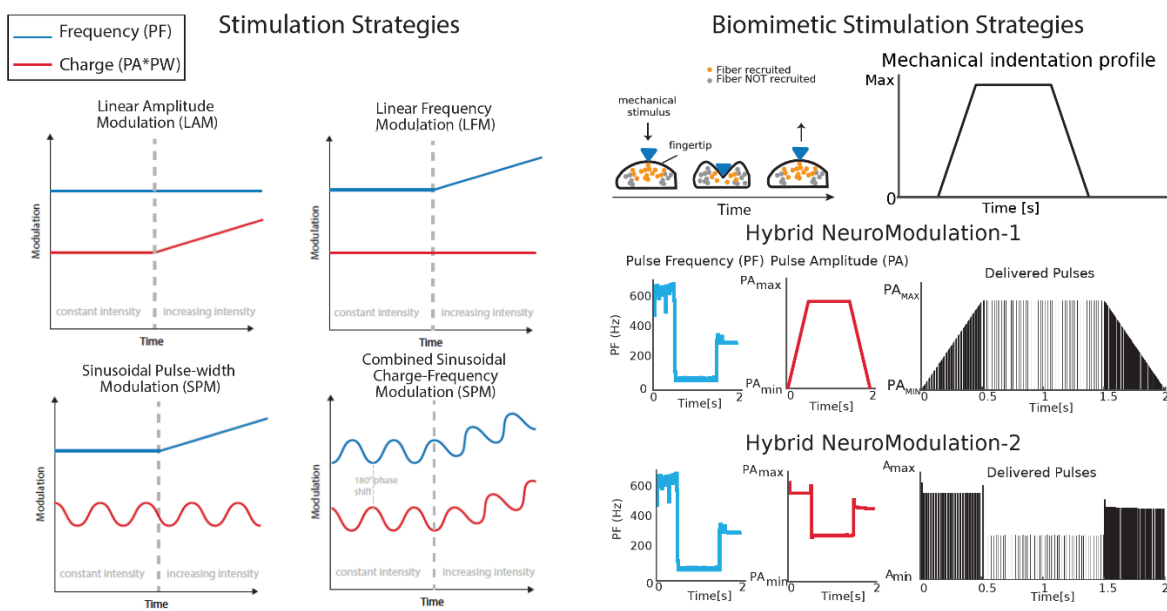


**Figure 1.6 Somatosensory Neuroprostheses.** The different approaches for targeting the peripheral nervous system in order to create a connection between the prosthesis and the sensory system are presented. Both the most effective approaches for upper and lower-limb amputees tested in humans are shown. Adapted from (Katic, Valle, and Raspopovic 2022) with permission.

### **1.4.2 Encoding strategies: Lack of natural, physiologically plausible touch**

The process of restoring sensory perception through electrical stimulation involves inducing action potentials in the existing axonal membranes using external electrical stimuli. It is crucial to design the stimulation in a manner that the brain perceives it as originating from a genuine sensory receptor, aligning with the response characteristics

observed in natural receptors mentioned earlier. Research efforts were firstly oriented to study the biocompatibility and basic functionality (Navarro et al. 2005; Wurth et al. 2017) of the proposed devices, however, the need for an exhaustive understanding of the interaction between implanted electrodes and the response of the neural tissue became evident (McIntyre and Grill 2001). This is due to the fact that neuroprostheses can stimulate by a range of different values for frequency, pulse width and amplitude, delivered through multiple active sites (ASs), located in various positions within the nervous system (Merrill, Bikson, and Jefferys 2005) (**Figure 1.7**). The proper selection of all these parameters contributes to a success of a neuroprosthetic device, and this high-dimensional problem is difficult to address by using empirical, experiment-based knowledge. Instead, computational models, being founded on precise physical knowledge of the problem, are better candidates to address the aforementioned questions.

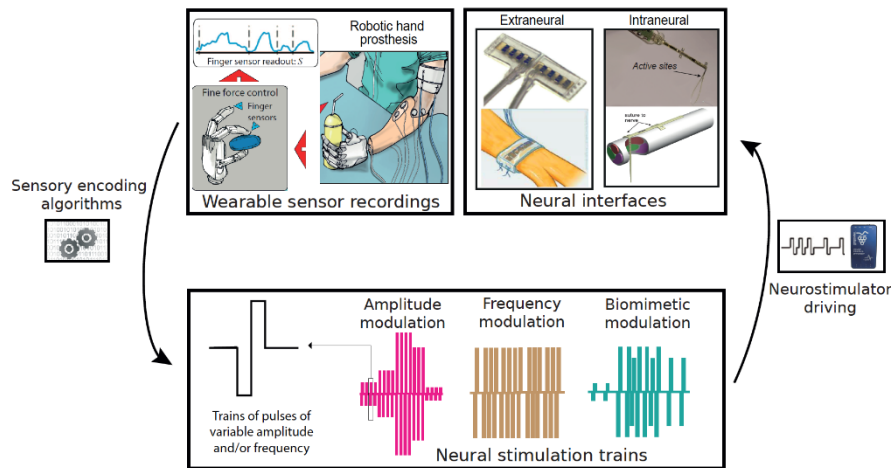


**Figure 1.7 Different sensory encoding strategies.** The neural stimulation can be modulated in different ways in order to encode as many information as possible to patient. In particular, the modulation of charge and frequency were presented in the past as the most promising approaches to encode sensory information. More recently more sophisticated algorithms (as the biomimetic stimulation strategies) have been presented. Taken from (Katic, Valle, and Raspopovic 2022) with permission.

Indeed, in the recent past, a major effort has been dedicated to optimizing the strategies adopted to convey sensory information from the prostheses to amputees. Different encoding strategies have been used to translate the readout of sensors embedded or added into the prosthesis into stimulation parameters (the amplitude, the pulse-width, the frequency and duration of pulse trains) (**Figure 1.8**).

The linear modulation of the injected charge (S. Raspopovic et al. 2014; M. Ortiz-Catalan, Hakansson, and Branemark 2014; Daniel W. Tan et al. 2014; Daniel W Tan et al. 2015; E. L. Graczyk et al. 2016; Francesco M. Petrini et al. 2019) or pulse frequency (G.S. Dhillon and Horch 2005; Horch et al. 2011; Clark et al. 2014; Davis et al. 2016; E. L. Graczyk et al. 2016) have been adopted to translate sensor information into neural modulation. Graczyk and collaborators showed that both the direct neural modulation of charge (i.e., the amplitude or the pulse duration) and of frequency similarly controlled the intensity of the evoked sensations reported by the subjects (E. L. Graczyk et al. 2016; G. Valle et al. 2018). This outcome is in accordance with the physiology of afferent fibers (according to the population

model (Muniak et al. 2007; Stanisa Raspopovic et al. 2017), which deliver information about the intensity of a sensation to the brain through population recruitment (i.e., more spiking fibers) or changes in firing activity (Poulos et al. 1984; Muniak et al. 2007; Pasluosta, Kiele, and Stieglitz 2018). Recruitment and firing activity are controlled by the modulation of the amplitude and frequency of stimulation, respectively.



**Figure 1.8 Contact with an object produces temporal patterns of pressure on a sensor at the fingertip of the prosthesis.** The sensor output is used as input to the sensory encoding algorithms. These functions indicate how to modulate frequency and/or amplitude to produce a certain pattern of stimulation. Stimulation trains are sent in real-time to a neurostimulator and are injected into the nerve by means of a neural interface. The outcome is that the prosthetic user can perceive sensation referred on the phantom limb in real-time. Taken from (Katic, Valle, and Raspopovic 2022) with permission.

The natural touch coding and the relationship between natural sensors and neural activity is more complex than those presently used in sensory neuroprosthetics. Indeed, the quality of the evoked percepts during peripheral nerve stimulation is not very natural (Daniel W. Tan et al. 2014; Giacomo Valle et al. 2018b). All the mechanoreceptors fire differently according to the stimulus features encoding different tactile information (Roland S. Johansson and Flanagan 2009). Ideally, neural stimulation should be able to provide sensory feedback that is functionally effective and highly natural, as the naturalness of the feedback plays a pivotal role in prostheses acceptance (Saal and Bensmaia 2015).

In the recent past, studies presented more complex stimulation approaches (Daniel W. Tan et al. 2014; Pasluosta, Kiele, and Stieglitz 2018) to encode tactile information using neural stimulation. In particular, the strategies that resemble the natural tactile coding are called ‘biomimetic’ (Saal and Bensmaia 2015; Okorokova, He, and Bensmaia 2018). Saal et al. developed a model (TouchSim) able to reproduce nerve activation patterns of the multifaceted mechanics of the skin and mechano-transduction (Saal et al. 2017). This model was implemented in a bidirectional hand prosthetics and test in a transradial amputees (Giacomo Valle et al. 2018b). In particular, the model was used to simulate the response of a peripheral nerve given a mechanical stimulus applied on the hand, and then this information was used for stimulating the nerve to restore a natural sensory feedback. The results showed that biomimetic stimulation was able to elicit more natural sensation than previous presented strategies. Moreover, this approach improved the gross manual dexterity of the subjects during functional task (F. Clemente et al. 2016) while maintaining high levels of manual accuracy and also improved prosthesis embodiment, reducing abnormal phantom limb perceptions (“telescoping effect (Rognini et al. 2018)”).

These outcomes show that sophisticated and biomimetic encoding approaches need to be used to restore more natural and useful sensory feedback and open up new opportunities for the extensive use of models for the neuroprosthetic technologies with disabled people (Table 1.1).

**Table 1.1 Results with different sensory encoding approaches.** Taken from (Katic, Valle, and Raspopovic 2022) with permission.

| NEURAL STIMULATION APPROACH             | SENSATION NATURALNESS | FUNCTIONAL BENEFITS | COGNITIVE BENEFITS | SENSITIVITY |
|---|-----------------------|---------------------|--------------------|-------------|
| Linear Amplitude Modulation (LAM)       | LOW                   | HIGH                | HIGH               | HIGH        |
| Linear Frequency Modulation (LFM)       | LOW                   | HIGH                | HIGH               | LOW         |
| Sinusoidal Pulse-Width Modulation (SPM) | HIGH                  | HIGH                | MEDIUM             | HIGH        |
| Biomimetic Neuro Modulation (BNM)       | HIGH                  | HIGH                | HIGH               | MEDIUM      |

Our understanding of tactile encoding mechanisms is limited due to the constraints of electrophysiological recordings, which can only detect responses from a small number of units at a time. As a result, we lack information about how the entire population of fibers on the surface reacts to specific stimuli. Moreover, techniques like microneurography require the subject to remain still, making it impractical to study neural responses in daily living situations. This hinders our ability to fully comprehend the role of different afferent classes and resolve the ongoing debate in the literature.

Previously, it was believed that each afferent class carries information about different stimuli (K. Johnson 2001), and the perception quality depended on the type of mechanoreceptor. However, recent experimental evidence has shown that many natural stimuli simultaneously excite multiple sensory types (Saal and Bensmaia 2014) and that the information carried by different unit classes is merged in the cortex. Computational modeling also supports these findings (Saal, Harvey, and Bensmaia 2015) and demonstrates that a population coding is crucial for the information processing of tactile sensation (Corniani et al. 2022).

Improvement in restoring somatosensory feedback lies in developing biomimetic stimulation strategies. Progress rely on a computational understanding of the transduction from forces acting on the foot sole to realistic neural responses. As a future step we believe that there is a need for developing a model that would define the stimulation biomimetic strategy based on the responses of multiple afferents from the foot sole and make this kind of models much more usable. Moreover, efforts need to be made for exploring the algorithms that translate the simulated activation of populations of sensory units into biomimetic patterns (Okorokova, He, and Bensmaia 2018) suitable for integration into bionic prostheses.

### **1.4.3 Touch, but not the proprioception.**

Accurate proprioceptive information is critical to achieve precise control of robotic prosthetics. Following the first works (Navarro et al. 2005) in animals, multiple independent clinical studies showed that electrical stimulation of peripheral sensory afferents through

epineural(D. W. Tan et al. 2014) and intraneural(S. Raspopovic et al. 2014; Davis et al. 2016; Francesco Maria Petrini, Bumbasirevic, et al. 2019; Francesco Maria Petrini, Valle, et al. 2019; Giacomo Valle, Saliji, et al. 2021) nerve stimulation, non-invasive transcutaneous stimulation (D’Anna et al. 2017), and even dorsal root stimulation (Chandrasekaran et al. 2019) could elicit localized and graded somato-sensations on the missing limb of people with amputations. In contrast, reports on the ability to elicit graded and controllable proprioception have been remarkably rare (Table 1.2). So, why is it that after decades of research in multiple independent clinical trials, reports of controlled proprioceptive sensations have been so scarce?

**Table 1.2, Review of the reported sensations in examined studies with electrical stimulation.** Peripheral nerve stimulation of upper-limb amputees using CUFF(Max Ortiz-Catalan et al. 2020; Zollo et al. 2019), FINE(D. W. Tan et al. 2014; Emily L Graczyk et al. 2018), TIME(Strauss et al. 2019; Francesco M. Petrini et al. 2019), Wire LIFE(Gurpreet S. Dhillon et al. 2004; Horch et al. 2011; Saal and Bensmaia 2015), tf - LIFE(Zollo et al. 2019; Overstreet, Cheng, and Keefer 2019) and USEA(Davis et al. 2016; George et al. 2019; Wendelken et al. 2017; Saal and Bensmaia 2015) electrodes. Peripheral nerve stimulation with lower-limb amputees using FINE(Charkhkar et al. 2018) and TIME(Francesco Maria Petrini, Bumbasirevic, et al. 2019; Francesco Maria Petrini, Valle, et al. 2019) electrodes

|                         | <b>Included subjects = 35</b> | <b>Common=</b> majority of responding contacts<br><b>Rare=</b> <10% of responding contacts | <b>Graded=</b> Sensation proportional to charge/frequency |
|-------------------------|-------------------------------|--|---|
| <b>Type of percepts</b> | <b>Reported in</b>            | <b>Number of contacts</b>  | <b>Properties</b>   |
| Touch/pressure          | 35/35                         | Common   | Graded/Controllable                                       |
| Tingling/paresthesia    | 22/35                         | Common   | Graded/Controllable                                       |
| <b>Proprioception</b>   | <b>27/35</b>                  | <b>Rare</b>  | <b>Episodic-not quantified</b>                            |
| Temperature             | 4/35                          | Rare   | Episodic-not quantified                                   |
| Pain                    | 3/35                          | Rare   | Episodic-not quantified                                   |

This overwhelming body of experimental evidence (Table 2) comes in stark contrast with intuitive understanding of electrophysiology. Indeed, large-diameter proprioceptive afferents should have the lowest threshold for electrical stimulation of the peripheral nerves. Therefore, they should be the easiest sensory afferents to recruit with neural interfaces(Rattay 1986; Capogrosso et al. 2013; M. A. Schiefer, Triolo, and Tyler 2008; McNeal 1976; Stanisa Raspopovic, Capogrosso, and Micera 2011) before eliciting any cutaneous percept. In fact, every pulse of electrical stimulation recruits myelinated axons with an efficiency that is inversely proportional to the distance from the electrode and directly proportional to the fiber diameter(McNeal 1976). In consequence, since fibers of different diameters are densely packed within nerve fascicles, practical implementation of electrical neurostimulation systems would always result, at least partially, in the recruitment of mixed diameter fiber distributions, hence, different sensory modalities(Capogrosso et al. 2013; Greiner et al. 2021; Stanisa Raspopovic et al. 2012). Therefore, cutaneous receptors are recruited concurrently to larger diameter afferents such as golgi (Ib) and spindle (Ia) afferents (Kibleur et al. 2020). These fibers converge to interneurons in the spinal cord where they undergo the first layer of sensory processing, and project to the gracilis (lower limb) or cuneate (upper limb) nuclei in the medulla oblongata, thalamus and then cortex(Kandel, E., Schwartz, J. & Jessel, T., n.d.). Given the discrepancy between experimental findings and theoretical considerations, we can hypothesize that there exist neurophysiological constraints that prevent the generation of functional proprioceptive percepts.



### 1.4.3.1 Understanding information processing along the somatosensory axes using populational analysis

The inability to properly restore proprioception raises questions about the non-specific recruitment of multiple sensory modalities commonly produced by neuroprosthetic systems. This indiscriminate recruitment may trigger neurophysiological constraints within the network targeted by artificially recruited afferents, which could hinder the neural processing of proprioceptive percepts.

While looking at the single-unit changes can unveil which interneurons are affected, and be the base for setting the hypotheses behind the underlying mechanisms, how different senses will be perceived depend on the complete, integrated processing of the whole neural population. Neurons within a network often work together to generate complex patterns of activity, and understanding these dynamics is crucial for unraveling the underlying mechanisms of information processing, sensory integration, and motor control. Studying the population activity in the spinal cord provides insights into the coordinated dynamics and interactions between different neurons. Moreover, neural activity is subject to variability, noise, and trial-to-trial variability. Single unit analysis may be influenced by the idiosyncrasies of individual neurons, making it harder to generalize the conclusion. Population analysis helps mitigate this issue by considering the collective activity of multiple neurons, which provides a more reliable and robust representation of the underlying neural processes.

Dimensionality reduction can help to capture the variance of high-dimensional neural activity representing the dynamics of an entire population and extract the information of interest while removing the background neural activity. Neural population analysis via neural manifold have been employed to unmask latent cortex dynamics in the context of learning (Perich et al. 2020; Sadtler et al. 2014; Gallego et al. 2017; 2020). Furthermore, this approach was used for understanding and controlling the movement (Gallego et al. 2017; 2018).

These advantages of the neural manifold analysis contribute to a deeper understanding of the functioning of the neural systems and facilitate the development of clinical interventions and neurotechnological applications.

## **1.5 Translational framework for novel sensory encoding strategies**

While the advancements are made in artificial communication with the brain through peripheral nerve stimulation, efforts are still needed for providing a truly natural sensory experience. This limitation has prompted the exploration of new avenues for converting sensory information into neural stimulation patterns, with the ultimate goal of enabling intuitive and authentic sensations. For going one step closer towards it, we need a novel neurostimulation framework for faster, easier and more robust developments. Biomimetic stimulation patterns can involve a range of different values for frequency, pulse width and amplitude. Creating stimulating patterns starting from the modeling output simulating the neural features neural response explaining a specific natural sensation, can be a potential way to slightly lower the complexity of the problem. Moreover, it is anticipated that this form of stimulation would more faithfully replicate the natural behavior. Studies were conducted for coding the touch sensation in somatosensory cortex (Callier, Suresh, and Bensmaia 2019b). However, currently there are no results on testing how the artificially induced stimulation propagates and translates from peripheral through central nervous system. Additionally, it is not known how these stimulation paradigms are processed within the first layers of somatosensory neuroaxis. Lastly, in order to prove a fully beneficial

aspect of biomimetic stimulation, it needs to be validated in humans, testing not only if the perception is more pleasant and natural, but also that the performance during the daily living tasks is improved.

## 1.6 Thesis objectives

Despite that peripheral nerve stimulation have shown promising potential for individuals with sensorimotor deficits, the efforts are still needed to define the proper language to artificially communicate with our nervous system.

The presented research is based on the following hypotheses:

- ❖ H1: Restoring natural sensation from the periphery holds tremendous potential for the application and improved performance of neural prostheses.
- ❖ H2: Defining a proper complex, biomimetic patterns of stimulation is necessary for restoring close-to-natural sensory feedback.
- ❖ H3: Starting from the microneurography recordings of the sensory afferents, it is possible to develop in silico model of foot sole mechanoreceptors that would be able to translate the applied mechanical stimulus into the neural afferent responses.
- ❖ H4: The reasons for certain limitations of neuroprostheses lie in insufficient understanding of the processing of artificially reconstructed sensations.
- ❖ H5: Similarity between natural sensations and sensory information elicited by biomimetic nerve stimulation can be found in analyzing the neural signals in the spinal cord and other segments of the somatosensory system.

The doctoral research fulfilled the expected scientific contributions:

- ❖ Construction of a realistic model of mechanoreceptors on the foot that would adequately imitate the natural activation of nerve fibers depending on the mechanical stimulus applied to the surface of the foot.
- ❖ Defining complex, biomimetic types of stimulation, starting from the outcomes of computational model, that would enable restoring close to natural sensation from the periphery.
- ❖ Analyzing the results of experiments on animals that revealed the reasons for major problems in restoring the sense of proprioception.
- ❖ Analysis of signals from the spinal cord of animals and other structures of the somatosensory system in order to set the hypotheses for possible mechanisms of processing the sensation of touch and proprioception. The results of the study will establish a scientific basis for defining new types of interfaces and methods of stimulation.
- ❖ The analysis of the experimental results in animals that showed that the processing of neural response in the spinal cord and other structures of the sensory system caused by nerve stimulation with some of the biomimetic types of stimulation is more similar to the processing of information caused by natural touch, which confirmed the reasons why the biomimetic type of stimulation causes a feeling closer to natural one.
- ❖ Defining guidelines for the development of new paradigms of stimulation and further improvement of neuroprosthetic design and neuromodulation approaches.

The main results of this theses are published in the following papers and book chapter:

- ❖ Katic, Natalija, Rodrigo Kazu Siqueira, Luke Cleland, Nicholas Strzalkowski, Leah Bent, Stanisa Raspopovic, and Hannes Saal. 2023. "Modeling Foot Sole Cutaneous Afferents: FootSim." *IScience* 26 (1): 105874. <https://doi.org/10.1016/j.isci.2022.105874>
- ❖ Katic Secerovic, Natalija, Josep-Maria Balaguer, Oleg Gorskii, Natalia Pavlova, Lucy Liang, Jonathan Ho, Erinn Grigsby, et al. 2021. "Neural Population Dynamics Reveals Disruption of Spinal Sensorimotor Computations during Electrical Stimulation of Sensory Afferents." Preprint. *Neuroscience*. <https://doi.org/10.1101/2021.11.19.469209>.
- ❖ Katic, Natalija, Giacomo Valle, and Stanisa Raspopovic. 2022. "Modeling of the Peripheral Nerve to Investigate Advanced Neural Stimulation (Sensory Neural Prosthesis)." In *Handbook of Neuroengineering*, edited by Nitish V. Thakor, 1-30. Singapore: Springer Singapore. [https://doi.org/10.1007/978-981-15-2848-4\\_100-1](https://doi.org/10.1007/978-981-15-2848-4_100-1).

## 1.7 Structure of the thesis

This dissertation is divided into five chapters.

The first chapter (Chapter 1) represents the general introduction of the thesis. It covers the motivation for the study, current state-of-the art, scientific and technological gaps and sets the main hypotheses and aims of the study.

This doctoral thesis was defined through studies covering three main aims and answering novel research questions, whose findings are presented in the next chapters (chapter 2-4):

- ❖ AIM 1: Developing in silico model of touch (Chapter 2)
  - a) Does the model enable the decoding of afferent activation in dynamic natural situations?
  - b) Can we use the model to define new biomimetic stimulation paradigms?
- ❖ AIM 2: Are there any limiting consequences of invasive neural encoding? (Chapter 3)
- ❖ AIM 3: Developing a novel, translational, multifaced framework for creating and testing biomimetic stimulation paradigms (Chapter 4)
  - a) How are these paradigms encoded in neural response in animals?
  - b) If we integrate these biomimetic paradigms into the neuromodulation device, will it be beneficial for the human usage?
  - c) Will the approach starting from computational modeling of specific behavior, followed with the animal testing and finalized by the human experiments give both scientific and neurotechnological beneficial outcomes?

The last chapter (Chapter 5) underlines the main findings of the theses while putting them in the broader context. Moreover, the limitations of the thesis and its future opportunities are listed as the final conclusive note.



# Chapter 2

## In silico modeling of foot afferents

*“All models are wrong, but some are useful”.*  
George Box

*Adapted from: Modeling foot sole cutaneous afferents: FootSim*

*Katic, Natalija, Rodrigo Kazu Siqueira, Luke Cleland, Nicholas Strzalkowski, Leah Bent, Stanisa Raspopovic, and Hannes Saal. 2023. “Modeling Foot Sole Cutaneous Afferents: FootSim.” IScience 26 (1): 105874. <https://doi.org/10.1016/j.isci.2022.105874>*

While walking and maintaining balance, humans rely on cutaneous feedback from the foot sole. Electrophysiological recordings reveal how this tactile feedback is represented in neural afferent populations, but obtaining them is difficult and limited to stationary conditions. We developed the FootSim model, a realistic replication of mechanoreceptor activation in the lower limb. The model simulates neural spiking responses to arbitrary mechanical stimuli from the combined population of all four types of mechanoreceptors innervating the foot sole. It considers specific mechanics of the foot sole skin tissue, and model internal parameters are fitted using human microneurography recording dataset. FootSim can be exploited for neuroscientific insights, to understand the overall afferent activation in dynamic conditions, and for overcoming the limitation of currently available recording techniques. Furthermore, neuroengineers can use the model as a robust in silico tool for neuroprosthetic applications and for designing biomimetic stimulation patterns starting from the simulated afferent neural responses.

## 2.1 Introduction

Complex sensorimotor integration of foot sole cutaneous feedback is crucial for gait and posture control (Takakusaki 2013; Pearcey and Zehr 2019). If somatosensory feedback is disrupted, postural stability is impaired, as demonstrated by an increase in sway and reduced gait stability in conditions of reduced feedback, such as under local anesthesia (McDonnell and Warden-Flood 2000) or cooling (Bent and Lowrey 2013). Neuropathic conditions such as amputation or severe diabetic neuropathy also result in compromised sensory feedback and motor control (Stanisa Raspopovic 2021). Conversely, gait can be stabilized and sway reduced by the use of balance-enhancing insoles with ridged surrounds if some sensitivity remains (Priplata et al. 2006; S. D. Perry et al. 2008; Christovão et al. 2013) or with neural implants where nerves have been damaged or severed (Stanisa Raspopovic, Valle, and Petrini 2021). Tactile sensibility on the foot sole relies on four classes of myelinated cutaneous afferents that provide information about touch and pressure (Kennedy and Inglis 2002; Strzalkowski et al. 2018). These sensory units carry information to circuits in the spinal cord and further towards the somatosensory cortex. Afferents are classified by the speed with which they adapt to constant stimulation, fast (FA) or slow (SA), and the size of their receptive fields, type 1 (small, with receptors close to the skin surface) and type 2 (large, with receptors embedded deeper in the skin).

Our understanding of how these afferents respond under natural conditions, such as standing and walking, is limited due to technical challenges related to in-vivo electrophysiological recordings from afferent fibers. Microneurography, a technique for recording electrophysiological responses from single fibers in human nerves, is difficult to implement, time-consuming and very unstable (and therefore not practicable in dynamic conditions such as walking and running). Experiments also require participants to remain motionless, so as not to dislocate the recording electrode from the single fiber of interest. Furthermore, the majority of such studies have focused on the glabrous skin of the hand and it is unclear how well these findings would apply to the different mechanical environment of the foot sole. Even though the palmar skin of the hand and the foot sole are innervated by the same classes of receptors, neural coding likely differs between them for a number of reasons. First, the usage of hands and feet differ greatly; while the hand experiences many small and delicate stimuli, such as during precision grips, the foot is usually exposed to a large spatial extent. Such usage differences will affect the nature of the signal being sent to the brain. Innervation densities also vary several-fold and are much lower on the foot than on the hand (Corniani and Saal 2020). The foot also displays an apparent medial-lateral increase in the density of afferents, with the FA1 units being the most prevalent (Strzalkowski et al. 2018), which is not evident on the hand (R S Johansson and Vallbo 1979). Finally, the hardness of the skin differs from the hand and varies considerably by region of the foot sole (Strzalkowski et al. 2015), which affects the propagation of mechanical stimuli and therefore the neural responses.

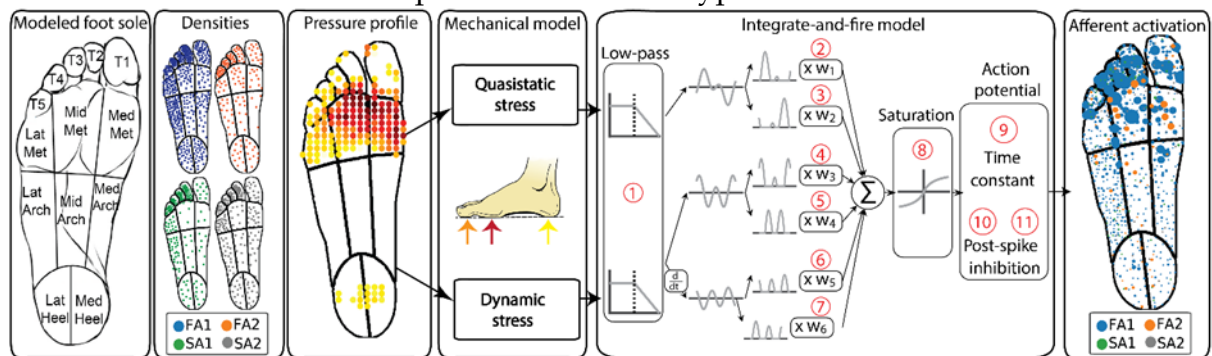
To address the need for a detailed understanding of foot afferent responses during standing and walking, which is impossible to access via existing recording techniques, we constructed a realistic in-silico model of their behavior. The model is based on experimentally recorded spiking responses from cutaneous afferents on the foot sole to arbitrary indentations of the skin. It is inspired by a previously constructed model replicating tactile responses from the hand for three classes of cutaneous afferents (Saal et al. 2017), but adapted to fit the mechanical environment and afferent response properties of the foot. We divided the foot sole into separate regions based on the mechanical properties of the skin and the estimated densities of different afferent classes. In a first step, the model

determines the stresses within the displaced skin arising from contact with an object and how these displacements propagate across it. In a second step, it generates the spiking responses of individual afferents, which are modeled by a set of 11 parameters each that are fit based on single-fiber recordings obtained from the human tibial nerve (Strzalkowski, Ali, and Bent 2017). We validate the obtained results by comparing modeled estimates for firing rates, thresholds and receptive field sizes with the ones recorded experimentally and afferent responses to ramp-and-hold stimuli reported in the literature. Finally, we estimate the population response originating from the foot sole during walking and demonstrate that the model can be used for understanding the activation of sensory units during dynamic conditions, overcoming a considerable limitation of available recording techniques.

## 2.2 Methods

### 2.2.1 FootSim model overview

We developed a model of an entire population of cutaneous afferents in the foot sole that is able to simulate their neural responses to different types of mechanical stimuli.



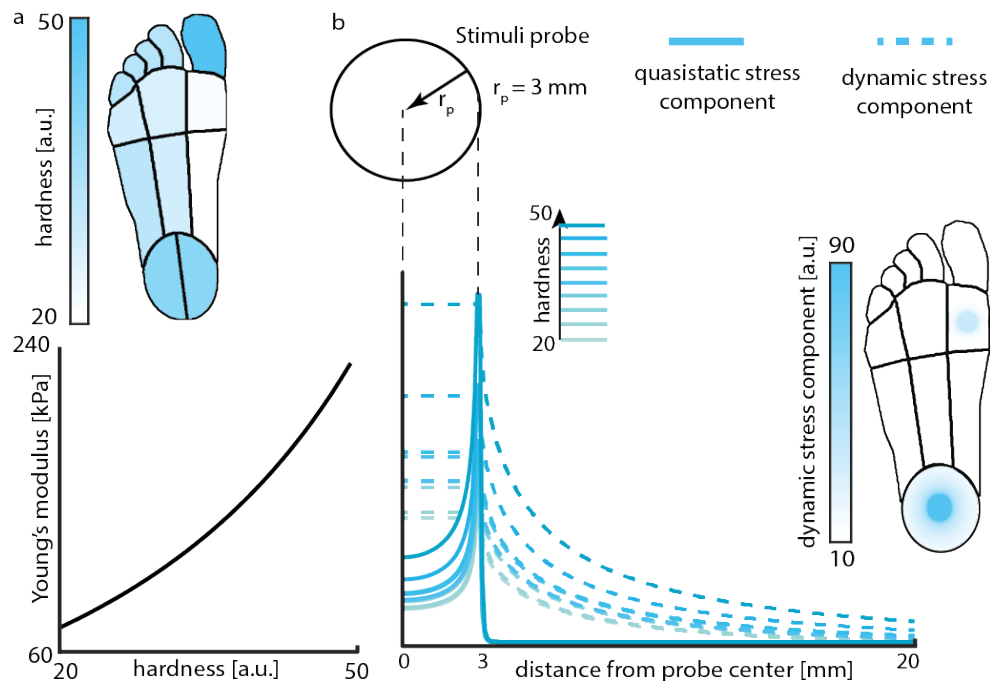
**Figure 2.1. Overview of the FootSim model mimicking the mechanotransduction process.** We divided the foot sole into 13 regions with different mechanical properties and tactile innervation: toes 1-5, lateral/middle/medial metatarsal/arch, and lateral/medial heel (box 1, from the left). We incorporated different densities of specific afferent types (fast adapting and slowly adapting type 1 and 2 – FA1, FA2, SA1, SA2) across regions of the foot sole based on empirically established innervation densities (Strzalkowski, Ali and Bent 2017). Stimuli are represented as spatiotemporal indentation profiles on the foot sole (box 3), creating an input to the mechanical model (box 4), where it is converted into quasistatic and dynamic stresses within the plantar skin at the locations of individual receptors (Saal et al., 2017). Quasistatic stress is associated with local vertical stress while dynamic component represents the pressure component propagated through the skin. Both stress components are passed through firing models (box 5) that simulate single afferent behavior. 11 parameters (1: low pass, 2:7:  $w_1$ - $w_6$ , 8: saturation, 9: time constant, 10,11: post spike inhibition parameters – slow and fast component) are fitted to replicate characteristics of individual afferent classes. As output, the FootSim model creates time-varying firing patterns for the desired afferent population (box 6). Taken from (Katic et al. 2023) with permission.

Taking into account mechanical (Strzalkowski, Mildren, and Bent 2015; Strzalkowski et al. 2015) and innervation properties (Strzalkowski et al. 2018), we divided the foot sole into separate regions (Figure 2.1, box 1 from the left) and included respective densities of different classes of mechanoreceptor afferents (Figure 2.1, box 2). To achieve a higher modularity which would enable easy and fast simulation of different realistic situations, we divided the foot sole into 13 regions which are differentially populated. The depth at which afferents terminate within the skin is set for each mechanoreceptor type and is constant across the foot sole. Tactile stimulation of the foot sole is modelled using a group of circular pins that indent the skin orthogonal to its surface. That is similar to monofilament testing

which is used to determine afferent firing thresholds and map the receptive fields. Mechanical stimuli that a user can apply on the place of interest on the foot sole can be defined in any shape. The indentation of every pin is set independently, such that arbitrary spatiotemporal patterns of indentation can be simulated (**Figure 2.1**, box 3) and given as input to the FootSim model. The FootSim model consists of two parts that jointly capture the complexity of mechanotransduction. The first part corresponds to a mechanical model that computes the deformation of the skin by the applied tactile stimulus (**Figure 2.1**, box 4): the calculated quasistatic stress reflects the perpendicular indentation of the skin, while the dynamic stress component simulates the stimulus propagation across the sole of the foot at higher frequencies. The second part consists of firing models that generate spiking output for individual fibers of different afferent classes based on the time-varying mechanical inputs (**Figure 2.1**, box 5).- Each firing model contains 11 unique parameters. A low-pass filter (parameter 1) reflects the fact that afferents become unresponsive to stimulation above a certain frequency of stimulation, dependent on the afferent class. To provide an acceleration signal we differentiated the dynamic skin response. Three mechanical signals (quasi-static, dynamic, and dynamic derivative) are then split into positive and negative signal contributions and rectified, resulting in six time-varying signals that are multiplied by six weight parameters (parameters 2-7) and summed. Since afferents' neural responses can saturate as a reaction to large skin deflections (Wheat, Salo, and Goodwin 2010), the resulting signal trace is passed through a saturating non-linear function (parameter 8). The resulting time-varying trace represents the input to the component that simulates the generation of the action potential. Its membrane potential decays to its resting value according to a time constant (parameter 9) and a post-spike inhibitory kernel is added to model the refractory period. Post-spike inhibition consists of a fast component (parameter 10), which decays after 4 ms, and a slow component, which peaks after 8 ms and decays completely after 36 ms (parameter 11), inspired by a previous model (Dong et al. 2013). As its final output, the model simulates neural responses of all afferent types innervating the foot sole (**Figure 2.1**, box 6), giving the user information about the type, position and firing pattern of each activated afferent.

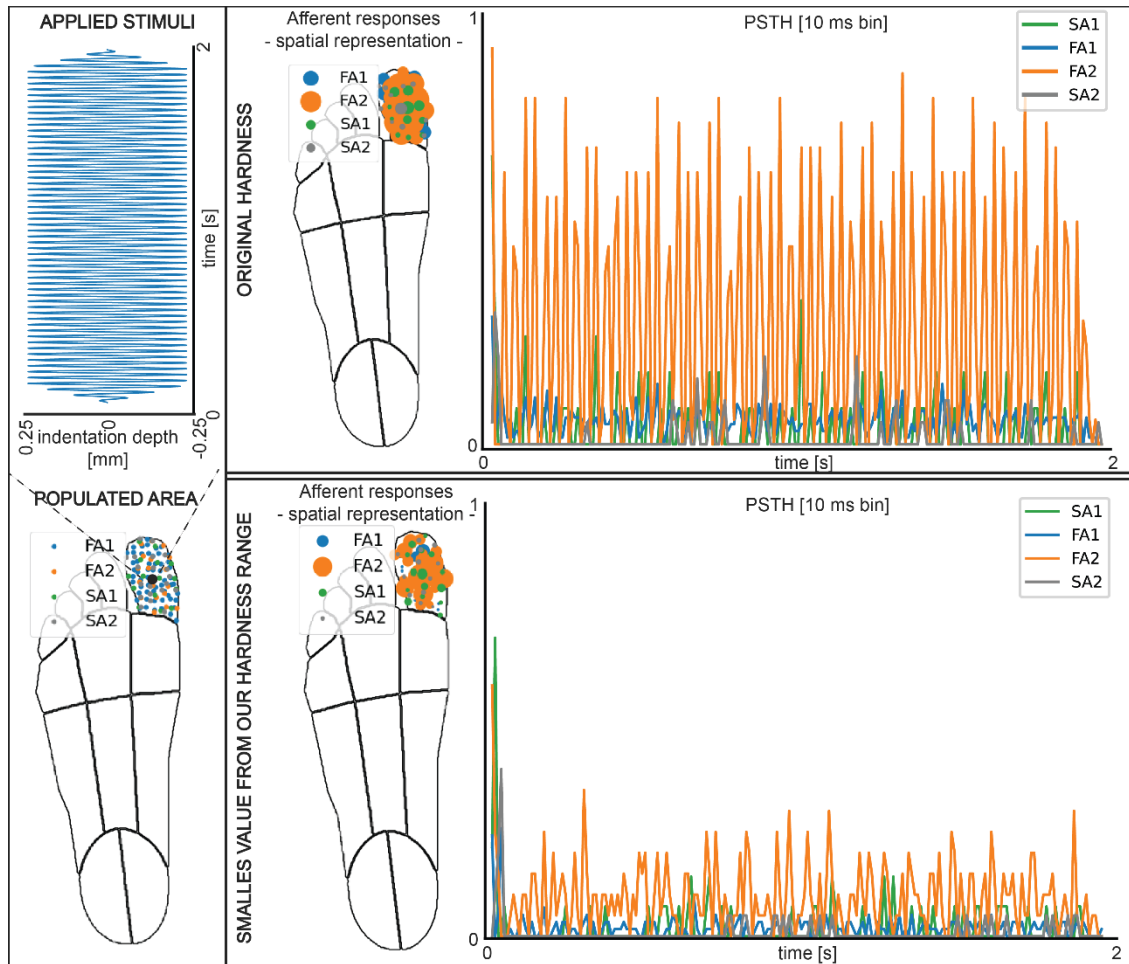
Mechanical properties of the glabrous skin of the foot differ compared to the hand, and also vary considerably across regions of the foot sole. These differences influence the propagation of the stimuli through the skin and consequently the mechanotransduction properties of the hand and foot. The FootSim model incorporates a physically plausible mechanism of dynamic stress propagation (Manfredi et al. 2012), which is similarly used in a previously published model for the hand. Yet there are important changes we implemented, to properly fit the specific properties of the foot sole. Poisson's ratio, a measure that describes the expansion of material in directions perpendicular to the direction of compression, is set as constant for all foot sites, based on previous measurements (Nakamura, Crowninshield, and Cooper 1981). Skin hardness represents how resistant the skin is to material deformation due to the constant compression load. It influences the stiffness, skin resistance to elastic elongation, characterized by Young's modulus of the skin, a mechanical property that defines the relationship between stress ( $\sigma$ ) and strain ( $\epsilon$ ) in the skin. We used experimentally obtained hardness measurements in arbitrary units recorded by a handheld durometer (Rx-1600-OO, with a 2 mm diameter, column-shaped indenter). For every single position of the recorded afferent, a hardness measurement was obtained. We averaged all values from the same foot region (regions defined as in **Figure 2.1**) and included them in the FootSim model. (**Figure 2.2a**, upper part). Based on a transformation appropriate for the type of durometer (Mitchell et al. 2011) we defined realistic values of

Young's modulus (**Figure 2.2a**, lower part). Skin hardness values affect both quasi-static and dynamic stress components, thereby influencing both the local vertical stress based on a quasi-static elastic model of the skin and the mechanical stimulus propagation on the surface of the foot sole. Figure 2.2b shows an example for how these two stress components propagate through the skin when stimuli are applied on regions with different hardness values. The foot representation on the right shows how the dynamic stress component is propagating spatially through the skin when stimuli are applied to the region with the highest hardness value (heel) and with the lowest one (medial arch).



**Figure 2.2 Mechanical model of FootSim simulates skin changes caused by the applied stimuli and its propagation through the sole of the foot.** a) Typical hardness of the skin in different regions of the foot sole (arbitrary units) as experimentally measured and incorporated into the model (upper part). We defined the Young's modulus, describing the stiffness of the skin, as a function of skin hardness (down part). b) We calculated the deflection produced by the applied stimuli. Quasistatic (solid line) and dynamic (dashed line) stress components as a result of sinusoidal stimulation with a circular probe (radius: 3 mm) at 10 Hz and amplitude of 0.25 mm. Different shades of turquoise indicate skin hardness values in different foot regions. Units on the vertical axis are arbitrary. Foot representation on the right indicates the values of dynamic component of stress showing how stress is propagating over the skin depending on the region where stimuli is applied. We used the same stimuli values reported above, but using circular probe of 15mm. Taken from (Katic et al. 2023) with permission.

In the **Figure 2.3** we show the differences in the firing rates spatially presented, and in form of PSTH, which are resulting from the use of different hardness values. It is a straightforward demonstration of the differences induced in the neural responses due to the variability of the hardness values, rather than maintaining them (Saal et al. 2017). We can observe big changes in PSTH of afferent responses, reflecting the influence of the hardness values used.



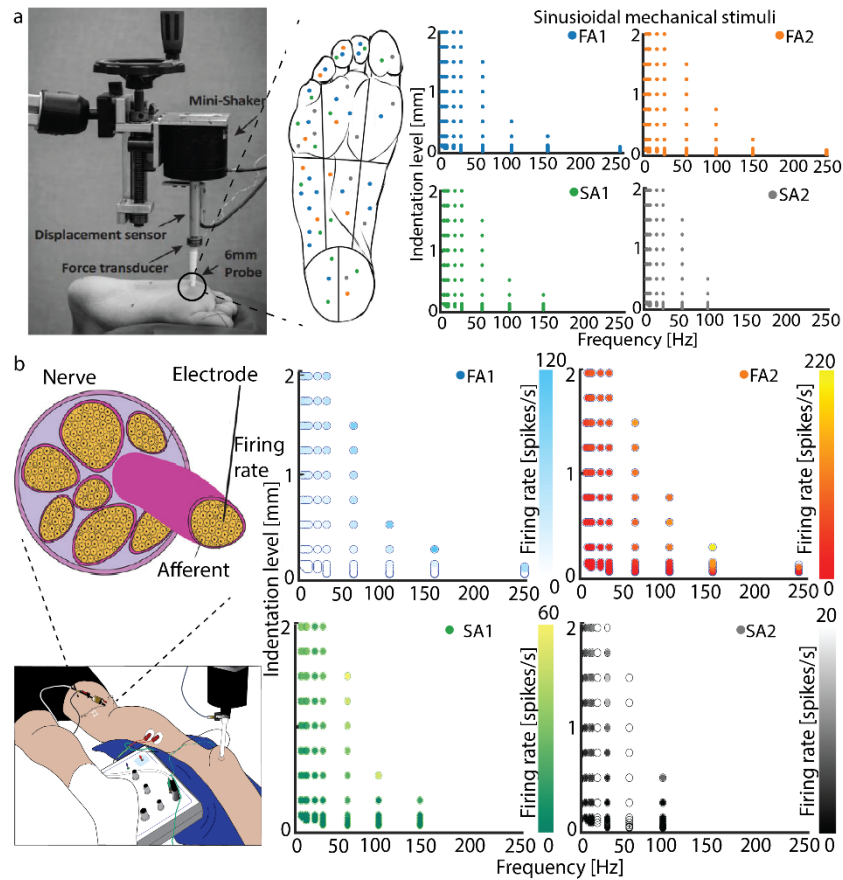
**Figure 2.3, Response of afferents innervating the great toe with different incorporated skin hardness values.** We populated the great toe with the afferents and applied sinusoidal stimuli at the middle point of this area. We show the responses of all afferents within that area when hardness was set to its original value (it is hard- maximum hardness). (left upper part) stimuli applied on the middle of the great toe. (left down part) populated great toe with all types of afferents. (right upper part) afferent responses on the applied stimuli with the high value of hardness – original one reported for the great toe. (right lower part) afferent responses on the applied stimuli with the low value of hardness. The responses are plotted spatially, where the area of each afferent dot corresponds to the firing rate of that afferent, as well as in the form of peristimulus time histogram of activity (PSTH), with a time bin of 10ms. Taken from (Katic et al. 2023) with permission.

### 2.2.2 Fitting model parameters

For fitting the parameter values of individual afferent models, we used the neural activity obtained in a previously published microneurography experiment (Strzalkowski et al., 2017), which we only briefly describe here for the sake of clarity. In short, afferent responses were recorded using 200um tungsten microelectrodes at the level of the popliteal fossa (**Figure 2.4b**, left). During the experiments, sinusoidal mechanical stimuli of varying amplitudes and frequencies were applied to the skin of the foot sole using a 6 mm diameter probe (**Figure 2.4a**, left). In total, 52 tactile afferents terminating in different locations on the foot sole (**Figure 2.4a**, middle) were stimulated using frequency/amplitude combinations that were changing depending on the afferent type (**Figure 2.4a**, right). The obtained dataset used for tuning of parameters contained neural responses from 52 single afferents stimulated by sinusoidal mechanical stimuli. Firing models were fitted to replicate the spiking responses of a single recorded afferent on the applied mechanical stimuli. Each firing model was governed by a set of 11 parameters (Saal et al. 2017). We searched for the best combination of these parameter values by using metaheuristic search algorithm (Abdel-



Basset, Abdel-Fatah, and Sangaiah 2018) that would result with the realistic simulation of afferent neural responses. We excluded from the dataset all afferents that were stimulated experimentally with less than 3 different frequencies (9 of them were discarded).

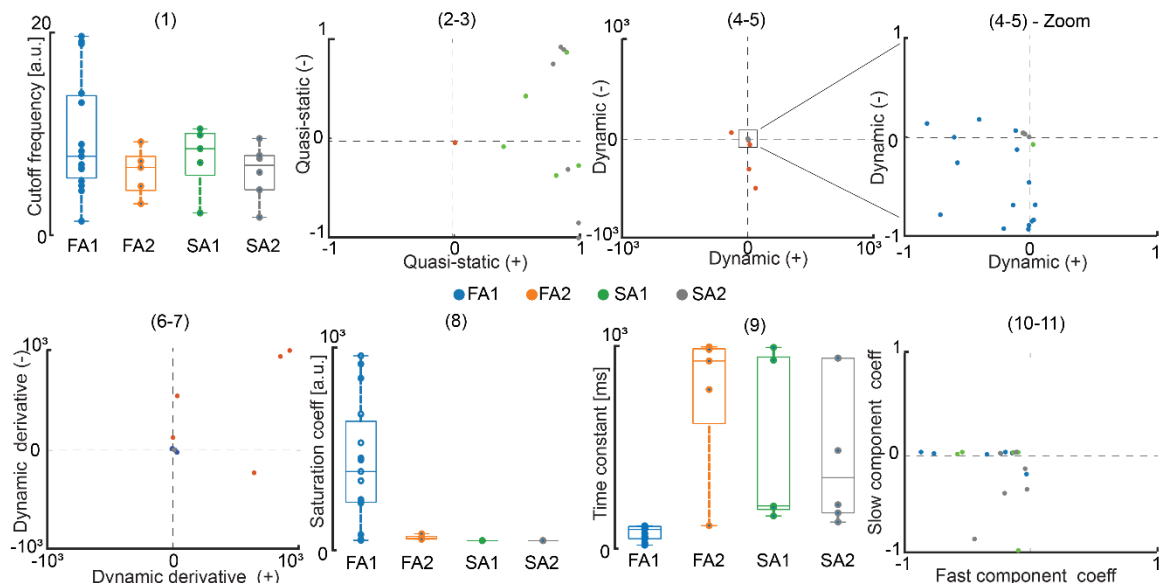


**Figure 2.4. Microneurography recordings in human tibial nerve.** (Strzalkowski, Ali, and Bent 2017) are used for fitting the model. a) Applied mechanical stimuli: using a 6 mm diameter probe (left side of the panel, taken and adapted from (Strzalkowski 2015) sinusoidal stimuli were with varying frequency and amplitude to excite afferents in different regions of the foot sole. Approximate positions of excited afferents are given on the foot sole representation (middle of the panel), color-coded (blue – FA1, orange – FA2, green – SA1, grey – SA2). 19 FAI, 9 FAII, 14 SAI and 10 SAII afferents were stimulated. Ranges of amplitude and frequency values of sinusoidal mechanical stimuli vary depending on the afferent type (representation on right). b) Illustration of the microneurography technique, recording from the tibial nerve at the level of the popliteal fossa. Two electrodes are inserted through the skin, one serves as a reference electrode, and the other is inserted into the nerve to record single afferents. Firing thresholds and firing rates [spikes/s] of single afferents were recorded. Here we present the average firing rate of responses that were stimulated with a specific frequency-amplitude combination. Taken from (Katic et al. 2023) with permission.

Our goal was to find a realistic replication of every afferent recorded during the microneurography experiment. That would ensure the enough variety of simulated afferent neural responses that is observed in different experiments. We applied a differential evolution algorithm (Storn and Price 1997), implemented in Python, for finding the sets of 11 parameter values that represent single afferents. The procedure follows several steps: within the FootSim environment, we place an afferent within the corresponding region where it was recorded during the experiment, ensuring that the mechanical parameters of this patch of skin matched those commonly observed for this region. Then we start the searching process by initializing the population of 11 parameters randomly. We generate the set of sinusoidal stimuli with all frequency-amplitude combination pairs applied experimentally and excite the afferent model. The cost function is defined as a sum of: i) errors between the simulated and recorded firing rate for each stimulus and ii) error in the

simulated and recorded threshold value. The differential evolution algorithm was then used to tune the parameters of the afferent models while minimizing this cost function. Initial parameters (starting values of the 11 parameter set) were changed based on the best set of values obtained in the previous optimization run and the procedure was repeated until the cost function did not decrease further over several consecutive runs. An individual optimization run was stopped when it approached the maximum number of iterations (500) or when the difference between the two populations of 11 parameters was less than 1%. For every recorded afferent, a separate model was fit. Models that failed a minimum performance threshold (set as a correlation between predicted and recorded firing rates less than 0.7) were excluded from the final model set. In total, we fit 5 SA1, 6 SA2, 15 FA1 and 5 FA2 individual afferent models that are the best-modeled replication of realistic afferents recorded during experimental procedure.

We achieved high accuracy of the fitting procedure for several models of each afferent type. Different models partially reflect the natural response variability of different afferents, which is observed in the empirical data. We did not observe strong trends in clustering the parameter values across the different afferent types (**Figure 2.5**). As they do not occupy the same parameter space, we ran a more extensive analysis of the parameter robustness as explained in a later section.



**Figure 2.5, Parameter values for individual models of afferents** (1) low-pass filter coefficients; (2-3) positive and negative values of quasi-static coefficients; (4-5) positive and negative values of dynamic coefficients; (6-7) positive and negative values of dynamic derivative coefficients; (8) saturation coefficient; (9) time constant; (10-11) fast and slow component coefficient of postspike inhibitory kernel. Taken from (Katic et al. 2023) with permission.

### 2.2.3 Fitting accuracy testing and model validation

In order to investigate the behavior of the fitted afferents, a Python toolbox was developed to perform validation of the model. We chose key metrics to investigate such as firing rate responses, absolute thresholds, response to ramp-and-hold stimuli and receptive field areas. In all tests, afferents generated with FootSim were placed on the foot sole following previously published afferent densities for each of the foot sole regions that have different mechanical properties and tactile innervation (Strzalkowski et al. 2018). A detailed description of the validation assessment will follow.



### 2.2.3.1 Firing rate responses

To analyze the responses of the fitted models to a given set of stimuli, we subjected the afferent models to an equivalent experiment to the one that generated our in vivo dataset (Strzalkowski, Ali, and Bent 2017). An initial challenge to reproducing such experiments was that not all afferents in the in vivo dataset received the whole range of stimuli. In turn, an individualized stimulus set was required for each fitted model.

The modelled firing rates were compared with the experimentally recorded ones for the same frequency and amplitude of stimulation received by the empirical counterpart. Sinusoidal waves of stimulation were modelled in Footsim indentation of a circular probe with 3 mm radius, which was indented and vibrated for two seconds. Firing rates were computed for each frequency-amplitude pair and compared with the empirical ones.

### 2.2.3.2 Afferent firing thresholds

Afferent firing thresholds (AFTs) were also compared with their empirical counterparts, a set of stimuli emulating the empirically given ones was applied to each of the fitted afferent models. In an effort to closely reproduce response thresholds, the minimum amplitude necessary to elicit a firing rate response of 1 Hz was classed as the model's afferent firing threshold.

### 2.2.3.3 Receptive Fields

Receptive field sizes were calculated analogous to the procedure established in (Saal et al. 2017). In short, we found the largest distance from the contact point of a simulated small probe (of one millimeter radius) at which an afferent model still responded to a short vibratory stimulus with an amplitude of several times the absolute threshold. This procedure was intended to mimic experimental determination of receptive fields. Empirically, afferent receptive fields were measured with monofilaments that applied a force 4-5 times greater than the absolute threshold.

### 2.2.3.4 Ramp-and-hold responses

Each afferent class exhibits well-known stereotypical responses to ramp-and-hold indentations. Aiming to interrogate these responses in our model we subjected each of the fitted models to a ramp-and-hold stimulus of 1 mm amplitude and one second of duration. The onset and offset of the stimulation lasted 0.2 seconds.

## **2.2.4 Simulation of neural responses during walking**

TekScan™ F-Scan™ (TekScan Inc., South Boston, MA, USA) Sport Insoles were worn by a single healthy participant (female, 19yrs, shoe size UK 5) during a period of four 6 m walking bouts at a self-selected speed. The insoles were cut to the size of the participant's foot, inserted into the shoe, and calibrated to the participant's mass. The insoles consist of equally spaced pressure sensors with an area of 0.26 cm<sup>2</sup>, spaced 0.51 cm apart on a grid. During the trial, a total of 446 pressure sensors were active, sampling the pressure signal at 100Hz. We extracted 16 steps (average length: 817ms, SD: 7.76) from straight line walking. The jogging step is representative of the other steps in that trial (average length=56.16ms, standard deviations=14.97 ms). All steps are normalized to 100 time points. Pressure data

for the left foot from all steps taken was averaged to create the spatiotemporal pressure profile of an average step. Recorded pressure is mapped into the FootSim by taking into consideration Poisson's ratio of the skin, Young's modulus of the skin and the radius of the flat-ended cylindrical indenter (radius equaling that of the pressure sensors). Instances of the participant turning were removed so that only full steps in a forward direction were processed. Each sensor input was represented by a separate simulated probe in the model, whose indentation trace was calculated from the measured average pressure profile, by considering the stiffness of each skin region as set in the model.

### 2.2.5 Quantification and statistical analysis

All statistical analyses were performed using Python, and specific statistical tests used for each experiment are described in the figure legends. Differences were considered significant if  $p < 0.05$ .

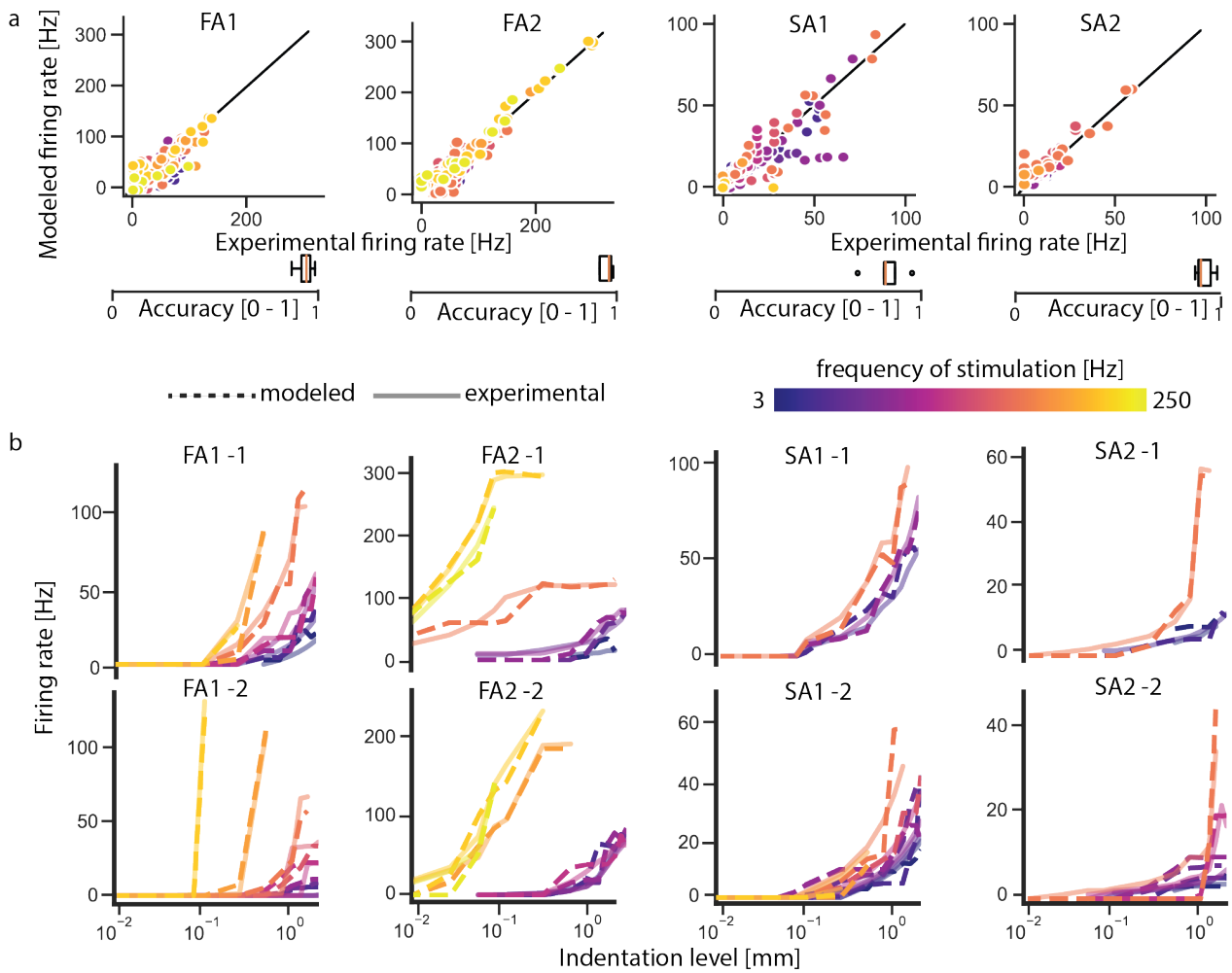
## 2.3 Results

### 2.3.1 FootSim model replicates experimental afferent neural responses

#### 2.3.1.1 Firing rates

We compared experimental and simulated firing rate responses to vibrotactile stimuli of different frequencies and amplitudes (skin indentation levels), covering a substantial range of the stimuli that the foot might be expected to encounter during natural behavior.

We found a close match between the experimental firing rates and the ones simulated by the model (**Figure 2.6a**), both across different afferent classes as well as for individual afferents. We show the rate-intensity functions of two examples of fitted models for each afferent type (**Figure 2.6b**). The model reproduced canonical response properties of different afferent classes. We observed an overall higher responsivity of FA afferents compared to SA afferents for vibrotactile stimuli. In addition, the frequencies eliciting the highest rates are higher for FA afferents than for either SA class (Muniak et al. 2007).



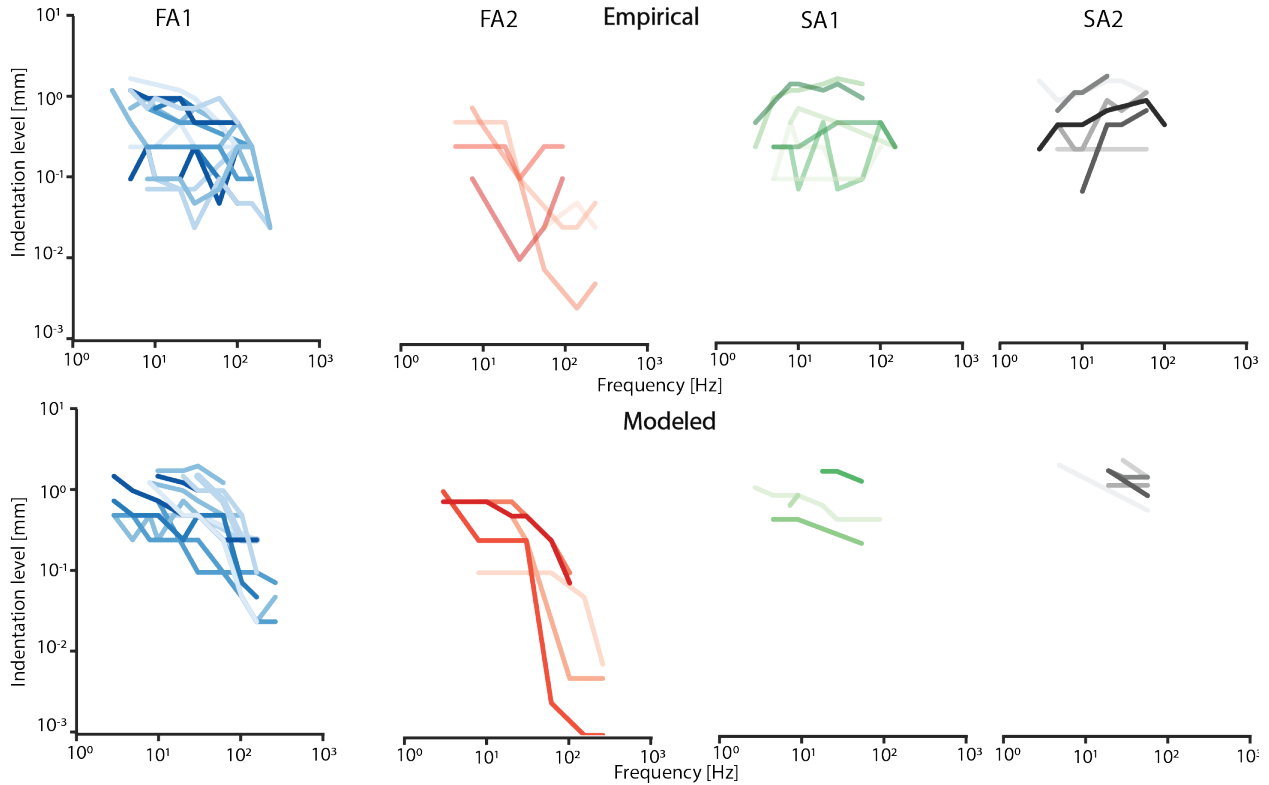
**Figure 2.6. FootSim accurately simulates afferent firing rates.** a) Scatter plots showing experimental versus modelled firing rates. Individual panels show comparisons for different afferent classes. Each dot corresponds to a tested frequency-amplitude pair, colored by frequency. Data from all afferents within a class is overlaid. Boxplots are showing the accuracy of the fitted models in predicting the firing rate of the afferents (FA1: median 0.94, min 0.87, max 0.98); FA2: median 0.96, min: 0.92, max: 0.98; SA1: median 0.85, min: 0.71, max: 0.98; SA2: median 0.91, min: 0.88, max: 0.99) b) Examples of two fitted models for each afferent class showing experimental and modelled rate-intensity functions. Solid semi-transparent lines denote experimental data, while dashed lines show the model results. Color scheme as in panel a. Taken from (Katic et al. 2023) with permission.

### 2.3.1.2 Response thresholds

As the frequency sensitivity profile of afferents is one of their main features and helps distinguish between different afferent types, we investigated afferents' absolute firing thresholds. These were defined as the minimum stimulation amplitude necessary to apply at each frequency to elicit afferent firing rates of at least 1 Hz. We compared the frequency profile simulated by FootSim with the empirical behavior of afferents. Within the boundaries of the range of frequencies evaluated, the model behavior closely matched experimentally derived counterparts (**Figure 2.7**).

We observe that FA afferents decrease their threshold at higher frequencies. Specifically, the FA2 afferent type displays very high responsiveness on frequencies higher than 90 Hz. On the other hand, SA1 afferents have high thresholds across all frequencies. Modelled SA2 afferents show slightly lower thresholds than the empirically recorded ones, especially on

the higher frequencies. This result matches the behavior of SA2 shown in **Figure 2.6a**, where we observe a higher firing rate on high frequencies compared to the experimentally measured ones. SA2 afferents were stimulated up to 100 Hz (**Figure 2.4a**) during the microneurography recording. Therefore, lack of the neural response data on higher frequencies limits the parameter fitting procedure and the accuracy of simulated responses.



**Figure 2.7. FootSim demonstrates realistic absolute firing threshold values.** Top row: Empirically measured absolute firing thresholds for afferents from all four classes over a range of different frequencies, obtained using a circular probe with 3 mm diameter. Each line with different color shade represents a different recorded afferent. Bottom row: Modeled absolute firing thresholds of the afferents using identical stimulation parameters as in experimental setup. Absolute threshold is defined as the minimal applied stimulation indentation level with specific frequency that results with the afferent firing rate of 1Hz. Each line represents a different model fit. Experimentally recorded afferent and its modelled replication in FootSim are presented with the same color on the top and bottom panel. Taken from (Katic et al. 2023) with permission.

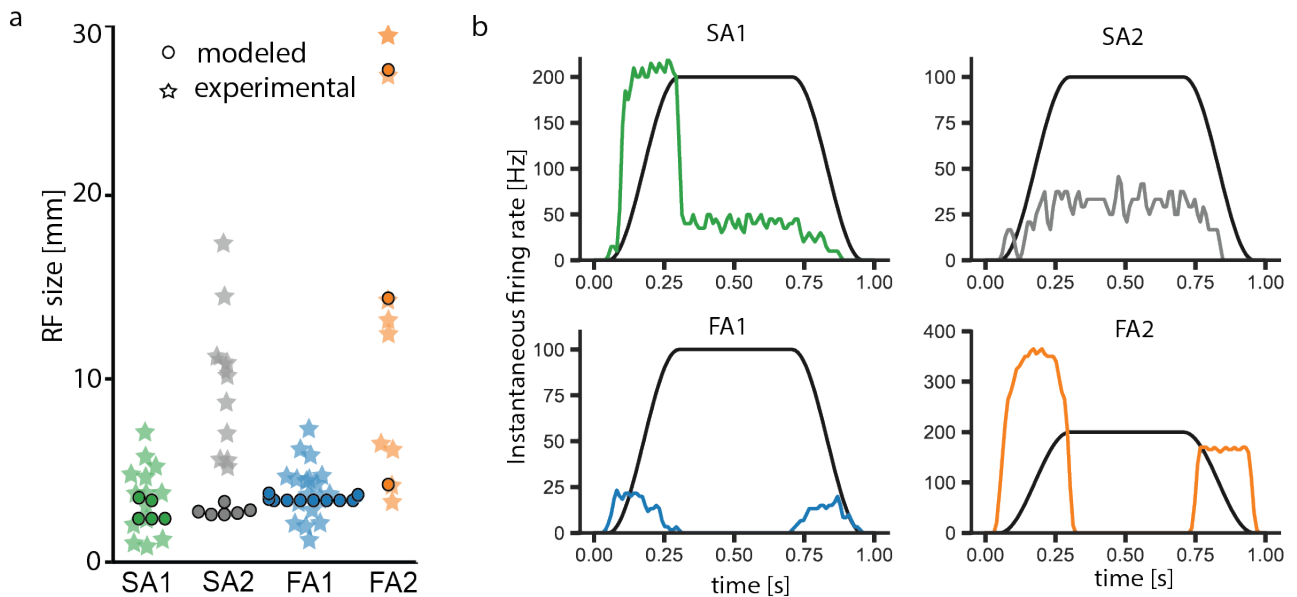
### 2.3.2 Model validation

We evaluated the performance of the model on a number of standard physiological metrics that are commonly used in the literature to characterize the response behavior of tactile afferents.

#### 2.3.2.1 Receptive fields

Tactile afferents differ in the size of their receptive fields (RFs) (Kennedy and Inglis 2002). This effect is most prominent across class, with type 1 fibers characterized by small receptive fields, while type 2 fibers possess much larger receptive fields that might also vary considerably between afferents of the same class. Receptive fields predicted by the model emerge “naturally” out of the interaction between skin mechanics and the fitted response

behavior of the different afferent models. We tested whether modelled receptive fields were comparable to experimentally recorded ones. We simulated the responses of all individual models to supra-threshold stimuli at fixed distances to determine the maximal distance at which a tactile stimulus would still elicit a response from the afferent. As our model of the skin is isotropic, modelled receptive fields will always be circular, while empirically measured receptive fields are often elliptical, likely caused by the structure of the skin and possibly properties of the receptors themselves. Nevertheless, when comparing RF sizes (expressed as the radius of a circular field of a given area), we found relatively good agreement between the modelled and empirical fields (**Figure 2.8a**).



**Figure 2.8. FootStim can produce realistic receptive field sizes and afferent responses to ramp and hold stimuli, replicating the natural behaviour of specific afferent types.** a) Receptive field sizes measured experimentally (stars) and simulated with FootSim (circles) for different afferent classes. Kruskal-Wallis test didn't show statistical difference ( $p > 0.05$ ) of modelled and experimentally measured receptive field sizes, except for SA2 ( $0.01 < p < 0.05$ ). b) Responses of different classes to the ramp and hold stimuli. Average population responses of the four different afferent classes (coloured lines) to a ramp-and-hold stimulus (indentation trace shown as black line). The model reproduces canonical response properties of the four afferent classes, as have been widely reported in the literature (Kaas 2004). Taken from (Katic et al. 2023) with permission.

SA1 and FA1 receptive fields were small and matched well though the measured fields showed higher size variability than the modelled ones. FA2 fields were large, but highly variable in size, and could cover a considerable portion of the foot sole. Modelled SA2 receptive fields, on the other hand, were smaller than those of real afferents. We ran a Kruskal-Wallis test to check whether the modelled and experimental values are statistically different. A significant difference was found only for SA2 afferents. Experimentally, SA2s are pretty insensitive to indentation so they have high monofilament thresholds. For that reason, very large monofilaments are used to map the receptive fields, which are required to induce skin stretch to evoke SA2 firing. Therefore, it is likely that the simple skin model we implemented, which reproduces stresses to normal indentation only, is not sufficient to capture the response profile of SA2 afferents accurately enough.

### 2.3.2.2 Afferent responses on ramp-and-hold stimuli

Different afferent classes are characterized by their stereotypical, canonical response profiles to ramp-and-hold stimuli: SA afferents respond during stimulus onset, but importantly also during sustained, constant indentation with a continued and graded dynamic response with SA2s having more uniform interspike intervals than SA1s. FA afferents only respond to dynamic phases during stimulus onset and offset (Kaas 2004). In order to test whether the model reproduced these stereotypical responses reported in the literature we simulated simple indentation traces with 2 mm depth and computed the firing responses of all afferent models in every region of the foot sole (**Figure 2.8b**). Stimulation was given in a one second window. In agreement with empirical expectations, SA1 afferents responded during the ramp onset and, less vigorously, during the plateau phase. Additionally, SA2 afferents responded weakly but consistently throughout the stimulus presentation. In contrast, both FA1 and FA2 afferents responded only during the onset and offset. We also tested the model with a slightly changed shape of ramp-and-hold stimuli, making the ramp phase steeper, reaching the plateau amplitude value in the short time period. In this scenario, FA afferents increased their firing rate, showing that the modeled afferent representatives are able to code the velocity. Thus, the model reproduces afferent behavior during ramp-and-hold stimuli as expected based on previous findings.

### 2.3.3 Robustness of model parameters

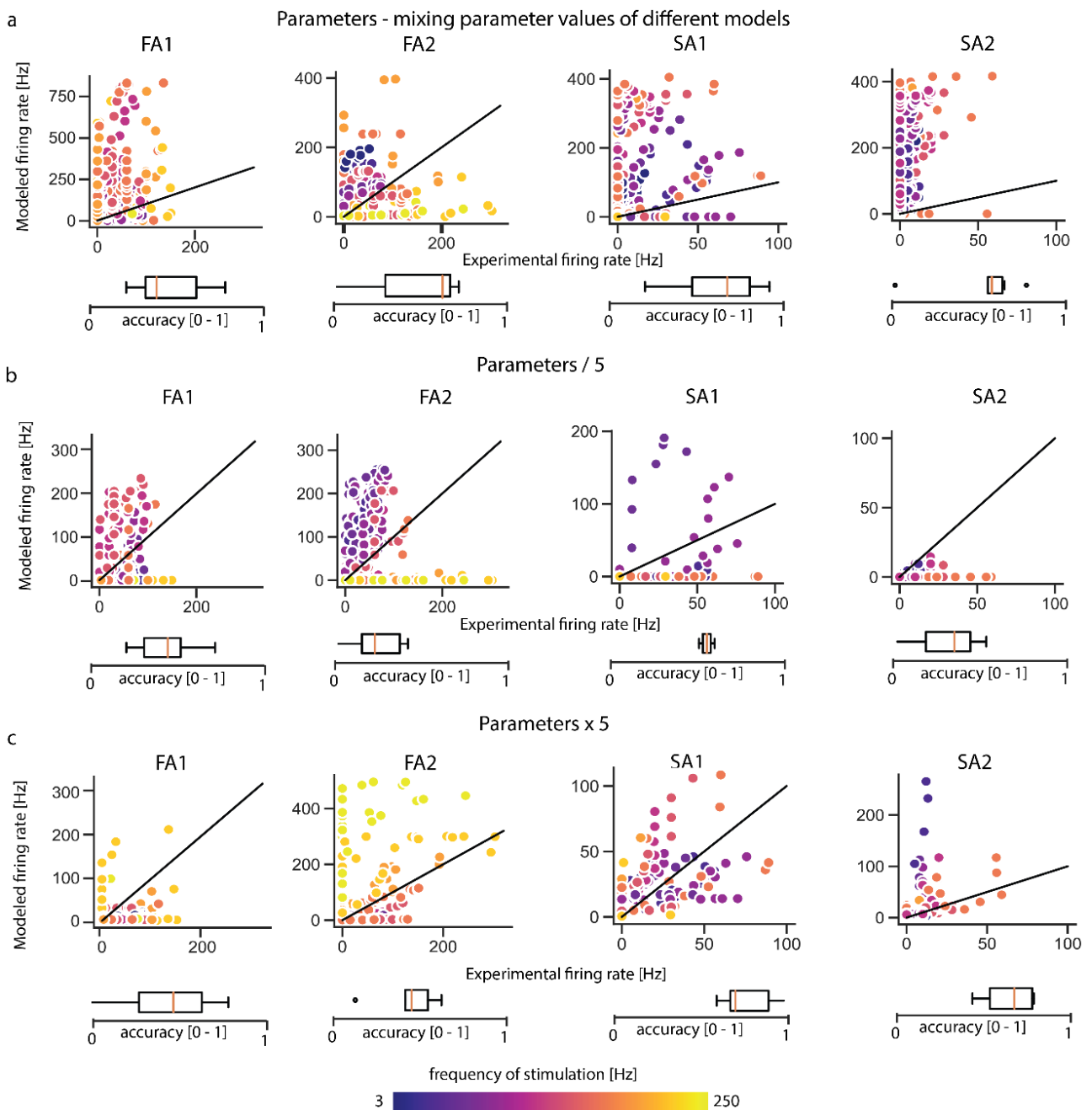
The firing model employed by FootSim is composed of eleven parameters (**Figure 2.1**) that form a non-linear dependence between the stress profile given as an input and the neural response as an output of the simulation. We ran several simulation experiments in order to explore the parameter space that is occupied by different neuron classes, validate the robustness of the fitted parameter values, and demonstrate the importance of both the absolute values and the relationships between parameters.

First, we sampled new models by “mixing and matching” different models of the same afferent type. We selected each parameter value of the new model by sampling it with replacement from the set of originally fitted values for that afferent type (**Figure 2.5**). This change highly reduced the accuracy in predicting the firing rates compared to the fitted models. As fitted parameters are not clustered based on the afferent type (**Figure 2.5**) this result was expected and additionally emphasizes that specific parameters are not independent of each other.

To address whether the relationship between values is a key feature of accurate and realistic behavior of afferent models, we substantially changed the absolute values of the model parameters, while keeping their relationship constant – increasing or decreasing all values five times (**Figure 2.9b** and **Figure 2.9c**, respectively). These changes mostly surpassed the behavior of mix-and-match models, however, accuracy was highly decreased.

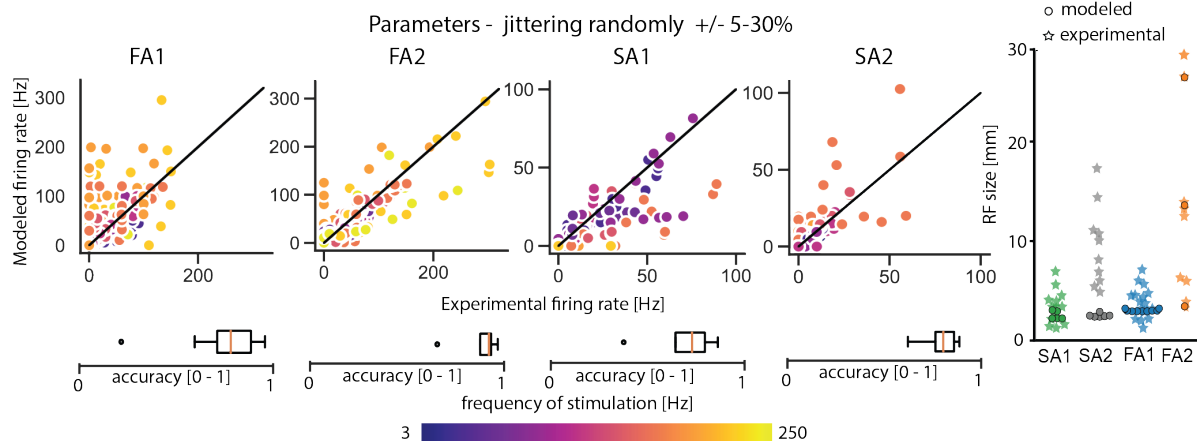
Finally, we examined whether slight changes of each parameter in the model would result in unexpected responses or whether the models are robust enough with respect to moderately small parameter jittering. We changed the value of each parameter by randomly jittering them between 5 and 30% of their value (**Figure 2.10**). The accuracy of the predicted firing rates was slightly decreased, as expected, but overall these models performed reasonably well. Estimated receptive field sizes remained very similar to the originally fitted models and responses on ramp and hold stimuli were very similar to the ones presented in

**Figure 2.8.** In summary, results show that slight jittering of parameters does not change significantly the neural responses.



**Figure 2.9, Exploring the individual models parameter space.** We changed afferent model parameters in 3 different ways and check their behavior. Scatter plots on the left side of the panels show empirical versus modelled firing rates. Individual panels show comparisons for different afferent classes. Each dot corresponds to a tested frequency-amplitude pair, colored by frequency. Boxplots are showing the accuracy of the f models in predicting the firing rate of the afferents. a) Changing the existing models of each afferent type by choosing a value for each parameter of the model from the set of all values for the specific parameter (sampling with repetition). b) reducing the single parameter values 5 times c) increasing the single parameter values 5 times. Taken from (Katic et al. 2023) with permission.





**Figure 2.10, Footstim is robust to modifications of parameters values but also to changes of relationships between parameters.** We changed parameter (11 parameters from the Figure 2.1) values by increasing or decreasing randomly by between 5 and 30 % of their nominal value. Scatter plots on the left show experimental versus modelled firing rates. Individual panels show comparisons for different afferent classes. Each dot corresponds to a tested frequency-amplitude pair, colored by frequency. Boxplots are showing the accuracy of the models in predicting the firing rate of the afferents. Plots on the right show the size of receptive fields for each afferent type. Taken from (Katic et al. 2023) with permission.

Based on the investigated variations of model parameters, we can conclude that both absolute values and the relationships between different values are important for realistic and accurate prediction of neural responses. Additionally, slight changes in these features will not cause a significant change in behavior, demonstrating the robustness of the fitted models.

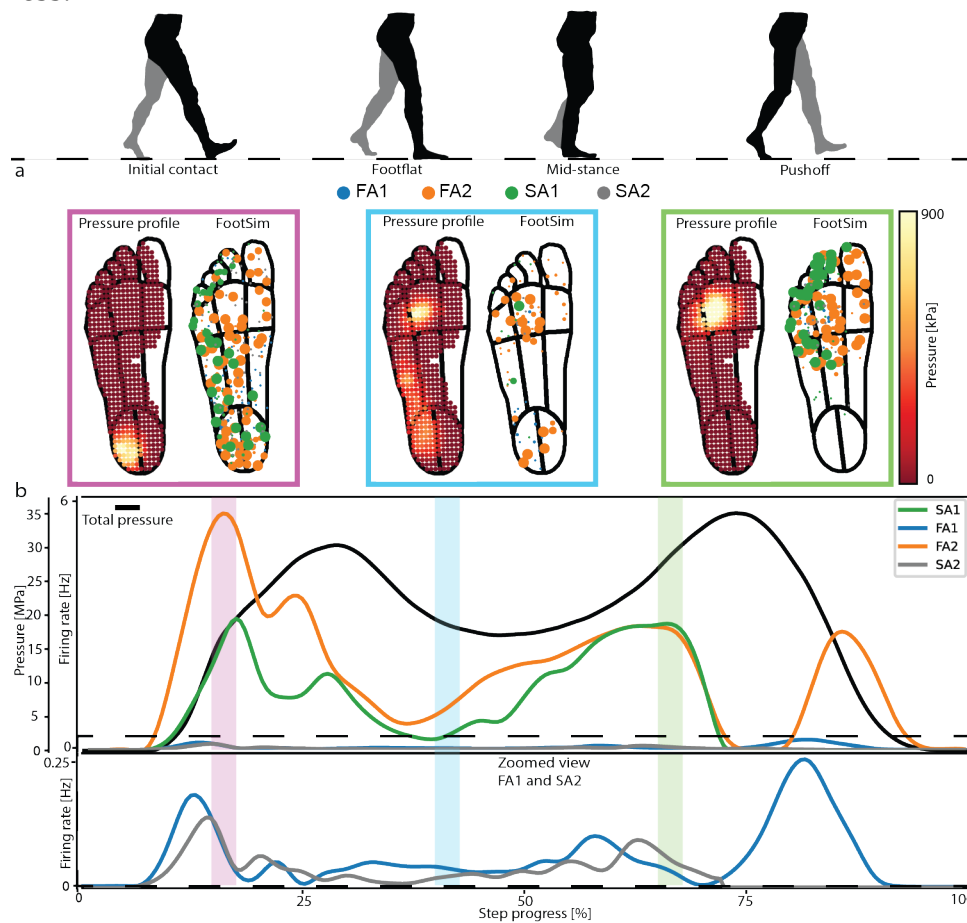
### 2.3.3 Neural afferent responses during walking cycle

Tactile responses during dynamic behavior are technically challenging to record as the microneurography technique requires the subject to be still. One of the benefits of the FootSim computational model is that it can be used to simulate neural responses to natural spatiotemporal pressure distributions during dynamic activities, such as walking, and thereby yield novel insights into neural population responses in behaviorally relevant scenarios. As a proof-of-concept for this application, we used pressure data from a healthy participant during walking, collected with a pressure-sensitive shoe insole. We averaged the spatiotemporal pressure profiles from multiple steps to create an average step profile and used this as an input to the model.

We present example frames of the input and the FootSim response in three different phases of the step – heel strike, mid-step and toe push-off – in **Figure 2.11a**. The simulated neural responses are color-coded depending on the afferent fiber type, and the size of the marker is correlated with the simulated firing rate. As the heel region has the highest skin hardness, propagation of stimuli is strong at the heel and it provokes the response of even some afferents in the metatarsal area or toes. In line with previous research (Bonneyoy and Armand 2015; Wiik et al. 2017), we noted that pressure increases rapidly during initial contact when the heel strikes the ground, then decreases and plateaus while the foot is flat on the ground and finally increases again, mostly around the metatarsal area, during push-off, before decaying as the foot lifts off (**Figure 2.11b**, black line). FootSim simulation responses for each afferent class were averaged across all afferents of that class that occur in the foot sole, with a time bin of 25 ms, and they are color-coded for different afferent types



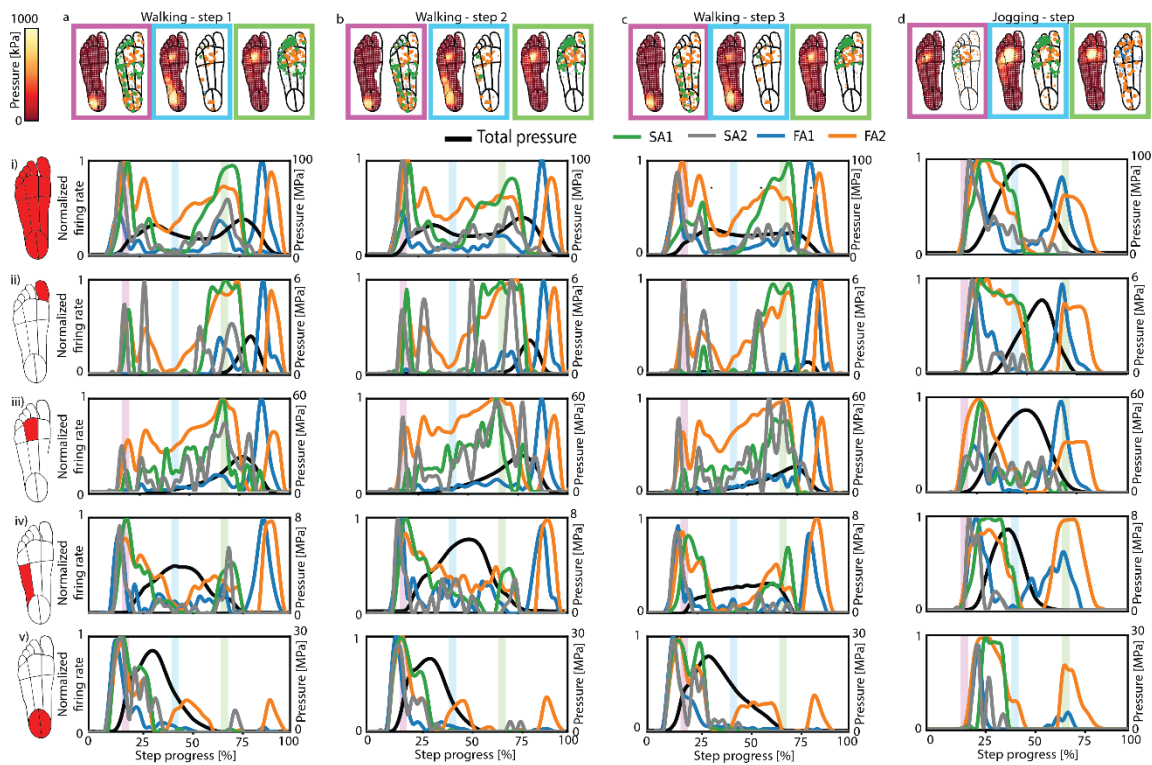
(Figure 2.11b). Across the four afferent populations, the largest responses were observed during heel strike, with smaller responses during push-off, while the mid-stance elicited the smallest responses. This result mirrors similar findings on the hand, where the population response is strongest during transient events and small during sustained forces (Callier, Suresh, and Bensmaia 2019b). Averaged firing rate curves (Figure 2.11b) show differences in the response profiles for the different afferent types during the walking cycle, implying potentially varied and specific roles during different moments of the gait cycle. Differences in the overall activity levels of the different afferent types partly reflect differences in local innervation densities, but might also be a consequence of the extrapolation from the relatively small probe used in data acquisition to the much larger contact areas simulated here. Future validation with experimental data is needed to validate such differences in responsiveness.



**Figure 2.11, FootSim can reveal dynamics of activation during the walking cycle.** a) The spatial indentation profile and the population response. Each afferent's marker is scaled by its firing rates during heel strike (pink box), mid-step (light blue box) and toe push-off (light green box). b) Total pressure during an average step as a function of time (black line). Shaded areas denote the three time periods depicted in panel b. We simulated average population responses divided by afferent class. Average firing rates for each class were divided by the number of fibers of the corresponding type that exist in the foot sole. Since FA1 and SA2 afferent have lower responses compared to the other afferents, we zoomed the view for better understanding of changes in activation of specific afferent type during walking cycle. Taken from (Katic et al. 2023) with permission.

Tactile feedback during walking is likely also employed in determining which part of the foot is in contact with the ground at any given moment. Indeed, afferent populations innervating different regions on the foot sole responded with different intensities and temporal profiles to the step (see responses for the heel, lateral arch, middle metatarsal, and great toe in Figure 2.12), signaling local time-varying pressure at different skin sites. Finally, neural responses also varied across different types of steps. The FootSim model responded consistently to similar pressure profiles (Figure 2.12 a, b and c), while producing markedly

different responses to different spatiotemporal pressure patterns, as present for example during jogging (**Figure 2.12d**).



**Figure 2.12, The spatial indentation profile and the population responses during different type of steps, analyzed by the location on the foot sole.** a), b) walking step c) walking step when person is turning d) jogging step. Top of all panels: the spatial indentation profile and the population response. Each afferent's marker is scaled by its firing rates during heel strike (pink box), mid-step (light blue box) and toe push-off (light green box). i) whole foot area ii) great toe area iii) middle metatarsal area iv) lateral arch area v) heel area of the foot sole. Total pressure during an average step as a function of time (black line). Shaded areas denote the three time periods depicted in the top of all panels. The firing rate of the afferents is averaged and normalized by afferent class over time (25ms window). Taken from (Katic et al. 2023) with permission.

Specifically, responses from different regions of the foot during walking and jogging were notably different. Afferents from the heel responded more during walking than in jogging, reflecting the differences in the pressure profile of the two activities, and specifically the decreased use of heel strikes during jogging. Conversely, afferents on the metatarsal location showed higher levels of activity in the jogging scenario, as this region is involved much more than while walking. Unlike when the person is walking, there is no second peak in SA1 activity, since SA1 are activated mostly during the slow change from the lateral to the metatarsal area of the foot.

## 2.4 Discussion

We assembled an in-silico model of the foot sole, that reconstructs the neural responses of individual tactile afferents innervating the foot sole in humans. It uses a mechanical part of the model to convert indentations into stress patterns, followed by firing models that reproduce the response properties of individual afferents. The model is fitted on a dataset of tactile afferents exposed to a wide range of vibrotactile stimuli at different frequencies and amplitudes, recorded in humans using microneurography. We showed that the model can reproduce the response properties of these neurons accurately, as determined by firing

rates, firing thresholds, and receptive field sizes. Characteristic response behaviors of different afferent types to ramp-and-hold stimuli are commonly taken as their specific feature. We confirmed that FootSim can replicate these features even though the models were not fit this type of stimuli, proving that model can generalize to novel stimuli. Finally, we showed how the model can be used to reconstruct approximate population activity during natural dynamic conditions, such as walking, which is difficult to measure experimentally (e.g. through microneurography). The model has direct possible neuroscientific and neuroprosthetic applicability.

### **2.4.1 FootSim emulates and reveals the role of specific tactile afferents for balance and gait**

For bipeds, such as humans, the soles of the feet are the only interface with the ground. Forces acting at this interface are sensed through the foot sole skin and this feedback is then used to aid in the control of body orientation and to manipulate the body center of mass (COM) (Kavounoudias, Roll, and Roll 1998; Oddsson, De Luca, and Meyer 2004). Consequently, a reduction of plantar cutaneous information results in an increase in postural sway (Orma 1957; Yun Wang, Watanabe, and Chen 2016) and compensatory stepping reactions to postural perturbations (Stephen D Perry, McIlroy, and Maki 2000). The importance of cutaneous feedback from the foot sole is also highlighted in patients with peripheral neuropathy, which causes a loss or degradation of tactile feedback, leading to concomitant decreased balance, distorted gait and even falls. Conversely, increasing cutaneous feedback from the foot sole border has been shown to increase gait stability in older adults (S. D. Perry et al. 2008).

Mechanoreceptors in the skin of the foot sole contribute to the representation of the COM with respect to the base of support (Kavounoudias, Roll, and Roll 1998) and are able to initiate postural reflexes that result in increased standing stability (Do, Bussel, and Breniere 1990). The toes, the heel, and the lateral border of the sole represent the physical limits of the base of support. Receptor densities in the toes are higher than in the rest of the foot sole, suggesting the significance of feedback from the toes in maintaining balance (Strzalkowski et al. 2018). FootSim simulation of activation during the walking cycle reveals an important increase of afferent activation in the heel and toes (**Figure 2.11** and **Figure 2.12**). The density of mechanoreceptors on the lateral side of the foot is also larger than that on the medial, and again this might afford fast and reliable feedback to react to balance loss. Specifically, if the COM moves beyond the base of support in the lateral direction, there is a need for a stepping reaction to prevent a fall (Maki and McIlroy 1996), while the medial movement of the COM can be compensated with the other leg and is, therefore, less critical. In addition, the medial region of the foot sole is arched upwards and it is therefore less often in contact with the ground compared to the lateral part, which provides an additional possible explanation for the low density of afferents in this region and their lower activity during walking. Furthermore, activation of specific skin regions on the sole of the foot through electrical stimulation has been shown to modulate the muscles of the lower limb to facilitate gait (Zehr et al. 2014). This very direct evidence, and direct measures of afferent coupling (Fallon et al. 2005) support the notion that feedback from specific mechanoreceptive sub-populations plays a significant role in spinal reflexes to control the magnitude of muscle activation for successful ambulation.

Apart from the location where an afferent terminates, its class also influences responsiveness to different types of stimuli and FootSim can help us understand the

dynamics of afferent activation (**Figures 2.8, Figure 2.11 and Figure 2.12**). Fast-adapting afferents are especially important in assisting balance control during human locomotion. They are likely responsive to the unevenness of the ground and unexpected slips and will serve as a feedback mechanism for balance maintenance and/or recovery. They are considered motion and velocity detectors, which explains their increased activity during transient events, such as foot-off and foot-contact. Since FA2 afferents are the most sensitive to perpendicular light touch, and have the biggest receptive fields which can cover up to the entire foot sole (Strzalkowski et al. 2018), it is expected that activity of these afferents is present during the whole gait cycle and especially high during the initial gait stance (Fig. 2.12). Merkel cells and Ruffini endings, corresponding to slow-adapting tactile afferent units type 1 and 2 participate in postural regulation, which generally involves movements and forces at frequencies below 5 Hz (Stephen D Perry, McIlroy, and Maki 2000). SA1 afferents are mostly associated with the maintained contact of the foot on support and they show high activity during the end of mid-stance when the metatarsal part of the foot is mostly on the ground and terminal gait stance when the subject is leaning on his toes. FA1 afferents and their connected Meissner corpuscles are associated with information related to foot contact (Kennedy and Inglis 2002) and their density is the highest in the toes (Strzalkowski et al. 2018), which explains their increased firing during the terminal, toe off phase of the gait. FA1 afferents are also strongly coupled to motor neurons in the lower (Fallon et al. 2005) and upper (Bent and Lowrey 2013) limbs highlighting their reflexive role in standing balance. As shear was not experimentally tested nor modelled, FA1 show lower activation as they respond a great deal to tangential forces along the skin. Low activity of SA2 is expected as they are stretch receptors and have a high threshold to orthogonal load and are characteristically the least sensitive type.

#### **2.4.2 Importance of specific FootSim features**

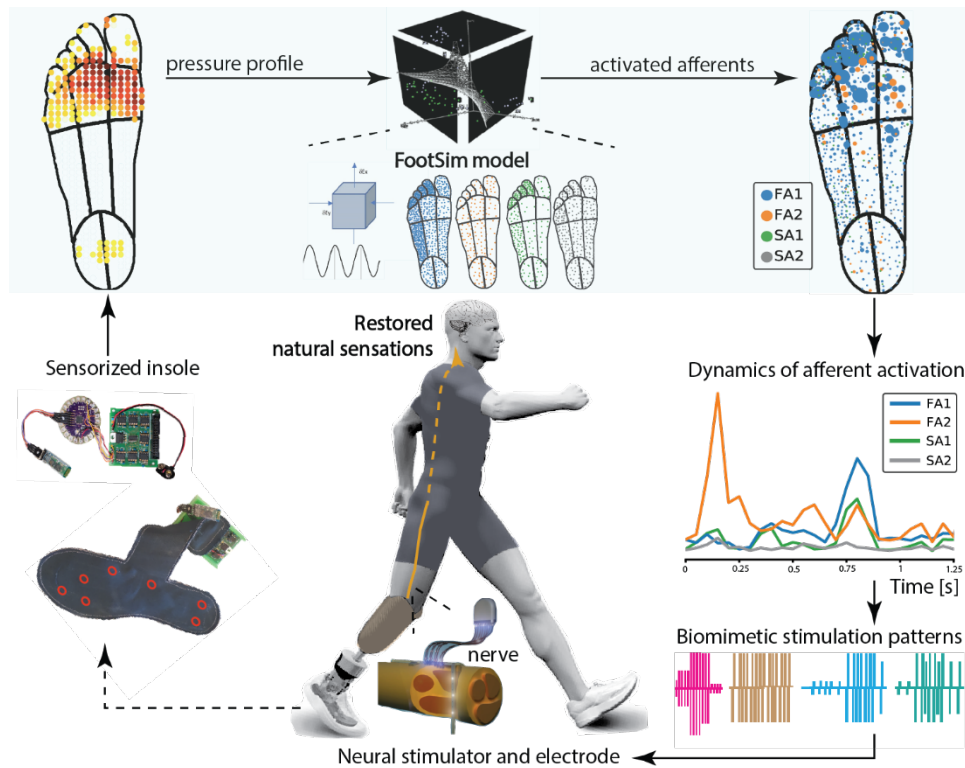
Differences in skin hardness across the foot sole produce non-linear changes in skin stiffness and, consequently, stress calculation and propagation are highly non-linear. Even though this variability does not correlate highly with single afferent firing rates (Strzalkowski et al. 2015), it influences the number of recruited fibers due to the differential spread of the mechanical stimuli through the skin of the foot sole. If stimuli with equal indentation amplitude are applied to a region of the skin with increased hardness, stress values will be higher and the dynamic component will propagate further on the skin of the foot sole, activating more afferents than when stimuli are applied to the region with low hardness values (**Figure 2.2b, Figure 2.11a, and Figure 2.3**). This effect is of importance for understanding the dynamics of afferent activation and translation of observed results for defining the biomimetic stimulating patterns for neuroprosthetic application. Additionally, the ability to implement modular values of skin hardness in FootSim is necessary when adapting the model for different groups of patients. For example, patients with diabetic neuropathy, as one of the conditions, develop increased skin hardness (Piaggese et al. 1999). In addition, afferent units from the foot sole lose their ability to transmit tactile information. In the FootSim model, the number of afferents can easily be easily modified. Therefore, we believe that the FootSim model design is suitable to be adapted for different groups of patients. The robustness of model parameters is very important as it is validating the strength of the designed model and its fitted values. Slight changes of parameter values in FootSim afferent models will not significantly change the neural response, therefore indicating that FootSim can be used as a unique, robust tool for simulating the neural responses of foot sole afferents.

The number of constructed afferents is restricted by the relatively small amount of experimentally recorded data. Hence, the FootSim model has a limited number of afferent replications and limited diversity of afferent responses. This variability, which is one of the natural features important for a realistic representation of foot sole afferent responses, could be accomplished by changing the fitted model parameter values on a small scale. Newly created models will not completely replicate the recorded afferent, but could conceivably portray information from different regions of the foot.

### ***2.4.3 FootSim model application in neuroprosthetics***

Lower-limb amputees are dealing with the loss of natural information about the interaction with the ground and currently available prostheses are not able to restore missing sensations (Stanisa Raspopovic 2020). This leads to reduced mobility, asymmetrical walking, lower embodiment, higher risk of falls and numerous consequent health issues (Francesco Maria Petrini, Bumbasirevic, et al. 2019). Electrical nerve stimulation shows promising results in restoring sensory feedback and improving amputees' condition (Francesco Maria Petrini, Bumbasirevic, et al. 2019; Francesco Maria Petrini, Valle, et al. 2019; Giacomo Valle, Saliji, et al. 2021). Multiple research groups are working on finding the best way to stimulate the nerve (Stanisa Raspopovic, Valle, and Petrini 2021) and have achieved distinct and spatially selective sensations that significantly improved motor tasks as well as the way the subject is perceiving the prostheses (Francesco Maria Petrini, Valle, et al. 2019; Preatoni et al. 2021). Most often, artificial encoding of linear stimulation has been tested, which has resulted in a range of perceived sensations: from undesirable paraesthesia, tingling or prickling, to more pleasant like touch and pressure, with limited reported perceived naturalness (Stanisa Raspopovic, Valle, and Petrini 2021). Since naturalness is among the features of the highest importance for prosthesis acceptance (Emily L. Graczyk et al. 2016), generating close-to-natural information for the nervous system (Saal and Bensmaia 2015), represents a critical clinical need. While hybrid modelling (Katic, Valle, and Raspopovic 2022) can help tackle the design of an optimal device to implant (Zelechowski, Valle, and Raspopovic 2020), we envisage the use of the FootSim model for defining the "biomimetic language": stimulation patterns to mimic the natural signals from the periphery. Indeed, the model has been designed to be effortlessly included in closed loop neuroprosthetics (**Figure 2.13**). Such a system is comprised of a sensorized insole that is able to record the pressure under the artificial foot sole, sending a reconstructed pressure profile as an input to the FootSim model, which simulates the neural responses of the fiber population. For an engineer, constructing the neuromodulation system, FootSim can be considered as a "plug & play" tool, able to reconstruct the afferent activity, and does not require any specific expertise for use. As an output, the model is producing the quasi-continuous dynamics of afferent activation during any activity (e.g. walking or running) of the subject, which can be used as a trigger for biomimetic stimulation policies. To do so, the function of transformation from the computed units' activities to the neurostimulator commands has to be assumed. We hypothesize a plausible option for such a transformation (**Figure 2.13**): the frequency of stimulation is defined directly from the summation of spike trains of all activated afferents, while the charge profile is coded in the number of recruited fibers (Giacomo Valle et al. 2018b). A direct translation of FootSim to biomimetic policy creation needs to be investigated further in light of the limitations of available neurostimulating technologies. Finally, developed stimulating paradigms could be transmitted to the neurostimulator through an appropriate transfer function. Potentially, such a biomimetic code encoded to nerves, through the neural implant, would be

transmitted to the spinal cord and somatosensory cortex, enabling the transfer of the information about contact with the ground. In this manner, we could potentially restore to a disabled subject close-to-natural sensation coming from the artificial foot. Yet, this use of FootSim to needs to be investigated, and validated in eventual future experiments.



**Figure 2.13. FootSim possible contribution to biomimetic stimulation patterns for tactile feedback restoration in future neuroprosthetics.** In a possible scenario, the user will be fitted with a leg prosthesis collecting real-time spatiotemporal pressure data via a sensorized insole (bottom left). This data will be provided as an input to the FootSim model. The model would convert the artificial pressure profiles into realistic neural response patterns (top, blue shaded box). FootSim output could be potentially used for generating biomimetic stimulation policies (bottom right). Neurostimulator would generate these paradigms and this type of stimulation could be used to transmit to the subject the information recorded with the insole in a future possible scenario. Taken from (Katic et al. 2023) with permission.

#### **2.4.4 Limitations of the study**

The importance of spike timing is well-known in tactile coding (Roland S Johansson and Birznieks 2004; Mackevicius et al. 2012). However, due to limitations in how precisely spike trains could be aligned with the precise stimulation profile, the fitting of the FootSim model relied on average firing rates, limiting the accuracy of predicting precise timings of generated action potentials. Still, when precise alignment of spike trains with skin oscillations is not required (and it is not clear whether precise spike timing at such fine temporal resolutions is behaviorally relevant on the foot), the model should reproduce time-varying firing rates on the order of around 100 ms with relatively high accuracy.

Second, we are simulating the stress propagation as quasi-continuous, without incorporating lateral sliding and shear forces. This is, together with the lack of experimentally recorded neural activity, one of the biggest reasons for the limited accuracy of SA2 responses. Yet, this simplification is not expected to significantly impact model accuracy, since a high correlation between tangential and normal forces is typically



observed during sliding (Yoshioka et al. 2007). Still, future models should incorporate more complex skin mechanics. In a related issue, we are approximating the skin as a two-dimensional surface, since 3D modelling of the involved tissues would drastically increase the complexity of the model, as well as limit the possibility of FootSim use in real-time. Lastly, and importantly, our experimental dataset is obtained by applying passive vibrotactile sinusoidal stimuli through a single relatively small probe over the receptive field of individual mechanoreceptor endings. For the simulation of neural responses during walking, we are predicting afferent responses in a dynamically loaded condition, where large parts of the foot are in contact with the ground and forces are high. Therefore, the model may be limited in its ability to accurately predict firing under high loads and with large contact areas, as well as when tangential forces are applied. Future experimental work should test and validate these predictions, within the limits of current technical capabilities, to improve future iterations of the model.

# Chapter 3

## Animal models can reveal novel insights about artificial somatosensory feedback

*"No amount of experimentation can ever prove me right; a single experiment can prove me wrong."  
Albert Einstein*

*Adapted from: Neural population dynamics reveals disruption of spinal sensorimotor computations during electrical stimulation of sensory afferents*

*Katic Secerovic, Natalija, Josep-Maria Balaguer, Oleg Gorskii, Natalia Pavlova, Lucy Liang, Jonathan Ho, Erinn Grigsby, et al. 2021. "Neural Population Dynamics Reveals Disruption of Spinal Sensorimotor Computations during Electrical Stimulation of Sensory Afferents." Preprint. Neuroscience. <https://doi.org/10.1101/2021.11.19.469209>.*

While neurostimulation technologies are rapidly approaching clinical applications for sensorimotor disorders, the impact of electrical stimulation on network dynamics is still unknown. Given the high degree of shared processing in neural structures, it is critical to understand if neurostimulation affects functions that are related to, but not targeted by the intervention. Here we approached this question by studying the effects of electrical stimulation of cutaneous afferents on unrelated processing of proprioceptive inputs. We recorded intra-spinal neural activity in four monkeys while generating proprioceptive inputs from the radial nerve. We then applied continuous stimulation to the radial nerve cutaneous branch and quantified the impact of the stimulation on spinal processing of proprioceptive inputs via neural population dynamics. Proprioceptive pulses consistently produced neural trajectories that were disrupted by concurrent cutaneous stimulation. This disruption propagated to the somatosensory cortex, suggesting that electrical stimulation can perturb natural information processing across the neural axis.



### 3.1 Introduction

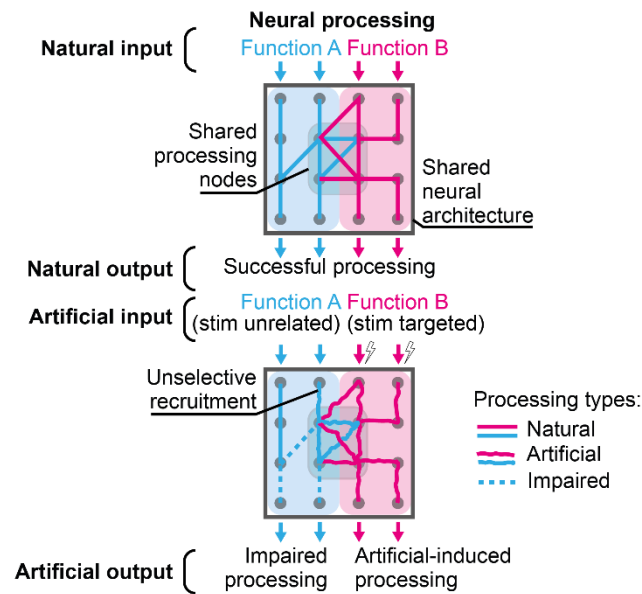
Decades of animal and human studies have shown that neurostimulation technologies can restore some level of neurological function in patients with sensorimotor deficits (Stanisa Raspopovic, Valle, and Petrini 2021; Edwards et al. 2017; Gill et al. 2018; Angeli et al. 2018; Formento et al. 2018; Greiner et al. 2021; Stanisa Raspopovic 2021; Kuiken 2009; Seáñez and Capogrosso 2021; Powell et al. 2023). These novel technologies produce immediate assistive effects, achieving a controlled restoration of multifaceted behavioral processes (Giacomo Valle, Saliji, et al. 2021). For instance, in humans peripheral neuroprostheses successfully restore touch sensations (S. Raspopovic et al. 2014; D. W. Tan et al. 2014; Francesco M. Petrini et al. 2019; Zollo et al. 2019; Francesco Maria Petrini, Valle, et al. 2019; Francesco Maria Petrini, Bumbasirevic, et al. 2019; Oddo et al. 2016; Francesco Clemente et al. 2019; M. Schiefer et al. 2016), and spinal cord stimulation enables the recovery of voluntary motor control (Gill et al. 2018; Wagner, Mignardot, Le Goff-Mignardot, et al. 2018; Angeli et al. 2018). While these remarkable results are fueling the translation of these technologies in clinical settings, the understanding of the short- and long-term effects of injecting electrical current into existing neural dynamics is still entirely unknown. In fact, virtually all these interventions suffer from a latent, yet critical caveat: the input delivered to the neural circuits is artificially generated, being widely different from naturally-generated neural activity.

Indeed, electrical stimulation produces synchronized volleys of neural activity in all recruited axons (or cells), rather than the asynchronous bursts of inputs that govern natural neural activity (Formento et al. 2020; Balaguer and Capogrosso 2021). What is the consequence of this stark difference with respect to neural function? Recently, some studies demonstrated that electrical stimulation actually triggers side effects at the neural level, which were initially unnoticed. For example, new data from epidural spinal cord stimulation for spinal cord injury showed that continuous stimulation of recruited sensory afferents produces a disruption of proprioceptive percepts at stimulation parameters commonly employed in clinical trials (Formento et al. 2018). Similarly, the inability to elicit robust proprioceptive percepts (Cimolato et al. 2023) is striking in the application of electrical stimulation of the peripheral nerves for the restoration of somato-sensations.

In fact, large-diameter proprioceptive afferents should have the lowest threshold for electrical stimulation. Therefore, these afferents should be the easiest sensory afferents to recruit with neural interfaces (Rattay 1986; Capogrosso et al. 2013; M. A. Schiefer, Triolo, and Tyler 2008; McNeal 1976). However, because of anatomical and geometrical constraints, in practice electrical neurostimulation leads to the activation of mixed diameter fiber distributions and, consequently, different sensory modalities (Capogrosso et al. 2013; Stanisa Raspopovic et al. 2012; Greiner et al. 2021). Therefore, cutaneous afferents are recruited concurrently, along with larger diameter afferents (Kibleur et al. 2020). These fibers converge on interneurons in the spinal cord where they undergo the first layer of sensory processing, representing a highly shared sensory network node.

It is conceivable that artificially-generated patterns of mixed neural activity hinder some of the computations of these shared network nodes, thus impairing natural circuit processing, hence, perception (**Figure 3.1**). In order to demonstrate this conjecture, we need tools that allow us to visualize and identify a direct measure of neural computation processes (Barack and Krakauer 2021). Analysis of population neural dynamics using neural manifolds is commonly employed to study computational objects that process information in the cortex (Sadler et al. 2014; Churchland et al. 2012; Gallego et al. 2017; 2018) and, more recently, in

the spinal cord. Indeed, one study showed that intraspinal population responses contain simple structures that enable the examination of complex processes such as walking (Lindén et al. 2022).



**Figure 3.1, Electrical stimulation disrupts computations of ongoing network processes.** Neural networks (cyan, magenta shaded areas) produce a desired neural function (Function A, B, respectively) within a highly shared neural architecture. These networks may share processing layers (or nodes) to process input information. Top, naturally-generated neural activity of unrelated neural functions successfully processes ongoing information input throughout the shared neural architecture. Bottom, artificially-generated neural activity targeted to restore Function B (magenta) artificially processes information input, while impairing information processing from an unrelated neural function (Function A, cyan). Specifically, artificially-induced processing in the shared processing nodes concurrently hinders computations of unrelated ongoing processing of Function B, which may also be unselectively recruited by the electrical stimulation. Taken from (Katic Secerovic et al. 2021) with permission.

Therefore, here we employed neural population analysis of intraspinal neural dynamics to 1) visualize neural computations underlying the processing of brief proprioceptive percepts elicited by single short pulses of electrical stimulation and 2) study how these computations were altered when concurrent electrical stimulation was delivered to sensory afferents from a different nerve. This experimental design offered a simplified version of the more general problem of the stimulation effects on unrelated neural functions, thus allowing us to execute casual manipulation and quantification of neural variables.

Therefore, we designed a series of electrophysiology experiments in anesthetized monkeys, who share distinguishable projections with the human nervous system distinct from all other animals (Lemon 2008; Sinopoulou et al. 2022). We recorded and analyzed artificially evoked proprioceptive neural signals both in the cervical spinal cord and somatosensory cortex. Specifically, we induced proprioceptive input in the hand and forearm by cuff electrode stimulation of the muscle branch of the radial nerve, which does not contain cutaneous afferents (Rudomin and Schmidt 1999; Confais et al. 2017). Then, we studied how concurrent stimulation of somatosensory afferents in the cutaneous branch of the radial nerve impacted the spinal and cortical proprioceptive responses. Using neural population analysis, we examined dorso-ventral intra-spinal spiking activity in response to muscle

nerve stimulation pulses and performed dimensionality reduction to observe the spinal neural trajectories. Concurrent stimulation of the cutaneous afferents disrupted these neural trajectories, suggesting a significant degradation of proprioceptive information processing in the spinal cord. Changes in proprioceptive information appeared as reduced cortical responses in the somatosensory cortex. Our results show that intraspinal neural population dynamics can capture the processing of sensorimotor information in spinal networks and its disruption of this information processing during artificial electrical stimulation.

## **3.2 Methods**

### **3.2.1 Animals**

The study was conducted according to the guidelines of the Declaration of Helsinki, and approved by the local (Research Institute of Medical Primatology) Institutional Ethics Committee (protocol № 38/1, October 31, 2019) and by the University of Pittsburgh Animal Research Protections and IACUC (ISOOO17081).

Three adult *Macaca Fascicularis* and one *Macaca Mulatta* monkeys were involved in the study (MK1 - MK 42286, male, 4 years old, 3.5 kg, MK2 - MK 42588, male, 4 years old, 3.35 kg, MK4 - MK 42328, male, 4 years old, 3.48 kg; MK3 - 219-21, male, 7 years old, 11.5 kg). Data for all *Macaca Fascicularis* monkeys were acquired in the National Research Centre "Kurchatov Institute", Research Institute of Medical Primatology, Sochi, Russia. Data for *Macaca Mulatta* monkey was acquired in the University of Pittsburgh, PA, US.

### **3.2.2 Surgical procedures**

All the surgical procedures were performed under full anesthesia induced with ketamine (10 mg/kg, i.m.) and maintained under continuous intravenous infusion of propofol (1% solution in 20 ml Propofol/20 ml Ringer 1.8 to 6 ml/kg/h), in addition to fentanyl (6-42 mcg/kg/hour) for the *Macaca Mulatta*, using standard techniques. Throughout the procedures, the veterinary team continuously monitored the animal's heart rate, respiratory rate, oxygen saturation level and temperature. Surgical implantations were performed during a single operation lasting approximately 8 hours. We fixed monkeys' heads in a stereotaxic frame securing the cervical spine in a prone and flat position. First, we implanted two silicon cuff electrodes (Microprobes for Life Science, Gaithersburg, MD 20879, U.S.A. and Micro-Leads, Somerville, MA 02144, U.S.A.) on the distal ends of the superficial branch and deep branch of radial nerve that we determined via anatomical landmarks. We then inserted EMG electrodes in the Extensor Digit. Communis, the Flexor Carpi Radialis and the Flexor Digit. Superficialis. We stimulated electrically two branches of the radial nerve and looked at the EMG response to verify which branch was the muscle branch and which one was the cutaneous branch. Second, we implanted the brain array using a pneumatic insertion system (Blackrock Microsystem). We performed a craniotomy and we incised the dura in order to get clear access to the central sulcus. We identified motor and sensory brain areas through anatomical landmarks and intra-surgical micro-stimulation. Specifically, we verified that electrical stimulation of the motor cortex induced motor responses in the hand muscles. We then determined the position of the somatosensory area S1 in relation to this spot and implanted the UTAH array electrode (Blackrock Microsystems, Salt Lake City, UT, U.S.A.) across Areas 1 and 2 (and Areas 3 and 4 for the *Mulatta* monkey), 1.2 mm lateral to

midline and 3.1 mm deep using a pneumatic inserter (Blackrock Microsystems, Salt Lake City, UT, U.S.A.).

Finally, we performed a laminectomy from C3 to T1 and then directly exposed the cervical spinal cord. We implanted a 32-channel linear probe (linear Probe with Omnetics Connector 32 pins - A1x32-15mm-50-177-CM32; NeuroNexus, Ann Arbor, MI, U.S.A.) and a 64-channel linear probe (double linear Probe with Omnetics Connector 64 pins - A2x32-15mm-100-200-177; NeuroNexus, Ann Arbor, MI, U.S.A.) in the gray matter at the C5 spinal segment. To implant the probe, we opened the dura mater and created a small hole in the pia using a surgical needle through which penetration of the probe with micromanipulators was possible. We implanted the arrays using MM-3 micromanipulators (Narishige, Tokyo, Japan; David Koff Instruments for the Mulatta monkey). Experiments in all four monkeys were terminal. At the end the animals were euthanized with a single injection of pentobarbital (60 mg/kg) and perfused with PFA for further tissue processing.

### **3.2.3 Electrophysiology in sedated monkeys**

Monkeys were sedated with a continuous intravenous infusion of propofol that minimizes effects on spinal cord stimulation (Toossi et al. 2019).

### **3.2.4 Data analysis**

We applied all data analysis techniques offline.

#### **3.2.4.1 Pre-processing**

We filtered raw signals recorded with 32 - electrode array implanted in the spinal cord, as well as signals documented with UTAH array in somatosensory cortex with comb filter to remove artefacts on 50 Hz/60 Hz (depending on the country where the experiments have been done) and its harmonics. We designed a digital infinite impulse response filter as a group of notch filters that are evenly spaced at exactly 50 Hz/60 Hz.

We detected single pulses of the deep branch of the radial nerve and extracted 430 ms of the intra-spinal and intra-cortical signal post stimulation.

#### **3.2.4.2 Identification of sensory volleys resulting from muscle nerve stimulation**

We were able to detect afferent volleys and the resulting gray matter response field evoked with muscle nerve stimulation in the spinal cord. We applied a 3rd order Butterworth digital filter and extracted the signal from 10 - 1000 Hz. Afferent volley is defined as a first volley after the stimulation pulse, occurring 3 - 4 ms after the stimulation (unique physiology of a single animal causes these variations) and followed with gray matter response field. We quantified the amount of processed proprioceptive information by neural network by measuring peak-to-peak amplitude values of the gray matter response field.

We applied a similar procedure to extract the muscle nerve evoked potentials recorded in the somatosensory cortex.

### 3.2.4.3 Characterization and quantification of neural spiking activity

We extracted neural spiking activity by applying a 3rd order Butterworth digital filter to the raw signal, separating the signal in frequency range from 800 Hz to 5000 Hz. We detected the spikes using thresholding algorithm (Quiroga, Nadasdy, and Ben-Shaul 2004). We determined the threshold value separately for each recording channel. To detect the accurate threshold value, we concatenated all data sets that we aim to analyze in a single file. All analyzed data sets were concatenated in a single file in order to detect proper threshold values. The same procedure was applied to intra-spinal and intra-cortical recordings.

Multiunit activity is presented in form of rasterplot and quantified with peri-stimulus time histogram (PSTH). Each dot in rasterplot represents a single detected spike. Every rasterplot row corresponds to the intra-spinal or intra-cortical activity perturbed with a single muscle nerve stimulus pulse. PSTH is quantified with mean event rate, defined as the average number of spikes across all single pulses of muscle nerve stimulation, within defined time frame.

### 3.2.4.4 Neural manifold and trajectory length

To project the trajectories in the neural manifold, we previously computed multiunit spiking activity for each condition. We calculated the spiking activity for every 100 ms with a sliding window of 10 ms over 430 ms around each muscle stimulation pulse. We zero-padded the first repetition for 90 ms and then overlapped 90ms from the previous repetition for the rest of repetitions. The final step to smooth the spiking activity was the application of a Gaussian kernel (s.d. 20 ms) to the binned square-root-transformed firings (10 ms bin size) of each recorded multiunit. For each condition, this resulted in a matrix of dimensions  $C \times T$ , where  $C$  is the number of channels in the dorso-ventral linear probe and  $T$  is the number of 10 ms windows in a repetition concatenated for all the repetitions within a condition. Subsequently, we proceed to eliminate noisy repetitions. We discarded those repetitions within each condition whose s.d. was greater than twice the total s.d. across all repetitions plus the total mean of the s.d. across all repetitions for that condition. For cortical data, we previously converted the distribution of s.d. to a lognormal distribution to apply this outlier cleaning rule.

To calculate the latent dynamics for each monkey, we z-scored each condition's spiking activity before applying dimensionality reduction principal component analysis (PCA) to the concatenated spike counts. We selected the first 3 principal components that explained most of the variance (~65% for all 3 monkeys, 54% for one monkey) as neural modes to define the neural manifold. Convergence points were reached at the first 3 to 5 dimensions according to the eigenspectrum of each monkey. In this low dimensionality space, we proceeded by eliminating repetitions as a function of the distance to the median trajectory. In particular, we computed the median trajectory for each 10 ms window for each condition. For each window, we calculated the distance between the median trajectory and the trajectory elicited by each repetition within a condition. 25th and 75th percentiles of the obtained distances allowed to discard trajectories whose distance was greater than the 75th percentile plus 1.5 times the interquartile range of the averaged trajectory for that repetition across all 10 ms windows. The same criterion was applied for the lower range. Finally, we quantified the trajectory length for the remaining repetitions for each condition and calculated the average trajectory length across all 10 ms windows.

### **3.2.5 Statistical Analysis**

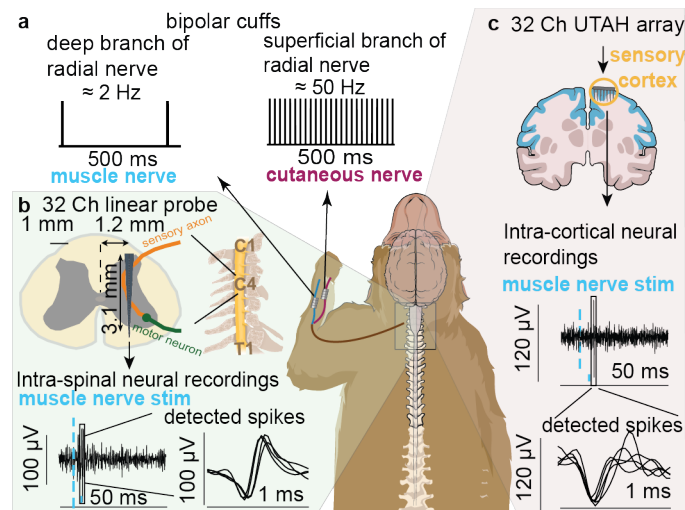
Multi-group significance comparison of data obtained from the neural manifold for each condition in all four monkeys was tested using Kruskal-Wallis test. The level of significance was set at \*\*\* $p < 0.005$ .

Significance of suppressed peak-to-peak amplitude values of afferent volleys was analyzed with one-way analysis of variance revealed (ANOVA). Each point represents the peak-to-peak amplitude as a response to a single stimulus pulse. Boxplots show: the central mark indicates the median, and the bottom and top edges of the box indicate the 25th and 75th percentiles, respectively. The whiskers extend to the most extreme data points not considered outliers, and the outliers are plotted individually using the 'o' symbol. The level of significance was set at \*\*\* $p < 0.001$ , \*\* $p < 0.01$  and \* $p < 0.05$ .

## **3.3 Results**

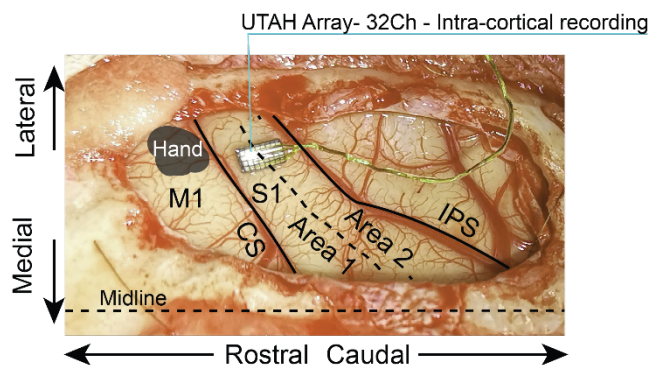
### **3.3.1 Simultaneous brain and spinal neural recordings during electrical nerve stimulation of multiple sensory modalities**

We designed a unique experimental setup in non-human primates as a proxy to understand how artificial inputs can influence neural network function in a controlled fashion. Specifically, we examined how stimulation of cutaneous afferents affects spinal network processing of proprioceptive pulses. The radial nerve, carrying sensory signals from the dorsal part of the forearm and hand, splits in proximity of the elbow into a pure-muscle and a pure-cutaneous branch (i.e., the deep and superficial branches of the radial nerve (Confais et al. 2017), respectively) offering the opportunity to provide modality-selective sensory stimuli. We implanted cuff electrodes on these two branches to elicit either proprioceptive or cutaneous inputs via electrical stimulation (**Figure 3.2a**). We artificially provided brief proprioceptive pulses by stimulating the muscle branch of the radial nerve with single electrical pulses (~2 Hz) below motor threshold. To assess the influence of artificial cutaneous input on the induced proprioceptive input, we provided cutaneous stimulation as continuous ~50 Hz pulses, a typical stimulation frequency used in human studies. Threshold (Thr) was defined as an amplitude that clearly evoked potentials in the spinal cord in response to low-frequency stimulation. We tested two conditions: stimulating the nerve at a low ( $0.9 \times \text{Thr}$ ) or high amplitude ( $1.1 \times \text{Thr}$ ). Stimulation amplitude corresponds to the amount of artificially recruited fibers. To study the transmission of artificially induced proprioceptive percepts from the periphery to the cerebral cortex, we recorded the Macaque monkeys' intra-spinal neural signals from a dorso-ventral 32-channel linear probe implanted in the gray matter of the spinal cord C5 segment (**Figure 3.2b**). Furthermore, we extracted intra-cortical neural signals (**Figure 3.2c**) using a 32-channel UTAH array placed in the somatosensory cortex (Area S1/S2, **Figure 3.3**).



**Figure 3.2, Experimental setup: Schematic illustration of experiments.** a) Stimulation: we implanted two nerve cuffs for stimulation on the superficial branch (cutaneous nerve) and the deep branch (muscle nerve) of the radial nerve. We stimulated the muscle nerve at  $\sim 2$  Hz, exclusively, or concurrently with  $\sim 50$  Hz stimulation of the cutaneous nerve branch. b) We recorded neural activity with a 32-channel dorso-ventral linear probe implanted in the gray matter of the spinal segment C5. Typical intra-spinal neural responses induced by stimulation of the muscle nerve. Zoom insets show examples of detected spike waveforms, e.g., single unit responses to proprioceptive pulses. c) We recorded neural activity with a 32-channel multi-electrode array in the somatosensory cortex and provided intra-cortical neural responses, similar as in b. Taken from (Katic Secerovic et al. 2021) with permission.

In summary, we recorded neural signals in the spinal cord and the somatosensory cortex of three anesthetized *Macaca Fascicularis* (MK1, MK2, MK4) and one *Macaca Mulatta* (MK3) monkey while stimulating only proprioceptive, or concurrently proprioceptive and cutaneous afferents.

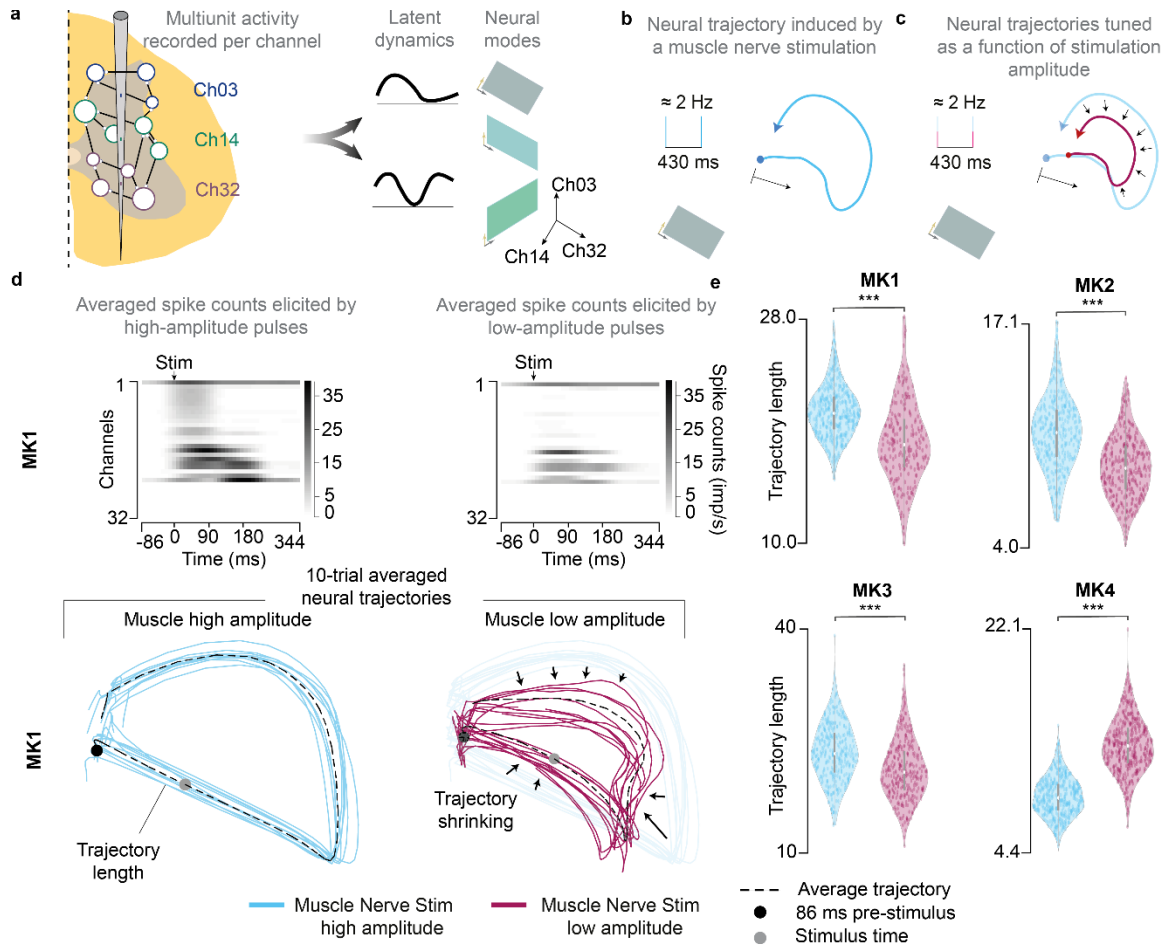


**Figure 3.3, Experimental procedure and electrophysiology details.** a) Representative picture showing the position of the UTAH array in relation to brain areas. We identified specific brain areas through anatomical landmarks and micro-stimulation of the cortex. We verified that a single pulse of stimulation delivered induced clear responses in the hand muscles. We determined the somatosensory area S1 in relation to the identified M1 anatomically and implanted the UTAH array electrode (Blackrock Microsystems) across Areas 1 and 2. Taken from (Katic Secerovic et al. 2021) with permission.



### 3.3.2 Proprioceptive inputs elicit robust trajectories in the spinal neural manifold

We explored the effect of brief pulses of artificially-generated proprioceptive inputs on the intraspinal neural population dynamics.



**Figure 3.4, Intra-spinal neural population analysis.** a) Latent dynamics and neural modes obtained from the multiunit recorded per channel. Left, a sketch of the dorso-ventral linear probe that recorded the activity of the spinal multiunit neural networks (each circle represents a recorded unit). Each color represents the neural activity recorded by each channel. Right, dimensionality reduction technique identifies the neural modes that define the low-dimensional spaces. In these subspaces, the neural activity followed precise dynamics. We hypothesized that b) a muscle nerve stimulation pulse elicits neural trajectories and that c) these neural trajectories shrink as a function of the stimulation amplitude. d) Top, averaged multiunit spike counts across all 32 channels, sorted by the highest spiking activity after the muscle nerve stimulation, for MK1. Bottom, resultant 10-trial averaged neural trajectories elicited by muscle nerve stimulation for MK1. This is plotted both at a high and low stimulation amplitude to appreciate the phenomenon of trajectory shrinking. e) Statistical quantification of the trajectory length for all monkeys for high and low stimulation amplitude of the muscle nerve (\*\*\* $p < 0.001$ ; \*\* $p < 0.01$ ; \* $p < 0.05$ ; Kruskal-Wallis test with 380 and 231 points for high and low amplitude, respectively, for MK1; 353 and 351 points for high and low amplitude, respectively, for MK2; 353 and 343 points, respectively, for MK3; 391 and 394 points, respectively, for MK4). Violin plots: each dot corresponds to the computed trajectory length for a trial, forming a Gaussian distribution of trajectory lengths. The central mark represented as a white dot indicates the median, and the gray line indicates the 25th and 75th percentiles. The whiskers extend to the most extreme data points not considered outliers. Trial corresponds to a stimulation pulse. Taken from (Katic Secerovic et al. 2021) with permission.

Because proprioceptive signals enter the spinal cord from the dorsal aspect and project towards medial and ventral laminae (Kandel, E., Schwartz, J. & Jessel, T., n.d.), we performed neural population analysis of the multiunit spiking data from all the channels of



our linear probe (**Figure 3.4a**) in response to 2 Hz muscle nerve stimulation. Specifically, we applied dimensionality reduction to unveil the latent properties of the spinal neural processing via principal component analysis (PCA). PCA identified three neural modes that sufficed to explain 54-65% of the variance of the spikes counts of multiunit threshold crossings recorded by the spinal probe for ~350 ms following each proprioceptive stimulus pulse. We then sought whether the neural manifold defined by these neural modes contained simple computational objects (e.g., clear neural trajectories that captured the changes of time-varying spikes, **Figure 3.4b, c**).

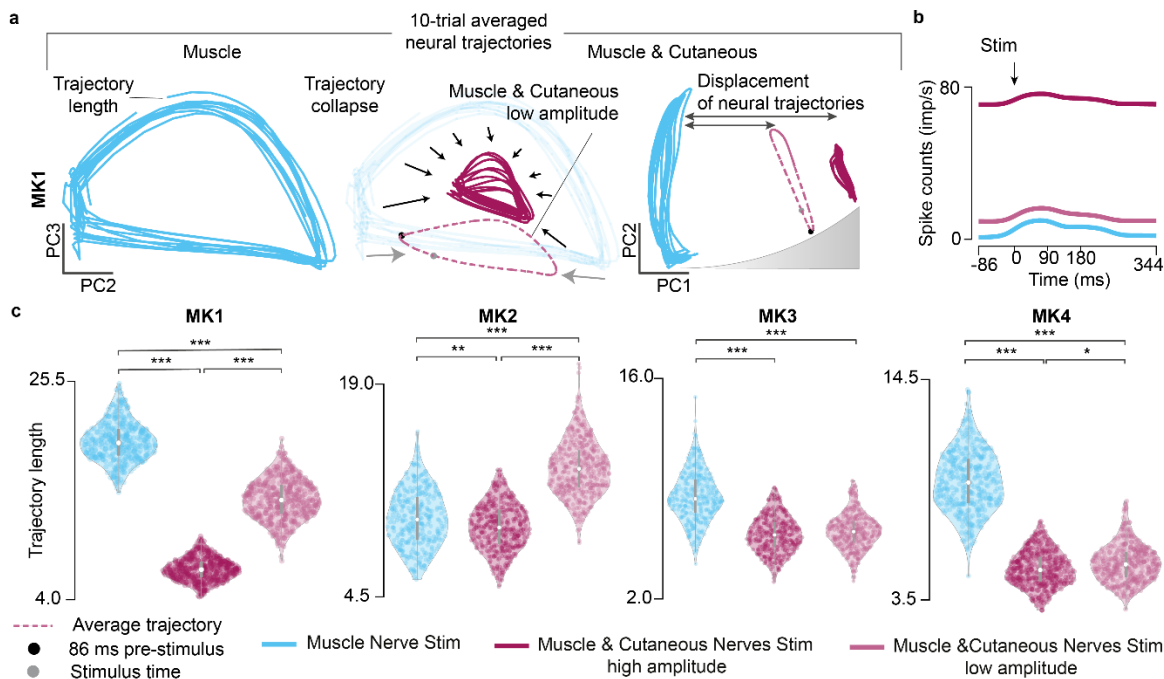
In the spinal manifold, the multiunit spike counts elicited very consistent dynamics after each stimulation pulse in the form of closed trajectories that were qualitatively similar in all monkeys (**Figure 3.4d**). Because averaged spiking responses initiated and terminated with baseline activity (i.e., no stimulation), the neural dynamics were represented by closed neural trajectories. Given the robustness and reproducibility of these trajectories, we hypothesized that estimated trajectory lengths could be used as a proxy to measure the amount of proprioceptive information processed within the recorded site. The logical consequence of this interpretation is that the length of the trajectories could be proportional to the amount of proprioceptive input processed.

Since the stimulation amplitude controls the number of recruited afferents, we tested this assumption by computing the neural trajectories induced by proprioceptive inputs both at high and low stimulation amplitudes (i.e., more or less recruited afferents, respectively). As expected, we found that muscle nerve stimulation at a higher amplitude elicited longer trajectories and vice versa (**Figure 3.4d**). This observation was consistent in MK1 (relative mean difference, +14.17%), MK2 (+24.05%) and MK3 (+44.21%, **Figure 3.4e**), but not in MK4 (-33.76%), probably due to the higher variability in the overall trajectories for this monkey.

In summary, we showed that population analysis of a dorso-ventral linear probe in the spinal cord shows highly robust and reproducible trajectories in the neural manifold in response to artificial proprioceptive pulses. We proposed to quantify the length of this trajectory as a means to assess the amount of proprioceptive information processed in the spinal cord.

### **3.3.3 Continuous electrical stimulation of the cutaneous nerve disrupts intra-spinal proprioceptive neural trajectories**

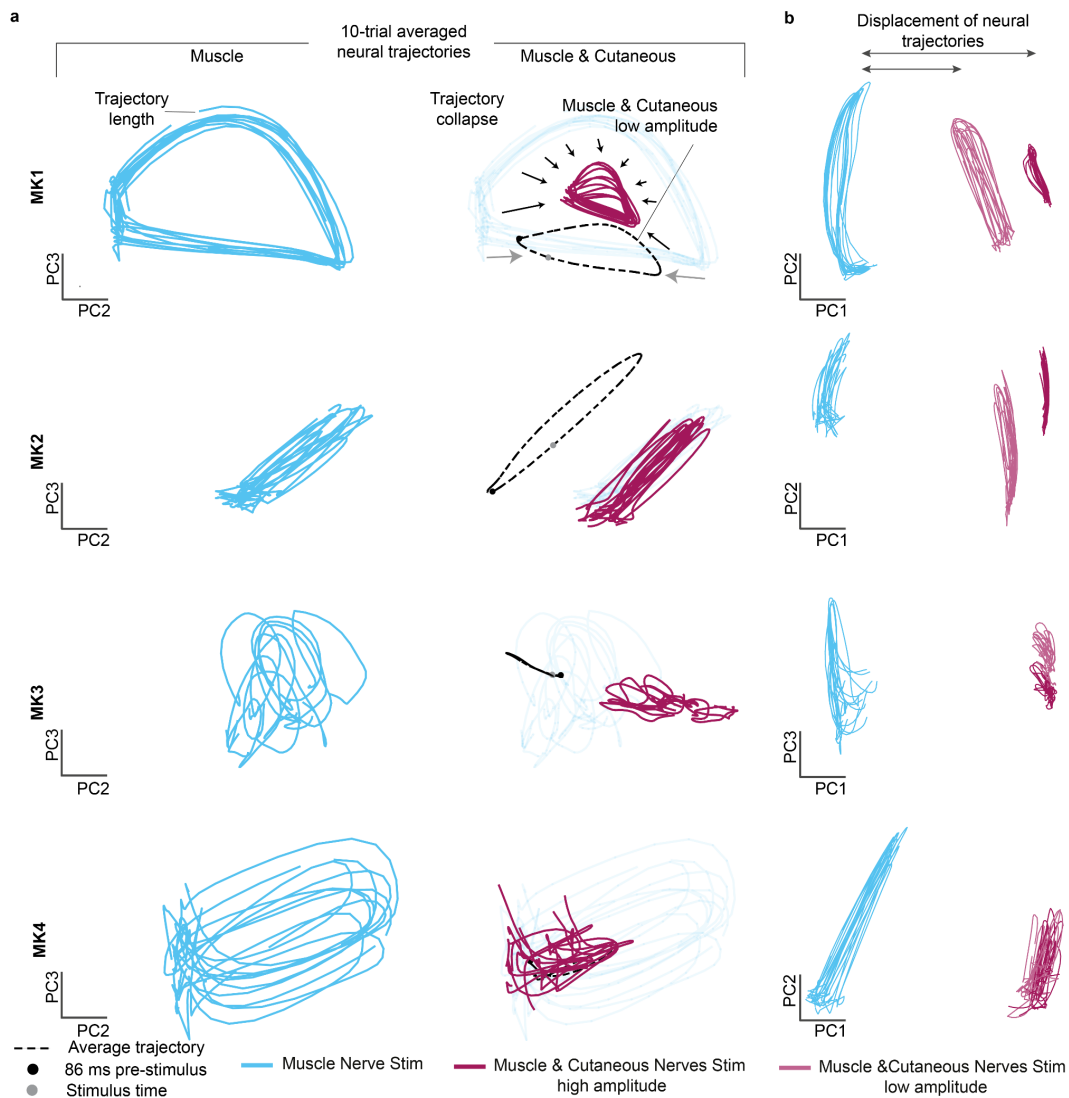
We next evaluated the impact of concurrent artificial cutaneous input on proprioceptive information processing. We projected on the neural manifold neural trajectories elicited by the stimulation of the proprioceptive branch. All four monkeys exhibited robust trajectories in response to proprioceptive inputs and, in all four monkeys, concurrent stimulation of cutaneous afferents significantly reduced the trajectory lengths (**Figure 3.5a**) or even completely disrupted their dynamics (**Figure 3.6**), albeit with different effect sizes. MK1 (relative mean difference, -66.03%), MK3 (-27.47%) and MK4 (-44.91%) exhibited the largest disruption, while MK2 (-5.89%) was significantly disrupted but to a lower effect size. To validate this result, we repeated the same experiment using lower amplitudes for the stimulation of the cutaneous afferents. Cutaneous stimulation at a low amplitude yielded less disruption (i.e., longer proprioceptive trajectory lengths) than at a high stimulation amplitude (**Figure 3.5c**), suggesting that the amount of neural computation disrupted is inversely proportional to stimulation intensity of cutaneous afferents.



**Figure 3.5, Neural trajectory lengths.** a) Comparison of the neural trajectories induced by muscle nerve stimulation and concurrent cutaneous stimulation across PC2-PC3 vs PC1-PC2. Gray dashed lines indicate average trajectory for muscle and cutaneous nerves stimulation at a low amplitude. b) Averaged spike counts across all trials and all channels for each stimulation condition for MK1. c) Statistical analysis of the trajectory lengths for each stimulation condition. Violin plots: each dot corresponds to the computed trajectory length for a trial, forming a Gaussian distribution of trajectory lengths. The central mark represented as a white dot indicates the median, and the gray line indicates the 25th and 75th percentiles. The whiskers extend to the most extreme data points not considered outliers. Trial corresponds to a stimulation pulse. (\*\* $p < 0.01$ ; \*\*\* $p < 0.001$ ; Kruskal-Wallis test with 381, 470 and 453 points for muscle nerve stimulation, concurrent cutaneous stimulation at high amplitude and low amplitude, respectively, for MK1; 369, 410 and 411 points, respectively, for MK2; 353, 376 and 397 points, respectively, for MK3; 392, 380 and 371 points, respectively, for MK4). Taken from (Katic Secerovic et al. 2021) with permission.

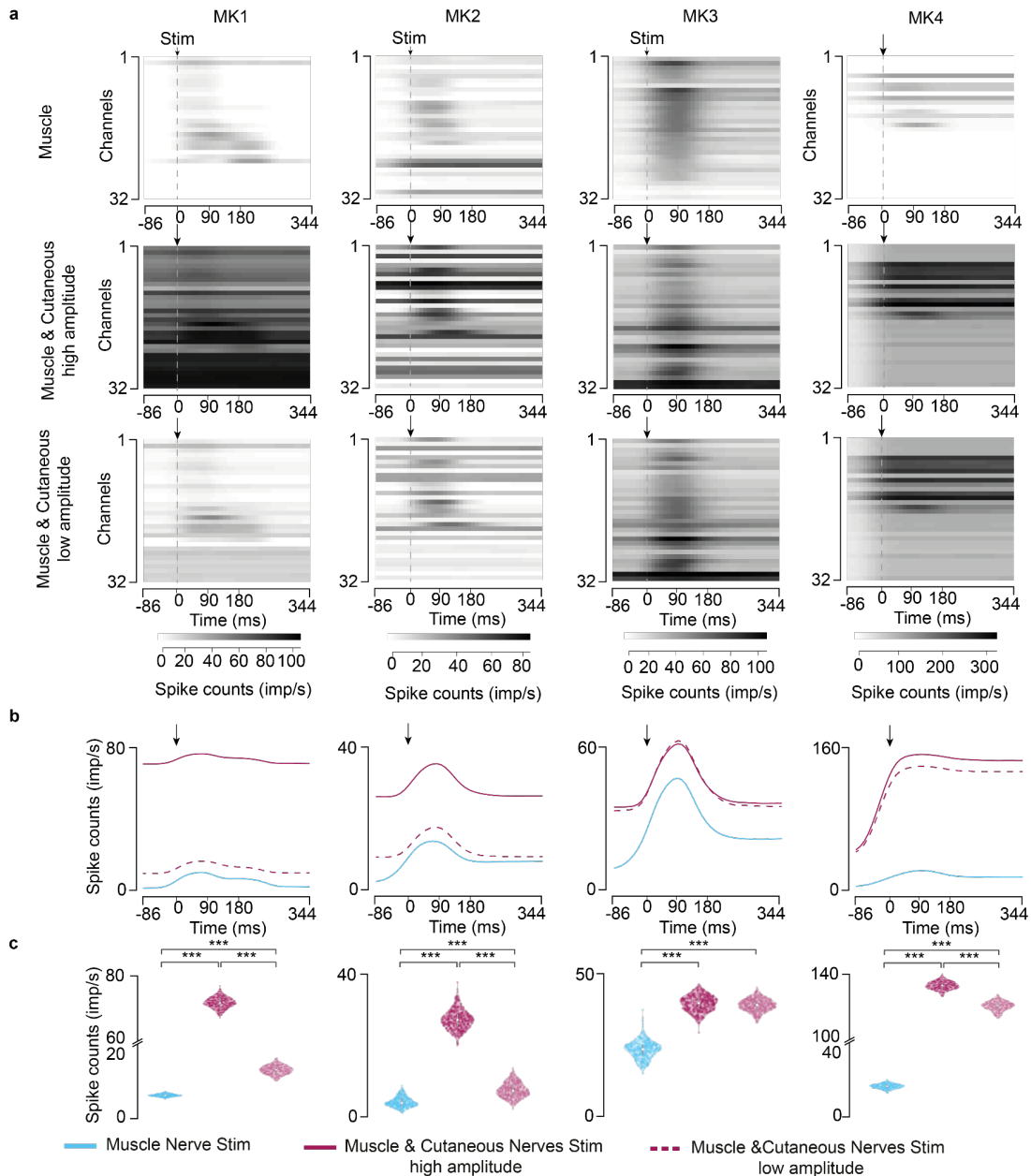
This observed trajectory disruption is particularly interesting considering that, during concurrent proprioceptive and cutaneous stimulation, the spinal cord received significantly more artificial input. Indeed, concurrent stimulation of the cutaneous afferents significantly increased overall spike counts in the recorded spinal circuitries (+5191.68% for MK1, +234.71% for MK2, +68.37% for MK3, +754.94% for MK4, **Figure 3.5b**, **Figure 3.7**). However, this increase was not captured by the neural trajectories, which strengthens the case that those trajectory lengths mainly represent proprioceptive information processing. - Additionally, we found that the disruption of information processing was captured in principal component (PC) 2 and PC3, where neural trajectories shrunk as a function of stimulation intensity. Moreover, PC1 depicted the displacement of these neural trajectories caused by the amount of concurrent cutaneous input (**Figure 3.5a**, **Figure 3.7**). In other words, when the spinal cord received inputs induced by concurrent muscle and cutaneous nerves stimulation, the neural trajectories were displaced across PC1, away from the proprioceptive neural trajectories. This displacement was proportional to the stimulation intensity and, in turn, to the computed spiking activity in the spinal cord (**Figure 3.7**). In particular, MK1 (+94.52%) and MK2 (+45.99%) produced longer proprioceptive trajectory lengths than MK3 (+3.49%) and MK4 (+5.22%) during concurrent cutaneous stimulation at a low amplitude. Indeed, the overall spike counts were very similar in MK3 and MK4 both at low and high stimulation amplitudes (**Figure 3.7**) (relative mean difference from

concurrent high to low amplitude, -84.44% for MK1, -59.82% for MK2, -1.69% for MK3, -8.40% for MK4), thereby eliciting similar neural trajectory lengths. These results infer that the main PCs clearly captured the amount of proprioceptive processed information as a function of concurrent stimulation amplitude. Indeed, neural trajectories that were further displaced across PC1 resulted in shorter neural trajectory lengths in PC2-PC3 (during concurrent high stimulation amplitude), whereas those that remained closer to the proprioceptive neural trajectories in PC1 were less disrupted in PC2-PC3 (during concurrent low stimulation amplitude, **Figure 3.5a**).



**Figure 3.6, Intraspinial neural trajectories.** a) Comparison of the neural trajectories induced by muscle nerve stimulation and concurrent cutaneous stimulation in all monkeys. Gray dashed lines indicate average trajectory for muscle and cutaneous nerves stimulation at a subthreshold amplitude. b) Visualization of the displacement of the neural trajectories across PC1 in all monkeys. The displacement is proportional to the spiking activity induced by each stimulation condition (i.e. the distance between neural trajectories induced by muscle nerve stimulation and concurrent cutaneous nerve at a low amplitude is lower than the distance between the neural trajectories induced by concurrent stimulation of the cutaneous nerve at a high amplitude). Taken from (Katic Secerovic et al. 2021) with permission.

In summary, we showed that concurrent stimulation of the cutaneous nerve significantly suppressed proprioceptive neural trajectory lengths, suggesting that concurrent artificial recruitment of cutaneous afferents hinders the processing of proprioceptive inputs in the spinal cord.

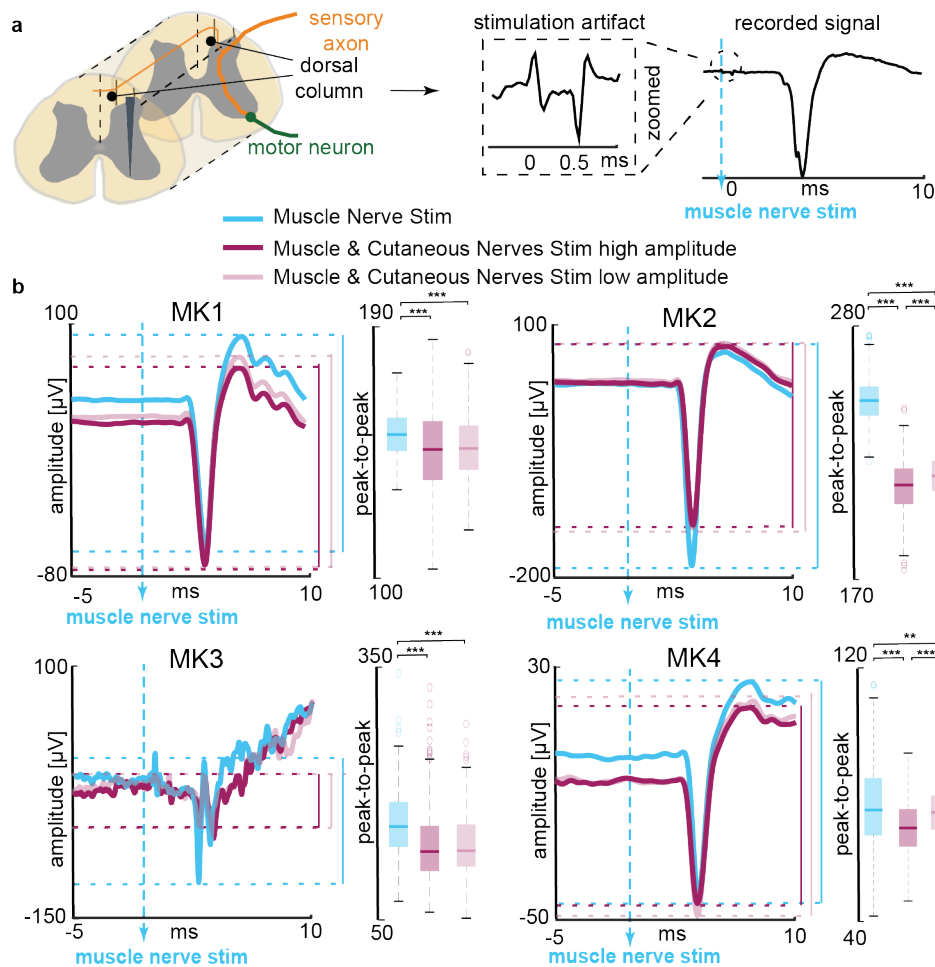


**Figure 3.7, Spinal spiking activity induced by concurrent cutaneous nerve stimulation.** a) Averaged spiking activity for each channel. Spike counts were averaged across all trials for each stimulation condition for four monkeys. Averaged multiunit spike counts across all 32 channels, sorted by the highest spiking activity after the muscle nerve stimulation. b) Averaged spiking activity. Spike counts were averaged across all trials and all channels for each stimulation condition for four monkeys. c) Statistical analysis of the spiking activity for each stimulation condition (\*\* $p < 0.01$ ; \*\*\* $p < 0.001$ ; \* $p < 0.05$ ; Kruskal-Wallis test with 387, 477 and 461 points for muscle nerve stimulation, concurrent cutaneous stimulation at high amplitude and low amplitude, respectively, for MK1; 374, 410 and 412 points, respectively, for MK2; 353, 400 and 399 points, respectively, for MK3; 401, 388 and 376 points, respectively, for MK4). Violin plots: each dot corresponds to the computed trajectory length for a trial, forming a Gaussian distribution of trajectory lengths. The central mark represented as a white dot indicates the median, and the gray line indicates the 25th and 75th percentiles. The whiskers extend to the most extreme data points not considered outliers. Trial corresponds to a stimulation pulse. Taken from (Katic Secerovic et al. 2021) with permission.

### **3.3.4 Cutaneous electrical stimulation reduced proprioceptive afferent volleys, spinal cord grey matter field potentials and multiunit responses**

To validate our findings, we looked for correlates using classical electrophysiology measures. We first inspected stimulation triggered average field potentials from the grey

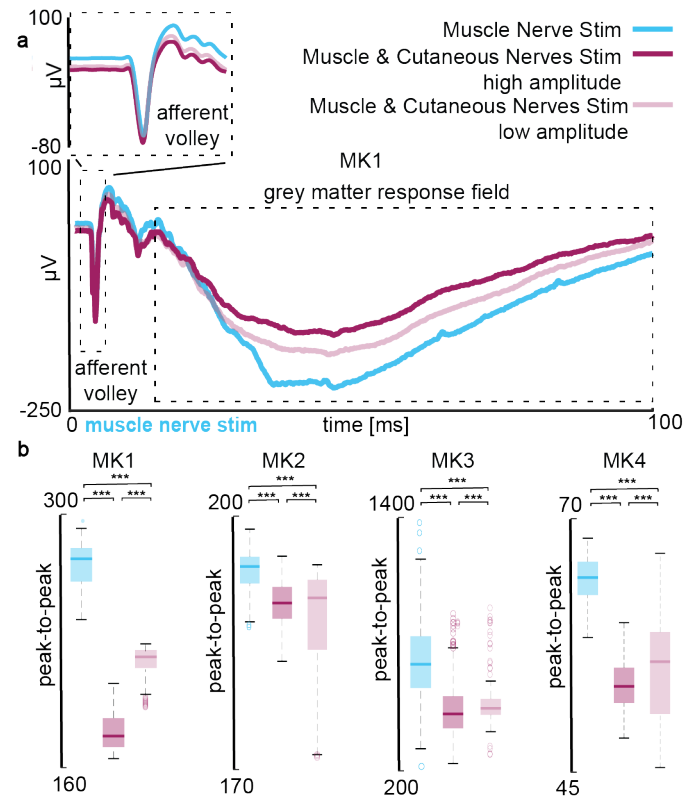
matter of the spinal cord, defined as the mean neural response across each single muscle nerve branch stimulation pulse (**Figure 3.9a**). Afferent volleys were detected at a latency between 3-4 ms after each proprioceptive pulse (**Figure 3.8** and **Figure 3.9a**).



**Figure 3.8, Proprioceptive afferent volley peak-to-peak amplitude suppression.** a) Definition of the afferent volley. Triggered-average signal showed stimulation artifacts in the signal (zoomed insight) around the time of muscle nerve stimulation (pulse width: 0.5 ms) while the afferent volley appeared 3-4 ms after the stimulation (depending on the monkey). b) Afferent volleys in four monkeys. Afferent volleys as a response to proprioceptive nerve stimulation (cyan), with concurrent cutaneous nerve stimulation (magenta; high stimulation amplitude – solid color; low stimulation amplitude – semi-transparent). Volleys are given as an example of a single dorsal channel and are averaged across all muscle nerve stimulation pulses. We compared peak-to-peak amplitude values of afferent volleys over 2 conditions with one-way ANOVA with 300 points, where each point represents the peak-to-peak amplitude as a response to a single stimulus pulse. Boxplots: The central mark indicates the median, and the bottom and top edges of the box indicate the 25th and 75th percentiles, respectively. The whiskers extend to the most extreme data points not considered outliers, and the outliers are plotted individually using the 'o' symbol. Asterisks: \*\*\* $p < 0.001$ ; \*\* $p < 0.01$ . Taken from (Katic Secerovic et al. 2021) with permission.

Continuous electrical stimulation of the cutaneous nerve reduced the peak-to-peak amplitude of these proprioceptive volleys in all four monkeys (**Figure 3.8**) and the reduction was proportional to stimulation intensity (muscle nerve stimulation vs muscle & cutaneous nerve stimulation high amplitude, mean values difference: MK1: -9%, MK2: -47%, MK3: -25%, MK4: -14%; muscle nerve stimulation vs muscle & cutaneous nerve stimulation low amplitude: MK1: -8%, MK2: -40%, MK3: -22%, MK4: -1%). Since volleys represent sensory inputs, these results suggest that part of the disruption that we observed in the neural trajectories may be a consequence of reduced proprioceptive inputs in the spinal cord.

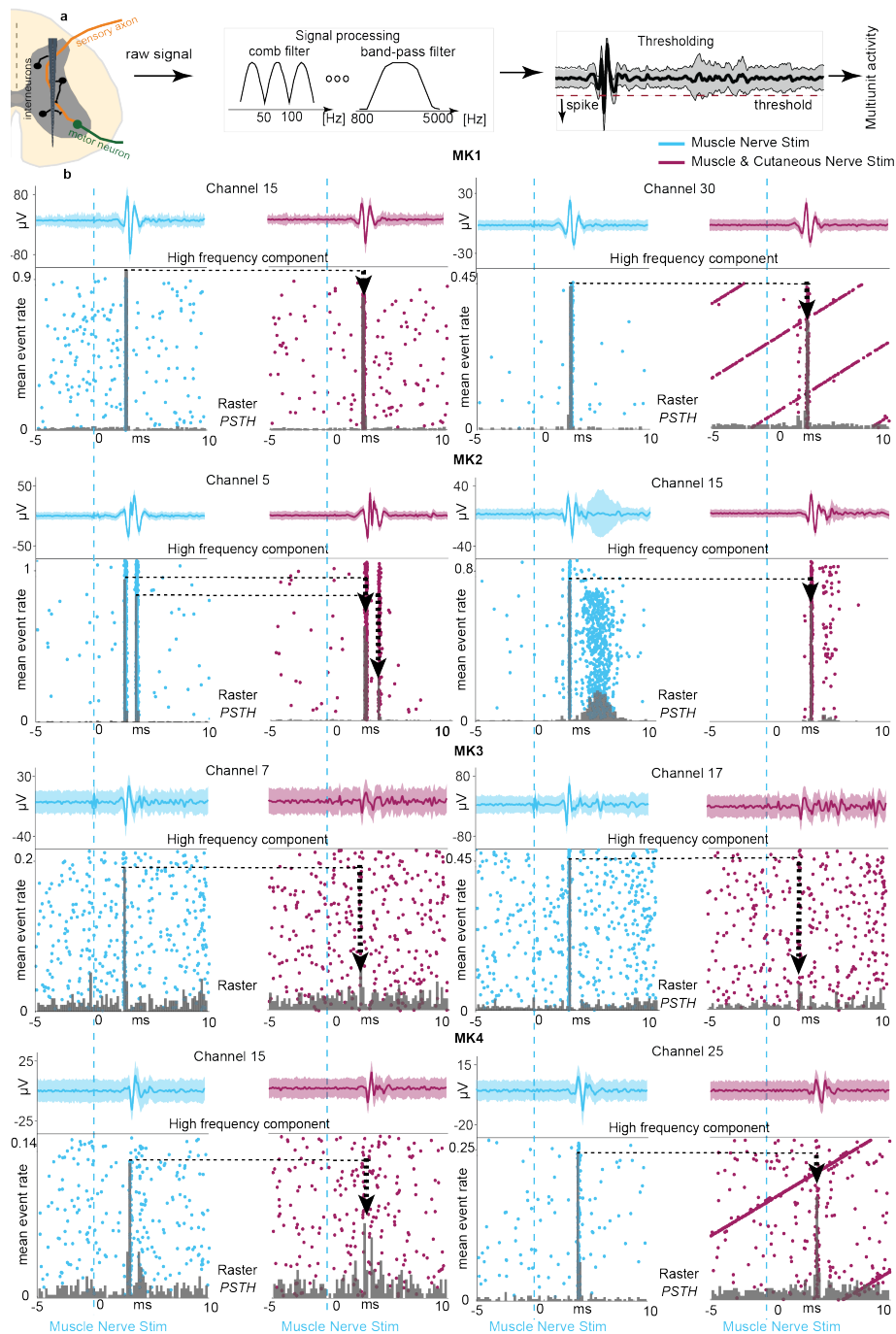
Additionally, grey matter response fields following each proprioceptive volley were also substantially suppressed during electrical stimulation. Peak-to-peak amplitude values of the fields were significantly reduced to a much larger extent than the volleys. Again, the suppression correlated to stimulation intensity: high amplitude of cutaneous stimulation resulted in greater suppression of afferent volleys and grey matter response fields peak to peak values than at a low stimulation amplitude (muscle nerve stimulation vs muscle & cutaneous nerve stimulation high amplitude, mean values difference: MK1: -83%, MK2: -18%, MK3: -46%, MK4: -56%; muscle nerve stimulation vs muscle & cutaneous nerve stimulation low amplitude: MK1: -48%, MK2: -15%, MK3: -42%, MK4: -43%, **Figure 3.9b**).



**Figure 3.9, Peak-to-peak amplitude suppression of spinal cord grey matter response fields.** a) MK1 triggered-average signal showing afferent volley, and grey matter response fields resulting from muscle nerve stimulation (cyan), with concurrent cutaneous nerve stimulation (magenta; high stimulation amplitude – solid color; low stimulation amplitude – semi-transparent). b) Peak-to-peak amplitude of grey matter response field in four monkeys, dorsal channels examples. Color coding the same as in a. We compared peak-to-peak amplitude values over two conditions with one-way ANOVA with 300 points, where each point represents the peak-to-peak amplitude as a response to a single stimulus pulse. Boxplots: The central mark indicates the median, and the bottom and top edges of the box indicate the 25th and 75th percentiles, respectively. The whiskers extend to the most extreme data points not considered outliers, and the outliers are plotted individually using the 'o' symbol. Asterisks: \*\*\* $p < 0.001$ . Taken from (Katic Secerovic et al. 2021) with permission.

The same trend was found in all 4 monkeys, suggesting that a significant component of the trajectory disruption may be related to reduced grey matter responses to proprioceptive volleys and not only to a simple reduction of proprioceptive inputs.





**Figure 3.10, Multiunit activity.** a) We filtered the signal to extract the spiking component and detected the neural action potentials using the thresholding algorithm (see methods). b) Examples of multiunit activity in two different channels (one in dorsal, one in ventral region) for each of the four monkeys. Single muscle nerve stimulation (cyan, left) and concurrent muscle and cutaneous nerve stimulation at a high amplitude (magenta, right). Dashed cyan line represents the muscle nerve stimulation pulse. Neural activity is presented and quantified with raster plots and peri-stimulus time histograms (PSTHs). Each row of the raster plots represents the response to a single muscle nerve stimulation pulse, while each dot corresponds to an action potential. Mean event rate is defined as an average number of spikes within a time frame of one bin (0.2 ms) across all single pulses of muscle nerve stimulation. Black lines highlight the PSTH bins that are reduced. Black arrows indicate the decreased mean event rate values of PSTH and their lengths correspond to the amount of reduction. Diagonal lines correspond to the units whose frequency is in line with frequency of stimulation. Taken from (Katic Secerovic et al. 2021) with permission.

Finally, we investigated whether changes in the population neural dynamics and grey matter field potentials could be reflected in changes of single neuron spiking activity. We

utilized multiunit threshold crossing analysis (**Figure 3.10a**) and identified channels in which a clear response to proprioceptive pulses was visible. In this multiunit analysis, the peak of neural activity after proprioceptive stimuli occurred at approximately 3 – 4 ms after each proprioceptive stimulation pulse. We present the neural responses of units that were activated by proprioceptive inputs. When continuous stimulation of the cutaneous nerve was overlapped with muscle nerve stimulation, we observed a reduction in these responses in all four monkeys, both in the dorsal and ventral horn of the spinal cord (**Figure 3.10b**).

In summary, we found that concurrent cutaneous nerve stimulation reduced peak-to-peak amplitude of afferent volleys, grey matter response fields and multiunit responses to proprioceptive stimuli. These results suggest that proprioceptive information processing may be disrupted by reducing both sensory input in the spinal cord as well as grey matter network computations.

### **3.3.5 Reduction of proprioceptive processing impacts somatosensory cortex**

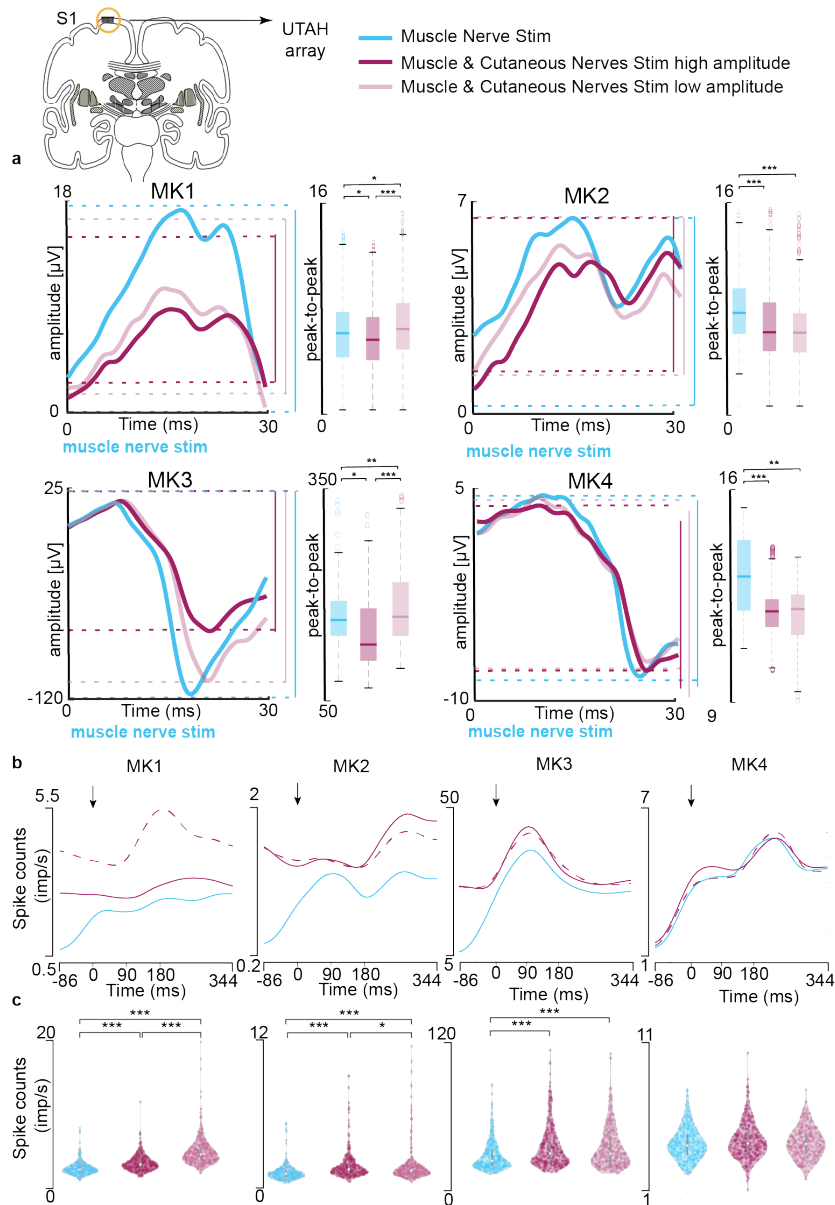
We showed that concurrent stimulation of cutaneous afferents suppresses proprioception information processing in the spinal cord and correlates to classic electrophysiology measures. We then hypothesized that this suppression in the spinal cord limits the amount of information transmitted upstream to the brain, which could impact conscious perception of proprioception.

To test this hypothesis, we analyzed intra-cortical neural signals extracted from area 2 of the somatosensory cortex in all four monkeys. We found cortical evoked potentials with a latency of around 22-25 ms, which is consistent with the longer distance between the cortex and the peripheral nerves and it has also been reported in similar experiments (Perich et al. 2020). Peak-to-peak analysis of the signal amplitude indicated similar results as in the spinal cord. We observed a reduction of proprioceptive evoked potentials during concurrent high amplitude stimulation of the cutaneous nerve in all monkeys (**Figure 3.11a**).

Observed suppression was detected in most of the channels in the array. Moreover, when we stimulated the cutaneous nerve at a low amplitude, peak-to-peak values of the signal increased (muscle nerve stimulation vs muscle & cutaneous nerve stimulation high amplitude, mean values difference: MK1: -8%, MK2: -19%, MK3: -30%, MK4: -29% ; muscle nerve stimulation vs muscle & cutaneous nerve stimulation low amplitude: MK1: +2%, MK2: -18%, MK3: +3%, MK4: -26%).

Surprisingly, when we inspected the spiking activity extracted from multiunits in the cortex, the spike counts induced by concurrent cutaneous nerve stimulation at a low amplitude were similar, or even greater, than those obtained at a high amplitude (relative mean difference from concurrent high to low amplitude, +53.69% for MK1, -7.65% for MK2, +3.14% for MK3, -6.40% for MK4, **Figure 3.11b,c**). This is markedly different from what we observed in the spinal cord (**Figure 3.6, Figure 3.7**). Indeed, we expected greater spiking activity consistently associated with higher stimulation amplitudes and not the opposite. In fact, this discrepancy seemed to reflect the spinal proprioceptive information processing, where concurrent cutaneous stimulation at a low amplitude yielded longer neural trajectory lengths.





**Figure 3.11, Somatosensory cortex evoked potentials and cortical spiking activity.** a) Somatosensory cortex evoked potentials in four monkeys. Examples of signals recorded as a response to muscle nerve stimulation, with concurrent cutaneous nerve stimulation (magenta; high stimulation amplitude – solid color; low stimulation amplitude – semi-transparent) or without it (cyan). Evoked potentials appeared with a latency between 22-25 ms. Signals are given as an example of a single channel in the somatosensory cortex and are averaged across all muscle nerve stimulation pulses. We compared peak-to-peak amplitude values of the signal over two conditions with one-way ANOVA with 300 points, where each point represents the peak-to-peak amplitude as a response to a single stimulus pulse. b) Spike counts were averaged across all trials and all channels for each stimulation condition for all monkeys. c) Statistical analysis of the spiking activity for each stimulation condition (Kruskal-Wallis test with 392, 474 and 460 points for muscle nerve stimulation, concurrent cutaneous stimulation at high amplitude and low amplitude, respectively, for MK1; 360, 389 and 392 points, respectively, for MK2; 335, 386 and 390 points, respectively, for MK3). Each dot corresponds to the computed trajectory length for a trial, forming a Gaussian distribution of trajectory lengths. Trial corresponds to a stimulation pulse. Taken from (Katic Secerovic et al. 2021) with permission.

Boxplots and violin plots: The central mark indicates the median, and the bottom and top edges of the box indicate the 25th and 75th percentiles, respectively. The whiskers extend to the most extreme data points not considered outliers, and the outliers are plotted individually using the 'o' symbol. Asterisks: \*\*\* $p < 0.001$ ; \*\* $p < 0.01$ ; \* $p < 0.05$ .

In summary, we observed a reduction of proprioceptive information during concurrent continuous stimulation of the cutaneous nerve also in the somatosensory cortex. This finding suggests that the effects that we observed in the spinal cord propagate through the higher layers of sensorimotor processing.

### **3.4 Discussion**

In this experimental study in four monkeys, we combined analysis of neural population dynamics with classical electrophysiology measures to analyze the impact of continuous electrical stimulation of the cutaneous afferents on the processing of proprioceptive information in the spinal cord. We found that the spinal sensorimotor computations of proprioceptive inputs were substantially disrupted when cutaneous afferents were concurrently stimulated and that this interference propagated to the brain. While limited to the stimulation of the cutaneous afferents, our findings suggest that artificially-generated neural input may disrupt ongoing neural processes that may be unrelated to the stimulation. More specifically, because of the highly shared neural architecture, even highly selective targeting of neural elements, like in our case the cutaneous afferents, can significantly undermine neural processing of seemingly unrelated neural functions, like proprioceptive percepts. Similar phenomena may occur in other regions of the nervous system and should therefore be studied. Hence, these results imply that efforts towards the development of naturalistic or biomimetic stimulation inputs should likely be employed in neurostimulation.

#### **3.4.1 Population analysis as a tool to explain network-level effects of electrical stimulation**

Electrical stimulation of the nervous system is widely applied in clinical practice and in clinical research trials in order to influence neural activity and ameliorate functions in a variety of disorders (Stanisa Raspopovic, Valle, and Petrini 2021; Edwards et al. 2017; Wagner, Mignardot, Le Goff-Mignardot, et al. 2018; Formento et al. 2018; Stanisa Raspopovic 2021). The most overt applications are sensorimotor neuroprostheses where a clear relationship can be found between stimulation parameters and strength of elicited movements (Gill et al. 2018; Wagner, Mignardot, Le Goff-Mignardot, et al. 2018; Formento et al. 2018; Powell et al. 2023) or evoked sensations (Stanisa Raspopovic, Valle, and Petrini 2021; Giacomo Valle et al. 2022; 2018b; Wendelken et al. 2017; Charkhkar et al. 2018). For example, epidural spinal cord stimulation has been applied for both motor recovery as well as, more recently, for restoration of sensory feedback. We know that spinal cord stimulation recruits sensory afferents. In motor applications, the recruitment of large proprioceptive afferents leads to an increased excitability of spinal motoneurons, thereby promoting movement. Instead, in sensory applications, the recruitment of the same afferents should in principle produce controllable conscious sensory experiences, similar to those elicited by stimulation of the peripheral nerve. However, beyond this simplistic vision, there is a fundamental lack of knowledge into what happens to neural networks that receive inputs from these afferents. In fact, the highly shared neural infrastructures involve neural sub-networks that are meant to produce the desired function (Kandel, E., Schwartz, J. & Jessel, T., n.d.; Koch, Acton, and Goulding 2018; Gordon et al. 2023). For instance, the motor network produces movement, but other networks may be involved in other unrelated processes such as perception, error estimation during movement execution and autonomic

function (Squair et al. 2021), among others (Gordon et al. 2023). These additional sub-networks may also share inputs from the same afferents and would thus be perturbed by stimulation.

In our work, we constructed a toy model to study this specific problem in a controlled fashion as a proxy to understand, more generally, how artificial inputs can influence neural network function. We focused on the spinal network effects caused by stimulation of the cutaneous afferents on the neural processing of a proprioceptive pulse. This toy model exemplifies that an ongoing neural process (proprioceptive input processing) is perturbed when seemingly unrelated electrical stimuli application (inducing touch percepts) is applied with typical stimulation pattern (fixed 50Hz square pulses). To explore network effects, we used modern population analysis tools that enable the quantification of information processing in the spinal circuits via analysis of neural trajectories in the neural space (Churchland et al. 2012). Specifically, we established a measure of proprioceptive information processing by quantifying neural trajectory lengths in spinal neural manifolds using intra-spinal population analysis (Lindén et al. 2022). Through the quantification of the trajectory length, we assessed the effect of concurrent cutaneous stimulation on the spinal proprioceptive information. We showed the collapse of proprioceptive neural trajectories during concurrent stimulation of cutaneous afferents, in other words, a suppression of proprioceptive information processed in the spinal cord, according to our interpretation. Importantly, simple analysis of total spike counts showed that the results of our trajectory length quantification were not trivial. Indeed, averaged multiunit spiking activity in response to proprioceptive stimuli were expectedly the highest during concurrent stimulation of the cutaneous afferents. This is an obvious result as general spinal activity is increased by the 50 Hz artificial cutaneous inputs. Thus, the actual total neural activity in the spinal cord is higher during cutaneous stimulation. Yet, the population analysis allows to extract only activity that explains the variance generated by proprioceptive inputs processes, enabling to infer the proprioceptive components of the neural dynamics against the background of cutaneous activity. Hence, the use of neural manifolds for population activity enabled the quantification of the stimulation effects on these computations.

We validated results obtained with neural manifold analysis with classical electrophysiology inspecting peak-to-peak amplitude of afferent volleys, spinal cord grey matter response fields and multiunit activity. These measures indicated a reduction in proprioceptive information during concurrent cutaneous stimulation.

### **3.4.2 Potential underlying neural mechanisms**

While successful in visualizing network effects, population analysis cannot offer an explanatory value on the specific neural mechanisms responsible for this suppression. Pre-synaptic inhibition is a likely candidate (Stein 1995). It is a well-known mechanism of sensory input gating that prevents transmission of excitatory post-synaptic potentials to neurons targeted by primary afferents (Rudomin and Schmidt 1999; Confais et al. 2017). In our experiments, the stimulation amplitude of the muscle nerve was the same across all conditions (i.e., fixed number of recruited afferents). Therefore, the reduction of unit responses to proprioceptive inputs during concurrent cutaneous afferent stimulation could be consistent with a reduction in synaptic inputs to these target units.

Nevertheless, the observed afferent volley reduction was not strong enough to explain complete diminishment of proprioceptive perception, which means that the disruption of neural trajectories was not caused only by reduced inputs, but also by affected processing.

We refer to this other potential mechanism as the “busy line” effect. Continuous, non-natural stimulation of the cutaneous afferents may produce highly synchronized activity in spinal circuits, which may receive both proprioceptive and cutaneous inputs. However, when artificially synchronized cutaneous inputs reach the spinal cord, they may saturate these circuits and reduce their capacity to respond to additional inputs (G. A. Miller 1956). When these neurons cannot be employed to process proprioceptive information, the neural network achieves a saturated state where no further processing can be carried out. This may explain why neural trajectories during cutaneous stimulation were displaced in the manifold space in a way that resembled a rigid geometric translation. Coincidentally, the modulated component of the neural dynamics was shorter or almost completely disrupted, suggesting that some of the neurons involved in performing the geometrical translation were not available to produce the modulated components of neural dynamics.

### **3.4.3 Effects within the brain**

We performed a large part of our analysis in the spinal cord, which is the first important layer of sensory processing, particularly, in regard to proprioception. However, conscious perception is processed at various layers above the spinal cord. Indeed, peak-to-peak amplitudes of cortex potentials evoked with muscle nerve stimulation were suppressed when overlapped with cutaneous input also in the sensory cortex area 2, which is known to integrate cutaneous and proprioceptive inputs (Gordon et al. 2023; London and Miller 2013). Moreover, if cortical signals were independent from spinal and brainstem processes, when looking at the global cortical spike counts we would have expected higher spike counts during high-amplitude stimulation of the cutaneous nerve and lower spiking activity during low amplitude stimulation of the cutaneous nerve. Instead, we found higher or similar spiking activity when we used low-amplitude stimulation of the cutaneous nerve. This may be indicative of the fact that high amplitude stimulation may convey more cutaneous input but less proprioceptive input to the cortex because of sub-cortical cancellation (Rudomin and Schmidt 1999). In contrast, cutaneous stimulation at a lower amplitude may mean less cutaneous input but more proprioceptive input to the cortex as a consequence of less cancellation occurring in sub-cortical structures. Nevertheless, these mechanistic conjunctures are strongly contingent on our experimental design. Future directions ought to design alternative experimental paradigms (i.e., including histological analysis) that uncover the spinal interneuron circuitry involved in the processing of proprioceptive information in response to concurrent input.

These overall results support the conclusion that conscious perception of proprioception may be also altered by sub-cortical interference. While this hypothesis cannot be tested in subjects with amputation because of their limb loss, recent data in humans with sensory incomplete spinal cord injury shows that spinal cord stimulation, which also recruits sensory afferents (Chandrasekaran et al. 2019), reduces proprioception acuity during supra-threshold stimulation (Formento et al. 2018). This result in humans further supports our hypothesis and we believe that it demands further investigation.

### **3.4.4 Conclusions and relevance for other brain circuits**

Our results showed that electrical stimulation of sensory afferents can alter the processing of proprioceptive information within spinal circuits. Similar phenomena may occur in brain networks during deep brain stimulation, where similar continuous electrical pulses are

delivered to thalamocortical projections and other large brain networks. In the brain, these effects, which in the spinal cord indicate the impossibility to appropriately process proprioception, could potentially alter cognitive processes unrelated to the stimulation goals within the cortex. A potential approach to minimize the interference of stimulation with ongoing neural processes is the use of “bio-mimetic” and model-based stimulation patterns (Cimolato et al. 2023; Giacomo Valle et al. 2018b; Bensmaia 2015; Katic et al. 2023; George et al. 2019). Instead of delivering unstructured and synchronized neural activity, they could produce more naturalistic patterns, thereby potentially avoiding these side effects. In conclusion, future stimulation strategies designs should consider the use of neural population analysis in order to analyze the effects of particular stimulation patterns on apparently unrelated neural network processes.

# Chapter 4

## From in silico modeling towards sophisticated application in humans

*"The science of today is the technology of tomorrow."  
Edward Teller*

*Adapted from: Biomimetic computer-to-brain communication restores naturalistic touch sensations via peripheral nerve stimulation*

*Giacomo Valle\*, Natalija Katic Secerovic\*, Dominic Eggemann, Oleg Gorskii, Natalia Pavlova, Thomas Stieglitz, Pavel Musienko, Marko Bumbasirevic and Stanisa Raspopovic – BioRxiv*

*\*equal contribution*

Artificial communication with the brain through peripheral nerve stimulation recently showed promising results in people with sensorimotor deficits. However, these efforts fall short in delivering close-to-natural rich sensory experience, resulting in the necessity to propose novel venues for converting sensory information into neural stimulation patterns, which would possibly enable intuitive and natural sensations. To this aim, we designed and tested biomimetic neurostimulation framework inspired by nature, able "to write" physiologically plausible information back into the residual healthy nervous system. Starting from in-silico model of mechanoreceptors, we designed biomimetic policies of stimulation, emulating activity of different afferent units. Then, we experimentally assessed these novel paradigms, alongside with mechanical touch and commonly used, linear neuromodulations. We explored the somatosensory neuroaxis by stimulating the nerve while recording the neural responses at the dorsal root ganglion and spinal cord of decerebrated cats. Biomimetic stimulation resulted in a neural activity that travels consistently along the neuroaxis, producing the spatio-temporal neural dynamic more like the naturally evoked one. Finally, we then implemented these paradigms within bionic device and tested it with patients. Biomimetic neurostimulations resulted in higher mobility and decreased mental effort compared to traditional approaches. Results of this neuroscience-driven technology inspired by the human body could be a model for development novel assistive neurotechnologies.

## 4.1 Introduction

Loss of the communication between the brain and the rest of the body due to an injury or a neurological disease severely impact sensorimotor abilities of disabled individuals. Often, they also experience the inability to sense their own body. The resulting low mobility and accompanying loss of independence cause a severe health problem and decline in quality of life with consequent necessary around-the-clock care. Recently developed neurotechnologies exploit direct electrical stimulation of the residual healthy peripheral or central nervous system to restore some of the lost sensorimotor functions (Edwards et al. 2017; Stanisa Raspopovic 2020; Stanisa Raspopovic, Valle, and Petrini 2021). Indeed, brain-computer interfaces (BCIs) exploiting implantable neural devices could potentially restore the bidirectional flow of information from and to the brain (Bensmaia, Tyler, and Micera 2020; Sharlene N. Flesher et al. 2021; Stanisa Raspopovic, Valle, and Petrini 2021). The implant of bio-compatible electrodes in the residual neural structures (Yang Wang et al. 2023), still functional after the injury, allows to create a direct communication channel. Indeed, neural stimulation of the peripheral somatic nerves (PNS) (Francesco Maria Petrini, Bumbasirevic, et al. 2019; Francesco M. Petrini et al. 2019; Max Ortiz-Catalan et al. 2020; Daniel W. Tan et al. 2014), spinal cord (Nanivadekar et al. 2022; Chandrasekaran et al. 2020; Wagner, Mignardot, Goff-Mignardot, et al. 2018; Angeli et al. 2018; Gill et al. 2018) or somatosensory cortex (S1) (Tabot et al. 2013; Salas et al. 2018; S. N. Flesher et al. 2016) showed the ability to restore missing sensations, resulting in closed-loop neuroprostheses able to establish a bidirectional link between human and machines. Sensory feedback restoration improved patients' ability to use bionic limbs and increased its acceptance rate (Francesco Clemente et al. 2019; Mastinu et al. 2020; Giacomo Valle, D'Anna, et al. 2020; Sharlene N. Flesher et al. 2021; M. Schiefer et al. 2016). However, the resulting dexterity of bionic hands is still far from that of natural hands in able-bodied individuals (Roland S. Johansson and Flanagan 2009), while mobility and endurance with bionic legs are to be improved (Stanisa Raspopovic 2021). This is most probably due to the multiple facts, among which that neurotechnologies are falling short regarding the naturalness of induced sensations (Stanisa Raspopovic, Valle, and Petrini 2021), often resulting in unpleasant paresthesia. Indeed, common neuromodulation devices do not stimulate neurons based on the human natural touch coding or using modelistic approach (Giacomo Valle, Strauss, et al. 2020; G. Valle et al. 2018; Cimolato et al. 2023), but rather with predefined constant stimulation frequency. With these stimulation patterns, all elicited neurons are simultaneously activated, contrary to what happens with neural activity during in-vivo natural touch (Saal and Bensmaia 2015). In fact, the natural asynchronous activation is driven in a part by the probabilistic nature of action potential generation in sensory organs, such as muscle spindles (Prochazka 2011) or retinal cells (Pillow 2005), and in second part by the stochastic nature of synaptic transmission (Abbott and Regehr 2004). The synchronization, which generates an unnatural aggregate activity within the neural tissue, could be among the main reasons of perceived paresthesia percepts (Francesco M. Petrini et al. 2019; G. Valle et al. 2018; Francesco Maria Petrini, Valle, et al. 2019). In fact, paresthetic sensations are likely to arise from this unnatural fibers activation (Formento et al. 2020), and can be due to over-excitation of afferents or a cross-talk between them (Torebjörk and Ochoa 1980). When caused by neuropathies, paresthesia is often chronic and do not improve over time, which might reflect an inability of central nervous system to learn how to interpret such aberrant neural responses (Saal and Bensmaia 2015). These percepts are unnatural and sometimes even uncomfortable, making the use of electrical stimulation challenging. Moreover, it can interfere with the individual's ability to sense and respond to other types of sensory information, such as touch or temperature. This can make it difficult to perform

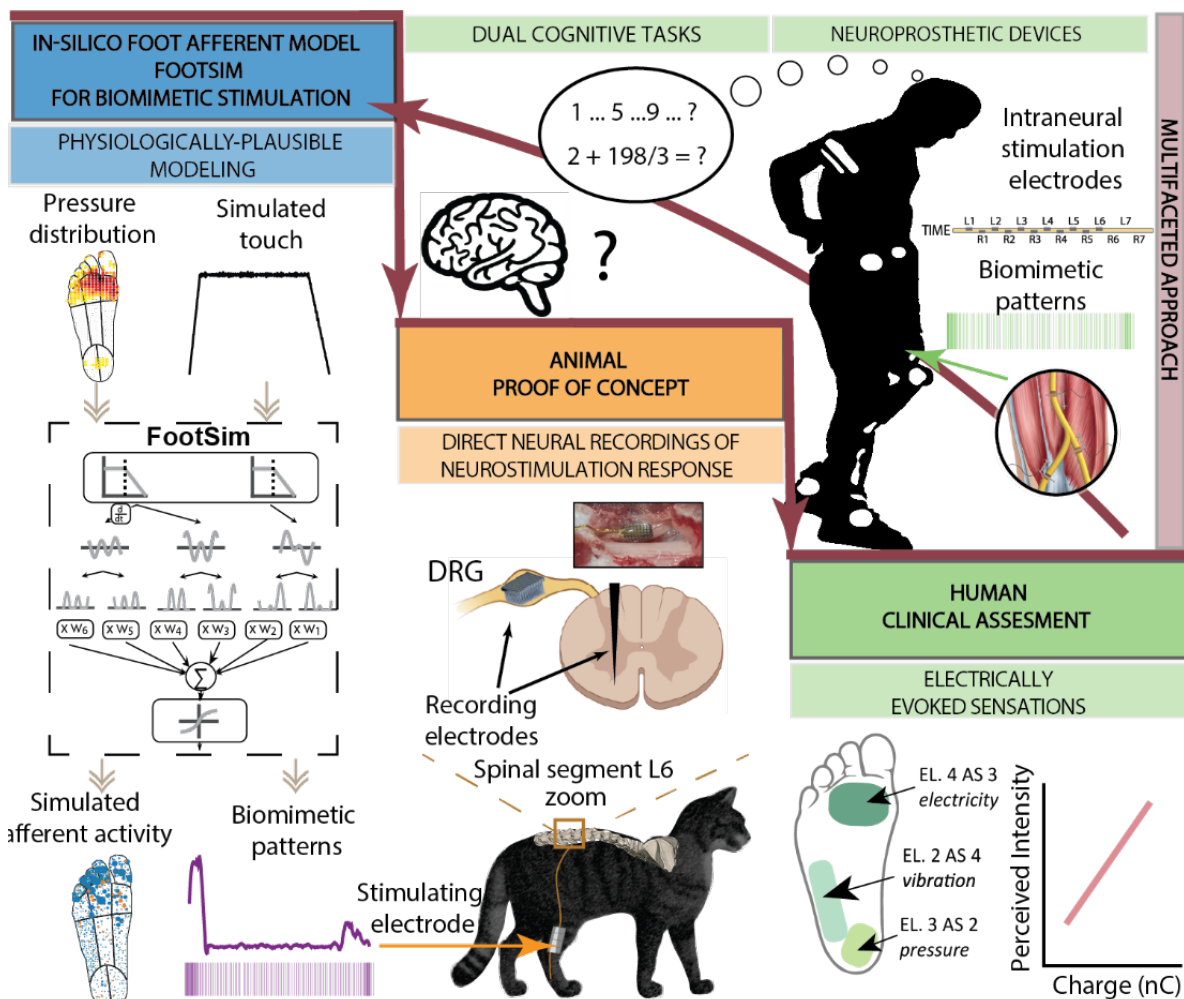
certain tasks or activities that require the use of multiple senses, or to interact with objects in the environment.

As a possible answer to this problem, the electrical stimulation built by mimicking the natural tactile signal (so called biomimetic sensory feedback (Saal and Bensmaia 2015; Okorokova, He, and Bensmaia 2018)) has shown to evoke more intuitive and natural sensations that better support interactions with objects, compared to non-biomimetic stimulation paradigms (George et al. 2019; Greenspon, Valle, Hobbs, Verbaarschot, Callier, Shelchikova, Sobinov, Jordan, Weiss, Fitzgerald, Prasad, Van Driesche, et al. 2023; Giacomo Valle et al. 2018b). These biomimetic approaches might have the ability to electrically evoke aggregate population response similar to the natural one (Callier, Suresh, and Bensmaia 2019a; Roland S. Johansson and Flanagan 2009). Previous studies on natural touch suggests that somatosensory information about most tactile features is encoded synergistically by all afferent classes in the nerve (Saal and Bensmaia 2014). Importantly, somatosensory cortex (Carter et al. 2014, 201; Pei et al. 2009) (or even in cuneate nucleus (Suresh et al. 2021)) are the earliest stages where signals coming from multiple fiber types converge and integrate with each other. It is allowing for the possibility that mimicking realistic neural responses of small mixed-type afferent populations will result in naturalistic patterns of cortical activation (Callier, Suresh, and Bensmaia 2019a), culminating in quasi-natural tactile percepts. However, despite the initial success of biomimetic approach in hand amputees, that is outperforming classical non-biomimetic stimulation patterns, this approach was never tested in lower-limb amputees. Moreover, it was evaluated while performing tasks of daily living, or in more complex scenario than a single user with a single-channel stimulation. Furthermore, we are still lacking the understanding how these patterns are transmitted and interpreted in the first layers of information processing along the somatosensory neuroaxis.

To this aim, we develop a neuroprosthetic framework constituted by realistic in-silico modeling, pre-clinical animal validation and clinical testing in human patients with intraneural devices (**Figure 4.1**). Using this unique multifaceted approach, we are aiming to test if the architecture established on the development of validated model-based neurotechnology can be effective for human applications. We designed biomimetic neurostimulation strategies for restoring somatosensory feedback by exploiting a realistic in-silico model of human touch (FootSim) (Katic et al. 2023). This computational model is able to emulate the neural activity of the sensory afferents, innervating the plantar area of the human foot, in response to any spatio-temporal skin deformation. FootSim allowed designing neurostimulation patterns that mimic some relevant temporal features of the natural touch coding. Together with developing new stimulation paradigms, we assessed the major challenge: how specific artificial stimulation patterns translate into a neural signal and in which form they travel towards the somatosensory neuroaxis. With this goal, we stimulated with cuff electrodes the tibial nerves of decerebrated cats, while simultaneously recording neural activity (in Dorsal Root Ganglion (DRG) with a 32-channels Utah array and in spinal cord (L6) a 32-channel shaft electrode). This setup allowed us to record and compare the electrically-induced activity (in response to biomimetic and non-biomimetic patterns of nerve stimulation) with the response of neurons to mechanical touch. We completed this multifaceted approach by implanting the electrodes in tibial nerve of three transfemoral amputees. Firstly, we tested the naturalness of the artificial sensation evoked using biomimetic and non-biomimetic encodings. Finally, we implemented the biomimetic neurostimulation in a real-time, closed-loop neuroprosthetic leg, comparing its performance with respect to previously-adopted neurostimulation strategies (linear and discrete



neuromodulations). The patients performance were assessed in ecological motor tasks (i.e. a stairs walking task (Giacomo Valle, Saliji, et al. 2021) and a double motor task (Preatoni et al. 2021)).



**Figure 4.1. Neuroscience-driven development of a biomimetic neuroprosthetic device.** The success development of a somatosensory neuroprosthesis is based on three main pillars: 1) In-silico models of the biological sensory processing have to be exploited for emulating the natural neural activation of the nervous system to external tactile stimuli; 2) proof of concept in animal models allows for an experimental validation of the mechanisms behind the use of specific neurostimulation strategies; 3) A rigorous clinical validation of the biomimetic technology in humans. The clinical assessment of invasive stimulation has to be performed in order to assess the functional outcomes in real-life scenarios. The results from the clinical trials will then allow to collect relevant data exploitable for improving computational modelling and deepening the understanding about the behavior.

Both the animal and human experiments indicate that time-variant, biomimetic paradigm could become the fundamental feature for designing the next generation of neuroprosheses, able to directly communicate with the brain while successfully encoding natural sensory information using artificial electrical stimulation.

## 4.2 Methods

### **4.2.1 Modeling of all tactile afferents innervating the glabrous skin of the foot (FootSim)**

In this study, we used FootSim (Katic et al. 2023), in-silico model of the afferents innervating the foot sole that simulates the neural responses on arbitrary mechanical stimuli. It is composed of the two parts i) mechanical part, calculating the deformation of the skin by applied stimulus and converting it into the skin stress ii) firing models that generate spiking output for individual fibers of different afferent classes. Each firing model contains 11 unique parameters. The model is fitted on a dataset of tactile afferents exposed to a wide range of vibrotactile stimuli at different frequencies and amplitudes, recorded in humans using microneurography. We fitted several models for each afferent type, reflecting partially the natural response variability of different afferents observed in the empirical data.

### **4.2.2 Design biomimetic neural stimulations using FootSim**

We designed 5 types of biomimetic patterns, based on the cumulative responses of specific afferent types. In FootSim model, we populated the foot sole with only one type of afferents (FA1/FA2/SA1/SA2) or with a complete population of afferents (FULL biomimetic), following their realistic distribution. We applied 2s stimuli covering the whole area of the foot. We combined ramp-and-hold stimuli (0.15s on phase, 0.3s off phase) with low-amplitude environmental noise (up to 0.5% of maximum amplitude of ramp-and-hold stimuli). FootSim model estimated the response of each single afferent placed on the sole of the foot. We aggregated the spiking activity of all units, smoothed the obtained function over time and used it as a modulated frequency of stimulation for each biomimetic pattern. Amplitude and pulsewidth of stimulation were constant and were chosen during the experimental procedure.

### **4.2.3 Electrophysiology in decerebrated cats**

Through the electrode contact of cuff electrodes we delivered single pulses of cathodic, charge balanced, symmetric square pulses (with pulse width of 0.5 ms). We provided the stimulation using AM stimulators Model 2100 (A-M Systems, Sequim, WA, USA). Electromyographic and neural signals were acquired using the RHS recording system with 96-channel headstages (Intan Technologies, Los Angeles, CA, U.S.A.) and at a sampling frequency of 30 kHz. We tuned the stimulation amplitude by observing the emergence of clear sensory volleys in the dorsal spinal cord in response to low-frequency stimulation.

We applied 5 types of biomimetic stimulation paradigms, repeating every pattern 90 times. Natural touch condition was applied by rubbing the cat's leg with cotton swab and was repeated 5 times.

### **4.2.4 Analysis of the animal neural data**

We applied all data analysis techniques offline.

#### 4.2.4.1 Pre-processing

We filtered raw signals recorded with 32 - electrode array implanted in the spinal cord, as well as signals documented with 32-channel Utah array in dorsal root ganglion with comb filter to remove artefacts on 50 Hz and its harmonics. We designed a digital infinite impulse response filter as a group of notch filters that are evenly spaced at exactly 50 Hz. We removed signal drift with a high-pass 3<sup>rd</sup> order Butterworth filter with a 30Hz cutoff frequency. High amplitude artifacts were detected when the signal crossed a threshold equal to  $15\sigma$ , where we estimated background noise standard deviation(Quian Quiroga and Panzeri 2009) as  $\sigma = \text{median } |x| \cdot 0.6745$ . Detected artifacts were zero-padded for 10 ms before and after the threshold crossing. We extracted neural signal of 2s recorded during stimulation with every defined paradigm. Natural touch condition produced response of 1s and the signal where neural activity was observable was extracted.

#### 4.2.4.2 Identification of local field potential

We isolated local field potentials by band passing the neural signal between 30Hz-300Hz and averaged the signal over multiple stimuli pattern repetitions.

#### 4.2.4.3 Characterization and quantification of neural spiking activity

We extracted neural spiking activity by applying a 3<sup>rd</sup> order Butterworth digital filter to the raw signal, separating the signal in frequency range from 800 Hz to 5000 Hz. We detected the spikes using unsupervised algorithm(Quiroga, Nadasdy, and Ben-Shaul 2004). We determined the threshold value separately for each recording channel. To detect the accurate threshold value, we concatenated all data sets recorded in one place (spinal cord/DRG) that we aim to analyze in a single file. All analyzed data sets were concatenated in a single file in order to detect proper threshold values. Threshold for detection of action potentials was set to negative  $3\sigma$  for signals recorded in the spinal cord and  $4\sigma$  for signals recorded in the DRG, where  $\sigma = \text{median } |x| \cdot 0.6745$  which represents an estimation of the background standard deviation.

Multiunit activity is presented in form of rasterplot and quantified with peri-stimulus time histogram (PSTH). Each dot in rasterplot represents a single detected spike. Every rasterplot row corresponds to the intra-spinal or intra-cortical activity perturbed with a single muscle nerve stimulus pulse. PSTH is quantified with mean event rate, defined as the average number of spikes across all single pulses of muscle nerve stimulation, within defined time frame.

### 4.2.5 Patient recruitment and surgical procedure in humans

Three unilateral transfemoral amputees were included in the study. All of them were active users of passive prosthetic devices (Ottobock 3R80) (**Table 4.1**). Ethical approval was obtained from the institutional ethics committees of the Clinical Center of Serbia, Belgrade, Serbia, where the surgery was performed (ClinicalTrials.gov identifier NCT03350061). All

the subjects read and signed the informed consent. During the entire duration of our study, all experiments were conducted in accordance with relevant EU guidelines and regulations.

Four TIMEs (Boretius et al. 2010) (14 ASs each) were obliquely implanted in the tibial branch of the sciatic nerve of each subject. The surgical approach used to implant TIMEs has been extensively reported elsewhere (Francesco Maria Petrini, Bumbasirevic, et al. 2019). Briefly, under general anesthesia, through a skin incision over the sulcus between the biceps femoris and semitendinosus muscles, the tibial nerve was exposed to implant 4 TIMEs. A segment of the microelectrodes cables was drawn through 4 small skin incisions 3 to 5 cm higher than the pelvis ilium. The cable segments were externalized (and secured with sutures) to be available for the transcutaneous connection with a neural stimulator. After 90 days, the microelectrodes were removed under an operating microscope in accordance with the protocol and the obtained permissions.

**Table 4.1. Participants' demographics.**

| Patient | Cause of Amputation | Level and Side of Amputation     | Age | Amputation Time | Phantom Limb Pain | Gender | Own Prosthesis                     | Frequency of Use |
|---------|---------------------|----------------------------------|-----|-----------------|-------------------|--------|------------------------------------|------------------|
| S1      | Trauma              | Distal two-thirds of right thigh | 49  | 2               | Medium            | M      | Passive prosthesis (3R80-Ottobock) | Daily            |
| S2      | Trauma              | Distal two-thirds of right thigh | 35  | 12              | Medium            | M      | Passive prosthesis (3R80-Ottobock) | Daily            |
| S3      | Trauma              | Distal two-thirds of left thigh  | 53  | 7               | Low               | M      | Passive prosthesis (3R80-Ottobock) | Daily            |

This study was performed within a larger set of experimental protocols aiming at assessing the impact of the restoration of sensory feedback via neural implants in leg amputees during a 3-month clinical trial (Francesco Maria Petrini, Bumbasirevic, et al. 2019; Francesco Maria Petrini, Valle, et al. 2019; Preatoni et al. 2021; Petrusic et al. 2022; Giacomo Valle, Saliji, et al. 2021). The data reported in this manuscript was obtained in multiple days during the 3-months trial in three leg amputees.

#### **4.2.6 Intraneural stimulation for evoking artificial sensations**

Each of the TIMEs (latest generation TIME-4H) implanted in the three amputees was constituted by 14 active sites and two ground-electrodes. Details concerning design and fabrication can be found in (Paul Čvančara et al. 2020; P. Čvančara et al. 2019). For each subject, 56 electrode channels were then accessible for stimulation on the tibial nerve. During the characterization procedure the stimulation parameters (i.e. amplitude and pulse-width of the stimulation train), for each electrode and AS, were recorded. The electrodes were connected to an external multichannel controllable neurostimulator, the STIMEP (Axonic, and University of Montpellier) (Guiho et al. 2016). The scope of this

procedure was to determine the relationships between stimulation parameters and the quality, location, and intensity of the electrically-evoked sensation, as described by Petrini et al. (Francesco Maria Petrini, Valle, et al. 2019). In brief, the injected charge was linearly increased at a fixed frequency (50 Hz (Francesco Maria Petrini, Valle, et al. 2019)) and pulse-width by modulating the amplitude of the stimulation for each electrode channel. In case the stimulation range was too small for the chosen pulse-width and the maximum injectable current, the pulse-width was increased, and the same procedure was repeated. When the subject reported to perceive any electrically-evoked sensation, the minimum charge (i.e. perceptual threshold) was registered. The maximum charge was collected in order to avoid that the sensation became painful or uncomfortable for the subject. This was repeated five times per channel and then averaged. Perceptual threshold and maximum charge were obtained for every electrode channel and have been used to choose the stimulation range. For each AS, the maximum injected charge was always below the TIME chemical safety limit of 120 nC (D'Anna et al. 2019). All the data were collected using a purposely-designed psychometric platform for neuroprosthetic applications. It indeed allows to collect data using standardized assessment questionnaires and scales, and to perform measurements over time. The psychometric platform is user-friendly and provides clinicians with all the information needed to assess the sensory feedback (Giacomo Valle, Iberite, et al. 2021).

#### **4.2.6 Assessment of sensation naturalness**

We first characterized the subjects' rating of the perceived naturalness of the stimulation delivered through TIMEs in S1, S and S3. We injected biphasic trains of current pulses lasting 2 s with an increasing phase (0.5 s), a static phase (1 s) and a decreasing phase (0.5 s) via TIMEs (**Fig.5c**) using Linear amplitude neuromodulation(G. Valle et al. 2018; Giacomo Valle et al. 2018a), Sinusoidal pulse-width neuromodulation(Daniel W. Tan et al. 2014; Max Ortiz-Catalan et al. 2019), Poissonian frequency neuromodulation (i.e. 50Hz stimulation with a poissonian spiking noise, consisting in a non-biomimetic, frequency-variant stimulation) and Biomimetic neurostimulation patterns constructed using FootSim (SAI-like, SAI-like, FAI-like, FAII-like and FULL Biomimetic).

The stimulation was delivered from 3 ASs for S1 and S2 eliciting sensation in the Frontal met, 3 ASs for S1 and S2 eliciting sensation in the Central met, 3 ASs for S1 and 2 ASs S2 eliciting sensation in the Lateral met and 5 ASs for S1 and 2 ASs S2 eliciting sensation in the Heel. For S3, only one AS per the four areas were tested (**Fig.S3**). The subjects were asked to report the location (i.e., Projected Field) and naturalness, rated on a scale from 0 to 5(G. Valle et al. 2018; Giacomo Valle et al. 2018a; Lenz et al. 1993). Each condition was randomized, and each stimulation trial was repeated three times. The injected charge (amplitude and pulse-width) was specific for each channel and set to the related threshold charge(Francesco Maria Petrini, Valle, et al. 2019). Moreover, intensity ratings were also collected during each stimulation to exclude relevant intensity difference among the encoding strategies (intensity bias). For the typical time scales involved in our experiments (trials lasting on the order of minutes), neither of our participants reported relevant changes in sensation intensity, which would indicate the presence of adaptation. The specific quality descriptors of the electrically-evoked sensations reported by the subjects were electrode-dependent, including a multitude of sensation types (natural and unnatural)(Giacomo Valle

et al. 2022; Francesco Maria Petrini, Valle, et al. 2019). The subjects were blinded to the sensory encodings used in each trial.

#### **4.2.7 Real-time biomimetic neurostimulation in a neuro-robotic leg**

The neuroprosthetic system included a robotic leg with a sensorized insole with embedded pressure sensors, along with a microcontroller and a neural stimulator (Guiho et al. 2016), implementing the encoding strategies and providing sensory feedback in real time by means of implanted TIMEs (Francesco Maria Petrini, Valle, et al. 2019). We implemented and tested: (i) no feedback (NF): the prosthesis did not provide any sensory feedback; (ii) linear amplitude neuromodulation (LIN): the prosthesis provided a linear feedback from three channels of the sensorized insole (heel, lateral or medial and frontal; more details in Petrini et al. (Francesco Maria Petrini, Valle, et al. 2019)); (iii) time-discrete neuromodulation feedback (DISC): the prosthesis delivered short trains of stimulation (0.5s) when a specific sensor was activated (heel, lateral or central and frontal) and again (0.5s) when the load was released from that sensor (neurostimulation delivered only at the transients); (iv) biomimetic neuromodulation feedback (BIOM): the neuroprosthetic device provided the biomimetic stimulation, reported as the one eliciting more natural sensation, from three channels of the sensorized insole (heel, lateral or central and frontal). For the model-based biomimetic approach (BIOM), the corresponding frequency trains were computed previously offline by the model to reach the appropriate speed during the real-time implementation. The amplitude of the stimulation was modulated linearly with the pressure sensor output, as proposed in Valle et al., (HNM-1) (Giacomo Valle et al. 2018a). In LIN and DISC, the stimulation frequency was fixed (tonic stimulation) to 50 Hz (Francesco Maria Petrini, Bumbasirevic, et al. 2019). During the functional experiments reported in this work, three tactile channels (those eliciting sensation on the heel, lateral or medial and frontal met areas) were used for sensory feedback in all the conditions. The delivered charge was similarly modulated on the three stimulating channels, but in a different range. In fact, each channel was modulated between its threshold and maximum charge values identified in the last mapping session. The biomimetic stimulation patterns adopted on the three channels were selected according to the naturalness perceived per foot area (**Fig.S3**) in each implanted subject. In particular, FAI Biomimetic for frontal, lateral and heel for both S1 and S2, while FULL Biomimetic neurostimulation for lateral met in both S1 and S2.

#### **4.2.8 Stairs Task**

During the stairs test (ST), S1 and S2 were asked to go through a course of stairs in sessions of 30s per 10 times per condition. The setup was configured as an angular staircase endowed with six steps with a height of 10 cm and a depth of 28 cm on one side and with four steps with a height of 15 cm and a depth of 27.5 cm on the other. Subjects were asked to walk clockwise climbing up the six steps and going down the four steps. Walking sessions were performed in four distinct conditions: (i) no feedback (NF); (ii) linear neuromodulation feedback (LIN); (iii) time-discrete neuromodulation feedback (DISC); (iv) biomimetic neuromodulation feedback (BIOM). All the stimulation conditions were randomly presented to the volunteers. The gait speed for this task was reported in terms of number of

laps, as previously performed (Francesco Maria Petrini, Valle, et al. 2019; Giacomo Valle, Saliji, et al. 2021). A lap is intended as going up and down the stairs and reaching the starting position again. A higher number of completed laps is indicative of a higher speed and vice versa. S1 and S2 performed this task.

#### **4.2.9 Cognitive double task**

In the cognitive double task (CDT), first S1 and S2 were instructed to walk forward for 5 m while timing them for 10 times per 4 conditions (BIOM, LIN, DISC and NF) performed in a random order. Subsequently, they were asked to walk for the same distance while performing a dual task (CDT). In particular, they had to spell backward in their mother-tongue language (Serbian) a five-letter word, which had not been previously presented. Also this task was performed 10 times per 4 conditions (BIOM, LIN, DISC and NF) performed in a random order. While the subjects were performing the CDT, both the walking speed (m/s) and the accuracy of the spelling (% of correct letters) were recorded. S1 and S2 performed this task.

#### **4.2.10 Self-reported confidence**

At the end of each session of ST, participants were asked to assess their self-confidence while performing the motor task, using a visual analog scale (from 0 to 10). The data were acquired in BIOM, LIN, DISC and NF conditions in S1 and S2.

#### **4.2.11 Statistics**

All data were exported and processed offline in Python (3.7.3, the Python Software Foundation) and MATLAB (R2020a, The MathWorks, Natick, USA). All data were reported as mean values  $\pm$  SD (unless otherwise indicated). The normality of data distributions was verified. In case of Gaussian distribution, two-tailed analysis of variance (ANOVA) test was applied. Elsewise, we performed the Wilcoxon rank-sum test. Post-hoc correction was executed in case of multiple groups of data. Significance levels were 0.05 unless differently reported in the figures' captions. In the captions of the figures, we reported the used statistical tests for each analysis and its result, along with the number of repetitions (n) and p values for each experiment.

### **4.3 Results**

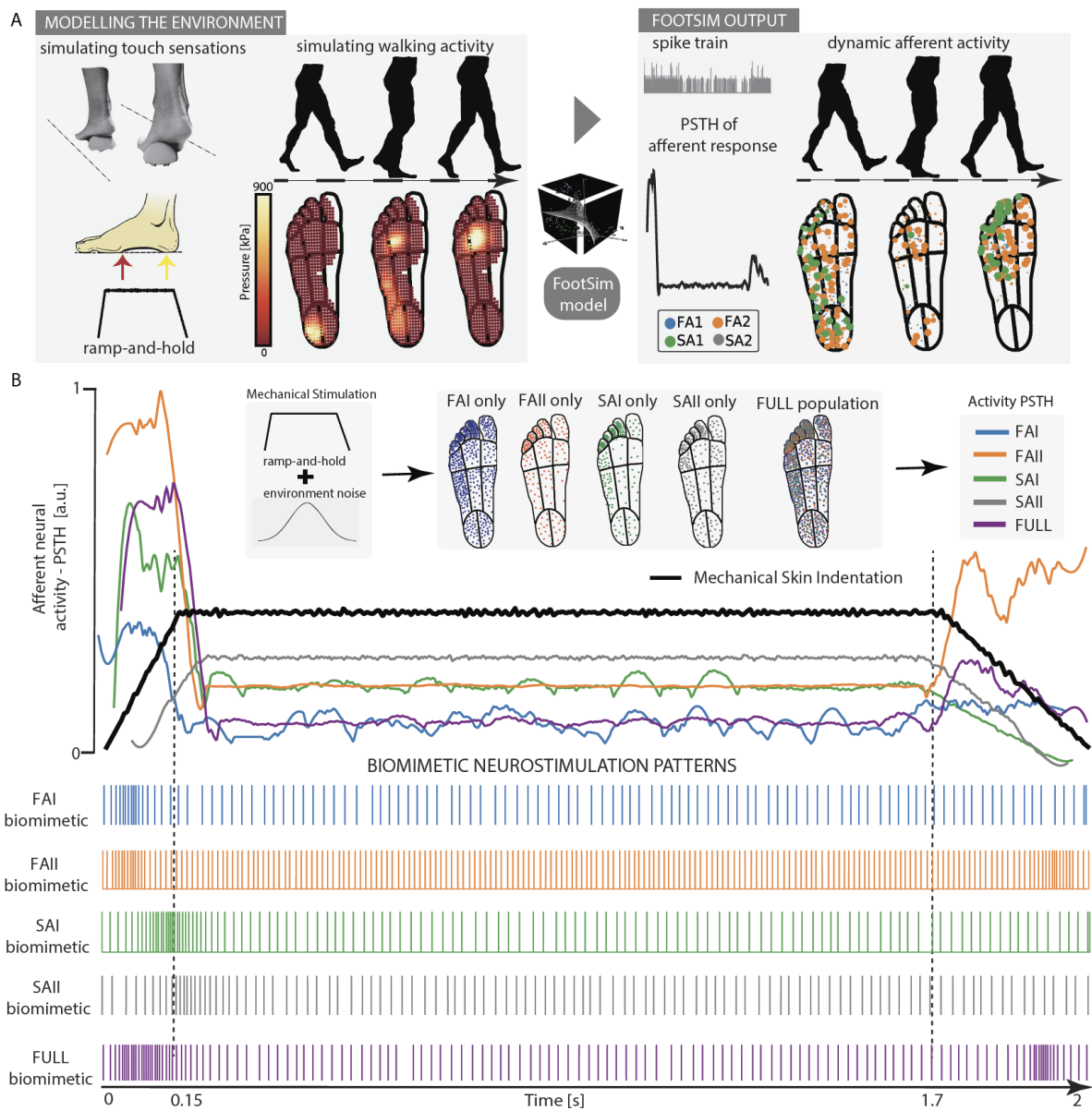
We exploited a trifold framework including modeling, animal and human experimentation (**Figure 4.1**) in order to design a neural stimulation strategy, based on a bio-inspired computation, effective for restoring somatosensation.

### 4.3.1 Biomimetic neurostimulation paradigms are designed by exploiting a realistic in-silico model of foot sole afferents (FootSim).

We used the computational model of foot sole cutaneous afferents (FootSim) (Katic et al. 2023) to recreate the natural coding of touch, and design new biomimetic stimulation strategies. FootSim is able to emulate the spatio-temporal dynamics of the natural touch code considering all tactile afferents innervating the plantar area of the foot. This model is a plug-and-play tool, fitted on the human microneurography data, which models external environment, defines a mechanical input, and gives on the output corresponding neural afferent activity (**Figure 4.2a**). While setting up the environment, user is populating the foot sole with desired distribution of all, or specific type of afferent, depending on the case and envisioned usage. Different mechanical stimuli could be applied. We can simulate single pressure stimuli on specific position of the plantar side of the foot, or, by extracting pressure distribution across the whole foot sole in different time steps, a scenario of a person walking or going through the obstacles (**Figure 4.2a** left). The FootSim output can be structured in several forms. We can extract spike train of a single afferent, of summed population activity, or spatially represent the activity of the afferents placed in the foot sole by coding their firing rates with the area of the circle (**Figure 4.2a** right).

When designing the biomimetic patterns, we also followed the aim to unveil if the naturalness can be coded in the neural responses specific to afferent type. We created 5 different scenarios by populating the foot sole with different types of afferents (**Figure 4.2b**: FAI/FAII/SAI/SAII only), or with a complete population realistically existing in the human foot (**Figure 4.2b**: FULL population). We applied a ramp-and-hold stimulus covering the whole foot sole with adding the environmental noise to mimic imperfection of the realistic pressure stimuli (**Figure 4.2b** black line). We calculated the peristimulus time histogram (PSTH) merging all afferent responses based on the scenario (**Figure 4.2b** colored lines) and used that as frequency patterns for creating biomimetic neurostimulation paradigms, while keeping the amplitude constant (**Figure 4.2b**: FAI/FAII/SAI/SAII/FULL biomimetic).

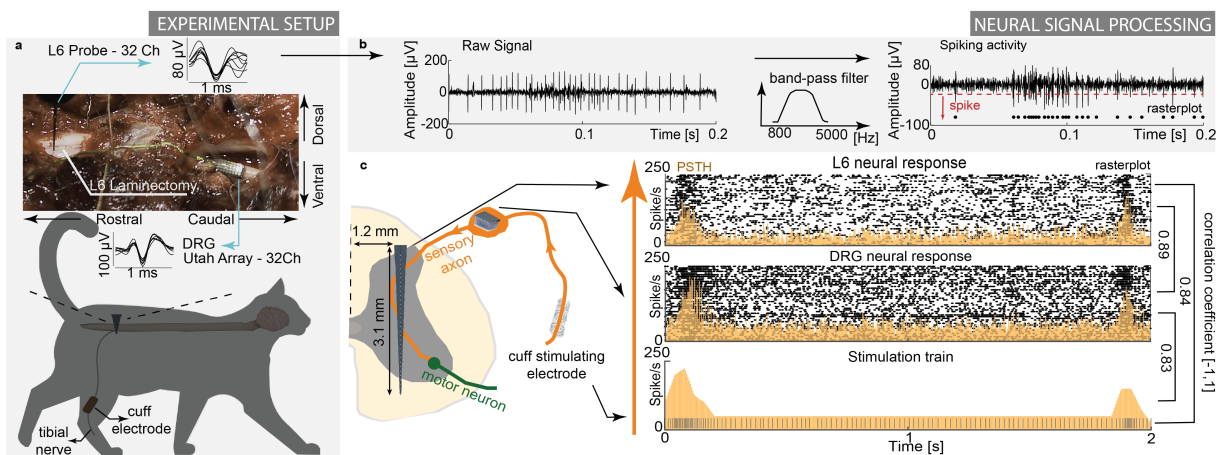




**Figure 4.2. Biomimetic neurostimulation patterns designed using a realistic in-silico model of foot sole afferents (FootSim).** (a) A schematic representation of practical use of FootSim plug-and-play model. Environment is modeled as a single, or continuous mechanical stimuli. The user can apply different types of stimulus, or simulate the walking scenario and the stimuli is given as an input to the model in form of pressure distribution across the foot sole. The output is afferent neural response that can be presented in several ways: as a single spike train, spatially represented on the foot sole by matching afferent firing rate with the area of the circle placed on the position of afferent, or as a populational response with peristimulus time histogram (PSTH). (b) Foot sole is populated with single type of afferent or with the whole realistic population (FAI/FAII/SAI/SAII/FULL population). We set the stimuli as a ramp-and-hold stimulus combined with the environmental noise and apply it on the whole foot area (black line). Neural responses of the whole applied population are given in the form of PSTH (colored lines). This was used as a function for the changes in frequency for defining biomimetic stimulating patterns. Amplitude remained constant in all biomimetic paradigms. All population distributions, afferent responses and respective biomimetic stimulation patterns are color coded: FAI: blue; FAII: orange; SAI: green; SAII: gray; FULL: purple.

### 4.3.2 The neurostimulation dynamics is transferred through somatosensory neuroaxis

We recorded intra-spinal neural response signals and activity in dorsal root ganglion (DRG) in two cats to be able to compare bio- and non-bioinspired stimulation patterns and study their transmission through somatosensory axes. Cats were decerebrated for enabling the analysis of only reflex responses, avoiding the signal interference with voluntary movements (Whelan 1996). Also, this procedure allows the testing without the use of anesthesia, that could potentially alter the neural responses. We implanted cuff electrode on tibial nerve for electrical stimulation and tuned the stimulation amplitude to be slightly above threshold. As multielectrode arrays showed to be the powerful tool for investigating the spinal cord processes (Greenspon et al. 2019), we extracted neural signals from a dorso-ventral 32-channel linear probe implanted within the L6 spinal segment. Additionally, with UTAH array with 32 channels (**Figure 4.3a**) we recorded neural signal in DRG at the L6 level.



**Figure 4.3. Purposely designed experiments to study neural dynamics through neurostimulation.** (a) Decerebrated cat experimental setup. We stimulated tibial nerve with cuff electrode and recorded neural response on the spinal level; upper part: exposed L6 vertebrae and dorsal root ganglion (DRG) with examples of recorded neural spikes from spinal linear electrode probe and DRG UTAH array. (b) Obtaining a multiunit neural activity. We filtered the signal to extract the spiking component and detect the neural action potentials using the thresholding algorithm. (c) Example of biomimetic stimulation paradigm and recorded response signal in one channel of spinal cord and DRG electrodes. Neural activity is presented and quantified with raster plot (black dots) and peri-stimulus time histogram (PSTH, yellow). Each row of the raster plot represents the response to a single biomimetic pattern (2s), while each dot corresponds to an action potential. Mean event rate (spikes/s) is defined as an average number of spikes within time frame of one bin (0.1 ms) across all single pulses of muscle nerve stimulation.

Stimulating tibial nerve with biomimetic paradigms and with constant stimulation of 50Hz that is commonly used in neuroprosthetics applications, allowed us to test the differences in resulting neural dynamics. We performed multi-unit threshold crossing analysis to identify the neural spiking activity (**Figure 4.3b**), presented the results in form of rasterplot, and quantified them using peri-stimulus time histogram (PSTH) (see Methods).

The temporal dynamics of the neural activation pattern was highly correlated to the frequency of the neurostimulation train (**Figure 4.3c**). In other words, by looking at the PSTH of single electrode channels, we can observe that multiple peripheral afferents

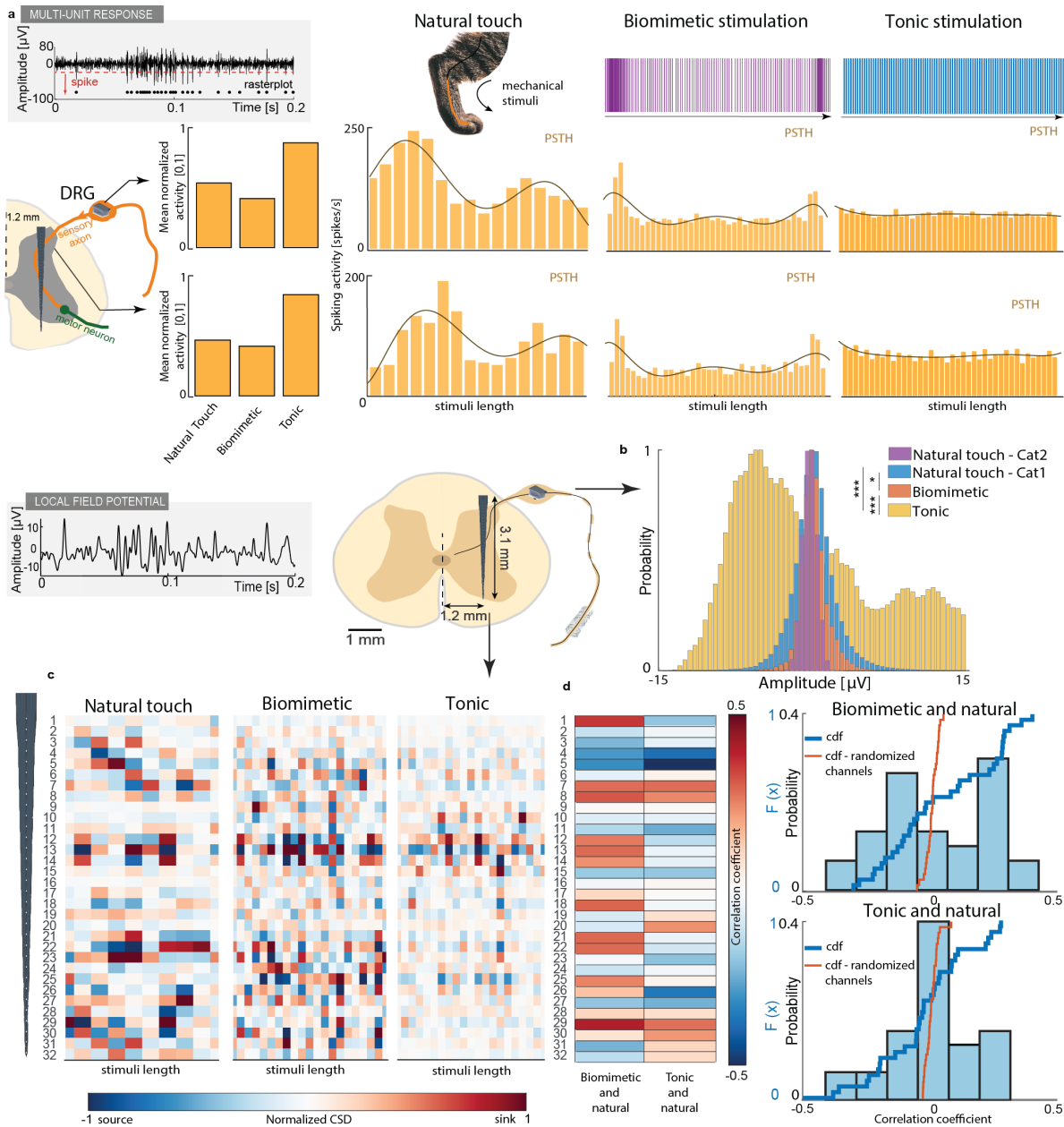
responses followed the biomimetic pattern and thus encoded the artificial tactile information. Biomimetic pattern of activation was transmitted to the DRG maintaining the same spatio-temporal neural dynamics ( $R=0.83$ ,  $p<0.05$ ) and then also to the spinal cord ( $R=0.89$ ,  $p<0.05$ ). This evidence proved how much the electrical neural stimulation could be used as an efficient tool to artificially generate patterns of neural activations able to be communicated to the upper parts of somatosensory system. Indeed, biomimetic patterns of neurostimulation, induced at the peripheral nerve level, showed to evoke a very similar spatio-temporal neural dynamics in the spinal cord ( $R=0.84$ ,  $p<0.05$ ).

### **4.3.3 Neural response evoked by biomimetic stimulation is more similar to the mechanically-induced activity than the one produced by tonic electrical stimulation**

We base our hypotheses of evoking close to natural perception with biomimetic stimulation on the ability to code and replicate natural neural response. We recorded and compared the neural responses in DRG and spinal cord resulting from different types of electrical stimulation with the naturally induced neural activity, produced by touching the cat's leg with the cotton bud.

Comparing the characteristics of the electrically-evoked neural dynamics with biomimetic, non-biomimetic and natural stimulation confirmed previous theories (Giacomo Valle et al. 2018a; Okorokova, He, and Bensmaia 2018; Saal and Bensmaia 2015). Indeed, the temporal pattern of the evoked-response exploiting biomimetic neurostimulation encoding was more similar to the one generated by mechanical stimulation of the skin of the animal, than the one induced with tonic stimulation. We represented multi-unit spiking activity with PSTH (**Figure 4.4a**). We calculated mean neural activity produced during the period of electrical or natural stimuli for estimating the overall amount of information occupying the spinal cord and DRG. Tonic stimulation showed much higher activity compared to the natural touch and biomimetic stimulation that have similar values, both in spinal cord and DRG recordings (**Figure 4.4a**, left). Shape of PSTH and its envelope gave an insight how neural activity is changing during the period of stimulation (natural, tonic or biomimetic). Biomimetic stimulation produces more similar activity as the natural touch compared to tonic stimulation (**Figure 4.4a**, right). Presented neural dynamics of activation codes the transmitted message and reveals that the information produced with biomimetic stimulation is matching better the natural touch neural coding than the commonly used tonic stimulation paradigm.

Local field potential (LFP) reflects summed activity of small population of neurons represented by their extracellular potentials (Destexhe and Goldberg 2015) and it captures the network dynamics (N. Maling and McIntyre 2016; Nicholas Maling and McIntyre 2016). We performed the analysis of the trigger averaged LFP signal for different stimulating conditions. We extracted the DRG most active channels and investigated their amplitude variations. More in detail, we compared the amplitude distribution of recorded LFP (**Figure 4.4b**).

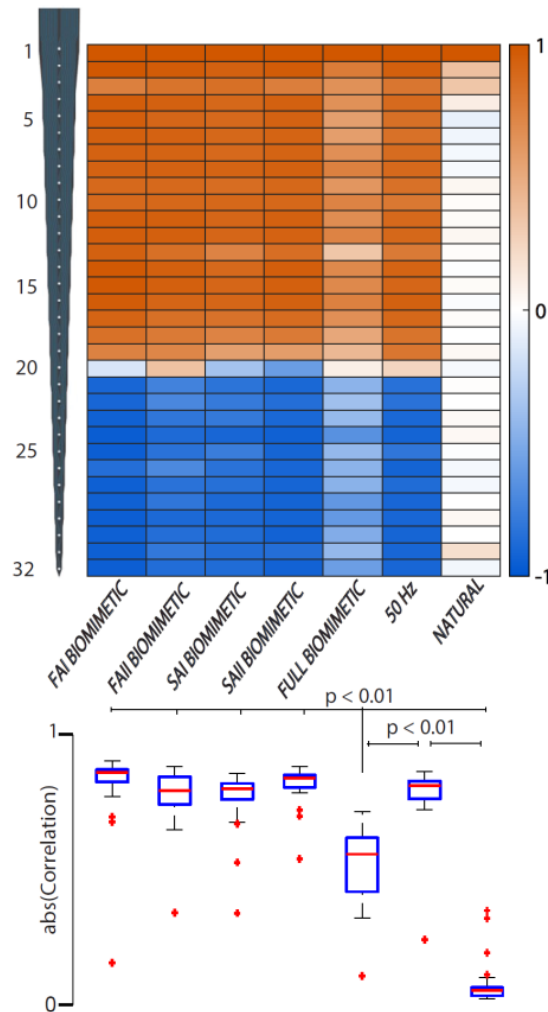


**Figure 4.4 Neural response on biomimetic stimulation is more similar to the response to natural touch than to tonic stimulation.** (a) Comparing multiunit neural activity as a response to natural touch, biomimetic or tonic (50 Hz) stimulation. We compared the signal recorded in DRG and spinal cord. Overall amount of neural activity during each condition is summed, normalized and presented with bars for comparison (left). Examples of spiking activity over time during each condition is presented using peri-stimulus time histogram (PSTH) (right) with the time bin of 50 ms. Brown lines represent the envelope of neural activity. (b) Comparing local field potential (LFP) recorded in DRG resulting from natural touch, biomimetic or tonic stimulation. Another natural touch response, recorded in cat 2, was added to analysis. We compared the distribution of specific signal amplitude values (\* $p < 0.01$ ; \*\*\* $p < 0.001$ ). (c) Comparing current source density (CSD) calculated from LFP recorded in spinal cord resulting from natural touch, biomimetic or tonic stimulation. CSD is normalized for each condition and presented along the length of the electrode with 100 ms bin. (d) Left: correlation of CSD between biomimetic/tonic and natural touch condition, channel by channel, color coded. Right: Histogram and cumulative distribution function (cdf) of the correlation coefficient values resulting from comparing biomimetic/tonic stimulation and natural touch condition (top/bottom). Blue line represents the cdf when the recording channels are matched and compared. Red line corresponds to cdf when channels are randomly shuffled and compared.

Stimulation of tonic response showed statistically different amplitude distribution compared to naturally evoked response as well as the neural response to biomimetic stimulation ( $p < 0.001$ ). Response on biomimetic stimulation was more similar to the natural condition ( $p > 0.05$ ). As an addition, we tested natural touch condition in one more cat to investigate the cross-subject similarities of neural dynamics. The distributions of LFP amplitude were similar ( $p > 0.05$ ), showing that the naturally evoked response follows a specific, potentially generalizable trend, rather than being completely individual. Current source density (CSD) is a technique for analyzing the extracellular current flow generated by the activity of neurons within a population of neurons. As it can estimate the location and magnitude of current sources and sinks that contribute to the measured electrical signals, we used it for comparing the spatial distribution of neural activity within a population of neurons in different conditions. We present the CSD estimated using local field potentials induced with biomimetic, tonic electrical stimulation, or natural touch (**Figure 4.4.c**). By looking at the spatial distribution of sinks and sources along the spinal axes, and comparing the overall resulting CSD, naturally induced touch response was more similar to the neural signal resulting from biomimetic stimulation (correlation coefficient 0.112) than to the one produced with constant, 50 Hz electrical stimulation (correlation coefficient 0.008). Additionally, we presented color coded channel-by-channel comparison of the resulting CSDs along the spinal electrode (**Figure 4.4d left**), and quantified the results with histogram and resulting cumulative distribution function (cdf) (**Figure 4.4d right**). CDF describes the probability that a random variable takes on a value less than or equal to a specified number. We used to compare distributions reflecting the comparison between CSD in different conditions. Tonic stimulation and natural touch produce neural responses with correlation coefficient very close to 0 in most of the channels, while that coefficient is higher for comparison between natural touch and biomimetic stimulation. In order to verify that this similarity is not produced by chance, we randomized the order of the channels in biomimetic and tonic electrical stimulation conditions and compared the recordings with the response of natural touch. It produced the correlation close to 0 for every electrode channel, confirming the validity of the used analyses.

Furthermore, we analyzed the similarity of neural signal along the transversal spinal axes. We compared the correlation between the LFP in the first channel of intraspinal array and all the other channels (**Figure 4.5**).

In the natural touch condition, similarity between the neural activity is high in the first few channels and it is diminished when looking at more ventral recordings, in both animals. When nerve was electrically stimulated, similarity between neural activity recorded with the different channels through spinal array is high. The biomimetic neurostimulation elicited a less similarity along the spinal axes than tonic stimulation. Full population biomimetic pattern showed to be the more promising one compared to the paradigms created by mimicking response of specific afferent types. Despite being significant different from the natural touch, biomimetic stimulation based on aggregate population of afferent responses shares a striking similarity with it, setting it significantly apart from the tonic, 50 Hz stimulation.



**Figure 4.5. Synchronization of the neural activity evoked in the spinal cord.** We compared and presented the correlation between the neural local field potential recording in the first electrode channel with all the other channel recordings. Upper part: Correlation values are color coded and presented along the spinal array electrode axes. Bottom part: We compared absolute values of correlation coefficient of natural with every biomimetic condition as well as 50 Hz stimulation with FULL biomimetic and natural touch condition with one-way ANOVA. Boxplots: The central mark indicates the median, and the bottom and top edges of the box indicate the 25th and 75th percentiles, respectively. The whiskers extend to the most extreme data points not considered outliers, and the outliers are plotted individually using the red '+' symbol. p values are indicated

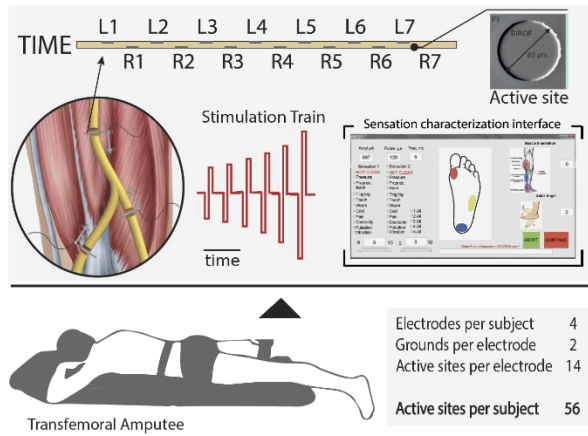
In summary, cumulative neural dynamics resulting from naturally induced touch is more similar to those produced by biomimetic stimulation than tonic electrical stimulation.

#### **4.3.4 Biomimetic neurostimulation evokes more natural sensations than non-biomimetic neurostimulation paradigms.**

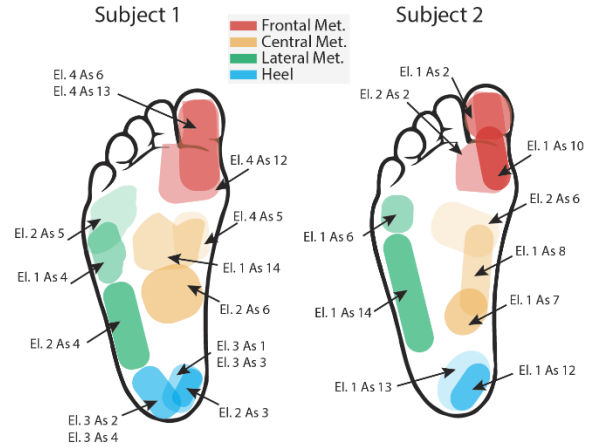
To test the functional implication of using biomimetic neurostimulations, we implemented and tested them in a human clinical trial. The scope was to firstly validate the biomimetic neurostimulation encoding assessing the quality of the evoked-sensations. Then, a real-time neuro-robotic device exploring biomimetic encoding strategies has to be compared to devices with previously-adopted encoding approaches in terms of functional performances. To this aim, three patients suffering from a transfemoral amputation (**Table 4.1**) were implanted with TIME electrodes in the tibial branch of the sciatic nerve (**Figure 4.6a**).



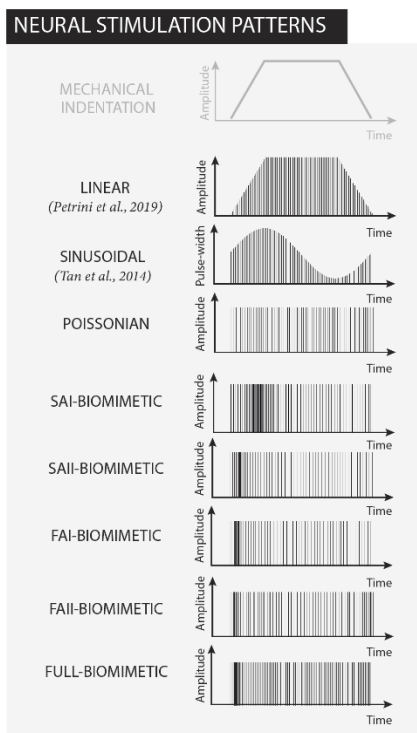
### A HUMAN PERIPHERAL NERVE IMPLANTS



### B ELECTRICALLY-EVOKED SENSATION LOCATIONS

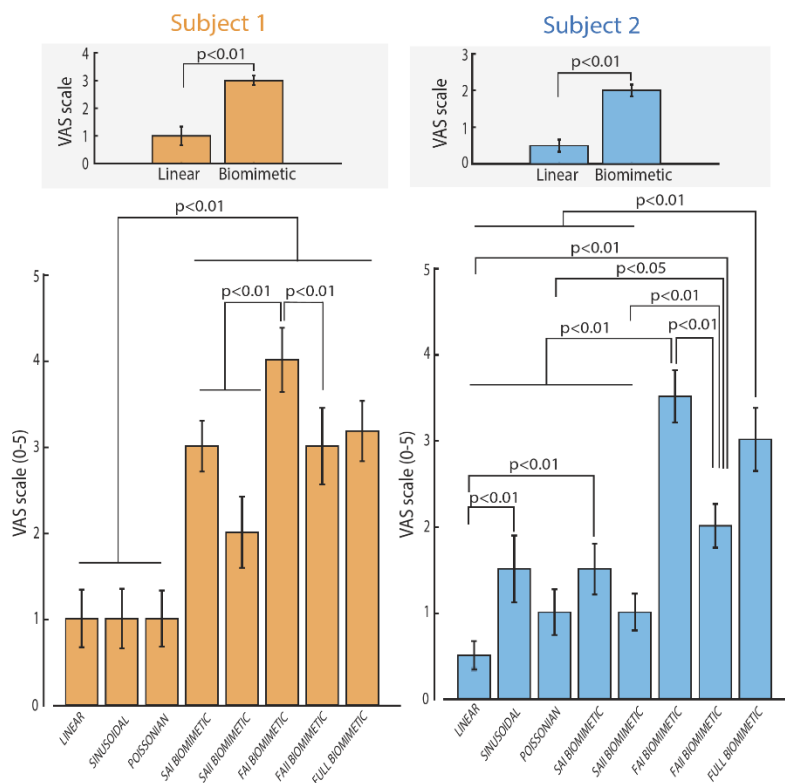


### C



### D

### PERCEIVED SENSATION NATURALNESS

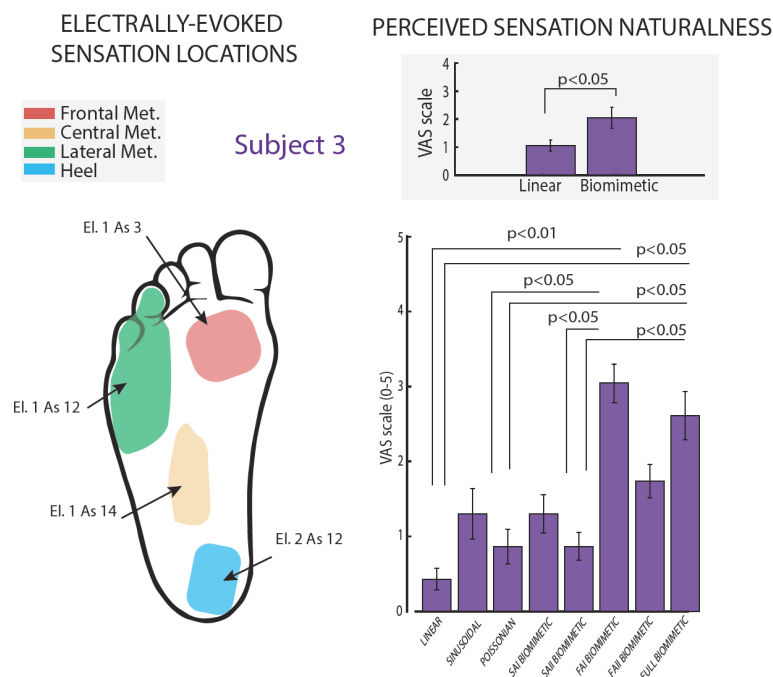


**Figure 4.6 Biomimetic neurostimulations evoke more natural perceptions in implanted humans than non-biomimetic approaches.** (a) Individuals with lower-limb amputation were implanted with TIME in their tibial nerves. The multichannel electrodes were used to directly stimulate the peripheral nerves evoking sensation directly referred to the phantom foot. (b) Projective fields maps of two implanted subjects (1 & 2) related to the active sites adopted to electrically stimulate the nerves. Different colors show the 4 main regions of the phantom foot (Frontal, Lateral and Central Metatarsus, and Heel). (c) Biomimetic and non-biomimetic neurostimulation strategies adopted for encoding a mechanical indentation of the foot sole. Linear neurostimulation is taken from (Francesco Maria Petrini, Valle, et al. 2019) and Sinusoidal neurostimulation by (Daniel W. Tan et al. 2014) (d) Naturalness ratings (VAS scale 0-5) of the perceived sensation elicited exploiting different stimulation strategies in two subjects. Insets: Group comparison between linear vs biomimetic stimulations.

After a phase, called sensation characterization procedure, where all the 56 electrode active sites have been tested (Francesco Maria Petrini, Valle, et al. 2019), a subgroup of electrode

channels were selected for this evaluation. Active sites eliciting sensations located in the frontal, central, lateral metatarsus and heel were identified (**Figure 4.6b** and **Figure 4.7**). In this way, the selected channels were electrically activating different groups of mixed afferents with projecting fields in different areas of the phantom foot (so with different distribution of innervating fibers). Then, multiple strategies, encoding a mechanical skin indentation, have been adopted to deliver neurostimulation trains through each selected channel of the intraneural implants (**Figure 4.6c**). The participants were asked to report the perceived sensation naturalness using a visual analogue scale (VAS) between 0 (totally non-natural sensation) and 5 (totally natural sensation – skin indentation) (Giacomo Valle et al. 2018a; Lenz et al. 1993).

In all the three implanted subjects and considering all the active sites tested (with different projected fields), the biomimetic neurostimulation patterns elicited sensations more natural than the linear neurostimulation encoding ( $3 \pm 0.18$  with Biomimetic compared to  $1 \pm 0.35$  in Linear for S1,  $2 \pm 0.16$  with Biomimetic compared to  $0.5 \pm 0.17$  in linear for S2, and  $2 \pm 0.36$  with Biomimetic compared to  $1 \pm 0.18$  in linear for S3 across all electrode tested,  $p < 0.01$ ) (**Figure 4.6d** and **Figure 4.7**) that was previously adopted in multiple neuroprosthetic applications (Francesco M. Petrini et al. 2019; G. Valle et al. 2018; Francesco Maria Petrini, Valle, et al. 2019). Moreover, biomimicry-based encodings often resulted in more natural perceived sensations compared to both sinusoidal (pulse width-variant) and poissonian (frequency-variant) neurostimulation strategies ( $p < 0.05$ ), indicating the importance of inducing a neural activation dynamic mimicking the natural biological code.

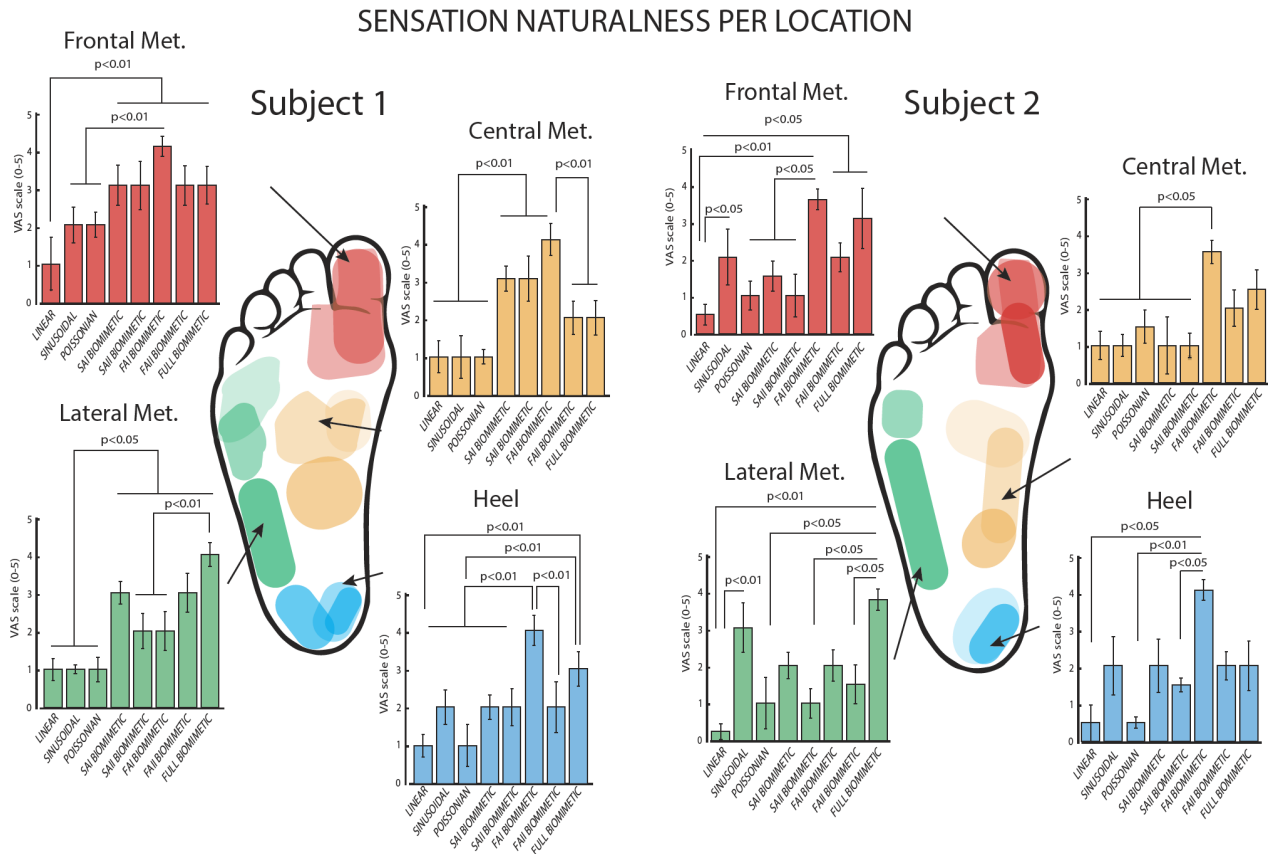


**Figure 4.7 Biomimetic neurostimulation elicits more natural sensations than non-biomimetic approaches in Subject 3.** Projective fields map of Subject 3 related to the active sites adopted to electrically stimulate the tibial nerve. Different colors show the 4 main regions of the phantom foot (Frontal, Lateral and Central Metatarsus, and Heel). Naturalness ratings (VAS scale 0-5) of the perceived sensation elicited exploiting different stimulation strategies. Insets: Group comparison between linear vs biomimetic stimulations.

Notably, although multiple biomimetic-like paradigms have been tested (SAI-, SAIL-, FAI-, FAII-like and Full biomimetic), none of them proved to be better. Although biomimetic stimulation was always eliciting more natural sensations than traditionally-adopted



encoding, analyzing the results per location in both subjects (**Figure 4.8**) did not show any clear evidence of an optimal biomimetic encoding schema. This was probably caused by the different composition of the fibers activated by the electrode channels in the different foot regions (Strzalkowski et al. 2018). In fact, the perceived areas were different according to the active site selected to stimulate, indicating a different group of mixed afferents recruited by the neurostimulation. We hypothesized that not only the proportion of SA and FA fibers is relevant, but also their role in encoding touch information in that specific region.



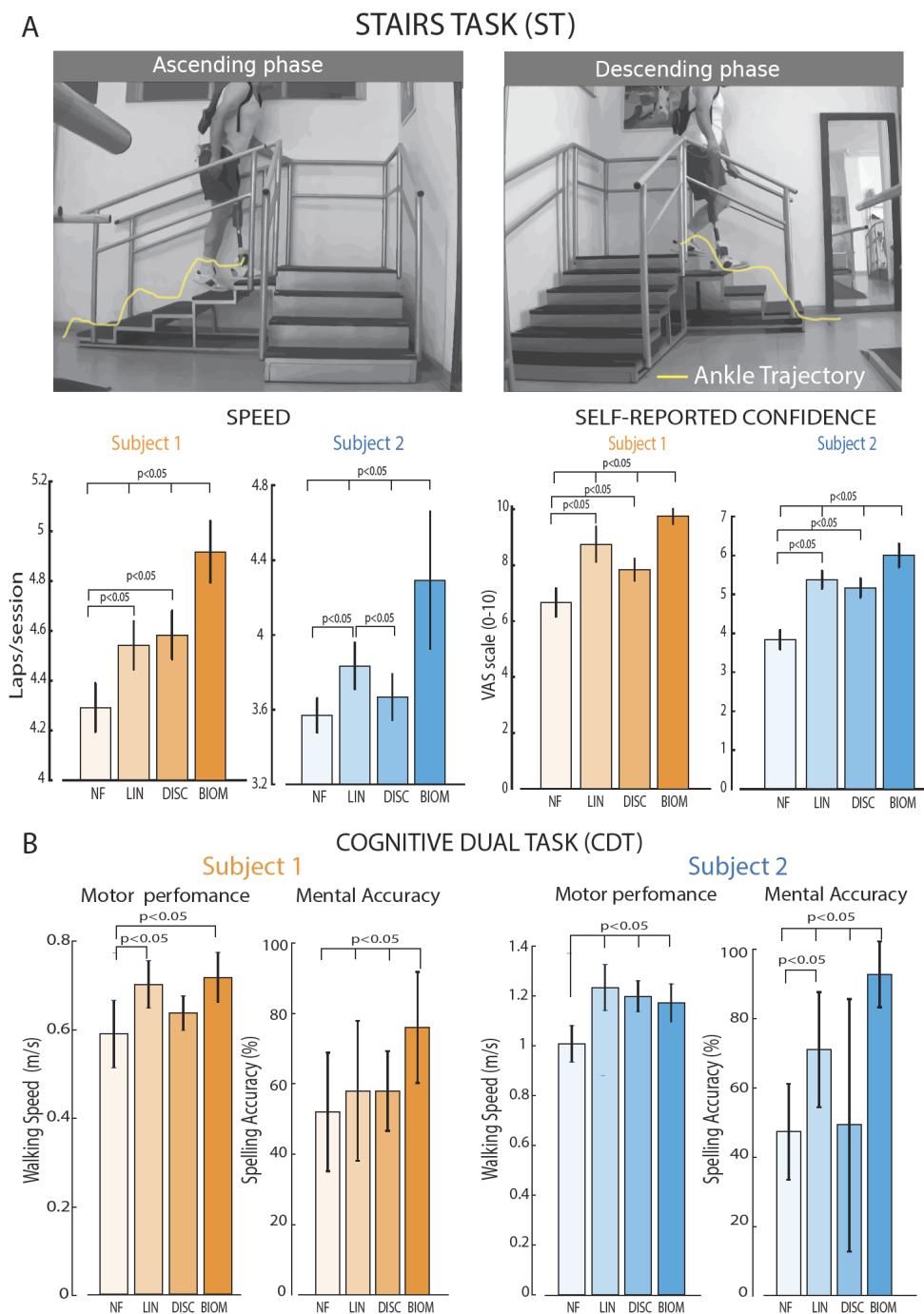
**Figure 4.8 Electrically-evoked sensation naturalness related to different projected fields location.** Projective fields maps of two implanted subjects (1 & 2) related to the active sites adopted to electrically stimulate the nerves. Different colors show the 4 main regions of the phantom foot (Frontal, Lateral and Central Metatarsus, and Heel). Naturalness ratings (VAS scale 0-5) of the perceived sensations breakdown per location of the projected fields.

These findings highlighted how biomimicry is a fundamental feature of the electrical neural stimulation for successfully restoring more natural somatosensory information.

#### **4.3.5 Biomimetic neurostimulation on a neuro-robotic device allows for a higher mobility and a reduced metal workload**

Aiming to develop a neuroprosthetic device able to replace the sensory-motor functions of a natural limb as much as possible, this biomimetic neurostimulation was then implemented in a real-time robotic system. This wearable system was composed by: i) a sensorized insole with multiple pressure sensors; ii) a microprocessor-based prosthetic knee with a compliant foot (Ossur, Iceland); iii) a portable microcontroller programmed with the biomimetic

sensory encoding algorithms; iv) a multichannel neurostimulator; v) intraneural electrodes implanted in the peripheral nerves (TIMES).



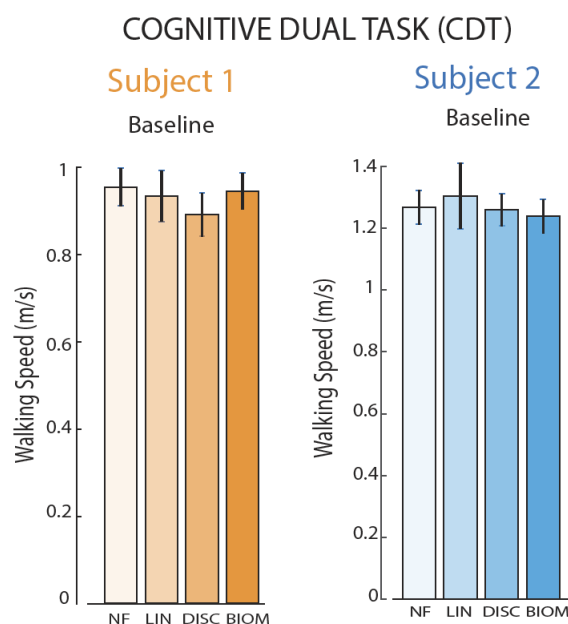
**Figure 4.9 Real-time biomimetic neural feedback allows for higher speed and lower cognitive workload while walking.** (a) In the Stairs Task (ST), the subjects (1 & 2) were asked to walk over stairs in both ascending and descending directions. (b) Speed (Laps/session) and self-reported confidence (VAS Scale 0-10) were measured in ST. (c) Motor performance (Walking Speed - m/s) and Mental Accuracy (Spelling Accuracy - %) of Subject 1 & 2 in the Cognitive Dual Task (CDT). In both tasks, conditions are NF (No Feedback), LIN (Linear Neurostimulation), DISC (Discrete Neurostimulation) and BIOM (Biomimetic Neurostimulation).

The neuroprosthetic device was working in real-time being able to record pressure information from the wearable sensors, while the patient was walking, and converting them

in patterns of biomimetic neurostimulation delivered through the TIMEs (see Method for implementation details). In this way, the users were able to perceive natural somatotopic sensations coming directly from the prosthetic leg without any perceivable delay.

After the implementation, we assessed the effects of exploiting the biomimetic encoding (BIOM) in a neuro-robotic device compared to a linear (LIN) or a time-discrete (DISC) neurostimulation strategy. In the LIN, the sensors' readouts were converted in neurostimulation trains following a linear relationship between applied pressure and injected charge (G. Valle et al. 2018; Francesco Maria Petrini, Valle, et al. 2019). In case of DISC, short-lasting, low-intensity electrical stimulation trains were delivered synchronously with gait-phase transitions (Crea et al. 2017; F. Clemente et al. 2016). Also the condition without the use of any neural feedback (NF) was included in the motor paradigms as a control condition.

The neuroprosthetic users were thus asked to perform two ecological motor tasks: Stairs Task (ST) (Giacomo Valle, Saliji, et al. 2021; Francesco Maria Petrini, Valle, et al. 2019) and Cognitive Double Task (CDT) (Preatoni et al. 2021).



**Figure 4.10 Walking speed baseline in the Cognitive Dual Task (CDT).** Motor performance (Walking Speed - m/s) of Subject 1 & 2 in the Cognitive Dual Task (CDT) at baseline (no mental task). The tested conditions are NF (No Feedback), LIN (Linear Neurostimulation), DISC (Discrete Neurostimulation) and BIOM (Biomimetic Neurostimulation).

In ST, results indicated that, when exploiting biomimetic neurostimulation in a neuro-robotic leg, both users improved their walking speed ( $4.9 \pm 0.1$  for S1 and  $4.3 \pm 0.4$  for S2 laps/session) compared to LIN ( $4.5 \pm 0.1$ ,  $p < 0.05$  for S1 and  $3.8 \pm 0.1$ ,  $p < 0.05$  for S2 laps/session), DISC ( $4.6 \pm 0.1$ ,  $p < 0.05$  for S1 and  $3.6 \pm 0.1$ ,  $p < 0.05$  for S2 laps/session) and NF ( $4.3 \pm 0.1$ ,  $p < 0.05$  for S1 and  $3.5 \pm 0.1$ ,  $p < 0.05$  for S2 laps/session) conditions (**Figure 4.9a**). Interestingly, also the self-reported confidence (VAS scale 0-10) in walking on stairs was increased, when the participants were exploiting the neuroprosthetic device with biomimetic neurofeedback ( $9.75 \pm 0.26$  for S1 and  $6 \pm 0.3$  for S2) compared to LIN ( $8.75 \pm 0.62$ ,

$p < 0.05$  for S1 and  $5.37 \pm 0.23$ ,  $p < 0.05$  for S2), DISC ( $7.83 \pm 0.39$ ,  $p < 0.05$  for S1 and  $5.17 \pm 0.25$ ,  $p < 0.05$  for S2) and NF ( $6.67 \pm 0.49$ ,  $p < 0.05$  for S1 and  $3.83 \pm 0.25$ ,  $p < 0.05$  for S2) conditions (**Figure 4.9a**).

In the CDT, both participants showed a higher mental accuracy in BIOM compared to the other conditions ( $p < 0.05$  in both subjects), while maintaining the same walking speed. In particular, the mental accuracy of S1 was  $76 \pm 16\%$  in BIOM,  $58 \pm 20\%$  in LIN,  $58 \pm 11\%$  in DISC and  $52 \pm 17\%$  in NF while in S2  $94 \pm 9.6\%$  in BIOM,  $72 \pm 17\%$  in LIN,  $50 \pm 37\%$  in DISC and  $48 \pm 14\%$  in NF. Notably, the walking speed was always higher in the feedback conditions compared to NF for S2 ( $p < 0.05$ ) and in BIOM and in LIN for S1 ( $p < 0.05$ ). As expected, without adding a secondary task, no difference was observed in the walking speed among the conditions in both subjects ( $p > 0.1$ , **Figure 4.10**). These findings indicated a higher decrease in mental workload, while the users were performing two tasks simultaneously (one motor and one cognitive) in the moment that a more bio-inspired neural stimulation was exploited in a neuro-robotic device.

## 4.4 Discussion

### 4.4.1 Multi-level approach for designing new stimulation strategies that would minimize paresthesia sensations

In this study, we designed, developed and tested a neuro-robotic device exploiting model-based biomimetic neurostimulations in people with limb amputation. Due to a multilevel framework, it was possible to design and test effective bio-inspired neurostimulation paradigms to elicit more natural feelings and better understand the reasoning behind the use of biomimetic approaches in the neuroprosthetic field. Indeed, thanks to realistic in-silico modeling of the foot touch coding, precise neural stimulation patterns were defined that could accurately emulate the firing of the cutaneous mechanoreceptors. Single-fiber (SAI, SAI, FAI, FAI) and mixed-fibers (FULL) type patterns have been implemented to encode a mechanical skin indentation into a neural stimulator. We modulated the stimulation frequency based on the fiber dynamics of activation since it showed to be beneficial for sculpting the artificial touch for bionic limbs (Emily L. Graczyk et al. 2022).

### 4.4.2 Comparing neural responses induced with natural touch and electrical nerve stimulation

The purposely-designed animal experiments allowed us to compare the neural dynamics as a response to natural touch, biomimetic or tonic electrical stimulation. The recordings in decerebrated cats via multiple neural interfaces along their somatosensory neuroaxis (somatic nerve, DRG and spinal cord) showed that biomimetic neurostimulations evoked spatio-temporal characteristics of the afferents' response more similar to the naturally induced one than tonic stimulation. These biomimetic patterns are going towards avoiding highly synchronized activity in spinal circuits that could saturate the circuits and limit the possibility to perceive touch sensations restored with electrical stimulation (G. A. Miller

1956). This is clear evidence of the effect of bio-inspired stimulation dynamics on the neural afferents activation, showing the possibility to artificially encode natural sensory messages into the nervous system. Indeed, previous researches have hypothesized the adoption of complex spatiotemporal patterns mimicking natural peripheral afferents activity (Saal and Bensmaia 2015; Okorokova, He, and Bensmaia 2018). This approach was also proposed for activity cortical activity using intracortical microstimulation (ICMS) to convey feedback of touch (Greenspon, Valle, Hobbs, Verbaarschot, Callier, Shelchkova, Sobinov, Jordan, Weiss, Fitzgerald, Prasad, van Driesche, et al. 2023) or of the entire movement trajectory (natural proprioceptive sensation) (Tomlinson and Miller 2016). Likewise, they also assumed that exploiting an ICMS interface that mimics natural sensations would be faster, and ultimately more effective than learning arbitrary associations with unnatural sensations or arbitrarily modulated ICMS (Bensmaia and Miller 2014). Our study validates these hypotheses on the use of biomimicry in PNS neuroprostheses. However, our experimental setup was focused to understanding the first layer of processing information coming from the periphery. We believe future experimental work should extend these findings investigating neural processes caused by electrical stimulation in gracilis (or cuneate for the upper limb) nucleus, thalamus or in somatosensory cortex.

#### **4.4.3 Biomimetic stimulation in neuromodulation devices is beneficial both for the perceived sensation and its functionality**

These biomimetic neurostimulation strategies were tested in three human subjects implanted in their peripheral leg nerves with intraneural electrodes. All the participants reported to feel more natural sensations, when stimulated with biomimetic encodings with respect to standard neuromodulation patterns from every stimulation channel on the electrodes. Neural stimulation gradually recruit all the sensory afferents within the fascicle (S. Raspopovic et al. 2017; Zelechowski, Valle, and Raspopovic 2020) depending on both distance from the electrode (threshold proportional to square of distance) and their diameter (threshold proportional to  $1/\text{square root of fiber diameter}$ ). Therefore, each stimulation pulse delivered through the active site is likely to recruit a mix of sensory afferents types, even if clustered (Jabaley, Wallace, and Heckler 1980). For this reason, how many and what tactile afferents will be stimulated by a given stimulation pattern through a specific electrode is unknown a priori. This might be the reason why different types of biomimetic encoding were reported as more natural by the participants according to the perceived foot location (**Fig.S3**) and, therefore, to the clusters of recruited afferents. This phenomenon can also explain the typology of sensation reported, while specific types of afferents were activated by neurostimulation (Torebjörk and Ochoa 1980; Ochoa and Torebjörk 1983) (flutter, vibration, touch). Likewise, why with simpler encoding (at the threshold level) the electrically-evoked sensation can be sometimes reported as naturalistic (Francesco M. Petrini et al. 2019; Daniel W. Tan et al. 2014; Francesco Maria Petrini, Valle, et al. 2019; Wendelken et al. 2017). Indeed, hypothesizing to recruit a cluster of only SAI-like afferents with intraneural electrical stimulation, the related evoked sensations could be sustained pressure (Ochoa and Torebjörk 1983). Nevertheless, in our study, biomimicry showed to be a fundamental feature for restoring more natural

sensations via neurostimulation in neuroprosthetic applications, regardless the groups of recruited afferents.

Finally, we implemented these algorithms in robotic prosthetic devices in a real-time fashion comparing their functional performance with previously-proposed technologies. Biomimetic neuroprosthetic legs allowed for a faster stair walking and a decreased mental workload in a double task paradigm in both subjects. These findings demonstrated that biomimicry is relevant also for device functionality and thus to enhance the beneficial effect of this intervention. In particular, a significant boost in mobility, on a difficult everyday life task as the stairs, is very relevant for people with lower-limb amputation. This improvement is likely connected to reported higher confidence in the prosthetic leg with biomimetic sensory feedback(Giacomo Valle, Saliji, et al. 2021) . The amputee is able to instantly sense the position of his leg with regard to the ground more naturally, which allows him to transition faster from heel strike to loading his prosthetic leg(Raja, Neptune, and Kautz 2012). Confidence and mobility have been previously proposed to be among the clearest and simplest parameters showing the impact of sensory feedback on gait(Giacomo Valle, Saliji, et al. 2021). Regarding the CDT, it represented a real-life scenario of multiple simultaneous tasks. It allowed us to obtain an objective measure of the better cognitive integration of the prosthesis with biomimetic neurostimulation(Giacomo Valle, D'Anna, et al. 2020; Preatoni et al. 2021), since both amputees improved their mental accuracy. In addition to our results, previous studies have also preliminarily shown these improvements in manual dexterity and object recognition in upper-limb amputees exploiting robotic hand prostheses(George et al. 2019; Giacomo Valle et al. 2018b).

#### **4.4.3 Future biomimetic neurostimulation devices**

This neuromodulation approach and framework based on biomimicry could also be very relevant for other sensory and motor neuroprostheses (e.g., Deep Brain Stimulation(de Hemptinne et al. 2015), epidural stimulation(Wagner, Mignardot, Goff-Mignardot, et al. 2018), ICMS(Sharlene N. Flesher et al. 2021; S. N. Flesher et al. 2016)) and for bioelectronic medicine applications (e.g. vagus stimulation(Marsal et al. 2021), stimulation of the autonomic nervous system(Donegà et al. 2021)) where there is the same necessity to evoke a natural pattern of activation in a certain nervous district using artificial electrical stimulation. Indeed, the biomimetic approach has been proven to be effective for improving functional performance in other type of neural prostheses (e.g., enhanced speech intelligibility for cochlear implants(Fumero et al. 2021); improved restoration of gaze stability in vestibular prostheses(Wiboonsaksakul et al. 2022)). Considering future biomimetic neuro-robotic devices restoring fully-natural sensations, spatial patterning can be achieved by stimulating different electrodes with spatially displaced projection fields, while temporal patterns can be elicited by temporally modulating the stimulation parameters delivered through each electrode, as proposed in our study. However, the extent to which artificially evoked neural activity must mimic that of the natural afferent inputs in order to be fully-exploitable also for more complex tactile features(Giacomo Valle, Strauss, et al. 2020; Mazzoni et al. 2020) (textures, object stiffness, shape, etc.) or proprioception remains a critical question.

Here we evaluated multiple types of biomimetic patterns that were developed using the distinct response characteristics of individual afferent types. When we stimulated the entire nerve during animal experiments, the biomimetic pattern based on the aggregate afferent response (FULL biomimetic) showed to be the most promising one compared to its natural counterpart. Notably, when these paradigms were delivered using TIME electrode in humans, smaller clusters of mixed afferents have been selectively activated by the different channels. Interestingly, the naturalness of the sensation, for the same encoding strategies, changed accordingly to specific areas of the foot sole. It suggests that the imposition of the aggregate dynamics for inducing natural sensations is not optimal for every fiber cluster recruited. It seems to depend on the distribution of activated afferents (mechanoreceptors) and their specific role in the sensory processing. We believe that neurostimulation strategies should be informed by computational modelling emulating realistic dynamic conditions.

In conclusion, our collected evidence not only amplifies the remarkable impact of biomimicry from a scientific perspective, but it also holds immense promise in heralding the advent of the next generation of neuroprosthetic devices. New technologies, inspired by nature, have a potential to fully emulate natural neural functions lost after a disease or an injury. The possibility to naturally communicate with the brain will open new doors for science in multiple fields.



# Chapter 5

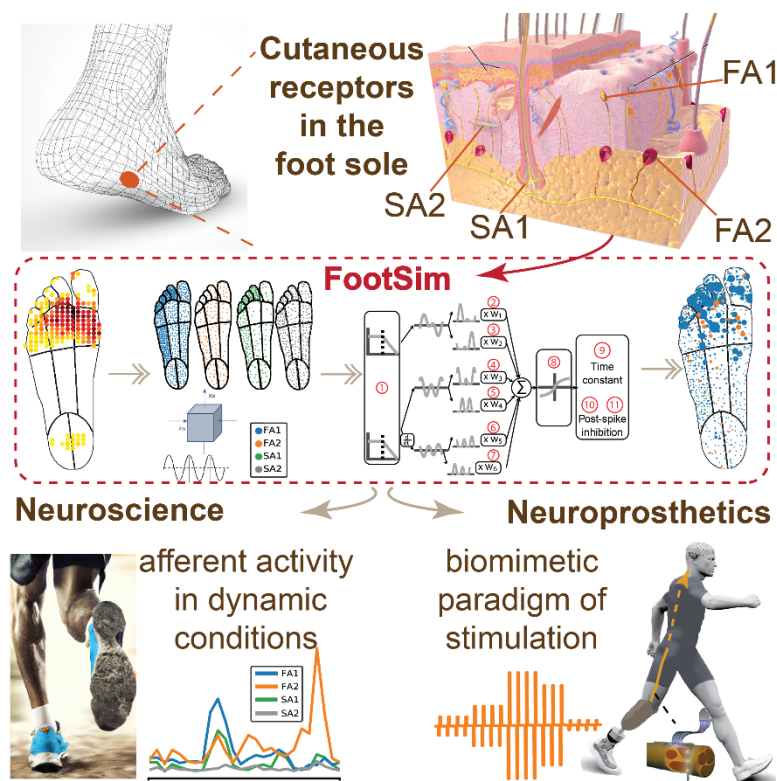
## Conclusion

*“Everything is hard before its easy.”*  
Goethe J.W.

## 5.1 In silico modeling of touch – scientific and engineering tool

Human gait and posture control heavily rely on the essential role of cutaneous feedback from the foot sole (Takakusaki 2013; Pearcy and Zehr 2019). Our knowledge about the coding the tactile feedback into the neural afferent responses is based on the electrophysiological recordings. Microneurography is the most commonly applied method for capturing electrophysiological responses from individual fibers in human nerves (Mano, Iwase, and Toma 2006). It uses the microelectrodes to directly record the neural traffic of myelinated and unmyelinated fibers (Ackerley and Watkins 2018). However, our ability to comprehend the responses of these afferents in realistic scenarios remains restricted because of technical obstacles (e.g. person has to be very still while needles are inserted deep until nerves) associated with conducting the microneurography procedure in vivo. It proves to be challenging, time-consuming, and highly unstable, rendering it impractical in dynamic conditions such as walking and running. Moreover, conducting experiments using this technique implies for participants to remain motionless to prevent displacement of the recording electrode from the targeted single fiber. Previous studies were mostly based on analyzing the responses of mechanoreceptors innervating the hand (Roland S. Johansson and Flanagan 2009). However, even though the hand and foot share the same afferent classes in their glabrous skin, their mechanical behavior is different, as well as distribution of specific afferent types, which is expected due to their completely different usage. While the hand often encounters numerous small and intricate stimuli, particularly during precision grips, the foot, on the other hand, is typically subjected to stimuli covering a broader spatial range. In order to tackle the challenge of comprehensively studying the responses of foot afferents during standing and walking, which cannot be accessed using current recording techniques, a sophisticated computational model was created. The FootSim (presented in Chapter 2) in silico model replicates the neural spiking reactions to diverse mechanical stimuli originating from the collective population of all four types of mechanoreceptors that innervate the foot sole, therefore confirming the *Hypothesis 3*. FootSim has a twofold impact: it is a tool suggested for both neuroprosthetic and neuroscientific use (**Figure 5.1**).

From the neuroscientific point of view, FootSim is able to simulate the activation foot sole afferents during dynamic conditions, like jogging, walking, or while maintaining balance, overcoming the limitations of present recording techniques. It can also reveal the specific role of afferent fiber types during daily situations. On the other side, accumulated knowledge about the cutaneous afferents' function is essential for designing effective interventions and therapies related to sensory deficits or disorders. Conditions that affect cutaneous afferents, such as neuropathies or sensory impairments, can significantly impact an individual's daily life, motor skills, and overall well-being. Understanding their role allows researchers and healthcare professionals to develop targeted approaches for rehabilitation and treatment. Since FootSim has parameters of skin features, as well as number and positioning of the fiber types, that are easily modulable by the user, the model can be adapted to the person with a specific condition. For example, diabetic patients often have higher hardness of the skin as well as they are dealing with the neuropathy which can cause the inability of some afferents to transmit the information from the periphery, therefore they do not feel when a rock is within a shoe, causing damage.



**Figure 5.1. FootSim possible contribution to biomimetic stimulation patterns for tactile feedback restoration in future neuroprosthetics.** In a possible scenario, the user will be fitted with a leg prosthesis collecting real-time spatiotemporal pressure data via a sensorized insole (bottom left). This data will be provided as an input to the FootSim model. The model would convert the artificial pressure profiles into realistic neural response patterns (top, blue shaded box). FootSim output could be potentially used for generating biomimetic stimulation policies (bottom right). Neurostimulator would generate these paradigms and this type of stimulation could be used to transmit to the subject the information recorded with the insole in a future possible scenario. Taken from (Katic et al. 2023) with permission.

Thinking about the neuroprosthetic perspective, the use of the FootSim model is envisaged for defining the biomimetic stimulation patterns mimicking the natural neural signals coming from the periphery.

Previously, similar type of model was developed for replicating the mechanoreceptor activation in the hand (Saal et al. 2017). It is a tool that enables the simulation of the responses of afferent innervating the glabrous skin of the hand, based on the data from monkeys. However it was limited (due to the constraints in fitting dataset) by replicating three out of four afferent classes that exist in the human hand, it caused a great response from the scientific audience. Moreover, the same group developed graphical user interface to generate a model that computes the firing rate and area of afferent activation from a dynamic stimulus applied to a specific skin area (Okorokova, He, and Bensmaia 2018). They envisioned the use of these model parameters for creating a biomimetic stimulation protocols restoring real-time tactile feedback in the hand. Yet, alongside with a missing class of afferents that was not implemented, they had a non-realistic mechanics of hand skin, and in my work regarding foot I addressed both of these limitations.

Also, finding a proper way to translate from the model outputs to the biomimetic paradigm able to be properly processed and restore close to natural sensation, is still a big open question (Cimolato, Katic, and Raspopovic 2021). The algorithm for creating this transformation can be based on the modeling approach, as previously done for stimulating the hand (Okorokova, He, and Bensmaia 2018). Yet, also simpler solutions as coding the frequency of stimulation directly from the summation of spike trains of all activated

afferents, while keeping the charge profile correlated with the number of recruited fibers, can be suitable for constructing predefined biomimetic paradigms (as showed in Chapter 4).

From the technological aspect, the final use of the Foot Sim model is in its real time application within neuroprosthetic systems (as suggested in **Figure 2.13**). For an engineer that is working on design of such a neuromodulation system, it can be considered as a “plug & play” tool, able to reconstruct the afferent activity, and does not require any specific expertise for use. FootSim is developed fully in Python and therefore can have a convenient processing speed, also for the large population sizes. For achieving this, the improvement needs to go in line with the advancements in the neurostimulation field regarding the novel interfaces and their materials (Giacomo Valle et al. 2022) while meticulously considering also limitations of the developed devices..

## **5.2 Understanding neural responses along the somatosensory axes**

### ***5.2.1 Unveiling hindered processing limitations with population analysis***

Modelling efforts(Cimolato et al. 2023) indicate that neuromodulation would elicit first, in easiest way the higher diameter fibers, as proprioceptive ones. However, multiple clinical evidences showing the inability of proprioceptive feedback restoration with neuromodulation techniques were the inspiration for the scientific study (presented in Chapter 3) aiming at investigation of the underlying mechanisms . Moreover, spinal cord stimulation in spinal cord injured patients showed that continuous stimulation of sensory afferents with commonly used stimulation paradigms produces a disruption of proprioceptive percepts at stimulation parameters commonly employed in clinical trials (Formento et al. 2018).

Given this discrepancy between experimental findings and theoretical considerations about expected outcomes of neurostimulation, we hypothesized that some neurophysiological constraints may exist, preventing the generation of functional proprioceptive percepts.

The processing of artificially induced proprioceptive information elicited with peripheral nerve stimulation is explored with purposely designed experiments in non-human primates. We analyzed spinal neural population dynamics using manifolds approach to estimate the impact of continuous electrical stimulation of the cutaneous afferents on the processing of proprioceptive information in the spinal cord. We confirmed and expanded the analysis with classical electrophysiology measures in both spinal cord and somatosensory cortex. Neural processing of proprioceptive inputs was disrupted during concurrent continuous stimulation of cutaneous afferents in both areas along the neural axes.

Neural population analysis with neural manifold techniques has been largely employed to study cortical processes (Gallego et al. 2018; 2020; Perich et al. 2020; Sadtler et al. 2014; Churchland et al. 2012). Recently, the manifold analysis was applied on the spinal cord neural data. Starting from the fact that generation of movements in the nervous system is not fully understood, they found that the neural population performs a continuous low-dimensional "rotation" in neural space during rhythmic behavior (Lindén et al. 2022). However, no study used manifold approach to analyze the sensory modalities integration among spinal neural circuits.

In this study, the use of neural manifolds for population activity analysis was crucial to assess phenomena of sensory interference. The population analysis allows to extract only activity that explains the variance generated by proprioceptive inputs. This enables us to understand the proprioceptive components of the neural dynamics against the background cutaneous activity. We established a measure of proprioceptive neural information processing by quantifying proprioceptive neural trajectories in spinal neural manifolds space.

While manifold based approach is beneficial for understanding the overall behavior of the neural circuits, the role and details of single unit processing remains unclear. Neural mechanisms causing this disruption are still unknown and should be investigated further. Potential reasons could be triggering of natural, but unwanted behavior (such as presynaptic inhibition of primary afferents), or could be caused by the inability of common neural resources to process two distinct artificial information streams when simultaneously activated.

Similar phenomena of the sensory interference might arise in different areas of the nervous system, for instance during deep brain stimulation. In the brain, these effects, which mirror the inability to adequately process proprioception in the spinal cord, have the potential to modify cognitive processes unrelated to the intended stimulation objectives within the cortex. It is necessary to conduct further investigation regarding these unwanted events.

Our findings show that fiber class selectivity is more important than what was intuitively thought because the failure to stimulate specific classes of afferents may lead to the triggering of natural sensory gating mechanisms that generates sensory interference (Rudomin and Schmidt 1999). In fact, one could say that the problem of selectivity has been underestimated, and that lack of selectivity not only limits the localization and extent of percept, but it affects their nature even by disrupting some of the information. In a way this reasoning is consistent with the interpretations arguing for “bio-mimetic” stimulation (Bensmaia 2015), but offering a new insight. Not only a truly “bio-mimetic” stimulation protocol would produce more natural sensations, but it may avoid the interference phenomena we observed, thus enabling perception. In support to our conjectures, human data show that the only device that reliably reported controllable proprioceptive percept is the penetrating, slanted UTAH array (Wendelken et al. 2017; Page et al. 2021). Indeed, the ability to recruit only few afferents near the electrode tips may be key to avoid sensory interference.

Although the motivation of this work was to understand if the cause of inability to restore proprioception lies in the neurophysiological constraints (and therefore confirming the *Hypothesis 4*, our study serves as a proxy to understand, more generally, how artificial inputs can influence neural network function (as pointed out in Chapter 3).

Future stimulation strategies and device designs ought to incorporate neural population analysis to assess the impact of specific stimulation patterns on seemingly unrelated neural network processes. Coupled with that, it should account for sensory interference in both electrode design and stimulation protocols to ensure the attainment of resilient, robust and reliable proprioceptive feedback.

## **5.2.2 Neural responses to artificial and natural stimuli**

While previous studies were focused on testing the functionality of various stimulation strategies and the perception of sensation by individuals, limited knowledge exists regarding the stimuli transmission and the form in which it enters the central nervous system.

Commonly used neuromodulation devices employ predefined (fixed) frequency stimulation paradigms (S. Raspopovic et al. 2014; Francesco Maria Petrini, Valle, et al. 2019; M. Ortiz-Catalan, Hakansson, and Branemark 2014), where all elicited neurons are simultaneously activated, in contrast to the neural activity during in-vivo natural touch (Saal and Bensmaia 2015). This synchronized and unnatural neural activity (Formento et al. 2020) could be one of the potential reasons for perceived paresthetic sensations (Francesco M. Petrini et al. 2019; G. Valle et al. 2018). In our animal experiments, we aimed to investigate whether biomimetic strategies, which replicate relevant temporal features of natural coding, elicit different neural responses compared to commonly used paradigms. Thus, we tested the afferent activation induced by applying different artificial but biomimetic stimuli and compared it with naturally induced touch and constant frequency stimulation patterns (presented in Chapter 4).

First, by analyzing the neural signal in the dorsal root ganglion, we showed that we are able to "write" the code into our nervous system, proving that the information traveled from periphery unaltered. While this finding may seem trivial, such evidence has not been previously presented. The information, in its original form, enters the spinal cord where it is processed by interneurons in the gray matter and transmitted to the upper parts of the somatosensory system. Furthermore, biomimetic stimulation elicited more similar neural response to the naturally induced one, than the constant frequency stimulation commonly applied in neuromodulation devices. This similarity was observed in both dorsal root ganglion and the spinal cord gray matter, confirming the *Hypothesis 5*. However, despite the demonstrated similarity, biomimetic strategies still exhibit distinct characteristics of artificially induced stimuli, and further efforts are required to create stimuli that fully replicate natural touch.

Our study provides compelling evidence regarding the impact of bio-inspired stimulation dynamics on the activation of neural afferents, demonstrating the potential to artificially encode natural sensory information into the nervous system. The presented findings validate the hypotheses regarding the use of biomimicry in neuromodulation devices. However, further testing is necessary, exploring new paradigms and investigating neural processing in upper parts of the nervous system, such as the thalamus or somatosensory cortex.

## **5.3 Multifaceted framework for creating novel stimulating patterns**

With the final goal of creating new more efficient stimulation paradigms, the workflow started by developing a computational knowledge about how the information is encoded on the periphery, converting the mechanical stimulus detected on the skin surface. Following that, we investigated in animal experiments how the information from the periphery is integrated and interpreted in the central nervous system.

As a final step, starting from our theoretical and modelistic findings, the new methodological approach of how to develop and test innovative neurotech is created. Framework represents novel strategy for designing biomimetic patterns that would elicit

close-to-natural sensation. Future studies should begin with computational modeling of the coding mechanism for the sensation we would like to restore. Biomimetic stimulation should be constructed based on such a model output. Applying the designed stimulation pattern in animal experiments can help us in understanding if there are some unexpected effects of the stimulation, and assure the overall safety of the stimuli paradigm. If possible, the testing should be finished with the human experiments, evaluating both the perceived quality of sensations and performance while doing daily tasks.

Chapter 4 is presenting suggested framework, accompanied with the results of its application. The biomimetic patterns we applied enhanced the evoked naturalness of sensation. More importantly, during ecological tasks testing (walking, climbing stairs) patients demonstrated much better results compared to the condition when traditional stimulating patterns were used. Therefore, our conceptually new multifaceted framework was experimentally demonstrated, validating the defined *Hypothesis 1 and Hypothesis 2*.

## **5.4 General outlook: Towards the development of novel neuroprosthetic approaches**

Together with the pioneering results showing effectiveness of biomimetic stimulation for restoring sensory feedback in the lower limb, we proved with unique multifaceted approach that architecture established on the development of validated model-based neurotechnology can be effective for human applications.

The philosophy of embracing the "circle of improvement" can extend its applicability to broader contexts and purposes. Understanding the underlying mechanism behind some behavior, modeling it and testing the proposed approach for achieving a goal, are closely related and inseparable three pillars. We should create models based on the scientific knowledge about the process, and it can also help us to even better understand the behavior we are modeling. It provides the insight about the novel solutions, and help us set the new hypotheses that should be evaluated. Moreover, model outputs are used as a guideline for designing optimal experimental setup which leads towards minimizing the amount of necessary testing. Both animal and human testing results have multifold usages. Validation of the model is a crucial step in developing a reliable structure, and more attention is needed to be directed towards that aspect. Experimental results are necessary to correct and improve the model and they gave us a new insight about the accumulated knowledge. All pillars are mutually changing and improving.

Findings of this thesis can help us in the development of the proper artificial, electrical language to speak with our nervous system. Our collected evidences not only highlight the remarkable impact of biomimicry from a scientific perspective, but also holds immense promise in revolutionizing the field of neuroprosthetics. Inspired by nature, these innovative technologies enabling direct communication with the brain and employing artificial electrical stimulation have the potential to fully emulate and restore natural neural functions that may be lost due to diseases or injuries. This breakthrough opens up new frontiers in scientific exploration and interdisciplinary collaboration. Both animal and human experiments consistently support the notion that a time-variant, biomimetic paradigm will serve as a fundamental feature in the design of future neuroprostheses.

Developing appropriate encoding of the information we would like to restore has to be followed with the technological advancements. Modeling efforts are already employed for defining the optimal interface design (Zelechowski, Valle, and Raspopovic 2020; Stanisa

Raspopovic et al. 2017; Katic, Valle, and Raspopovic 2022), exploring new materials (Giacomo Valle et al. 2022; Wurth et al. 2017) and their safety of use (Francesco M. Petrini et al. 2019; Grill, Norman, and Bellamkonda 2009). Connected with that, the future development should go in line with the possibilities of the neural stimulators. The testing of new paradigms is limited with the possible complexity of stimulation patterns, as well as the tolerable delay of information transfer. Moreover, we should always think about investigating possible natural limitations, challenges in sensory integration process, or side effects that could possibly occur.

## 5.5 Limitations of the thesis

The causes of main limitations of the thesis can be structured into three classes: limitations of dataset available, complexity of experimental setup, constrains of technology used.

Parameters of the FootSim model were fitted using the overall spike rates of single units, without recorded precise spike trains. While in hand tactile coding, the importance of the spike timing is known to be very high, it is not clear whether precise spike timing at such fine temporal resolutions is behaviorally relevant for the foot. Also, the model has limited accuracy of predicting the SA2 type afferents' response. This cell type transmits the information about skin stretch. When converting the stimuli propagation on the skin of the foot sole, we are not incorporating shear forces or lateral sliding, but stimulating it as a quasi-continuous stress. The amount of SA2 responses in the provided experimental dataset we used for fitting was not big enough to completely overcome this barrier.

All the performed experimental setups are technologically extremely challenging. In order to be able to test only reflexes and avoid usage of the anesthesia that could potentially alter the neural responses, we did one part of the experiments in decerebrated cats. That made testing of the information processing in the cortex impossible. On the other hand, decerebration is not considered ethical while performing experiments in non-human primates, therefore all the procedures in monkeys have been done in fully anesthetized animals. Furthermore, we believe additional testing for analyzing the data processed in the dorsal column nuclei or thalamus would be a necessary step for complementing and expanding the understanding of the processes explained throughout this thesis. Placing the recording electrodes in these structures is a complicated procedure that would drastically increase a complexity and the length of such experiments that were already longer than twelve hours.

Finally, even though we tested the biomimetic patterns in the closed-loop neuroprosthetic system, these paradigms were predefined. While we believe that the stimulation strategies could be defined in the real time as an output of the model, based on the sensory input insole recordings input, it requires technological improvements. The insole data transmission, model predictions, system controller algorithm and stimulator should in total have a maximum delay smaller than around 100 ms. From the technological aspect it is possible, however engineering efforts are needed to make the complete system fully functionable in real time.



## 5.6 Opportunities

The evidence collected during my thesis not only amplifies the remarkable impact of biomimicry from a scientific perspective, but it also holds immense promise in heralding the advent of the next generation of neuroprosthetic devices.

Worldwide, a lot of effort is placed on developing the interfaces to record and stimulate the nervous system, understanding and predicting the neural output, with the final aim to restore some missing sensation. This thesis follows the same inspiration. Indeed present moment in human history is a “golden one” for the artificial communication with brain, with several companies aiming to achieve it. Neuralink (“Neuralink,” n.d.), a widely known company, is working on the development of a brain-machine interface (Fiani et al. 2021) that could restore both sensory and motor function in individuals with neurological disorders improving such as spinal cord injuries, neurodegenerative diseases, and neurobiological shortfalls (Musk and Neuralink 2019). They are developing cutting-edge technology for the recording of neural signals from the cortex and stimulating it properly. Recently, they have received the FDA approval for a clinical trial testing brain implants in humans. In addition to helping patients with paralysis, experts believe that similar system could someday help treat conditions like blindness and mental illness. Similar idea was previously created by their opponents, Blackrock Neurotech (“Blackrock Neurotech,” n.d.), that are focused on developing new recording electrodes that would be used in novel brain-computer interfaces (BCI) while trying to decrease the invasiveness of the implant. Their commercialized Utah MEA electrode has already been used in several studies, mostly in restoring object interactions in patients with tetraplegia (Rastogi et al. 2021; Simeral et al. 2021). Moreover, the company's precision electrode technology is at the core of many worldwide innovations in BCI, enabling dozens of early users to MoveAgain, SeeAgain, HearAgain, TalkAgain and more.

Significant human resources, investments and efforts are dedicated to bridge the gap and reestablish the sensory experiences that have been lost due to various circumstances. The restoration of lost. The commitment reflects the recognition of their profound importance in enhancing the quality of life and facilitating a comprehensive understanding of our surroundings.

When performing all these tasks, the ethical aspects are to be considered with high scrutiny. This is especially important because these devices could potentially influence the subjective sense of the persons, and influence their free will.

As a closing remark, technological advancements in the industry area indicate this is a historical moment when the results and methods of this thesis can have the direct application in the translational framework, helping millions of disabled individuals.

## Bibliography

- Abbott, L. F., and Wade G. Regehr. 2004. "Synaptic Computation." *Nature* 431 (7010): 796–803. <https://doi.org/10.1038/nature03010>.
- Abdel-Basset, Mohamed, Laila Abdel-Fatah, and Arun Kumar Sangaiah. 2018. "Metaheuristic Algorithms: A Comprehensive Review." In *Computational Intelligence for Multimedia Big Data on the Cloud with Engineering Applications*, 185–231. Elsevier. <https://doi.org/10.1016/B978-0-12-813314-9.00010-4>.
- Abraira, Victoria E., and David D. Ginty. 2013. "The Sensory Neurons of Touch." *Neuron* 79 (4): 618–39. <https://doi.org/10.1016/j.neuron.2013.07.051>.
- Ackerley, Rochelle, and Roger Holmes Watkins. 2018. "Microneurography as a Tool to Study the Function of Individual C-Fiber Afferents in Humans: Responses from Nociceptors, Thermoreceptors, and Mechanoreceptors." *Journal of Neurophysiology* 120 (6): 2834–46. <https://doi.org/10.1152/jn.00109.2018>.
- Andersen, Richard A., Eun Jung Hwang, and Grant H. Mulliken. 2010. "Cognitive Neural Prosthetics." *Annual Review of Psychology* 61 (1): 169–90. <https://doi.org/10.1146/annurev.psych.093008.100503>.
- Angeli, Claudia A., Maxwell Boakye, Rebekah A. Morton, Justin Vogt, Kristin Benton, Yangshen Chen, Christie K. Ferreira, and Susan J. Harkema. 2018. "Recovery of Over-Ground Walking after Chronic Motor Complete Spinal Cord Injury." *New England Journal of Medicine* 379 (13): 1244–50. <https://doi.org/10.1056/NEJMoa1803588>.
- Balaguer, Josep-Maria, and Marco Capogrosso. 2021. "A Computational Model of the Interaction Between Residual Cortico-Spinal Inputs and Spinal Cord Stimulation After Paralysis." In *2021 10th International IEEE/EMBS Conference on Neural Engineering (NER)*, 251–54. Italy: IEEE. <https://doi.org/10.1109/NER49283.2021.9441219>.
- Barack, David L., and John W. Krakauer. 2021. "Two Views on the Cognitive Brain." *Nature Reviews. Neuroscience* 22 (6): 359–71. <https://doi.org/10.1038/s41583-021-00448-6>.
- Bensmaia, Sliman J. 2015. "Biological and Bionic Hands: Natural Neural Coding and Artificial Perception." *Philosophical Transactions of the Royal Society B: Biological Sciences* 370 (1677): 20140209. <https://doi.org/10.1098/rstb.2014.0209>.
- Bensmaia, Sliman J., and Lee E. Miller. 2014. "Restoring Sensorimotor Function through Intracortical Interfaces: Progress and Looming Challenges." *Nature Reviews Neuroscience* 15 (5): 313–25. <https://doi.org/10.1038/nrn3724>.
- Bensmaia, Sliman J., Dustin J. Tyler, and Silvestro Micera. 2020. "Restoration of Sensory Information via Bionic Hands." *Nature Biomedical Engineering*, November, 1–13. <https://doi.org/10.1038/s41551-020-00630-8>.
- Bent, Leah R., and Catherine R. Lowrey. 2013. "Single Low-Threshold Afferents Innervating the Skin of the Human Foot Modulate Ongoing Muscle Activity in the Upper Limbs." *Journal of Neurophysiology* 109 (6): 1614–25. <https://doi.org/10.1152/jn.00608.2012>.
- "Blackrock Neurotech." n.d. <https://blackrockneurotech.com/>.
- Bonnefoy, Alice, and Stéphane Armand. 2015. "Normal Gait." *Orthopedic Management of Children with Cerebral Palsy: A Comprehensive Approach*, 567.
- Boretius, Tim, Jordi Badia, Aran Pascual-Font, Martin Schuettler, Xavier Navarro, Ken Yoshida, and Thomas Stieglitz. 2010. "A Transverse Intrafascicular Multichannel Electrode (TIME) to Interface with the Peripheral Nerve." *Biosensors and Bioelectronics* 26 (1): 62–69. <https://doi.org/10.1016/j.bios.2010.05.010>.

- Borton, D., S. Micera, J. d. R. Millan, and G. Courtine. 2013. "Personalized Neuroprosthetics." *Science Translational Medicine* 5 (210): 210rv2-210rv2. <https://doi.org/10.1126/scitranslmed.3005968>.
- Brand, Rubia van den, Janine Heutschi, Quentin Barraud, Jack DiGiovanna, Kay Bartholdi, Michèle Huerlimann, Lucia Friedli, et al. 2012. "Restoring Voluntary Control of Locomotion after Paralyzing Spinal Cord Injury." *Science* 336 (6085): 1182-85. <https://doi.org/10.1126/science.1217416>.
- Callier, Thierry, Aneesha K. Suresh, and Sliman J. Bensmaia. 2019a. "Neural Coding of Contact Events in Somatosensory Cortex." *Cerebral Cortex (New York, N.Y.: 1991)*, January. <https://doi.org/10.1093/cercor/bhy337>.
- Callier, Thierry, Aneesha K Suresh, and Sliman J Bensmaia. 2019b. "Neural Coding of Contact Events in Somatosensory Cortex." *Cerebral Cortex* 29 (11): 4613-27. <https://doi.org/10.1093/cercor/bhy337>.
- Capogrosso, M., N. Wenger, S. Raspopovic, P. Musienko, J. Beauparlant, L. Bassi Luciani, G. Courtine, and S. Micera. 2013. "A Computational Model for Epidural Electrical Stimulation of Spinal Sensorimotor Circuits." *Journal of Neuroscience* 33 (49): 19326-40. <https://doi.org/10.1523/JNEUROSCI.1688-13.2013>.
- Carter, Andrew W., Spencer C. Chen, Nigel H. Lovell, Richard M. Vickery, and John W. Morley. 2014. "Convergence across Tactile Afferent Types in Primary and Secondary Somatosensory Cortices." *PLOS ONE* 9 (9): e107617. <https://doi.org/10.1371/journal.pone.0107617>.
- Chandrasekaran, Santosh, Ameya C Nanivadekar, Gina McKernan, Eric R Helm, Michael L Boninger, Jennifer L Collinger, Robert A Gaunt, and Lee E Fisher. 2020. "Sensory Restoration by Epidural Stimulation of the Lateral Spinal Cord in Upper-Limb Amputees." Edited by Tamar R Makin, Richard B Ivry, Tamar R Makin, and Matthew G Perich. *ELife* 9 (July): e54349. <https://doi.org/10.7554/eLife.54349>.
- Chandrasekaran, Santosh, Ameya C. Nanivadekar, Gina P. McKernan, Eric R. Helm, Michael L. Boninger, Jennifer L. Collinger, Robert A. Gaunt, and Lee E. Fisher. 2019. "Sensory Restoration by Epidural Stimulation of Dorsal Spinal Cord in Upper-Limb Amputees." Preprint. *Rehabilitation Medicine and Physical Therapy*. <https://doi.org/10.1101/19009811>.
- Charkhkar, Hamid, Courtney E. Shell, Paul D. Marasco, Gilles J. Pinault, Dustin J. Tyler, and Ronald J. Triolo. 2018. "High-Density Peripheral Nerve Cuffs Restore Natural Sensation to Individuals with Lower-Limb Amputations." *Journal of Neural Engineering* 15 (5): 056002. <https://doi.org/10.1088/1741-2552/aac964>.
- Christovão, Thaluanna Calil Lourenço, Hugo Pasini Neto, Luanda André Collange Grecco, Luiz Alfredo Braun Ferreira, Renata Calhes Franco de Moura, Maria Eliege de Souza, Luis Vicente Franco de Oliveira, and Claudia Santos Oliveira. 2013. "Effect of Different Insoles on Postural Balance: A Systematic Review." *Journal of Physical Therapy Science* 25 (10): 1353-56. <https://doi.org/10.1589/jpts.25.1353>.
- Churchland, Mark M., John P. Cunningham, Matthew T. Kaufman, Justin D. Foster, Paul Nuyujukian, Stephen I. Ryu, and Krishna V. Shenoy. 2012. "Neural Population Dynamics during Reaching." *Nature* 487 (7405): 51-56. <https://doi.org/10.1038/nature11129>.
- Cimolato, Andrea, Federico Ciotti, Jelena Kljajić, Giacomo Valle, and Stanisa Raspopovic. 2023. "Symbiotic Electroneural and Musculoskeletal Framework to Encode Proprioception via Neurostimulation: ProprioStim." *IScience* 26 (3): 106248. <https://doi.org/10.1016/j.isci.2023.106248>.

- Cimolato, Andrea, Natalija Katic, and Stanisa Raspopovic. 2021. "Modern Approaches of Signal Processing for Bidirectional Neural Interfaces." In *Somatosensory Feedback for Neuroprosthetics*, 631–59. Elsevier. <https://doi.org/10.1016/B978-0-12-822828-9.00016-2>.
- Clark, G. A., S. Wendelken, D. M. Page, T. Davis, H. A. C. Wark, R. A. Normann, D. J. Warren, and D. T. Hutchinson. 2014. "Using Multiple High-Count Electrode Arrays in Human Median and Ulnar Nerves to Restore Sensorimotor Function after Previous Transradial Amputation of the Hand." In *2014 36th Annual International Conference of the IEEE Engineering in Medicine and Biology Society*, 1977–80. <https://doi.org/10.1109/EMBC.2014.6944001>.
- Clemente, F., M. D'Alonzo, M. Controzzi, B. B. Edin, and C. Cipriani. 2016. "Non-Invasive, Temporally Discrete Feedback of Object Contact and Release Improves Grasp Control of Closed-Loop Myoelectric Transradial Prostheses." *IEEE Transactions on Neural Systems and Rehabilitation Engineering* 24 (12): 1314–22. <https://doi.org/10.1109/TNSRE.2015.2500586>.
- Clemente, Francesco, Giacomo Valle, Marco Controzzi, Ivo Strauss, Francesco Iberite, Thomas Stieglitz, Giuseppe Granata, et al. 2019. "Intraneural Sensory Feedback Restores Grip Force Control and Motor Coordination While Using a Prosthetic Hand." *Journal of Neural Engineering* 16 (2): 026034. <https://doi.org/10.1088/1741-2552/ab059b>.
- Clites, Tyler R., Matthew J. Carty, Jessica B. Ullauri, Matthew E. Carney, Luke M. Mooney, Jean-François Duval, Shriya S. Srinivasan, and Hugh. M. Herr. 2018. "Proprioception from a Neurally Controlled Lower-Extremity Prosthesis." *Science Translational Medicine* 10 (443): eaap8373. <https://doi.org/10.1126/scitranslmed.aap8373>.
- Collinger, Jennifer L, Brian Wodlinger, John E Downey, Wei Wang, Elizabeth C Tyler-Kabara, Douglas J Weber, Angus JC McMorland, Meel Velliste, Michael L Boninger, and Andrew B Schwartz. 2013. "High-Performance Neuroprosthetic Control by an Individual with Tetraplegia." *The Lancet* 381 (9866): 557–64. [https://doi.org/10.1016/S0140-6736\(12\)61816-9](https://doi.org/10.1016/S0140-6736(12)61816-9).
- Comitato, Antonella, and Rita Bardoni. 2021. "Presynaptic Inhibition of Pain and Touch in the Spinal Cord: From Receptors to Circuits." *International Journal of Molecular Sciences* 22 (1): 414. <https://doi.org/10.3390/ijms22010414>.
- Confais, Joachim, Geehee Kim, Saeka Tomatsu, Tomohiko Takei, and Kazuhiko Seki. 2017. "Nerve-Specific Input Modulation to Spinal Neurons during a Motor Task in the Monkey." *The Journal of Neuroscience* 37 (10): 2612–26. <https://doi.org/10.1523/JNEUROSCI.2561-16.2017>.
- Corniani, Giulia, Miguel A. Casal, Stefano Panzeri, and Hannes P. Saal. 2022. "Population Coding Strategies in Human Tactile Afferents." Edited by Daniele Marinazzo. *PLOS Computational Biology* 18 (12): e1010763. <https://doi.org/10.1371/journal.pcbi.1010763>.
- Corniani, Giulia, and Hannes P. Saal. 2020. "Tactile Innervation Densities across the Whole Body." *Journal of Neurophysiology* 124 (4): 1229–40. <https://doi.org/10.1152/jn.00313.2020>.
- Crea, Simona, Benoni B. Edin, Kristel Knaepen, Romain Meeusen, and Nicola Vitiello. 2017. "Time-Discrete Vibrotactile Feedback Contributes to Improved Gait Symmetry in Patients With Lower Limb Amputations: Case Series." *Physical Therapy* 97 (2): 198–207. <https://doi.org/10.2522/ptj.20150441>.
- Čvančara, P., G. Valle, M. Müller, T. Guiho, A. Hiarrassary, F. Petrini, S. Raspopovic, et al. 2019. "On the Reliability of Chronically Implanted Thin-Film Electrodes in Human

- Arm Nerves for Neuroprosthetic Applications." *BioRxiv*, May, 653964. <https://doi.org/10.1101/653964>.
- Čvančara, Paul, Tim Boretius, Víctor M. López-Álvarez, Pawel Maciejasz, David Andreu, Stanisa Raspopovic, Francesco Petrini, et al. 2020. "Stability of Flexible Thin-Film Metallization Stimulation Electrodes: Analysis of Explants after First-in-Human Study and Improvement of in Vivo Performance." *Journal of Neural Engineering* 17 (4): 046006. <https://doi.org/10.1088/1741-2552/ab9a9a>.
- D'Anna, Edoardo, Francesco M. Petrini, Fiorenzo Artoni, Igor Popovic, Igor Simanić, Stanisa Raspopovic, and Silvestro Micera. 2017. "A Somatotopic Bidirectional Hand Prosthesis with Transcutaneous Electrical Nerve Stimulation Based Sensory Feedback." *Scientific Reports* 7 (1). <https://doi.org/10.1038/s41598-017-11306-w>.
- D'Anna, Edoardo, Giacomo Valle, Alberto Mazzoni, Ivo Strauss, Francesco Iberite, Jérémy Patton, Francesco M. Petrini, et al. 2019. "A Closed-Loop Hand Prosthesis with Simultaneous Intraneural Tactile and Position Feedback." *Science Robotics* 4 (27): eaau8892. <https://doi.org/10.1126/scirobotics.aau8892>.
- Davis, T S, H A C Wark, D T Hutchinson, D J Warren, K O'Neill, T Scheinblum, G A Clark, R A Normann, and B Greger. 2016. "Restoring Motor Control and Sensory Feedback in People with Upper Extremity Amputations Using Arrays of 96 Microelectrodes Implanted in the Median and Ulnar Nerves." *Journal of Neural Engineering* 13 (3): 036001. <https://doi.org/10.1088/1741-2560/13/3/036001>.
- Delmas, Patrick, Jizhe Hao, and Lise Rodat-Despoix. 2011. "Molecular Mechanisms of Mechanotransduction in Mammalian Sensory Neurons." *Nature Reviews Neuroscience* 12 (3): 139–53. <https://doi.org/10.1038/nrn2993>.
- Destexhe, Alain, and Joshua A. Goldberg. 2015. "LFP Analysis: Overview." In *Encyclopedia of Computational Neuroscience*, edited by Dieter Jaeger and Ranu Jung, 52–55. New York, NY: Springer New York. [https://doi.org/10.1007/978-1-4614-6675-8\\_782](https://doi.org/10.1007/978-1-4614-6675-8_782).
- Dhillon, G.S., and K.W. Horch. 2005. "Direct Neural Sensory Feedback and Control of a Prosthetic Arm." *IEEE Transactions on Neural Systems and Rehabilitation Engineering* 13 (4): 468–72. <https://doi.org/10.1109/TNSRE.2005.856072>.
- Dhillon, Gurpreet S., Stephen M. Lawrence, Douglas T. Hutchinson, and Kenneth W. Horch. 2004. "Residual Function in Peripheral Nerve Stumps of Amputees: Implications for Neural Control of Artificial Limbs." *The Journal of Hand Surgery* 29 (4): 605–15; discussion 616–618. <https://doi.org/10.1016/j.jhssa.2004.02.006>.
- Dietrich, Caroline, Sandra Nehrlich, Sandra Seifert, Kathrin R. Blume, Wolfgang H. R. Miltner, Gunther O. Hofmann, and Thomas Weiss. 2018. "Leg Prosthesis With Somatosensory Feedback Reduces Phantom Limb Pain and Increases Functionality." *Frontiers in Neurology* 9: 270. <https://doi.org/10.3389/fneur.2018.00270>.
- Dillingham, Timothy R., Liliana E. Pezzin, and Andrew D. Shore. 2005. "Reamputation, Mortality, and Health Care Costs among Persons with Dysvascular Lower-Limb Amputations." *Archives of Physical Medicine and Rehabilitation* 86 (3): 480–86. <https://doi.org/10.1016/j.apmr.2004.06.072>.
- Do, M. C., B. Bussel, and Y. Breniere. 1990. "Influence of Plantar Cutaneous Afferents on Early Compensatory Reactions to Forward Fall." *Experimental Brain Research* 79 (2): 319–24. <https://doi.org/10.1007/BF00608241>.
- Donegà, Matteo, Cathrine T. Fjordbakk, Joseph Kirk, David M. Sokal, Isha Gupta, Gerald E. Hunsberger, Abbe Crawford, et al. 2021. "Human-Relevant near-Organ Neuromodulation of the Immune System via the Splenic Nerve." *Proceedings of the National Academy of Sciences* 118 (20): e2025428118. <https://doi.org/10.1073/pnas.2025428118>.

- Dong, Yi, Stefan Mihalas, Sung Soo Kim, Takashi Yoshioka, Sliman Bensmaia, and Ernst Niebur. 2013. "A Simple Model of Mechanotransduction in Primate Glabrous Skin." *Journal of Neurophysiology* 109 (5): 1350–59. <https://doi.org/10.1152/jn.00395.2012>.
- Edwards, Christine A., Abbas Kouzani, Kendall H. Lee, and Erika K. Ross. 2017. "Neurostimulation Devices for the Treatment of Neurologic Disorders." *Mayo Clinic Proceedings* 92 (9): 1427–44. <https://doi.org/10.1016/j.mayocp.2017.05.005>.
- Eisen, Marc D. 2003. "Djourno, Eyries, and the First Implanted Electrical Neural Stimulator to Restore Hearing." *Otology & Neurotology* 24 (3): 500.
- Fallon, James B., Leah R. Bent, Penelope A. McNulty, and Vaughan G. Macefield. 2005. "Evidence for Strong Synaptic Coupling Between Single Tactile Afferents From the Sole of the Foot and Motoneurons Supplying Leg Muscles." *Journal of Neurophysiology* 94 (6): 3795–3804. <https://doi.org/10.1152/jn.00359.2005>.
- Fiani, Brian, Taylor Reardon, Benjamin Ayres, David Cline, and Sarah R Sitto. 2021. "An Examination of Prospective Uses and Future Directions of Neuralink: The Brain-Machine Interface." *Cureus*, March. <https://doi.org/10.7759/cureus.14192>.
- Flesher, S. N., J. L. Collinger, S. T. Foldes, J. M. Weiss, J. E. Downey, E. C. Tyler-Kabara, S. J. Bensmaia, A. B. Schwartz, M. L. Boninger, and R. A. Gaunt. 2016. "Intracortical Microstimulation of Human Somatosensory Cortex." *Science Translational Medicine* 8 (361): 361ra141-361ra141. <https://doi.org/10.1126/scitranslmed.aaf8083>.
- Flesher, Sharlene N., John E. Downey, Jeffrey M. Weiss, Christopher L. Hughes, Angelica J. Herrera, Elizabeth C. Tyler-Kabara, Michael L. Boninger, Jennifer L. Collinger, and Robert A. Gaunt. 2021. "A Brain-Computer Interface That Evokes Tactile Sensations Improves Robotic Arm Control." *Science (New York, N.Y.)* 372 (6544): 831–36. <https://doi.org/10.1126/science.abd0380>.
- Flor, Herta, Lone Nikolajsen, and Troels Staehelin Jensen. 2006. "Phantom Limb Pain: A Case of Maladaptive CNS Plasticity?" *Nature Reviews Neuroscience* 7 (11): 873–81. <https://doi.org/10.1038/nrn1991>.
- Formento, Emanuele, Edoardo D'Anna, Sandra Gribi, Stéphanie P. Lacour, and Silvestro Micera. 2020. "A Biomimetic Electrical Stimulation Strategy to Induce Asynchronous Stochastic Neural Activity." *Journal of Neural Engineering* 17 (4): 046019. <https://doi.org/10.1088/1741-2552/aba4fc>.
- Formento, Emanuele, Karen Minassian, Fabien Wagner, Jean Baptiste Mignardot, Camille G. Le Goff-Mignardot, Andreas Rowald, Jocelyne Bloch, Silvestro Micera, Marco Capogrosso, and Gregoire Courtine. 2018. "Electrical Spinal Cord Stimulation Must Preserve Proprioception to Enable Locomotion in Humans with Spinal Cord Injury." *Nature Neuroscience* 21 (12): 1728–41. <https://doi.org/10.1038/s41593-018-0262-6>.
- Fumero, Milagros J., Almudena Eustaquio-Martín, José M. Gorospe, Rubén Polo López, M. Auxiliadora Gutiérrez Revilla, Luis Lassaletta, Reinhold Schatzer, Peter Nopp, Joshua S. Stohl, and Enrique A. Lopez-Poveda. 2021. "A State-of-the-Art Implementation of a Binaural Cochlear-Implant Sound Coding Strategy Inspired by the Medial Olivocochlear Reflex." *Hearing Research* 409 (September): 108320. <https://doi.org/10.1016/j.heares.2021.108320>.
- Gallego, Juan A., Matthew G. Perich, Raed H. Chowdhury, Sara A. Solla, and Lee E. Miller. 2020. "Long-Term Stability of Cortical Population Dynamics Underlying Consistent Behavior." *Nature Neuroscience* 23 (2): 260–70. <https://doi.org/10.1038/s41593-019-0555-4>.
- Gallego, Juan A., Matthew G. Perich, Lee E. Miller, and Sara A. Solla. 2017. "Neural Manifolds for the Control of Movement." *Neuron* 94 (5): 978–84. <https://doi.org/10.1016/j.neuron.2017.05.025>.

- Gallego, Juan A., Matthew G. Perich, Stephanie N. Naufel, Christian Ethier, Sara A. Solla, and Lee E. Miller. 2018. "Cortical Population Activity within a Preserved Neural Manifold Underlies Multiple Motor Behaviors." *Nature Communications* 9 (1): 4233. <https://doi.org/10.1038/s41467-018-06560-z>.
- George, J. A., D. T. Kluger, T. S. Davis, S. M. Wendelken, E. V. Okorokova, Q. He, C. C. Duncan, et al. 2019. "Biomimetic Sensory Feedback through Peripheral Nerve Stimulation Improves Dexterous Use of a Bionic Hand." *Science Robotics* 4 (32): eaax2352. <https://doi.org/10.1126/scirobotics.aax2352>.
- Gill, Megan L., Peter J. Grahn, Jonathan S. Calvert, Margaux B. Linde, Igor A. Lavrov, Jeffrey A. Strommen, Lisa A. Beck, et al. 2018. "Neuromodulation of Lumbosacral Spinal Networks Enables Independent Stepping after Complete Paraplegia." *Nature Medicine* 24 (11): 1677–82. <https://doi.org/10.1038/s41591-018-0175-7>.
- Gordon, Evan M., Roselyne J. Chauvin, Andrew N. Van, Aishwarya Rajesh, Ashley Nielsen, Dillan J. Newbold, Charles J. Lynch, et al. 2023. "A Somato-Cognitive Action Network Alternates with Effector Regions in Motor Cortex." *Nature* 617 (7960): 351–59. <https://doi.org/10.1038/s41586-023-05964-2>.
- Graczyk, E. L., M. A. Schiefer, H. P. Saal, B. P. Delhaye, S. J. Bensmaia, and D. J. Tyler. 2016. "The Neural Basis of Perceived Intensity in Natural and Artificial Touch." *Science Translational Medicine* 8 (362): 362ra142–362ra142. <https://doi.org/10.1126/scitranslmed.aaf5187>.
- Graczyk, Emily L., Breanne P. Christie, Qinpu He, Dustin J. Tyler, and Sliman J. Bensmaia. 2022. "Frequency Shapes the Quality of Tactile Percepts Evoked through Electrical Stimulation of the Nerves." *The Journal of Neuroscience* 42 (10): 2052–64. <https://doi.org/10.1523/JNEUROSCI.1494-21.2021>.
- Graczyk, Emily L., Benoit P. Delhaye, Matthew A. Schiefer, Sliman J. Bensmaia, and Dustin J. Tyler. 2018. "Sensory Adaptation to Electrical Stimulation of the Somatosensory Nerves." *Journal of Neural Engineering* 15 (4): 046002. <https://doi.org/10.1088/1741-2552/aab790>.
- Graczyk, Emily L., Linda Resnik, Matthew A. Schiefer, Melissa S. Schmitt, and Dustin J. Tyler. 2018. "Home Use of a Neural-Connected Sensory Prosthesis Provides the Functional and Psychosocial Experience of Having a Hand Again." *Scientific Reports* 8 (1): 9866. <https://doi.org/10.1038/s41598-018-26952-x>.
- Graczyk, Emily L., Matthew A. Schiefer, Hannes P. Saal, Benoit P. Delhaye, Sliman J. Bensmaia, and Dustin J. Tyler. 2016. "The Neural Basis of Perceived Intensity in Natural and Artificial Touch." *Science Translational Medicine* 8 (362). <https://doi.org/10.1126/scitranslmed.aaf5187>.
- Granata, Giuseppe, Riccardo Di Iorio, Roberto Romanello, Francesco Iodice, Stanisa Raspopovic, Francesco Petrini, Ivo Strauss, et al. 2018. "Phantom Somatosensory Evoked Potentials Following Selective Intraneural Electrical Stimulation in Two Amputees." *Clinical Neurophysiology* 129 (6): 1117–20. <https://doi.org/10.1016/j.clinph.2018.02.138>.
- Greenspon, Charles M., Emma E. Battell, Ian M. Devonshire, Lucy F. Donaldson, Victoria Chapman, and Gareth J. Hathway. 2019. "Lamina-Specific Population Encoding of Cutaneous Signals in the Spinal Dorsal Horn Using Multi-Electrode Arrays." *The Journal of Physiology* 597 (2): 377–97. <https://doi.org/10.1113/JP277036>.
- Greenspon, Charles M., Giacomo Valle, Taylor G. Hobbs, Ceci Verbaarschot, Thierry Callier, Natalya D. Shelchkova, Anton R. Sobinov, Patrick M. Jordan, Jeffrey M. Weiss, Emily E. Fitzgerald, Dillan Prasad, Ashley Van Driesche, et al. 2023. "Biomimetic Multi-Channel Microstimulation of Somatosensory Cortex Conveys High Resolution Force

- Feedback for Bionic Hands." Preprint. Neuroscience. <https://doi.org/10.1101/2023.02.18.528972>.
- Greenspon, Charles M., Giacomo Valle, Taylor G. Hobbs, Ceci Verbaarschot, Thierry Callier, Natalya D. Shelchkova, Anton R. Sobinov, Patrick M. Jordan, Jeffrey M. Weiss, Emily E. Fitzgerald, Dillan Prasad, Ashley van Driesche, et al. 2023. "Biomimetic Multi-Channel Microstimulation of Somatosensory Cortex Conveys High Resolution Force Feedback for Bionic Hands." Preprint. Neuroscience. <https://doi.org/10.1101/2023.02.18.528972>.
- Greiner, Nathan, Beatrice Barra, Giuseppe Schiavone, Henri Lorach, Nicholas James, Sara Conti, Melanie Kaeser, et al. 2021. "Recruitment of Upper-Limb Motoneurons with Epidural Electrical Stimulation of the Cervical Spinal Cord." *Nature Communications* 12 (1): 435. <https://doi.org/10.1038/s41467-020-20703-1>.
- Grill, Warren M., Sharon E. Norman, and Ravi V. Bellamkonda. 2009. "Implanted Neural Interfaces: Biochallenges and Engineered Solutions." *Annual Review of Biomedical Engineering* 11: 1-24. <https://doi.org/10.1146/annurev-bioeng-061008-124927>.
- Guiho, T, D Andreu, VM López-Alvarez, P Cvancara, A Hiarrassary, G Granata, L Wauters, et al. 2016. "Advanced 56 Channels Stimulation System to Drive Intrafascicular Electrodes." In *Converging Clinical and Engineering Research on Neurorehabilitation II. Proceedings of the 3rd International Conference on NeuroRehabilitation (ICNR2016), October 18-21, 2016, Segovia, Spain*, edited by González-Vargas J Ibáñez J, 2:743-47. Biosystems & Biorobotics; 15.
- Hasan, Z., and D. G. Stuart. 1988. "Animal Solutions to Problems of Movement Control: The Role of Proprioceptors." *Annual Review of Neuroscience* 11: 199-223. <https://doi.org/10.1146/annurev.ne.11.030188.001215>.
- Hasan, Ziaul. 1992. "Role of Proprioceptors in Neural Control." *Current Opinion in Neurobiology* 2 (6): 824-29. [https://doi.org/10.1016/0959-4388\(92\)90140-G](https://doi.org/10.1016/0959-4388(92)90140-G).
- Hebert, J. S., J. L. Olson, M. J. Morhart, M. R. Dawson, P. D. Marasco, T. A. Kuiken, and K. M. Chan. 2014. "Novel Targeted Sensory Reinnervation Technique to Restore Functional Hand Sensation After Transhumeral Amputation." *IEEE Transactions on Neural Systems and Rehabilitation Engineering* 22 (4): 765-73. <https://doi.org/10.1109/TNSRE.2013.2294907>.
- Heller, B W, D Datta, and J Howitt. 2000. "A Pilot Study Comparing the Cognitive Demand of Walking for Transfemoral Amputees Using the Intelligent Prosthesis with That Using Conventionally Damped Knees." *Clinical Rehabilitation* 14 (5): 518-22. <https://doi.org/10.1191/0269215500cr345oa>.
- Hemptinne, Coralie de, Nicole C. Swann, Jill L. Ostrem, Elena S. Ryapolova-Webb, Marta San Luciano, Nicholas B. Galifianakis, and Philip A. Starr. 2015. "Therapeutic Deep Brain Stimulation Reduces Cortical Phase-Amplitude Coupling in Parkinson's Disease." *Nature Neuroscience* 18 (5): 779-86. <https://doi.org/10.1038/nn.3997>.
- Horch, Kenneth, Sanford Meek, Tyson G. Taylor, and Douglas T. Hutchinson. 2011. "Object Discrimination With an Artificial Hand Using Electrical Stimulation of Peripheral Tactile and Proprioceptive Pathways With Intrafascicular Electrodes." *IEEE Transactions on Neural Systems and Rehabilitation Engineering* 19 (5): 483-89. <https://doi.org/10.1109/TNSRE.2011.2162635>.
- Horgan, Olga, and Malcolm MacLachlan. 2004. "Psychosocial Adjustment to Lower-Limb Amputation: A Review." *Disability and Rehabilitation* 26 (14-15): 837-50. <https://doi.org/10.1080/09638280410001708869>.
- Iggo, A. 1977. "CUTANEOUS AND SUBCUTANEOUS SENSE ORGANS." *British Medical Bulletin* 33 (2): 97-102. <https://doi.org/10.1093/oxfordjournals.bmb.a071432>.



- Jabaley, Michael E., William H. Wallace, and Frederick R. Heckler. 1980. "Internal Topography of Major Nerves of the Forearm and Hand: A Current View." *The Journal of Hand Surgery* 5 (1): 1–18. [https://doi.org/10.1016/S0363-5023\(80\)80035-9](https://doi.org/10.1016/S0363-5023(80)80035-9).
- Johansson, R S. 1978. "Tactile Sensibility in the Human Hand: Receptive Field Characteristics of Mechanoreceptive Units in the Glabrous Skin Area." *The Journal of Physiology* 281 (1): 101–25. <https://doi.org/10.1113/jphysiol.1978.sp012411>.
- Johansson, R S, and A B Vallbo. 1979. "Tactile Sensibility in the Human Hand: Relative and Absolute Densities of Four Types of Mechanoreceptive Units in Glabrous Skin." *The Journal of Physiology* 286 (1): 283–300. <https://doi.org/10.1113/jphysiol.1979.sp012619>.
- Johansson, R. S., and A. B. Vallbo. 1980. "Spatial Properties of the Population of Mechanoreceptive Units in the Glabrous Skin of the Human Hand." *Brain Research* 184 (2): 353–66. [https://doi.org/10.1016/0006-8993\(80\)90804-5](https://doi.org/10.1016/0006-8993(80)90804-5).
- Johansson, Roland S, and Ingvars Birznieks. 2004. "First Spikes in Ensembles of Human Tactile Afferents Code Complex Spatial Fingertip Events." *Nature Neuroscience* 7 (2): 170–77. <https://doi.org/10.1038/nn1177>.
- Johansson, Roland S., and J. Randall Flanagan. 2009. "Coding and Use of Tactile Signals from the Fingertips in Object Manipulation Tasks." *Nature Reviews Neuroscience* 10 (5): 345–59. <https://doi.org/10.1038/nrn2621>.
- Johansson, Roland S., and Åke B. Vallbo. 1983. "Tactile Sensory Coding in the Glabrous Skin of the Human Hand." *Trends in Neurosciences* 6 (January): 27–32. [https://doi.org/10.1016/0166-2236\(83\)90011-5](https://doi.org/10.1016/0166-2236(83)90011-5).
- Johnson, K. 2001. "The Roles and Functions of Cutaneous Mechanoreceptors." *Current Opinion in Neurobiology* 11 (4): 455–61. [https://doi.org/10.1016/S0959-4388\(00\)00234-8](https://doi.org/10.1016/S0959-4388(00)00234-8).
- Johnson, K. O., and S. S. Hsiao. 1992. "Neural Mechanisms of Tactual Form and Texture Perception." *Annual Review of Neuroscience* 15: 227–50. <https://doi.org/10.1146/annurev.ne.15.030192.001303>.
- Kaas, Jon H. 2004. "Somatosensory System." In *The Human Nervous System*, 1059–92. Elsevier. <https://doi.org/10.1016/B978-012547626-3/50029-6>.
- Kandel, E., Schwartz, J. & Jessel, T. n.d. *Principles of Neuro Science*. The McGraw-Hill Companies, 2000.
- Katic, Natalija, Rodrigo Kazu Siqueira, Luke Cleland, Nicholas Strzalkowski, Leah Bent, Stanisa Raspopovic, and Hannes Saal. 2023. "Modeling Foot Sole Cutaneous Afferents: FootSim." *IScience* 26 (1): 105874. <https://doi.org/10.1016/j.isci.2022.105874>.
- Katic, Natalija, Giacomo Valle, and Stanisa Raspopovic. 2022. "Modeling of the Peripheral Nerve to Investigate Advanced Neural Stimulation (Sensory Neural Prosthesis)." In *Handbook of Neuroengineering*, edited by Nitish V. Thakor, 1–30. Singapore: Springer Singapore. [https://doi.org/10.1007/978-981-15-2848-4\\_100-1](https://doi.org/10.1007/978-981-15-2848-4_100-1).
- Kavounoudias, Anne, Régine Roll, and Jean-Pierre Roll. 1998. "The Plantar Sole Is a 'Dynamometric Map' for Human Balance Control." *NeuroReport* 9 (14): 3247–52. <https://doi.org/10.1097/00001756-199810050-00021>.
- Kennedy, Paul M., and J. Timothy Inglis. 2002. "Distribution and Behaviour of Glabrous Cutaneous Receptors in the Human Foot Sole." *The Journal of Physiology* 538 (3): 995–1002. <https://doi.org/10.1113/jphysiol.2001.013087>.
- Kibleur, Pierre, Shravan R. Tata, Nathan Greiner, Sara Conti, Beatrice Barra, Katie Zhuang, Melanie Kaeser, Auke Ijspeert, and Marco Capogrosso. 2020. "Spatiotemporal Maps of Proprioceptive Inputs to the Cervical Spinal Cord During Three-Dimensional

- Reaching and Grasping." *IEEE Transactions on Neural Systems and Rehabilitation Engineering* 28 (7): 1668–77. <https://doi.org/10.1109/TNSRE.2020.2986491>.
- Knibestöl, M. 1973. "Stimulus-Response Functions of Rapidly Adapting Mechanoreceptors in the Human Glabrous Skin Area." *The Journal of Physiology* 232 (3): 427–52. <https://doi.org/10.1113/jphysiol.1973.sp010279>.
- Knibestöl, M., and Å. B. Vallbo. 1970. "Single Unit Analysis of Mechanoreceptor Activity from the Human Glabrous Skin." *Acta Physiologica Scandinavica* 80 (2): 178–95. <https://doi.org/10.1111/j.1748-1716.1970.tb04783.x>.
- Koch, Stephanie C., David Acton, and Martyn Goulding. 2018. "Spinal Circuits for Touch, Pain, and Itch." *Annual Review of Physiology* 80 (February): 189–217. <https://doi.org/10.1146/annurev-physiol-022516-034303>.
- Kuiken, Todd A. 2009. "Targeted Muscle Reinnervation for Real-Time Myoelectric Control of Multifunction Artificial Arms." *JAMA* 301 (6): 619. <https://doi.org/10.1001/jama.2009.116>.
- Kuiken, Todd A., Paul D. Marasco, Blair A. Lock, Robert Norman Harden, and Julius P. A. Dewald. 2007. "Redirection of Cutaneous Sensation from the Hand to the Chest Skin of Human Amputees with Targeted Reinnervation." *Proceedings of the National Academy of Sciences of the United States of America* 104 (50): 20061–66. <https://doi.org/10.1073/pnas.0706525104>.
- Lemon, Roger N. 2008. "Descending Pathways in Motor Control." *Annual Review of Neuroscience* 31: 195–218. <https://doi.org/10.1146/annurev.neuro.31.060407.125547>.
- Lenz, F. A., M. Seike, R. T. Richardson, Y. C. Lin, F. H. Baker, I. Khoja, C. J. Jaeger, and R. H. Gracely. 1993. "Thermal and Pain Sensations Evoked by Microstimulation in the Area of Human Ventrocaudal Nucleus." *Journal of Neurophysiology* 70 (1): 200–212. <https://doi.org/10.1152/jn.1993.70.1.200>.
- Limakatso, Katleho, Gillian J. Bedwell, Victoria J. Madden, and Romy Parker. 2020. "The Prevalence and Risk Factors for Phantom Limb Pain in People with Amputations: A Systematic Review and Meta-Analysis." Edited by Arezoo Eshraghi. *PLOS ONE* 15 (10): e0240431. <https://doi.org/10.1371/journal.pone.0240431>.
- Lindén, Henrik, Peter C. Petersen, Mikkel Vestergaard, and Rune W. Berg. 2022. "Movement Is Governed by Rotational Neural Dynamics in Spinal Motor Networks." *Nature* 610 (7932): 526–31. <https://doi.org/10.1038/s41586-022-05293-w>.
- London, Brian M., and Lee E. Miller. 2013. "Responses of Somatosensory Area 2 Neurons to Actively and Passively Generated Limb Movements." *Journal of Neurophysiology* 109 (6): 1505–13. <https://doi.org/10.1152/jn.00372.2012>.
- Macefield, Vaughan G. 2005. "Physiological Characteristics of Low-Threshold Mechanoreceptors in Joints, Muscle and Skin in Human Subjects." *Clinical and Experimental Pharmacology and Physiology* 32 (1–2): 135–44. <https://doi.org/10.1111/j.1440-1681.2005.04143.x>.
- Mackevicius, E. L., M. D. Best, H. P. Saal, and S. J. Bensmaia. 2012. "Millisecond Precision Spike Timing Shapes Tactile Perception." *Journal of Neuroscience* 32 (44): 15309–17. <https://doi.org/10.1523/JNEUROSCI.2161-12.2012>.
- Maki, Brian E., and William E. McIlroy. 1996. "Postural Control in the Older Adult." *Clinics in Geriatric Medicine* 12 (4): 635–58. [https://doi.org/10.1016/S0749-0690\(18\)30193-9](https://doi.org/10.1016/S0749-0690(18)30193-9).
- Makin, Tamar R., Frederique De Vignemont, and A. Aldo Faisal. 2017. "Neurocognitive Barriers to the Embodiment of Technology." *Nature Biomedical Engineering* 1 (1): 0014. <https://doi.org/10.1038/s41551-016-0014>.

- Maling, N., and C. McIntyre. 2016. "Local Field Potential Analysis for Closed-Loop Neuromodulation." In *Closed Loop Neuroscience*, 67–80. Elsevier. <https://doi.org/10.1016/B978-0-12-802452-2.00005-6>.
- Maling, Nicholas, and Cameron McIntyre. 2016. "Local Field Potential Analysis for Closed-Loop Neuromodulation." In *Closed Loop Neuroscience, 2016, ISBN 978-0-12-802452-2, Págs. 67-80*, 67–80. <https://dialnet.unirioja.es/servlet/articulo?codigo=5896944>.
- Manfredi, Louise R., Andrew T. Baker, Damian O. Elias, John F. Dammann, Mark C. Zielinski, Vicky S. Polashock, and Sliman J. Bensmaia. 2012. "The Effect of Surface Wave Propagation on Neural Responses to Vibration in Primate Glabrous Skin." Edited by Miguel Maravall. *PLoS ONE* 7 (2): e31203. <https://doi.org/10.1371/journal.pone.0031203>.
- Mano, Tadaaki, Satoshi Iwase, and Shinobu Toma. 2006. "Microneurography as a Tool in Clinical Neurophysiology to Investigate Peripheral Neural Traffic in Humans." *Clinical Neurophysiology* 117 (11): 2357–84. <https://doi.org/10.1016/j.clinph.2006.06.002>.
- Marasco, Paul D., Jacqueline S. Hebert, Jon W. Sensinger, Courtney E. Shell, Jonathon S. Schofield, Zachary C. Thumser, Raviraj Nataraj, et al. 2018. "Illusory Movement Perception Improves Motor Control for Prosthetic Hands." *Science Translational Medicine* 10 (432). <https://doi.org/10.1126/scitranslmed.aao6990>.
- Marasco, Paul D., Keehoon Kim, James Edward Colgate, Michael A. Peshkin, and Todd A. Kuiken. 2011. "Robotic Touch Shifts Perception of Embodiment to a Prosthesis in Targeted Reinnervation Amputees." *Brain* 134 (3): 747–58. <https://doi.org/10.1093/brain/awq361>.
- Marsal, Sara, Héctor Corominas, Juan José de Agustín, Carolina Pérez-García, María López-Lasanta, Helena Borrell, Delia Reina, et al. 2021. "Non-Invasive Vagus Nerve Stimulation for Rheumatoid Arthritis: A Proof-of-Concept Study." *The Lancet Rheumatology* 3 (4): e262–69. [https://doi.org/10.1016/S2665-9913\(20\)30425-2](https://doi.org/10.1016/S2665-9913(20)30425-2).
- Mastinu, Enzo, Leonard F. Engels, Francesco Clemente, Mariama Dione, Paolo Sassu, Oskar Aszmann, Rickard Brånemark, et al. 2020. "Neural Feedback Strategies to Improve Grasping Coordination in Neuromusculoskeletal Prostheses." *Scientific Reports* 10 (1): 11793. <https://doi.org/10.1038/s41598-020-67985-5>.
- Mazzoni, Alberto, Calogero M. Oddo, Giacomo Valle, Domenico Camboni, Ivo Strauss, Massimo Barbaro, Gianluca Barabino, et al. 2020. "Morphological Neural Computation Restores Discrimination of Naturalistic Textures in Trans-Radial Amputees." *Scientific Reports* 10 (1): 1–14. <https://doi.org/10.1038/s41598-020-57454-4>.
- McDonnell, Michelle, and Andrea Warden-Flood. 2000. "Effect of Partial Foot Anaesthesia on Normal Gait." *Australian Journal of Physiotherapy* 46 (2): 115–20. [https://doi.org/10.1016/S0004-9514\(14\)60319-6](https://doi.org/10.1016/S0004-9514(14)60319-6).
- McIntyre, Cameron C., and Warren M. Grill. 2001. "Finite Element Analysis of the Current-Density and Electric Field Generated by Metal Microelectrodes." *Annals of Biomedical Engineering* 29 (3): 227–35. <https://doi.org/10.1114/1.1352640>.
- McNeal, Donald R. 1976. "Analysis of a Model for Excitation of Myelinated Nerve." *IEEE Transactions on Biomedical Engineering* BME-23 (4): 329–37. <https://doi.org/10.1109/TBME.1976.324593>.
- Merrill, Daniel R., Marom Bikson, and John G.R. Jefferys. 2005. "Electrical Stimulation of Excitable Tissue: Design of Efficacious and Safe Protocols." *Journal of Neuroscience Methods* 141 (2): 171–98. <https://doi.org/10.1016/j.jneumeth.2004.10.020>.

- Miller, George A. 1956. "The Magical Number Seven, plus or Minus Two: Some Limits on Our Capacity for Processing Information." *Psychological Review* 63 (2): 81-97. <https://doi.org/10.1037/h0043158>.
- Miller, William C., Mark Speechley, and Barry Deathe. 2001. "The Prevalence and Risk Factors of Falling and Fear of Falling among Lower Extremity Amputees." *Archives of Physical Medicine and Rehabilitation* 82 (8): 1031-37. <https://doi.org/10.1053/apmr.2001.24295>.
- Mitchell, M. R., R. E. Link, A. W. Mix, and A. J. Giacomini. 2011. "Standardized Polymer Durometry." *Journal of Testing and Evaluation* 39 (4): 103205. <https://doi.org/10.1520/JTE103205>.
- Moxey, P. W., P. Gogalniceanu, R. J. Hinchliffe, I. M. Loftus, K. J. Jones, M. M. Thompson, and P. J. Holt. 2011. "Lower Extremity Amputations - a Review of Global Variability in Incidence: Lower Extremity Amputations-a Global Review." *Diabetic Medicine* 28 (10): 1144-53. <https://doi.org/10.1111/j.1464-5491.2011.03279.x>.
- Muniak, M. A., S. Ray, S. S. Hsiao, J. F. Dammann, and S. J. Bensmaia. 2007. "The Neural Coding of Stimulus Intensity: Linking the Population Response of Mechanoreceptive Afferents with Psychophysical Behavior." *Journal of Neuroscience* 27 (43): 11687-99. <https://doi.org/10.1523/JNEUROSCI.1486-07.2007>.
- Musk, Elon and Neuralink. 2019. "An Integrated Brain-Machine Interface Platform With Thousands of Channels." *Journal of Medical Internet Research* 21 (10): e16194. <https://doi.org/10.2196/16194>.
- Nakamura, S., R. D. Crowninshield, and R. R. Cooper. 1981. "An Analysis of Soft Tissue Loading in the Foot--a Preliminary Report." *Bulletin of Prosthetics Research* 10-35: 27-34.
- Nanivadekar, Ameya C., Santosh Chandrasekaran, Eric R. Helm, Michael L. Boninger, Jennifer L. Collinger, Robert A. Gaunt, and Lee E. Fisher. 2022. "Closed-Loop Stimulation of Lateral Cervical Spinal Cord in Upper-Limb Amputees to Enable Sensory Discrimination: A Case Study." *Scientific Reports* 12 (1): 17002. <https://doi.org/10.1038/s41598-022-21264-7>.
- Navarro, Xavier, Thilo B. Krueger, Natalia Lago, Silvestro Micera, Thomas Stieglitz, and Paolo Dario. 2005. "A Critical Review of Interfaces with the Peripheral Nervous System for the Control of Neuroprostheses and Hybrid Bionic Systems." *Journal of the Peripheral Nervous System: JPNS* 10 (3): 229-58. <https://doi.org/10.1111/j.1085-9489.2005.10303.x>.
- "Neuralink." n.d. <https://neuralink.com/>.
- Nolan, Lee, Andrzej Wit, Krzysztof Dudziński, Adrian Lees, Mark Lake, and Michał Wychowański. 2003. "Adjustments in Gait Symmetry with Walking Speed in Trans-Femoral and Trans-Tibial Amputees." *Gait & Posture* 17 (2): 142-51. [https://doi.org/10.1016/S0966-6362\(02\)00066-8](https://doi.org/10.1016/S0966-6362(02)00066-8).
- Ochoa, J, and E Torebjörk. 1983. "Sensations Evoked by Intraneural Microstimulation of Single Mechanoreceptor Units Innervating the Human Hand." *The Journal of Physiology* 342 (September): 633-54.
- Oddo, Calogero Maria, Stanisa Raspopovic, Fiorenzo Artoni, Alberto Mazzoni, Giacomo Spigler, Francesco Petrini, Federica Giambattistelli, et al. 2016. "Intraneural Stimulation Elicits Discrimination of Textural Features by Artificial Fingertip in Intact and Amputee Humans." *ELife* 5 (March): e09148. <https://doi.org/10.7554/eLife.09148>.

- Oddsson, Lars I. E., Carlo J. De Luca, and Peter F. Meyer. 2004. "The Role of Plantar Cutaneous Sensation in Unperturbed Stance." *Experimental Brain Research* 156 (4): 505–12. <https://doi.org/10.1007/s00221-003-1804-y>.
- Okorokova, Elizaveta, Qinqu He, and Sliman J. Bensmaia. 2018. "Biomimetic Encoding Model for Restoring Touch in Bionic Hands through a Nerve Interface." *Journal of Neural Engineering*, September. <https://doi.org/10.1088/1741-2552/aae398>.
- Orma, E. J. 1957. "The Effects of Cooling the Feet and Closing the Eyes on Standing Equilibrium. Different Patterns of Standing Equilibrium in Young Adult Men and Women." *Acta Physiologica Scandinavica* 38 (3–4): 288–97. <https://doi.org/10.1111/j.1748-1716.1957.tb01392.x>.
- Ortiz-Catalan, M., B. Hakansson, and R. Branemark. 2014. "An Osseointegrated Human-Machine Gateway for Long-Term Sensory Feedback and Motor Control of Artificial Limbs." *Science Translational Medicine* 6 (257): 257re6–257re6. <https://doi.org/10.1126/scitranslmed.3008933>.
- Ortiz-Catalan, Max, Enzo Mastinu, Paolo Sassu, Oskar Aszmann, and Rickard Brånemark. 2020. "Self-Contained Neuromusculoskeletal Arm Prostheses." *The New England Journal of Medicine* 382 (18): 1732–38. <https://doi.org/10.1056/NEJMoa1917537>.
- Ortiz-Catalan, Max, Johan Wessberg, Enzo Mastinu, Autumn Naber, and Rickard Brånemark. 2019. "Patterned Stimulation of Peripheral Nerves Produces Natural Sensations With Regards to Location but Not Quality." *IEEE Transactions on Medical Robotics and Bionics* 1 (3): 199–203. <https://doi.org/10.1109/TMRB.2019.2931758>.
- Osborn, Luke E, Andrei Dragomir, Joseph L Betthausen, Christopher L Hunt, Harrison H Nguyen, Rahul R Kaliki, and Nitish V Thakor. 2018. "Prosthesis with Neuromorphic Multilayered E-Dermis Perceives Touch and Pain." *SCIENCE ROBOTICS*, 12.
- Overstreet, Cynthia K., Jonathan Cheng, and Edward W. Keefer. 2019. "Fascicle Specific Targeting for Selective Peripheral Nerve Stimulation." *Journal of Neural Engineering* 16 (6): 066040. <https://doi.org/10.1088/1741-2552/ab4370>.
- Page, David M., Jacob A. George, David T. Kluger, Christopher Duncan, Suzanne Wendelken, Tyler Davis, Douglas T. Hutchinson, and Gregory A. Clark. 2018. "Motor Control and Sensory Feedback Enhance Prosthesis Embodiment and Reduce Phantom Pain After Long-Term Hand Amputation." *Frontiers in Human Neuroscience* 12.
- Page, David M., Jacob A. George, Suzanne M. Wendelken, Tyler S. Davis, David T. Kluger, Douglas T. Hutchinson, and Gregory A. Clark. 2021. "Discriminability of Multiple Cutaneous and Proprioceptive Hand Percepts Evoked by Intraneural Stimulation with Utah Slanted Electrode Arrays in Human Amputees." *Journal of NeuroEngineering and Rehabilitation* 18 (1): 12. <https://doi.org/10.1186/s12984-021-00808-4>.
- Pasluosta, Cristian, Patrick Kiele, and Thomas Stieglitz. 2018. "Paradigms for Restoration of Somatosensory Feedback via Stimulation of the Peripheral Nervous System." *Clinical Neurophysiology* 129 (4): 851–62. <https://doi.org/10.1016/j.clinph.2017.12.027>.
- Pearcey, Gregory E. P., and E. Paul Zehr. 2019. "We Are Upright-Walking Cats: Human Limbs as Sensory Antennae During Locomotion." *Physiology* 34 (5): 354–64. <https://doi.org/10.1152/physiol.00008.2019>.
- Pei, Yu-Cheng, Peter V. Denchev, Steven S. Hsiao, James C. Craig, and Sliman J. Bensmaia. 2009. "Convergence of Submodality-Specific Input Onto Neurons in Primary Somatosensory Cortex." *Journal of Neurophysiology* 102 (3): 1843–53. <https://doi.org/10.1152/jn.00235.2009>.

- Perich, Matthew G., Sara Conti, Marion Badi, Andrew Bogaard, Beatrice Barra, Sophie Wurth, Jocelyne Bloch, et al. 2020. "Motor Cortical Dynamics Are Shaped by Multiple Distinct Subspaces during Naturalistic Behavior." Preprint. Neuroscience. <https://doi.org/10.1101/2020.07.30.228767>.
- Perry, S. D., A. Radtke, W. E. McIlroy, G. R. Fernie, and B. E. Maki. 2008. "Efficacy and Effectiveness of a Balance-Enhancing Insole." *The Journals of Gerontology Series A: Biological Sciences and Medical Sciences* 63 (6): 595–602. <https://doi.org/10.1093/gerona/63.6.595>.
- Perry, Stephen D, William E McIlroy, and Brian E Maki. 2000. "The Role of Plantar Cutaneous Mechanoreceptors in the Control of Compensatory Stepping Reactions Evoked by Unpredictable, Multi-Directional Perturbation." *Brain Research* 877 (2): 401–6. [https://doi.org/10.1016/S0006-8993\(00\)02712-8](https://doi.org/10.1016/S0006-8993(00)02712-8).
- Petrini, Francesco M., Giacomo Valle, Ivo Strauss, Giuseppe Granata, Riccardo Di Iorio, Edoardo D'Anna, Paul Čvančara, et al. 2019. "Six-Month Assessment of a Hand Prosthesis with Intraneural Tactile Feedback." *Annals of Neurology* 85 (1): 137–54. <https://doi.org/10.1002/ana.25384>.
- Petrini, Francesco Maria, Marko Bumbasirevic, Giacomo Valle, Vladimir Ilic, Pavle Mijović, Paul Čvančara, Federica Barberi, et al. 2019. "Sensory Feedback Restoration in Leg Amputees Improves Walking Speed, Metabolic Cost and Phantom Pain." *Nature Medicine* 25 (9): 1356–63. <https://doi.org/10.1038/s41591-019-0567-3>.
- Petrini, Francesco Maria, Giacomo Valle, Marko Bumbasirevic, Federica Barberi, Dario Bortolotti, Paul Cvancara, Arthur Hiairassary, et al. 2019. "Enhancing Functional Abilities and Cognitive Integration of the Lower Limb Prosthesis." *Science Translational Medicine* 11 (512): eaav8939. <https://doi.org/10.1126/scitranslmed.aav8939>.
- Petrusic, Igor, Giacomo Valle, Marko Dakovic, Dusan Damjanovic, Marko Bumbasirevic, and Stanisa Raspopovic. 2022. "Plastic Changes in the Brain after a Neuro-Prosthetic Leg Use." *Clinical Neurophysiology*, April. <https://doi.org/10.1016/j.clinph.2022.04.001>.
- Piaggese, Alberto, Marco Romanelli, Elena Schipani, Fabrizio Campi, Antonio Magliaro, Fabio Baccetti, and Renzo Navalesi. 1999. "Hardness of Plantar Skin in Diabetic Neuropathic Feet." *Journal of Diabetes and Its Complications* 13 (3): 129–34. [https://doi.org/10.1016/S1056-8727\(98\)00022-1](https://doi.org/10.1016/S1056-8727(98)00022-1).
- Pillow, J. W. 2005. "Prediction and Decoding of Retinal Ganglion Cell Responses with a Probabilistic Spiking Model." *Journal of Neuroscience* 25 (47): 11003–13. <https://doi.org/10.1523/JNEUROSCI.3305-05.2005>.
- "Postural Control Part 1 - Proprioception." n.d. <https://yourpinnacle.com.au/blog/postural-control-part-1-proprioeption/>.
- Poulos, Da, J Mei, Kw Horch, Rp Tuckett, Jy Wei, Mc Cornwall, and Pr Burgess. 1984. "The Neural Signal for the Intensity of a Tactile Stimulus." *The Journal of Neuroscience* 4 (8): 2016–24. <https://doi.org/10.1523/JNEUROSCI.04-08-02016.1984>.
- Powell, Marc P., Nikhil Verma, Erynn Sorensen, Erick Carranza, Amy Boos, Daryl P. Fields, Souvik Roy, et al. 2023. "Epidural Stimulation of the Cervical Spinal Cord for Post-Stroke Upper-Limb Paresis." *Nature Medicine* 29 (3): 689–99. <https://doi.org/10.1038/s41591-022-02202-6>.
- Preatoni, Greta, Giacomo Valle, Francesco M. Petrini, and Stanisa Raspopovic. 2021. "Lightening the Perceived Weight of a Prosthesis with Cognitively Integrated Neural Sensory Feedback." *Current Biology* 31: 1–7. <https://doi.org/10.1016/j.cub.2020.11.069>.

- Priplata, Attila A., Benjamin L. Patritti, James B. Niemi, Richard Hughes, Denise C. Gravelle, Lewis A. Lipsitz, Aristidis Veves, Joel Stein, Paolo Bonato, and James J. Collins. 2006. "Noise-Enhanced Balance Control in Patients with Diabetes and Patients with Stroke." *Annals of Neurology* 59 (1): 4–12. <https://doi.org/10.1002/ana.20670>.
- Prochazka, Arthur. 2011. "Proprioceptive Feedback and Movement Regulation." In *Comprehensive Physiology*, 89–127. American Cancer Society. <https://doi.org/10.1002/cphy.cp120103>.
- Quian Quiroga, Rodrigo, and Stefano Panzeri. 2009. "Extracting Information from Neuronal Populations: Information Theory and Decoding Approaches." *Nature Reviews. Neuroscience* 10 (3): 173–85. <https://doi.org/10.1038/nrn2578>.
- Quiroga, R. Quian, Z. Nadasdy, and Y. Ben-Shaul. 2004. "Unsupervised Spike Detection and Sorting with Wavelets and Superparamagnetic Clustering." *Neural Computation* 16 (8): 1661–87. <https://doi.org/10.1162/089976604774201631>.
- Raja, Bhavana, Richard R. Neptune, and Steven A. Kautz. 2012. "Quantifiable Patterns of Limb Loading and Unloading during Hemiparetic Gait: Relation to Kinetic and Kinematic Parameters." *Journal of Rehabilitation Research and Development* 49 (9): 1293–1304.
- Raspopovic, S., M. Capogrosso, F. M. Petrini, M. Bonizzato, J. Rigosa, G. Di Pino, J. Carpaneto, et al. 2014. "Restoring Natural Sensory Feedback in Real-Time Bidirectional Hand Prostheses." *Science Translational Medicine* 6 (222): 222ra19–222ra19. <https://doi.org/10.1126/scitranslmed.3006820>.
- Raspopovic, S., F. M. Petrini, M. Zelechowski, and G. Valle. 2017. "Framework for the Development of Neuroprostheses: From Basic Understanding by Sciatic and Median Nerves Models to Bionic Legs and Hands." *Proceedings of the IEEE* 105 (1): 34–49. <https://doi.org/10.1109/JPROC.2016.2600560>.
- Raspopovic, Stanisa. 2020. "Advancing Limb Neural Prostheses." *Science* 370 (6514): 290–91. <https://doi.org/10.1126/science.abb1073>.
- — —. 2021. "Neurorobotics for Neurorehabilitation." *Science* 373 (6555): 634–35. <https://doi.org/10.1126/science.abj5259>.
- Raspopovic, Stanisa, Marco Capogrosso, Jordi Badia, Xavier Navarro, and Silvestro Micera. 2012. "Experimental Validation of a Hybrid Computational Model for Selective Stimulation Using Transverse Intrafascicular Multichannel Electrodes." *IEEE Transactions on Neural Systems and Rehabilitation Engineering* 20 (3): 395–404. <https://doi.org/10.1109/TNSRE.2012.2189021>.
- Raspopovic, Stanisa, Marco Capogrosso, and Silvestro Micera. 2011. "A Computational Model for the Stimulation of Rat Sciatic Nerve Using a Transverse Intrafascicular Multichannel Electrode." *IEEE Transactions on Neural Systems and Rehabilitation Engineering* 19 (4): 333–44. <https://doi.org/10.1109/TNSRE.2011.2151878>.
- Raspopovic, Stanisa, Francesco Maria Petrini, Marek Zelechowski, and Giacomo Valle. 2017. "Framework for the Development of Neuroprostheses: From Basic Understanding by Sciatic and Median Nerves Models to Bionic Legs and Hands." *Proceedings of the IEEE* 105 (1): 34–49. <https://doi.org/10.1109/JPROC.2016.2600560>.
- Raspopovic, Stanisa, Giacomo Valle, and Francesco Maria Petrini. 2021. "Sensory Feedback for Limb Prostheses in Amputees." *Nature Materials* 20 (7): 925–39. <https://doi.org/10.1038/s41563-021-00966-9>.
- Rastogi, Anisha, Francis R. Willett, Jessica Abreu, Douglas C. Crowder, Brian A. Murphy, William D. Memberg, Carlos E. Vargas-Irwin, et al. 2021. "The Neural Representation of Force across Grasp Types in Motor Cortex of Humans with Tetraplegia." *Eneuro* 8 (1): ENEURO.0231-20.2020. <https://doi.org/10.1523/ENEURO.0231-20.2020>.

- Rattay, Frank. 1986. "Analysis of Models for External Stimulation of Axons." *IEEE Transactions on Biomedical Engineering* BME-33 (10): 974-77. <https://doi.org/10.1109/TBME.1986.325670>.
- Risso, G., G. Valle, F. Iberite, I. Strauss, T. Stieglitz, M. Controzzi, F. Clemente, et al. 2019. "Optimal Integration of Intraneural Somatosensory Feedback with Visual Information: A Single-Case Study." *Scientific Reports* 9 (1): 7916. <https://doi.org/10.1038/s41598-019-43815-1>.
- Rognini, G., F. M. Petrini, S. Raspopovic, G. Valle, G. Granata, I. Stauss, M. Solca, et al. 2018. "Multisensory Bionic Limb to Achieve Prosthesis Embodiment and Reduce Distorted Phantom Limb Perceptions. J Neurol Neurosurg Psychiatry 0:1-3. Doi:10.1136/Jnnp-2018-318570."
- Rossini, Paolo M., Silvestro Micera, Antonella Benvenuto, Jacopo Carpaneto, Giuseppe Cavallo, Luca Citi, Christian Cipriani, et al. 2010. "Double Nerve Intraneural Interface Implant on a Human Amputee for Robotic Hand Control." *Clinical Neurophysiology* 121 (5): 777-83. <https://doi.org/10.1016/j.clinph.2010.01.001>.
- Rudomin, P., and Robert F. Schmidt. 1999. "Presynaptic Inhibition in the Vertebrate Spinal Cord Revisited." *Experimental Brain Research* 129 (1): 1-37. <https://doi.org/10.1007/s002210050933>.
- Rusaw, David, Kerstin Hagberg, Lee Nolan, and Nerrolyn Ramstrand. 2012. "Can Vibratory Feedback Be Used to Improve Postural Stability in Persons with Transtibial Limb Loss?" *Journal of Rehabilitation Research and Development* 49 (8): 1239-54.
- Saal, Hannes P., and Sliman J. Bensmaia. 2014. "Touch Is a Team Effort: Interplay of Submodalities in Cutaneous Sensibility." *Trends in Neurosciences* 37 (12): 689-97. <https://doi.org/10.1016/j.tins.2014.08.012>.
- — —. 2015. "Biomimetic Approaches to Bionic Touch through a Peripheral Nerve Interface." *Neuropsychologia* 79 (December): 344-53. <https://doi.org/10.1016/j.neuropsychologia.2015.06.010>.
- Saal, Hannes P., Benoit P. Delhaye, Brandon C. Rayhaun, and Sliman J. Bensmaia. 2017. "Simulating Tactile Signals from the Whole Hand with Millisecond Precision." *Proceedings of the National Academy of Sciences* 114 (28): E5693-5702. <https://doi.org/10.1073/pnas.1704856114>.
- Saal, Hannes P., Michael A. Harvey, and Sliman J. Bensmaia. 2015. "Rate and Timing of Cortical Responses Driven by Separate Sensory Channels." *ELife* 4 (December): e10450. <https://doi.org/10.7554/eLife.10450>.
- Sadtler, Patrick T., Kristin M. Quick, Matthew D. Golub, Steven M. Chase, Stephen I. Ryu, Elizabeth C. Tyler-Kabara, Byron M. Yu, and Aaron P. Batista. 2014. "Neural Constraints on Learning." *Nature* 512 (7515): 423-26. <https://doi.org/10.1038/nature13665>.
- Salas, Michelle Armenta, Luke Bashford, Spencer Kellis, Matiar Jafari, HyeonChan Jo, Daniel Kramer, Kathleen Shanfield, et al. 2018. "Proprioceptive and Cutaneous Sensations in Humans Elicited by Intracortical Microstimulation." *ELife* 7 (April): e32904. <https://doi.org/10.7554/eLife.32904>.
- Schiefer, Matthew A., Ronald J. Triolo, and Dustin J. Tyler. 2008. "A Model of Selective Activation of the Femoral Nerve With a Flat Interface Nerve Electrode for a Lower Extremity Neuroprosthesis." *IEEE Transactions on Neural Systems and Rehabilitation Engineering* 16 (2): 195-204. <https://doi.org/10.1109/TNSRE.2008.918425>.
- Schiefer, Matthew, Daniel Tan, Steven M Sidek, and Dustin J Tyler. 2016. "Sensory Feedback by Peripheral Nerve Stimulation Improves Task Performance in Individuals with



- Upper Limb Loss Using a Myoelectric Prosthesis." *Journal of Neural Engineering* 13 (1): 016001. <https://doi.org/10.1088/1741-2560/13/1/016001>.
- Seáñez, Ismael, and Marco Capogrosso. 2021. "Motor Improvements Enabled by Spinal Cord Stimulation Combined with Physical Training after Spinal Cord Injury: Review of Experimental Evidence in Animals and Humans." *Bioelectronic Medicine* 7 (1): 16. <https://doi.org/10.1186/s42234-021-00077-5>.
- Secerovic, Natalija Katic, Josep-Maria Balaguer, Oleg Gorskii, Natalia Pavlova, Lucy Liang, Jonathan Ho, Erinn Grigsby, et al. 2021. "Neural Population Dynamics Reveals Disruption of Spinal Sensorimotor Computations during Electrical Stimulation of Sensory Afferents." Preprint. Neuroscience. <https://doi.org/10.1101/2021.11.19.469209>.
- Simeral, John D., Thomas Hosman, Jad Saab, Sharlene N. Flesher, Marco Vilela, Brian Franco, Jessica N. Kelemen, et al. 2021. "Home Use of a Percutaneous Wireless Intracortical Brain-Computer Interface by Individuals With Tetraplegia." *IEEE Transactions on Biomedical Engineering* 68 (7): 2313–25. <https://doi.org/10.1109/TBME.2021.3069119>.
- Sinopoulou, Eleni, Ephron S. Rosenzweig, James M. Conner, Daniel Gibbs, Chase A. Weinholtz, Janet L. Weber, John H. Brock, et al. 2022. "Rhesus Macaque versus Rat Divergence in the Corticospinal Projectome." *Neuron* 110 (18): 2970-2983.e4. <https://doi.org/10.1016/j.neuron.2022.07.002>.
- Squair, Jordan W., Matthieu Gautier, Lois Mahe, Jan Elaine Soriano, Andreas Rowald, Arnaud Bichat, Newton Cho, et al. 2021. "Neuroprosthetic Baroreflex Controls Haemodynamics after Spinal Cord Injury." *Nature* 590 (7845): 308–14. <https://doi.org/10.1038/s41586-020-03180-w>.
- Stein, R. B. 1995. "Presynaptic Inhibition in Humans." *Progress in Neurobiology* 47 (6): 533–44. [https://doi.org/10.1016/0301-0082\(95\)00036-4](https://doi.org/10.1016/0301-0082(95)00036-4).
- Storn, Rainer, and Kenneth Price. 1997. "Differential Evolution – A Simple and Efficient Heuristic for Global Optimization over Continuous Spaces." *Journal of Global Optimization* 11 (4): 341–59. <https://doi.org/10.1023/A:1008202821328>.
- Strauss, I., G. Valle, F. Artoni, E. D'Anna, G. Granata, R. Di Iorio, D. Guiraud, et al. 2019. "Characterization of Multi-Channel Intraneural Stimulation in Transradial Amputees." *Scientific Reports* 9 (1): 19258. <https://doi.org/10.1038/s41598-019-55591-z>.
- Strzalkowski, Nicholas D J. 2015. "Tactile Perception Across the Human Foot Sole as Examined by the Firing Characteristics of Cutaneous Afferents and Mechanical Properties of the Skin." <https://doi.org/10.13140/RG.2.2.12911.02721>.
- Strzalkowski, Nicholas D. J., R. Ayesha Ali, and Leah R. Bent. 2017. "The Firing Characteristics of Foot Sole Cutaneous Mechanoreceptor Afferents in Response to Vibration Stimuli." *Journal of Neurophysiology* 118 (4): 1931–42. <https://doi.org/10.1152/jn.00647.2016>.
- Strzalkowski, Nicholas D. J., Robyn L. Mildren, and Leah R. Bent. 2015. "Thresholds of Cutaneous Afferents Related to Perceptual Threshold across the Human Foot Sole." *Journal of Neurophysiology* 114 (4): 2144–51. <https://doi.org/10.1152/jn.00524.2015>.
- Strzalkowski, Nicholas D. J., Ryan M. Peters, J. Timothy Inglis, and Leah R. Bent. 2018. "Cutaneous Afferent Innervation of the Human Foot Sole: What Can We Learn from Single-Unit Recordings?" *Journal of Neurophysiology* 120 (3): 1233–46. <https://doi.org/10.1152/jn.00848.2017>.
- Strzalkowski, Nicholas D. J., John J. Triano, Chris K. Lam, Cale A. Templeton, and Leah R. Bent. 2015. "Thresholds of Skin Sensitivity Are Partially Influenced by Mechanical

- Properties of the Skin on the Foot Sole." *Physiological Reports* 3 (6): e12425. <https://doi.org/10.14814/phy2.12425>.
- Suresh, Aneesha K., Charles M. Greenspon, Qinpu He, Joshua M. Rosenow, Lee E. Miller, and Sliman J. Bensmaia. 2021. "Sensory Computations in the Cuneate Nucleus of Macaques." *Proceedings of the National Academy of Sciences* 118 (49): e2115772118. <https://doi.org/10.1073/pnas.2115772118>.
- Tabot, G. A., J. F. Dammann, J. A. Berg, F. V. Tenore, J. L. Boback, R. J. Vogelstein, and S. J. Bensmaia. 2013. "Restoring the Sense of Touch with a Prosthetic Hand through a Brain Interface." *Proceedings of the National Academy of Sciences* 110 (45): 18279–84. <https://doi.org/10.1073/pnas.1221113110>.
- Takakusaki, Kaoru. 2013. "Neurophysiology of Gait: From the Spinal Cord to the Frontal Lobe: Neurophysiology of Gait." *Movement Disorders* 28 (11): 1483–91. <https://doi.org/10.1002/mds.25669>.
- Tan, D. W., M. A. Schiefer, M. W. Keith, J. R. Anderson, J. Tyler, and D. J. Tyler. 2014. "A Neural Interface Provides Long-Term Stable Natural Touch Perception." *Science Translational Medicine* 6 (257): 257ra138–257ra138. <https://doi.org/10.1126/scitranslmed.3008669>.
- Tan, Daniel W, Matthew A Schiefer, Michael W Keith, J Robert Anderson, and Dustin J Tyler. 2015. "Stability and Selectivity of a Chronic, Multi-Contact Cuff Electrode for Sensory Stimulation in Human Amputees." *Journal of Neural Engineering* 12 (2): 026002. <https://doi.org/10.1088/1741-2560/12/2/026002>.
- Tan, Daniel W., Matthew A. Schiefer, Michael W. Keith, James Robert Anderson, Joyce Tyler, and Dustin J. Tyler. 2014. "A Neural Interface Provides Long-Term Stable Natural Touch Perception." *Science Translational Medicine* 6 (257): 257ra138. <https://doi.org/10.1126/scitranslmed.3008669>.
- The Global Lower Extremity Amputation Study Group, and N Unwin. 2002. "Epidemiology of Lower Extremity Amputation in Centres in Europe, North America and East Asia." *British Journal of Surgery* 87 (3): 328–37. <https://doi.org/10.1046/j.1365-2168.2000.01344.x>.
- "The Sense of Touch." n.d. [http://www.corpshumain.ca/en/Touche\\_en.php](http://www.corpshumain.ca/en/Touche_en.php).
- Tomlinson, Tucker, and Lee E. Miller. 2016. "Toward a Proprioceptive Neural Interface That Mimics Natural Cortical Activity." *Advances in Experimental Medicine and Biology* 957: 367–88. [https://doi.org/10.1007/978-3-319-47313-0\\_20](https://doi.org/10.1007/978-3-319-47313-0_20).
- Toossi, Amirali, Dirk G Everaert, Richard R E Uwiera, David S Hu, Kevin Robinson, Ferrante S Gragasin, and Vivian K Mushahwar. 2019. "Effect of Anesthesia on Motor Responses Evoked by Spinal Neural Prostheses during Intraoperative Procedures." *Journal of Neural Engineering* 16 (3): 036003. <https://doi.org/10.1088/1741-2552/ab0938>.
- Torebjörk, H. Erik, and José L. Ochoa. 1980. "Specific Sensations Evoked by Activity in Single Identified Sensory Units in Man." *Acta Physiologica Scandinavica* 110 (4): 445–47. <https://doi.org/10.1111/j.1748-1716.1980.tb06695.x>.
- Tuthill, John C., and Eiman Azim. 2018. "Proprioception." *Current Biology* 28 (5): R194–203. <https://doi.org/10.1016/j.cub.2018.01.064>.
- Vallbo, A. B., and R. S. Johansson. 1984. "Properties of Cutaneous Mechanoreceptors in the Human Hand Related to Touch Sensation." *Human Neurobiology* 3 (1): 3–14.
- Valle, G., F. M. Petrini, I. Strauss, F. Iberite, E. D'Anna, G. Granata, M. Controzzi, et al. 2018. "Comparison of Linear Frequency and Amplitude Modulation for Intraneural Sensory Feedback in Bidirectional Hand Prostheses." *Scientific Reports* 8 (1): 16666. <https://doi.org/10.1038/s41598-018-34910-w>.

- Valle, Giacomo, Giovanna Aiello, Federico Ciotti, Paul Cvancara, Tamara Martinovic, Tamara Kravic, Xavier Navarro, Thomas Stieglitz, Marko Bumbasirevic, and Stanisa Raspopovic. 2022. "Multifaceted Understanding of Human Nerve Implants to Design Optimized Electrodes for Bioelectronics." *Biomaterials* 291 (December): 121874. <https://doi.org/10.1016/j.biomaterials.2022.121874>.
- Valle, Giacomo, Edoardo D'Anna, Ivo Strauss, Francesco Clemente, Giuseppe Granata, Riccardo Di Iorio, Marco Controzzi, et al. 2020. "Hand Control With Invasive Feedback Is Not Impaired by Increased Cognitive Load." *Frontiers in Bioengineering and Biotechnology* 8. <https://doi.org/10.3389/fbioe.2020.00287>.
- Valle, Giacomo, Francesco Iberite, Ivo Strauss, Edoardo D'Anna, Giuseppe Granata, Riccardo Di Iorio, Thomas Stieglitz, et al. 2021. "A Psychometric Platform to Collect Somatosensory Sensations for Neuroprosthetic Use." *Frontiers in Medical Technology* 3: 8. <https://doi.org/10.3389/fmedt.2021.619280>.
- Valle, Giacomo, Alberto Mazzoni, Francesco Iberite, Edoardo D'Anna, Ivo Strauss, Giuseppe Granata, Marco Controzzi, et al. 2018a. "Biomimetic Intraneural Sensory Feedback Enhances Sensation Naturalness, Tactile Sensitivity, and Manual Dexterity in a Bidirectional Prosthesis." *Neuron* 100 (1): 37-45.e7. <https://doi.org/10.1016/j.neuron.2018.08.033>.
- Valle, Giacomo, Alberto Mazzoni, Francesco Iberite, Edoardo D'Anna, Ivo Strauss, Giuseppe Granata, Marco Controzzi, et al. 2018b. "Biomimetic Intraneural Sensory Feedback Enhances Sensation Naturalness, Tactile Sensitivity, and Manual Dexterity in a Bidirectional Prosthesis." *Neuron* 100 (1): 37-45.e7. <https://doi.org/10.1016/j.neuron.2018.08.033>.
- Valle, Giacomo, Albulena Saliji, Ezra Fogle, Andrea Cimolato, Francesco M. Petrini, and Stanisa Raspopovic. 2021. "Mechanisms of Neuro-Robotic Prosthesis Operation in Leg Amputees." *Science Advances* 7 (17): eabd8354. <https://doi.org/10.1126/sciadv.abd8354>.
- Valle, Giacomo, Ivo Strauss, Edoardo D'Anna, Giuseppe Granata, Riccardo Di Iorio, Thomas Stieglitz, Paolo Maria Rossini, Stanisa Raspopovic, Francesco Maria Petrini, and Silvestro Micera. 2020. "Sensitivity to Temporal Parameters of Intraneural Tactile Sensory Feedback." *Journal of NeuroEngineering and Rehabilitation* 17 (1): 110. <https://doi.org/10.1186/s12984-020-00737-8>.
- Wagner, Fabien B., Jean-Baptiste Mignardot, Camille G. Le Goff-Mignardot, Robin Demesmaeker, Salif Komi, Marco Capogrosso, Andreas Rowald, et al. 2018. "Targeted Neurotechnology Restores Walking in Humans with Spinal Cord Injury." *Nature* 563 (7729): 65-71. <https://doi.org/10.1038/s41586-018-0649-2>.
- Wagner, Fabien B., Jean-Baptiste Mignardot, Camille G. Le Goff-Mignardot, Robin Demesmaeker, Salif Komi, Marco Capogrosso, Andreas Rowald, et al. 2018. "Targeted Neurotechnology Restores Walking in Humans with Spinal Cord Injury." *Nature* 563 (7729): 65-71. <https://doi.org/10.1038/s41586-018-0649-2>.
- Wang, Yang, Xinze Yang, Xiwen Zhang, Yijun Wang, and Weihua Pei. 2023. "Implantable Intracortical Microelectrodes: Reviewing the Present with a Focus on the Future." *Microsystems & Nanoengineering* 9 (1): 1-17. <https://doi.org/10.1038/s41378-022-00451-6>.
- Wang, Yun, Kazuhiko Watanabe, and Liang Chen. 2016. "Effect of Plantar Cutaneous Inputs on Center of Pressure during Quiet Stance in Older Adults." *Journal of Exercise Science & Fitness* 14 (1): 24-28. <https://doi.org/10.1016/j.jesf.2016.02.001>.

- Waters, R. L., J. Perry, D. Antonelli, and H. Hislop. 1976. "Energy Cost of Walking of Amputees: The Influence of Level of Amputation." *The Journal of Bone and Joint Surgery. American Volume* 58 (1): 42-46.
- Waters, Robert L., and Sara Mulroy. 1999. "The Energy Expenditure of Normal and Pathologic Gait." *Gait & Posture* 9 (3): 207-31. [https://doi.org/10.1016/S0966-6362\(99\)00009-0](https://doi.org/10.1016/S0966-6362(99)00009-0).
- Wendelken, Suzanne, David M. Page, Tyler Davis, Heather A. C. Wark, David T. Kluger, Christopher Duncan, David J. Warren, Douglas T. Hutchinson, and Gregory A. Clark. 2017. "Restoration of Motor Control and Proprioceptive and Cutaneous Sensation in Humans with Prior Upper-Limb Amputation via Multiple Utah Slanted Electrode Arrays (USEAs) Implanted in Residual Peripheral Arm Nerves." *Journal of NeuroEngineering and Rehabilitation* 14 (1): 121. <https://doi.org/10.1186/s12984-017-0320-4>.
- Wheat, H. E., L. M. Salo, and A. W. Goodwin. 2010. "Cutaneous Afferents From the Monkeys Fingers: Responses to Tangential and Normal Forces." *Journal of Neurophysiology* 103 (2): 950-61. <https://doi.org/10.1152/jn.00502.2009>.
- Whelan, PATRICK J. 1996. "CONTROL OF LOCOMOTION IN THE DECEREBRATE CAT." *Progress in Neurobiology* 49 (5): 481-515. [https://doi.org/10.1016/0301-0082\(96\)00028-7](https://doi.org/10.1016/0301-0082(96)00028-7).
- Wiboonsaksakul, Kantapon Pum, Dale C. Roberts, Charles C. Della Santina, and Kathleen E. Cullen. 2022. "A Prosthesis Utilizing Natural Vestibular Encoding Strategies Improves Sensorimotor Performance in Monkeys." *PLOS Biology* 20 (9): e3001798. <https://doi.org/10.1371/journal.pbio.3001798>.
- Wiik, Anatole Vilhelm, Adeel Aqil, Mads Brevadt, Gareth Jones, and Justin Cobb. 2017. "Abnormal Ground Reaction Forces Lead to a General Decline in Gait Speed in Knee Osteoarthritis Patients." *World Journal of Orthopedics* 8 (4): 322. <https://doi.org/10.5312/wjo.v8.i4.322>.
- Wurth, S., M. Capogrosso, S. Raspopovic, J. Gandar, G. Federici, N. Kinany, A. Cutrone, et al. 2017. "Long-Term Usability and Bio-Integration of Polyimide-Based Intra-Neural Stimulating Electrodes." *Biomaterials* 122: 114-29. <https://doi.org/10.1016/j.biomaterials.2017.01.014>.
- Yoshioka, T., S. J. Bensmaïa, J. C. Craig, and S. S. Hsiao. 2007. "Texture Perception through Direct and Indirect Touch: An Analysis of Perceptual Space for Tactile Textures in Two Modes of Exploration." *Somatosensory & Motor Research* 24 (1-2): 53-70. <https://doi.org/10.1080/08990220701318163>.
- Zehr, E Paul, Tsuyoshi Nakajima, Trevor Barss, Taryn Klarner, Stefanie Miklosovic, Rinaldo A Mezzarane, Matthew Nurse, and Tomoyoshi Komiyama. 2014. "Cutaneous Stimulation of Discrete Regions of the Sole during Locomotion Produces 'Sensory Steering' of the Foot." *BMC Sports Science, Medicine and Rehabilitation* 6 (1): 33. <https://doi.org/10.1186/2052-1847-6-33>.
- Zelechowski, Marek, Giacomo Valle, and Stanisa Raspopovic. 2020. "A Computational Model to Design Neural Interfaces for Lower-Limb Sensory Neuroprostheses." *Journal of NeuroEngineering and Rehabilitation* 17 (1): 24. <https://doi.org/10.1186/s12984-020-00657-7>.
- Zollo, Loredana, Giovanni Di Pino, Anna L. Ciancio, Federico Ranieri, Francesca Cordella, Cosimo Gentile, Emiliano Noce, et al. 2019. "Restoring Tactile Sensations via Neural Interfaces for Real-Time Force-and-Slippage Closed-Loop Control of Bionic Hands." *Science Robotics* 4 (27): eaau9924. <https://doi.org/10.1126/scirobotics.aau9924>.



## Биографија

Наталија Катић рођена је 1995. године у Београду. Завршила је основну школу као ђак генерације, и гимназију као вуковац. Дипломирала је 2017. године на Електротехничком факултету у Београду, одсек Сигнали и системи са просечном оценом 9,51. Њен дипломски рад проглашен је од стране Математичког института САНУ за најбољи рад у категорији дипломских и мастер радова 2018. године. Мастер студије завршила је 2018. године на истом смеру са просечном оценом 10. Докторске студије уписала је 2018. године на изборном подручју Управљање системима и обрада сигнала. Положила је све испите на докторским студијама са просечном оценом 10.

Запослена је у Институту Михајло Пупин и уједно је и екстерни члан Лабораторије за неуроинжењеринг на ЕТХ у Цириху. Радила је на европском „ERC“ пројекту „Feel Again“, под менторством руководиоца проф. др Станише Распоповића. Тренутно је члан тима на пројектима Фонда за Иновациону делатност и Фонда за науку Републике Србије.

Објавила је радове у часописима „Nature Medicine“, „iScience“ и „Journal of Neural Engineering“, један рад је послат на ревизију и објављен је тренутно на платформи „BioRxiv“. Објавила је поглавља у књигама издавачких кућа „Academic Press Books - Elsevier“ и „Springer Nature Singapore“. Остварила је сарадњу са Универзитетима у Питсбургу, Санкт Петербургу и Шефилду, кроз низ истраживачких пројеката. Добитница је стипендије Швајцарског националног центра за истраживања у домену роботике („NCCR Robotics“). Свој рад излагала је на међународним конференцијама „Society for Neuroscience“, по позиву била члан скупа „Frontiers of Engineering symposium“. Била је једини стипендиста ван Сједињених Америчких Држава организатора „NSF DARE Conference: Transformative Opportunities for Modeling in Neurorehabilitation“ у Лос Анђелесу ове године.

Име и презиме аутора: Наталија Катић

Број индекса: 5020/18

## Изјава о ауторству

### Изјављујем

да је докторска дисертација под насловом „Декодирање неуралних механизма помоћу „in silico“ модела и експеримената на животињама са циљем обнављања соматосензорног осећаја променом неуропротеза“:

- резултат сопственог истраживачког рада;
- да дисертација у целини ни у деловима није била предложена за стицање друге дипломе према студијским програмима других високошколских установа;
- да су резултати коректно наведени и
- да нисам кршио/ла ауторска права и користио/ла интелектуалну својину других лица.

У Београду, 19. 06. 2023.

Потпис аутора



## Изјава о истоветности штампане и електронске верзије докторског рада

Име и презиме аутора: Наталија Катић

Број индекса: 5020/18

Студијски програм: Управљање системима и обрада сигнала

Наслов рада: Декодирање неуралних механизма помоћу „in silico“ модела и експеримената на животињама са циљем обнављања соматосензорног осећаја променом неуропротеза

Ментори: Др Жељко Ђуровић, редовни професор; Др Милица Јанковић, ванредни професор

Изјављујем да је штампана верзија мог докторског рада истоветна електронској верзији коју сам предао/ла ради похрањивања у **Дигиталном репозиторијуму Универзитета у Београду**.

Дозвољавам да се објаве моји лични подаци везани за добијање академског назива доктора наука, као што су име и презиме, година и место рођења и датум одбране рада.

Ови лични подаци могу се објавити на мрежним страницама дигиталне библиотеке, у електронском каталогу и у публикацијама Универзитета у Београду.

У Београду, 19. 06. 2023.

Потпис аутора



Наталија Катић



## Изјава о коришћењу

Овлашћујем Универзитетску библиотеку „Светозар Марковић“ да у Дигитални репозиторијум Универзитета у Београду унесе моју докторску дисертацију под насловом:

„Декодирање неуралних механизма помоћу „in silico“ модела и експеримената на животињама са циљем обнављања соматосензорног осећаја променом неуропротеза“ која је моје ауторско дело.

Дисертацију са свим прилозима предао/ла сам у електронском формату погодном за трајно архивирање. Моју докторску дисертацију похрањену у Дигиталном репозиторијуму Универзитета у Београду и доступну у отвореном приступу могу да користе сви који поштују одредбе садржане у одабраном типу лиценце Креативне заједнице (Creative Commons) за коју сам се одлучио/ла.

1. Ауторство (CC BY)
2. Ауторство – некомерцијално (CC BY-NC)
3. Ауторство – некомерцијално – без прерада (CC BY-NC-ND)
4. Ауторство – некомерцијално – делити под истим условима (CC BY-NC-SA)
5. Ауторство – без прерада (CC BY-ND)
6. Ауторство – делити под истим условима (CC BY-SA)

(Молимо да заокружите само једну од шест понуђених лиценци. Кратак опис лиценци је саставни део ове изјаве).

У Београду, 19. 06. 2023.

Потпис аутора



1. Ауторство. Дозвољаваате умножавање, дистрибуцију и јавно саопштавање дела, и прераде, ако се наведе име аутора на начин одређен од стране аутора или даваоца лиценце, чак и у комерцијалне сврхе. Ово је најслободнија од свих лиценци.
2. Ауторство – некомерцијално. Дозвољаваате умножавање, дистрибуцију и јавно саопштавање дела, и прераде, ако се наведе име аутора на начин одређен од стране аутора или даваоца лиценце. Ова лиценца не дозвољава комерцијалну употребу дела.
3. Ауторство – некомерцијално – без прерада. Дозвољаваате умножавање, дистрибуцију и јавно саопштавање дела, без промена, преобликовања или употребе дела у свом делу, ако се наведе име аутора на начин одређен од стране аутора или даваоца лиценце. Ова лиценца не дозвољава комерцијалну употребу дела. У односу на све остале лиценце, овом лиценцом се ограничава највећи обим права коришћења дела.
4. Ауторство – некомерцијално – делити под истим условима. Дозвољаваате умножавање, дистрибуцију и јавно саопштавање дела, и прераде, ако се наведе име аутора на начин одређен од стране аутора или даваоца лиценце и ако се прерада дистрибуира под истом или сличном лиценцом. Ова лиценца не дозвољава комерцијалну употребу дела и прерада.
5. Ауторство – без прерада. Дозвољаваате умножавање, дистрибуцију и јавно саопштавање дела, без промена, преобликовања или употребе дела у свом делу, ако се наведе име аутора на начин одређен од стране аутора или даваоца лиценце. Ова лиценца дозвољава комерцијалну употребу дела.
6. Ауторство – делити под истим условима. Дозвољаваате умножавање, дистрибуцију и јавно саопштавање дела, и прераде, ако се наведе име аутора на начин одређен од стране аутора или даваоца лиценце и ако се прерада дистрибуира под истом или сличном лиценцом. Ова лиценца дозвољава комерцијалну употребу дела и прерада. Слична је софтверским лиценцама, односно лиценцама отвореног кода.